MASS TRANSFER TO THIN LIQUID FILMS ON ROTATING SURFACES, WITH AND WITHOUT CHEMICAL REACTION

by

S. R. MOORE

Thesis submitted for the degree of Doctor of Philosophy in the Faculty of Engineering of the University of Newcastle Upon Tyne.

Department of Chemical & Process Engineering,
University of Newcastle Upon Tyne,
England.

October, 1986

FOR PAULA

ACKNOWLEDGEMENTS

The contributions of the following people are gratefully acknowledged-

- Mr. K. Peet in whose laboratories the work was completed.

- Mr. J.E. Porter for many useful suggestions and advice during our frequent and lively discussions.

- The S.E.R.C. for funding the research.

- Shell EXPRO (UK) for helping with the cost of preparing the thesis.

- All the technical staff. Particularly Eric, Brian, Chris, Ian and George for creating a superb experimental facility.

- Agnes for the time and effort involved in typing the final draft.

- All friends and fellow students for the encouragement which was needed at certain times.

- Paula for patience, understanding and a usefully placed condenser.

ABSTRACT

This investigation was concerned with the ability of perforated discs to act as the active mass transfer surface in rotary contact devices. Of particular interest were discs constructed of a woven stainless steel mesh. This material had a high fractional free area and an irregular surface, which is desirable if interfacial turbulence is to be promoted. The characteristics of three grades of mesh were compared with those of a plate perforated with punched holes and a smooth plane disc. A hydrodynamic study indicated that a stable film could be maintained on these flexible materials at speeds in excess of 200 RPM. However it was also demonstrated that at higher speeds dry areas tended to form around the periphary. The mass transfer performance was analysed in a specially designed rotary test rig using a carbon dioxide/water system. These experiments indicated that high transfer rates are attainable provided that operation is restricted to conditions where film breakdown does not occur. At 1500 RPM flowrates in excess of 200 cm^3/sec must be utilised. The same apparatus was adapted so that the enhancement due to a chemical reaction in the liquid phase could be determined. Aqueous solutions of diethanolamine were used in these experiments. The results were compared with predictions based upon a penetration type theory. The results of the investigation were applied to the design of a scrubber for an underwater closed-cycle nitro diesel engine and conclusions as to the relative merits of physical and chemical systems made.

LIST OF CONTENTS

4.2 Study of films flowing on rotating mesh discs

4.2.1 Preliminary experiments and observations

4.2.1.1 Introduction and description of equipment

4.2.1.2 Description of disc construction

4.2.1.3 Experimental work

4.2.1.3.1 Discs running dry

4.2.1.3.2 Discs running wet

4.2.2 Leakage measurements

4.2.2.1 Introduction

4.2.2.2 Experimental procedure

4.2.2.3 Discussion of results

5.0 Mass transfer processes (with and without an associated chemical reaction)

5.1 Physical mass transfer processes

5.1.1 Introduction

5.1.2 General concepts

5.1.3 Mass transfer models

5.1.4 Mass transfer to a liquid film on a rotating disc

5.2 Physical mass transfer in relation to the present investigation

5.2.1 Introduction

5.2.2 Calculation of mass transfer coefficients in the present investigation

5.2.3 Analysis of previous mass transfer results

5.2.4 Use of mass transfer models

5.3 Mass transfer accompanied by chemical reaction

5.3.1 Introduction

5.3.2 Calculation of acceleration factors for the case of a second order irreversible reaction

5.3.2.1 Psuedo first order reaction

5.3.2.2 Fast pseudo fist order

J Miscellaneous tables showing properties of the system carbon dioxide/aqueous diethanolamine

K Miscellaneous calculations

K1 Annular correction for mass transfer

K2 Calculation of required gas flowrate

L Operation of the regeneration system

a) Priming of the reboiler with CO_2 free DEA

b) Elevation of the reboiler to the operational (boiling) temperature

c) Feed of loaded solution to the column

d) Storage of regenerated solution

1.0. INTRODUCTION

1.1. Mass transfer and the concept of a rotary contact machine

Some of the most important processes in the chemical industry are concerned with the transfer of mass or energy, or a combination of the two, either at solid surfaces or through one of the many phase boundary combinations. Thus, the theory and practice of heat and mass transfer are constantly subject to intense study since any improvement in their efficiency, or the equipment within which such processes occur, could lead to considerable economic benfits. Similarily, with the development of offshore oil and processing operations, space is a limiting economic factor and therefore miniaturisation of transfer equipment is equally beneficial. Not only does this allow extra equipment to be carried in the given space, but it also means that operations normally only available on 'the beach' can be carried out at the well head, thus reducing the amount of material to be pumped to shore.

In order to develop compact equipment to meet these requirements the fundamentals of the processes of mass and energy transfer must be subject to a degree of intensification. When considering mass transfer a particularly important system is that involving gas and liquid phases. In some equipment used for these operations the interface between the two phases expands as the operation proceeds. Such an expansion is desirable as it exposes to the gas a fresh area of liquid from which, or too which, transfer can take place. The bubble growth period on the plate of a distillation column is an example of this phenomenom as is the spreading of a liquid film over a solid object.

One method to intensify the mass transfer process, in the case of gas/liquid systems, is by forcing the liquid to flow in a thin film over a solid object. Thus, for a given volumetric through-put a thin film presents a large gas/liquid interface, and transfer involves small diffusion lengths. The promotion of mixing in such films, either by the effect of surface waves, or the inducement of turbulence, further intensifies the mass transfer process.

The present work is an extension of a programme of research which developed from the study of thin films formed under the action of gravity on stationary, inclined and vertical plane , and later roughened plates. The usefulness of such equipment is limited by the minimum film thickness attainable. This is dependent on the forces available to 'spread' the liquid film, which in the case of stationary plates is fixed at the gravitational norm. By using a rotating disc as the surface on which the film is formed, not only are thinner films obtainable for a given through-put but they are attained in short distances measured in the direction of flow. This effect is achieved since elements of the film, even at modest radial positions and modest speeds of surface rotation, are subjected to centrifugal forces considerably in excess of that due to gravitational acceleration (9.81 m/s^2). For a packed device this means the minimum size of packing required to prevent flooding can be reduced thus allowing micro-packings

to be used in conditions of high gas and liquid loadings. Therefore the size of equipment needed for a given performance and through-put can be smaller than if a stationary contact surface is used.

Early research on rotating films concentrated on the hydrodynamics of the liquid and was limited to the use of smooth discs. A number of authors studied the flow regimes developed over various ranges of both flowrate and rotational speed and attempted to measure, by numerous methods, the thickness of the film and its surface velocity. The formation of ripples and waves were observed, noted,categorised and compared with similar features associated with films produced by gravitational forces. A number of preliminary design reports aimed at various practical applications were published. These include an apparatus for water de-salination (1) and equipment associated with the transfer of oxygen to blood (2). Venkatarraman (3) used a rotating film to investigate mass transfer to an expanding interface with a water/carbon dioxide system. The mass transfer section of this research was limmited to laminar films since these were the easiest to model.

Recent developments in rotating disc technology (4,5) have indicated that further improvements in mass transfer coefficients can be obtained by promoting internal circulation of the liquid in the film. This can be achieved by using a disc surface which provides a 'turbulent' film. In addition, it has recently been demonstrated over a wide range of flowrates and speeds of rotation, that a virtually stable, continuous film can be developed on a rough, perforated plate (5). Thus the gas/liquid interface can be increased by a factor equal to the plate voidage, as the liquid will be exposed to gas below, via the perforations, as well as above the rotating disc.

In an attempt to increase mass transfer coefficients even further it has been suggested that a selection of fine, regular meshes could be employed as the active mass transfer surface in a rotating machine. Since no information was available pertaining to the stability or hydrodynamics of a film formed on a mesh disc, a series of preliminary experiments were necessary to enable the influence of such factors on the mass transfer to be determined.

In addition to attaining further experimental data on the performance of rotary discs it was hoped that the research could be used to investigate the possibilities of using such a system as the stripping section of a nitro-diesel engine. Thus, although the machine structure and experimental conditions, solvents, etc., were, to a limited extent, chosen to study the mass transfer performance of a device suitable for diesel engine application, operation over a wide range of flowrate and rotary speeds provides data appropriate to the design and development of machines for general processing duties.

1.2. The concept of a closed-cycle diesel engine as an underwater power system

The advent of offshore oil operations has identified a demand for a practical, autonomous, subsea power-supply system that is flexible enough to cope with the numerous underwater activities currently practised. These include wellhead completion, rig inspection and maintenance, trenching, corring, bulldozing, hardware retrieval and personnel rescue. Additionally, recent surveys indicate that there is an increasing demand for a system capable of supporting missions with a duration in the region of ten hours and where work is required below two hundered metres.

At the present time and in the majority of cases, power is supplied through an umbilical cable linking the underwater operator with a surface mothership. Alternatively, when a modest power supply is required, the simple lead/acid battery can be used. This bestows the advantage of complete autonomous movement during the relatively short mission duration allowed by such a limited power source. Although both systems have worked well it is apparent that they are limited in their application to the future requirements as outlined above. Umbilical cables are expensive, rather clumsy and even at present depths are prone to snarling, breaking and drifting. When working at the prosed depths such problems are likely to be intolerable. Limitations on power levels and mission length are the obvious restriction of the lead/acid battery system. Future improvements in battery technology could decrease these limitations to a certain extent. Thus it follows that what is required is a power source that combines the capacity and durability of the umbilical with the autonomy of the battery.

As the result of an extensive survey undertaken by the department of Marine Engineering at the University of Newcastle Upon Tyne, (23,24) it was concluded that the use of a diesel engine, with conventional fuels would constitute an ideal system so long as the problems accosiated with breathing, exhausting, control and dynamic performance could be adequately resolved.

For subsea operations the diesel engine must be provided with a synthetic atmosphere containing oxygen to sustain combustion. This requirement can be attained in two ways; closed cycle operation or open cycle operation. In an open system, oxygen would be carried as a liquid and would be fed continuously to the engine. The exhaust gasses formed would then be compressed to a pressure where they could be discharged overboard. However, this is not a practical mode of operation if the overall power/weight/volume ratio is to be kept at an efficient level. Even when a diesel engine is running at full load it only consumes approximately 10% of the induced charge, therefore a vast quantity of virtually redundant working fluid has to be stored and exhausted. In a closed cycle the exhaust gasses are cleaned up and the initial inlet oxygen content re-established by addition of stored gas. In this way the volume of liquid oxygen to be carried is kept to a minimum. Before such a system becomes a practical solution a number of associated problems have to be solved. Broadly defined these are:

1. Provision of engine cylinder conditions compatible with the normal dual-cycle combustion process, including apportioning of suitable quantities of dilutent gas to fulfil the functions of a working fluid, whilst simultaneously limiting maximum cylinder temperatures.

2. Provision of total-system dynamic capability to match the rapid response of the diesel engine following load changes.

3. The replenishment of the depleted charge with oxygen in the required proportions.

4. The design of a compact stripper to remove combustion products from the exhaust gasses.

Set against the advantages of the closed cycle system are the obvious weight, volume and cost penalties associated with the scrubber and its consumable chemicals. The present work is, in part, an attempt to improve the design of the scrubber by applying the concept of rotary films to the problem. Thus it is hoped that one result of this work will be a practical solution to problem 4 above.

The scrubber used at present on the test rig constructed in the marine engineering department is a simple contraflow tower packed with plastic pall rings. It uses a 50% aqueous solution of pottasium hyroxide (KOH), pumped from a battery of 100 litre storage tanks, as the solvent into which a percentage of the carbon dioxide in the exhaust gasses is absorbed. As the reaction associated with KOH and carbon dioxide is irreversible it means that the solution can be used just once before being discarded. Obviously such a scheme in an underwater environment is impractical. A mission of a reasonable length would require a vast volume of tankage to carry the fresh solution down and return the used solution to the surface for disposal. More importantly a system relying on a scrubbing column would be unoperable as it relies on gravity to produce the contraflow and thus it would only function correctly when in a vertical position. Any realistic scheme has to be operable with the submersible at any inclination and thus a system that functions indepently of gravity has to be employed. Although rotary contact devices have so far only been used horizontally it is believed that as the centrifugal forces generated are far greater than gravity that such a system could meet this requirement. This is tested in the present work.

The choice of solvent to operate in such a system is important as it vitally effects the power/weight/volume ratio and thus the overall attractiveness of the system. In order to reduce the tankage requirements it was felt that a once through solvent (such as KOH) was impractical, and was of no use unless a superior alternative could not be devised. Thus two choices remained. Firstly, sea water could be used. This has the advantages that it is in a plentiful supply and that it can be returned to the sea once it has been used. Thus in that respect it can be thought of as a once through solvent without the disadvantages of KOH. However, water only absorbs carbon dioxide physically and thus a

greater transfer area (and therefore disc diameter) is needed to produce the same degree of scrubbing as a chemical solvent. Consequently the disc diameter may prove too big to be practical. Alternatively a chemical solvent which undergoes a reversible reaction with carbon dioxide can be employed. In such a case the gas would be absorbed under conditions which promote the forward reaction and then, in a separate device, be released by altering the conditions so that the reverse reaction is favoured. Therefore the amount of solvent needed is reduced to that which is required in the actual device and the associated pipework. The choice of solvent for such a process would have to consider any problems associated with such a choice. These could include the reaction of the solvent with other constituents of the gas stream, corrosion of the machinery, degradation of the solvent and the generation of the conditions to promote re-release of absorbed carbon dioxide.

Mass transfer processes which employ chemical solvents are widely used in industry. Therefore the present work, using these regenerable processes as its basis, investigates the applicability of this technique to the problem outlined above. The solvents and conditions used in the mass transfer experiments were chosen as a result of these considerations. The selection of solvent and the effect this had on the project as a whole is discussed in section 3. The results of the investigation are applied to the specific case of the nitro-diesel engine scrubber in Appendix C.

2.0. THE DEVELOPMENT OF ROTARY CONTACT DEVICES AND THE SIGNIFICANCE OF PAST WORK TO THE PRESENT INVESTIGATION

Since rotary discs were first used to produce thin films only a small volume of work has been published concerning their application to mass transfer systems. In comparison, a considerable amount has been written on their use in heat transfer operations and on the hydrodynamics of the thin films formed when the surface of the rotary disc is smooth. The work on mass transfer that has been presented, in general deals with plane discs, where, under most conditions, laminar flow prevails. Theoretical equations have been developed to model these processes accurately. The use of roughened surfaces to induce mixing of the liquid film has only recently been considered. The results of this work indicate that greater rates of mass transfer can be achieved than when surface waves are the only source of mixing. No work has been published on the use of rotary discs where mass transfer is enhanced by a chemical reaction (although such work has been suggested (6)).

The idea of using rotating discs to produce thin films developed from investigations of the behaviour of liquids flowing down stationary, inclined and vertical plane plates. It was found (8,9,10) that for this geometry the measured rates of mass transfer were significantly (up to 20 times) higher than those predicted assuming the film was laminar. It was observed that these high mass transfer rates were associated with liquid films which exhibited surface waves. These waves are characteristic of thin film flow and, for any particular geometry, are related to flowrate and the rheological properties of the film liquid. Under conditions where the film surface is essentially smooth, mass transfer measurements are consistent with predictions based on the assumption of laminar flow within the film. The formation and properties of these waves are well documented and have been extensively reviewed by Bell (7). It was suggested that the increased performance was a result of two effects; the mixing created by the interfacial waves (11,12,13) and the increase in interfacial area due to these waves (11,14,15). However, it has been shown since, that the increase in area is negligible (4,14, 16) and that the improvement is solely due to mixing.

By using a rotating disc as the plane on which the film is formed, not only are thinner films obtainable for a given through put, but they are attained in a short distance, measured in the direction of flow. This effect is achieved because the centrifugal forces induced by rapidly spinning a disc are much greater than that due to gravitational acceleration. The first, detailed study of mass transfer involving a liquid flowing across the surface of a rotating disc was that of Venkataraman (3). He used this system as an example of mass transfer to an expanding interface. The research was concerned with the absorption of carbon dioxide into water (at 25°C) as it flowed across the surface of a small disc ($\simeq$ 12.5 cm diameter). The range of liquid flow rates and rotary speeds investigated (2.9 to 7.6 cm^3/sec and 44 to 76 radians/sec respectively) were such that the free surface of liquid was essentially smooth. The measured mass transfer rates were compared with a number of models of increasing

complexity. The simplest model, the author's so called 'crude' model, was essentially an application of the penetration concept to this configuration, assuming purely radial flow. In this case measured mass transfer rates were some 23% higher than predicted values. Improvement of the model to take account of velocity components in the liquid film, normal to the plane of the surface, produced predicted values 3 to 7% greater than the measured results. Modification of the model to consider small and large depths of penetration indicated that sufficient differences could only be expected at film flows <1cm^3/sec. For the 'smooth' film flow regime, investigated in this study, additional refinements to include the influence of inertia, and the Coriolis acceleration, on film dynamics produced good agreement (within 4%) between measured and predicted values.

It was noted above that under certain conditions waves are formed on the surface of thin films flowing down inclined planes. A number of investigations have also been undertaken to study the various flow regimes encountered with thin films flowing on a rotating surface. These studies have been limited to smooth discs. Charwat et al (19) produced a plot of flowrate against speed of rotation for the ranges 0-7 cm^3/sec and 6 to 75 radians/sec respectively. This indicated that the boundaries between the regimes where concentric waves, spiral waves and a smooth surface were observed. Bell (7) extended such observations for flowrates up to 300 cm^3/sec showing the existance of additional areas where film breakdown and nozzle jetting occur. The graphs are reproduced in section 4 (see figure 4.1) where the hydrodynamics of thin films are covered in more detail.

The onset of waves in falling films gives rise to an increased rate of mass transfer. Likewise, it would seem reasonable to expect that waves formed on rotating films would produce the same effect. Watts (6,18) measured the rates of mass transfer of carbon dioxide to water over a range of flowrates and speeds (37.5 to 187.5 cm^3/sec and 33.5, 69 and 115 radians/sec) where spiral waves are present. For these experiments he used a smooth disc of approximately 34cm diameter which was run so that the plane of the liquid surface was vertical. The equipment was modified from previous heat transfer experiments by sealing the disc inside a stationary cover so that leakages to and from the gas chamber were avoided. Liquid samples were taken from the edge of the disc via a 1/4" copper tube and analysed for total carbon dioxide using a method outlined by Perciful (17). The author developed equations to predict the rate of gas absorption in a similar way to the laminar flow, entry length approach to heat transfer. However, these equations were never successfully solved. The results are presented (6,18) as graphs of the rate of mass transfer, calculted from the carbon dioxide analysis of the water, against flowrate at the three speeds used. To compare these with a theoretical model the predicted results from Venkataraman's 'approximate' theory (as outlined above) are plotted on the same graph for each speed. Although mass transfer rates give an effective feel for the efficiency of a piece of equipment it is hard to use them to compare the performance of separate rotary devices operating at different conditions. Therefore using the disc dimensions and gas conditions stated (6), the overall liquid phase mass transfer coefficients have been

calculated from the mass transfer results presented. These values can then be compared with the results of other investigations and with the results gained from the present work.

The characteristic of Charwat et al (19) noted previously indicates that the work of Venkataraman (3) falls within the 'smooth-film' regime and thus, as found, mass transfer coefficients can be predicted by accurately constructed laminar models. However, the range of experimental conditions used by Watts (6) fall within the 'spiral-waves' zone on the graphs of Bell (7) and Charwat (19). When comparing the results of Watts' investigations with the predictions of Venkataraman's 'approximate' theory (shown to be a reasonably good laminar model), Watts' results fall considerably ($\simeq$ 20%) lower than the predicted values. The author does not discuss this discrepancy in the light of the wave behaviour on the disc, and in fact concludes that the agreement is 'fairly good'. If it is assumed that Watts' experimental and analytical techniques give reliable results then it is possible to draw a number of conclusions from this discrepancy which the author fails to make. The fact that the results fall below predictions of a proven laminar model are significant, as this would imply a difference in the mass transfer characteristics of thin films formed on rotating plates and thin films formed on inclined plates. That is, that instead of enhancing mass transfer, the spiral waves observed, decrease the rates of transfer from that which would be expected for a laminar film under the same conditions. It would seem hard to justify such a conclusion. Alternatively this phenomenom could be an effect of arranging the rotating disc in the vertical plane. Such a suggestion has important conotations in the present work, as a scrubber for a commercially viable nitro-diesel engine would have to be able to operate at any inclination. Again it is hard to justify why a change in inclination of the rotating disc should effect the performance so drastically. It would appear that the effect of gravitational acceleration should be negligible compared with the centrifugal forces generated. To study the effect that disc inclination has on the mass transfer characteristics of a rotary unit, special attention was paid to the design of the experimental rig so, that with only minimal alterations the disc could be aligned either vertically or horizontally. Such design considerations are discussed in more detail in Chapter 7. In mass transfer investigations the most likely area where error can occur is in the analysis of the dissolved gas in solution. At best this can be a difficult operation to perform accurately. Thus when considering methods of measuring dissolved carbon dioxide in water (in Chapter 6) the method used by Watts was studied to determine whether the cause of the foregoing discrepancy was a result of his analysis technique.

Lim (4) studied the absorption of oxygen into water flowing over a smooth rotating disc at 25°C. He purposely chose the operating conditions employed in the research so that waves were formed on the liquid surface. This enabled their effect on mass transfer to be measured. Additionally the experimental rig was constructed so that the variation of mass transfer coefficients with radius could be investigated. Some three hundred readings were taken using liquid flowrates in the range 14.5 to 60.5 cm^3/sec rotational speeds from 24.0 to 117.3 radians/sec and at disc radii

between 6 and 18 cm. So that the effect of the spray section at the edge of the disc could be quantified the equipment was constructed so that liquid samples could be withdrawn from the disc surface as well as from the sump of the retaining vessel. Samples were taken from the surface by the use of a probe which was designed so that it caused the least amount of disturbance to the liquid surface. The design of the probe did however cause problems. As the liquid velocity at the probe inlet was small, it was found in most cases that an insufficient amount of fluid could be delivered to the measuring device at a steady rate. Therefore during all experiments it was necessary to use a syphoning effect to produce the required flowrate. At disc speeds below 42 radians/sec the problem was particularly severe as the flow had to be controlled manually using needle valves. The author sites these difficulties as a possible cause of the scattering shown at low speeds, for the results at the edge of the disc. Such scatter was not found in the readings taken with the liquid after the spray section. A gas sensing electrode was used as an on-line analysis technique to measure the oxygen content of the sampled water. This had the advantages of giving a real time measurement of the mass transfer rate and removed the possible inaccuracies (including sample collection and storage) involved with a titrative method.

The measured data was presented in graphical form with mass transfer coefficients and rates of mass transfer plotted against flowrate at the various rotational speeds used. The experimental data is again compared with the theoretical models devised by Venkataraman. Therefore as these models predict mass transfer rates assuming laminar flow the difference shown by the measured rates will give an indication of the effect of the waves. Over the range of variables studied the mass transfer rates were always substantially higher than those predicted by the 'approximate' model. The increase in some cases was up to three times. This the author concludes, emphasises the influence and importance of the waves. As can be seen such observations disagree drastically with those of Watts. Lim (4) modified Venkataraman's 'approximate' model to take account of the effect of the waves. He modified the model by assuming that mixing and exposure takes place in concentric rings with a width which is equal to the wave-length of the waves on the disc. He showed that this model was capable of describing his results for mass transfer on the smooth disc. He warns, however, that by choosing the correct value of the wave length, results to agree with any set of data could be calculated. As the work carried out on wave length determination was limited he recommends that further investigations are needed before the reliability of this model can be established.

Lim's results also indicated that, at a particular disc speed, there is a tendancy for the effect of waves on mass transfer to decrease with increasing flowrate. This characteristic indicates a problem when relying on the arbitrary nature of surface waves to enhance mass transfer rates. As future commercial applications of rotary mass transfer equipment may require high flowrates the magnitude of mixing caused by surface waves may, under these conditions, make smooth discs economically unviable.

A solution to this problem would be to induce mixing in the film via an external stimuli which is not a function of the operating conditions. Davies and Warner (20) have shown that mass transfer rates can be increased up to three fold by employing roughened surfaces in place of smooth inclined plates. Thus, it has been suggested, that an extension such as this to rotating films might further increase mass transfer rates. This would be more attractive than relying on the intrinsic surface waves.

Since its initial suggestion only a limited amount of research has been undertaken to investigate the use of roughened surfaces to increase the mass transfer characteristics of rotary devices. In order that such processes could be modelled the first work was carried out using a 'grooved' disc. This disc was constructed from a flat aluminium plate upon the surface of which was cut a series of concentric grooves, 10mm broad and 2mm deep. In order to produce a model of mass transfer on this surface it was assumed that the laminar film formed was completely mixed when passing from one groove to the next. Therefore a model based upon Higbie's penetration theory could be devised. The theoretical 'exposure-time' defined by Higbie (22) would in this case be equal to the time taken for liquid to cross a groove. Therefore, while a smooth plate can be considered analagous to a wetted wall column a grooved disc would find its analogy in a sphere column.

Lim (21) employed grooved as well as plane discs, when using the same equipment as in previous investigations, to study the de-oxygenation of sea water. The results of this investigation are presented by Koerfer (5) who used them as a comparison of the results he gained from his own investigations. The aim of this work was to analyse if a further improvement of mass transfer properties could be achieved by using a perforated disc. Employing such a surface would enable the liquid film to be partially exposed to the gas below, as well as above the rotating surface. It was recognised that in order to achieve an enhancement of mass transfer rates due to this increase in gas/liquid interfacial area the film would have to be stablized above the perforations. Additionally liquid leakage through the holes would have to be minimised. The perforated material used is produced by punching a series of 2mm diameter holes on a 3mm triangle pitch in a 1mm thick stainless steel plate. While this left a smooth upper surface, burrs, with an average depth of 0.1mm remained around the perforations on the underside. Preliminary studies carried out to investigate the stability of the film formed on this rotating surface indicated the importance of these burrs. With the smooth side up leakage measurements demonstrated that a stable film could only be maintained at low speeds of rotation. However, when the disc was reversed only minimal leakage occured even at the highest speeds. Leakage measurements were taken for liquid flowrates between 32 and 180 cm^3/sec at speeds in the range 16 to 129 radians/sec. It was observed that the surface of the film formed on the rough side appeared more agitated ('turbulent') than the film formed on the smooth side. A photographic study of the film using a synchronized stroboscope to 'freeze' the disc, reinforced these experimental observations.

Koerfer (5) employed the same experimental conditions, equipment and operating procedures as Lim (21) had used in his desorption experiments with grooved and plane discs. Comparison of the results of each investigation was thus simple. To gain the benefits of the increased 'turbulence' and film stability the perforated disc was used with its 'rough' side up. Liquid flowrates between 300 and 950 cm^3/sec were applied at speeds between 10.5 and 63 radians/sec. Visual inspection of the film under these conditions indicated that the liquid behaved in the same manner as in the leakage experiments. However, due to the increased flowrates and slight irregularities of the disc surface more spray was formed especially at the highest speeds. The results of these experiemnts were again plotted as graphs of mass transfer rates and coefficients against flowrate at each of the speeds used. Additionally the results of Lim's investigations were presented on the same graphs. Thus the enhancement due to the perforated surface was easily measured. The free liquid surface area, that is the area on the surface of the disc plus that due to the perforations, was used to calculate the mass transfer coefficients from the measured rates of desorption. Thus, any improvement shown in the mass transfer characteristics was solely due to the change in the hydrodynamics of the film. At all speeds and flowrates the smooth plate was the least efficient. At all except the highest flowrate and lowest speed, the perforated disc provided the higher transfer coefficients. Koerfer assumed that the high liquid loading here must have caused considerable leakage. The author concludes that the mass transfer coefficients measured at high rotational speeds are remarkable. He recommended that future work should invesigate the radial distribution of mass transfer on this disc. Additionally, he noted that discs with a rougher surface quality and higher fractional free area may produce even greater enhancement than the perforated surface used.

The aim of the present work was to investigate possible methods of further intensifying the mass transfer processes occuring in a rotary device. The choice of gas/liquid systems used in the investigation was determined by the desire to apply the results gained to the design of a scrubber for a closed cycle nitro-diesel engine. Koerfer demonstrated that the promotion of 'turbulence' in the thin film leads to greatly enhanced mass transfer coefficients. Additionally the use of a perforated surface increases the interfacial area per unit volume thus improving the efficiency of a machine of given size. Alternatively, this would facilitate further miniaturisation of process equipment while retaining the same overall rate of mass transfer. This assumes that a stable film can be formed above the perforations. These conclusions have resulted in the postulation of the existance of an ideal hydrodynamic condition for the thin film.

It has been proposed that the mass transfer coefficient of a rotating system would be maximised if a stable film that was turbulent, and yet unsupported by any physical means could be generated. Such a film would promote eddy rather than molecular diffusion and would allow gas/liquid contact over the whole of both interfaces.

Therefore one aim of the present project is to discover if discs constructed from a fine steel mesh produce a film which is closer to this ideal case than that formed on the perforated plate used by Koerfer. Discs constructed of this material would have a high fractional free area (up to 50%) and provide a rough surface for flow. Due to their open structure it was felt that if a stable film could be formed that it would possibly exist on both sides of the disc surface. If this was the case then the interfacial area would attain its maximum possible value and the film would function as if the disc were not present. Therefore the above proposal would be satisfied. As mesh discs had never been used in rotary machines previously a preliminary study was undertaken to discover how a flexible, woven surface behaved when rotated. Observations were taken of the disc surface running dry and again when liquid was introduced at the centre. Due to the semi-transparent nature of the discs, great difficulty was encountered when attempting to view the film formed. Use of the stroboscopic technique outlined by Koerfer (5) helped only at high rotational speeds. These difficulties plus additional problems associated with the flexibility of the surface limited the quantitative analysis of film hydrodynamics to a series of leakage measurements. The results of these experiments together with the qualitative observations taken are presented in Section 4 where the hydrodynamics of thin films are discussed.

Numerous mass transfer processes commonly used in the chemical and gas purification industries make use of solvents that react with the gas to be absorbed. A chemical reaction effects the mass transfer characteristics of a piece of equipment in two ways. Firstly, as the absorbed gas is effectively removed (in irreversible reactions) from the bulk of the solvent, the concentration driving force is not reduced as the process proceeds. Secondly, if a chemical solvent is used that exhibits the same hydrodynamics as the original physical solvent then the rate of mass transfer will be increased by an amount which is dependent on the rate of the reaction. That is, a fast reaction will dramatically increase the rate of mass transfer, while a slow reaction may have negligible effect. The speed of a reaction must be judged relative to the magnitude of the mass transfer coefficient of the physical system. Efficient mass transfer systems are less effectively enhanced by a particular reaction rate than systems characterised by low mass transfer coefficients. With the correct choice of chemical solvent the mass transfer properties of a particular device can be greatly enhanced. This provides an additional method of intensifying the mass transfer process that takes place on a rotating surface. The present investigation examines the effect that a chemical reaction has on the rate of mass transfer by comparing the efficiencies of a physical and chemical solvent with identical hydrodynamic properties. The choice of solvents was determined by the desire to apply the results of the investigation to the solution of the nitro-diesel engine problem. A number of models have been published which can be used to predict the effect that a chemical reaction has on the rate of mass transfer. These were developed assuming flow through packed beds. Methods have been presented that are based on the assumptions of Whitman's, Higbie's and Dankwert's mass transfer models. Therefore the data gained from

the mass transfer experiments of the present investigation has been used to study whether such methods are applicable to rotary devices. Additionally, it was hoped that the discrepancies between predictions based on these models would suggest which best described the mass transfer process on a rotating disc.

3.0 REGENERABLE MASS TRANSFER PROCESSES

3.1 Introduction

In certain mass transfer operations involving a gas/liquid system it is desirable to use a liquid phase with which the solute gas reacts. To be of commercial interest the chemical solvent used must be regenerable. This implies that by changing the conditions from those used during the absorption process (i.e. the temperature, pressure, or a combination of the two) the chemical absorption reaction can be reversed, the dissolved gas removed and the solvent effectively regenerated. Replacement of a physical solvent by an applicable chemical solvent in a particular mass transfer system can have a number of advantages, these include:

- Increased capacity, especially when removing acid gasses having low partial pressures.
- High degree of removal (clean-up) of acid gas
- Absorption mass transfer coefficient increased (provided that the reaction is fast enough to occur near the interface - see section 5.3)
- Desorption mass transfer coefficient increased
- Potential for selectively absorbing one reacting gas over another based on a difference in rates of absorption.

Against these considerable advantages certain disadvantages must be considered, including the cost of chemical bases, high heat of absorption, corrosion of carbon steel, side reactions (base degradation) and possible environmental concerns.

This section considers the chemical solvent used during the present investigation, indicating why it was chosen and how its choice influenced the form of the research.

3.2 Choice of Solvent

Two types of chemical solvent are of particular interest in systems where carbon dioxide is to be absorbed, promoted hot carbonates and solvents containing amines. Which category is most applicable to a particular system depends largely on the inlet acid gas partial pressure and the depth of removal required. Chemical solvents containing amines are generally preferred when the partial pressure of carbon dioxide in the feed gas is relatively low and/or when its concentration must be reduced to a very low level in the treated gas. At high partial pressures and where deep removal is not required, physical solvents usually prove economically more attractive than either type of chemical solvent. Promoted potassium carbonate processes are used at intermediate carbon dioxide partial pressures. Astarita et al (54) provide a useful graph which shows the approximate ranges of application of different types of gas treating processes for carbon dioxide removal where no hydrogen sulphide or other acid gas impurities are present in the gas. This is reproduced as figure 3.1. Using the specifications provided by the Department of Marine Engineering (Appendix C) the required inlet and outlet carbon dioxide partial pressures were calculated and the point representing this condition plotted on figure 3.1. This indicated that an aqueous amine solution was the most suitable in the present investigation.

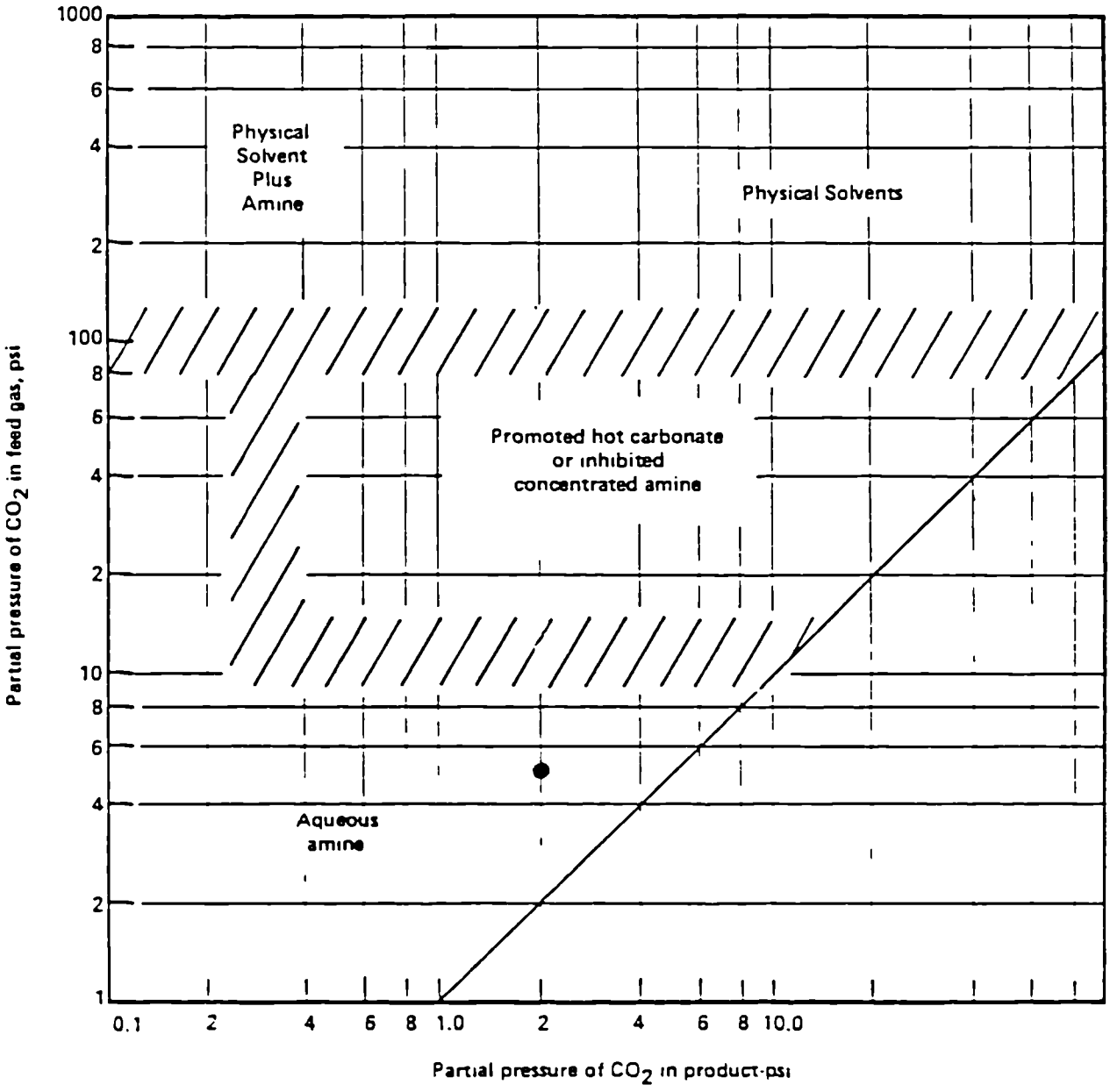

● inlet conditions appropriate to the nitro-diesel engine

figure 3.1 Determination of chemical solvent for a particular operation

A large number of amines are available for use in industrial carbon dioxide absorption processes. The choice of process solution is determined by the pressure and temperature conditions of the gas to be treated, its composition with respect to major and minor constituents, and the purity requirements of the treated gas. Aqueous monoethanolamine (MEA) (is in most situation) the preferred solvent for gas streams containing relatively low, concentrations of carbon dioxide and no minor contaminents such as COS and CS_2. The low molecular weight of MEA resulting in high solution capacity at moderate concentrations, its high alkalinity and the relative ease with which it can be reclaimed from contaminated solutions are advantages which in many industrial cases more than counterbalance inherent disadvantages. These include the fact that MEA solutions are appreciably more corrosive than solutions of other amines, and that the relatively high vapour pressure of MEA causes significant vapourization losses. More importantly, with respect to the present investigation, MEA has been shown by Hofmeyer et al (109) to be subject to oxidative degradation which results in the formation of formic acid, ammonia, substituted amides and high molecular weight polymers. It appears that MEA is considerably more vulnerable to oxidative degradation than the other ethanolamines. This is important when considering its use in the context of a nitro-diesel engine where a significant proportion of the inlet gas (i.e. exhaust from the engine) consists of oxygen.

Secondary amines are much less reactive than primary amines and thus aqueous solutions of diethanolamine (DEA) are less prone to oxidative degradation than those of MEA. In addition the reaction products are less corrosive and thus higher amine concentrations can be used. Therefore although the solution capacity of DEA is less than that of MEA the use of higher concentrations means that if the same liquid throughput is used and the same overall performance is attained. The low vapour pressure of DEA makes it suitable for low pressure operations as vapourization losses are quite negligible. It should be noted that DEA is more prone to thermal degradation than MEA. However, careful design of the regeneration system can minimise the importance of this disadvantage.

Tertiary amines, such as triethanolamine (TEA) are not widely used in the absorption of carbon dioxide. This is largely because of their low capacity (resulting from higher equivalent weight), their low reactivity and relatively poor stability.

Recently, aqueous solutions of Diglycolamine (DGA) have been used in the industrial absorption of acid gases. This solvent is in many respects similar to MEA, except that its low vapour pressure permits its use in relatively high concentrations, typically 40 to 60 weight percent. This results in lower circulation rates and steam consumption when compared to typical MEA solutions. Disadvantages of DGA are its relatively high cost as well as its somewhat higher corrosivity toward carbon steel. Also, chemical losses due to the formation of nonregenerable products from reactions with CO_2, COS and CS_2 appear to be higher than in MEA and DEA systems. Again DGA suffers from an appreciable degree of oxidative degradation resulting in the formation of acids, including formic acid

Diisopropanolamine (DIPA) has found widespread use in the treatment of refinery gases and liquids which besides, H_2S and CO_2, also contain COS in appreciable amounts. Relatively concentrated

aqueous solutions (30 to 40 weight percent) have been used and it is reported that these have a low regeneration steam requirement and are non corrosive (111). Little has been published concerning the properties of DIPA and no information on its susceptability to thermal or oxidative degeneration could be located.

Methyldiethanolamine (MDEA) is used in a number of processes in which selective removal of H_2S from refinery gases containing H_2S and CO_2 is required. This tertiary amine has the same limitations as TEA when used for the absorption of carbon dioxide.

Pilot plant tests have recently demonstrated the performance of a high strength proprietary agent that permits operation in the presence of oxygen and other impurities normally associated with solution degeneration (112,113). Developed by Dow Chemical Company (Midland, Michigan) this proprietary alkanolamine based solvent, called Gas/Spec FS-IL has been formulated with corrosion inhibitors. The solvent has been used to process fluegasses which had an oxygen and carbon dioxide of 4-7 mol% and 8-10 mol% respectively. These tests indicated that the regenerative chemical absorption system could be operated at very high CO_2 loadings without the excessive corrosion that is characteristic of more conventional (MEA, DEA etc) acid-gas processing routes. The reduction in chemical degradation significantly lowers both the capital and operating costs.

The choice of amine for operation in a stripping unit associated with a closed cycle nitro-diesel engine is obviously limited by its ability to cope with the oxygen contained in the exhaust gases. Thermal degradation and corrosion can also limit the use of some solutions, but in general these problems can be solved by good design of absorption and regeneration equipment. Of the solvents available, only the proprietary Gas/Spe FS-IL has a demonstrative resistance to oxidative degeneration. This was therefore the ideal choice of solvent for use in the chemical mass transfer experiments of the present investigation. UNfortunately a necessary volume of this solution could not be obtained so as to allow its performance to be analysed. Diethanolamine was therefore used as an alternative. Although aqueous DEA solutions suffer to a certain degree from oxidative degradation, this is less marked than that of MEA solutions. In addition a number of researchers suggest that this problem can be minimised by the addition of certain soluble inorganic salts to the circulating solution. This is discussed below.

3.3 Properties of Diethanolamine which effect the present Investigation

3.3.1 Physical properties of Diethanolamine

The physical properties of diethanolamine and of various aqueous solutions (i.e. density, viscosity, surface tensions etc) are presented in many texts dealing with the sweetening of flue gases (54,101,103). The properties required in the present investigation are discussed in section 5.4 (where the physio-chemical data for the mass transfer calculations are outlined) and presented graphically in Appendix J.

3.3.2 Oxidation

As noted above diethanolamine is oxidised readily in the presence of oxygen to form corrosive organic acids. This reaction is generally enhanced when free carbon dioxide is present, and at high temperatures.

To prevent oxidation the storage vessels used to hold the amine solution should be gas blanketted to keep air out of the system. Nitrogen is an ideal gas for this purpose. If, as is the case with the flue gases from a diesel engine, the aqueous solution has to come in contact with oxygen, the degree of degradation (and hence the corrosion rate) can be reduced by injecting a suitable oxygen scavenger. Hydrazine, sodium sulphite and many other soluble inorganic salts have proved useful for this purpose(114). However, their use should be carefully controlled because in high concentrations they themselves can cause serious corrosion difficulties.

3.3.3 Thermal Decomposition

Although solutions of diethanolamine are stable at low temperatures, when the pure compound or the aqueous solutions are heated to above 150°C some decomposition is noticed. The decomposition products formed tend to be corrosive. Problems associated with thermal decomposition can thus be minimised by avoiding high surface temperatures. Low pressure steam heating is therefore the ideal choice in these systems.

3.3.4 Chemical Reaction/Degradation

A number of papers have been published in which the chemical degradation of solutions of diethanolamine has been analysed. (115, 116, 117, 118). However in general this work has been rather unsystematic in its approach. That due to Kennard and Melson provides the most informative analysis of this problematic subject, and presents a number of guidelines to minimise this form of degradation.

·As well as causing the thermal degradation of DEA into amine derivatives such as piperazine and diamines, high temperatures can also promote the chemical combination of CO_2 and DEA to form heat stable carbamates. These stable compounds cannot be removed by heat or distillation and cannot be neutralized by the addition of soda ash. In addition high temperatures also promote irreversible reactions with contaminants in the flue gases such as carbonary sulfide, hydrogen cyanide and carbon disulfide. Kennard and Melson thus recommend that the surface temperature of heat exchangers should be minimised and the flowrate of DEA maximised.

·The partial pressure of carbon dioxide effects the degree of diethanolamine degradation. To minimise this, the partial pressure should be kept as low as possible. The authors go as far as recommending than an acid-gas with a high carbon dioxide concentration should be mixed with a sweeter gas before it is treated even though this would increase the size of absorber required.

·To minimise degradation, dilute solutions of DEA should be employed (if possible below concentrations of 20wt%). Higher concentrations increase the rate of degradation (to HEOD (3-(hydroxethyl)-2-oxazolidone) particularly at temperatures in excess of 140°C.

3.3.5 Foaming

Foaming can cause severe problems in absorbers using solutions of diethanolamine, in particular where a high degree of solution degradation has occured or where excessive amount of corrosion inhibitors have been added. Dissolved hydrocarbons, organic acids and finely divided suspended solids also contribute to this problem. If foaming occurs it can cause a considerable reduction in plant throughout, increase DEA losses, prevent adequate regeneration and adversly effect the sweetening efficiency. Foaming also causes poor contact between the gas and the amine solution; therefore, the acid gas removal rate is decreased.

Foaming can be initiated by excessive turbulence and high liquid to vapour contacting velocities. Conditions such as these occur in rotary equipment and thus all available methods of minimising solution degradation were employed during the experimental section of the present investigation.

3.3.6. The reaction of diethanolamine and carbon dioxide

The product of the reaction between carbon dioxide and primary or secondary amines is the amine salt of the carbamic acid (tertiary amines, because of the absence of a hydrogen atom attached to the nitrogen, simply act as bases and form bicarbonates) i.e.,

$$CO_2 + 2R_2NH \rightarrow R_2NCOO^- + R_2NH_2^+ \qquad 3.1$$

Most evidence suggests that this reaction is second order (see section 5.4) i.e.,

$$\text{Rate of reaction (mol/}\ell\text{.sec)} = k_2[Am][CO_2] \qquad 3.2$$

where k_2 is the second order rate constant for the amine (ℓ/mol.sec) and [Am] is the concentration of amine [mol/ℓ]. It is found that the contributions of the reactions with water and with hydroxyl ions to the overall rate of reaction are negligible under conditions used in practice for the absorption of CO_2 in aqueous MEA or DEA solutions.

Equation 3.1 indicates that in the primary reaction, two moles of amine react for every mole of carbon dioxide absorbed. However, a slow secondary reaction takes place owing to the reaction of the small equilibruim concentration of carbon dioxide with hydroxyl ions or water:-

$$RNH_3^+ + RNHCOO^- \rightleftharpoons$$

$$\rightleftharpoons 2RNH_2 = CO_2 \begin{cases} \xrightarrow{H_2O} HCO_3^- + RNH_3^+ + RNH_2 \\ \xrightarrow{OH} HCO_3^- + 2RNH_2 \end{cases} \qquad 3.3$$

4.0. HYDRODYNAMICS OF A THIN FILM FORMED ON A ROTATING DISC

4.1. Review of previous work

4.1.1 Introduction

When studying the mass transfer properties of a system it is important that the hydrodynamic condition of the liquid phase is known. Such knowledge enables the mass transfer performance to be explained with respect to the flow pattern occuring. It is equally useful when preparing theoretical models of the transfer process.

This section contains a brief description of work so far published which is concerned with the study of the hydrodynamics of thin films formed on rotating surfaces. As extensive reviews of this topic have already been published (Bell (7) and Lim (4)), the present work only considers elements which were useful when preparing the mass transfer study, or when analyzing the results gained. The following section gives brief details of the hydrodynamic studies undertaken in the present investigation. These were required because no previous work had been concerned with surfaces constructed from regular stainless steel meshes.

The hydrodynamic work published in the past can be divided into two areas; the development of theoretical flow models and the practical investigation of thin film flow. These are obviously inter-related as the conclusions of the former should be capable of predicting the results of the latter once a successful model has been devised. Theoretical models have in general been restricted to the case of laminar flow on smooth discs although some thought has been given to films where turbulance is present (7,4 and Koerfer (5)). This, like the turbulent mass transfer theories discussed in section 5, is of little use at the moment due to an inability to characterise the properties of turbulent flows (eddy diffusivity in mass transfer and a velocity profile in hydrodynamics). Practical investigations have concentrated on the study of film breakdown, wave formation, film thickness, surface velocity and, in the case of perforated plates, leakage behaviour. This section is therefore divided into two sub-sections. The first is concerned with theoretical developments and outlines in full a simple flow model used during the analysis of the mass transfer results. The second introduces the concepts of wave formation, film breakdown and leakage behaviour thus enabling past work to be related to the results of the hydrodynamic study of mesh discs (section 4.2).

4.1.2. Theoretical hydrodynamic models

4.1.2.1. Introduction

This section presents the so-called 'centrifugal' model which can be used to predict the properties of thin-laminar films formed on smooth discs at low rotational speeds. Although other models, which allow for the effect of Coriolis and inertial forces, have been presented, the 'centrifugal' model has found wide spread use even in cases where the assumptions inherent in its derivation are not obeyed. This is mainly due to its simplicity. This model was used to determine the hydrodynamic properties required for the analysis of the mass transfer results. The more accurate models were useful for estimating the approximate error associated with the use of the centrifugal model.

4.1.2.2. The 'centrifugal' model

In the 'centrifugal' model it is assumed that liquid flows in a purely radial direction i.e. there is no 'slip' on the disc. This motion is caused by the centrifugal force of the spinning system and is balanced by the viscous drag. Furthermore it is assumed that there is a steady flow of liquid on the disc, that the thickness of the film is small compared to the radius and that the influence of gravity, surface tension and friction with the surrounding medium is insignificant. Thus the general form of the Navier-Stokes equation reduces to a simple force balance i.e.

$$\frac{\nu d^2 Vr}{dy^2} = -\omega^2 r \qquad 4.1$$

This expression can be integrated subject to the boundary conditions;

$y = 0 \quad Vr = 0$ at the disc surface

$y = \delta \quad \frac{dVr}{dy} = 0$ at the free surface

to give an expression for the radial velocity of;

$$Vr = \frac{\omega^2 r}{\nu}\left(\delta y - \frac{y^2}{2}\right) \qquad 4.2$$

The average velocity $\bar{V}r$, is therefore given by;

$$\bar{V}r = \frac{1}{\delta}\int_0^{\delta} Vr\,dy = \frac{\omega^2 r \delta^2}{3\nu} \qquad 4.3$$

The film thickness can be given in terms of the system parameters by substituting the radial velocity Vr (from equation 4.2) into equation 4.3 and equating the resulting expression to the flowrate per unit area available, i.e.

$$\bar{V}r = \frac{\omega^2 r \delta^2}{3\nu} = \frac{Q}{2\pi r \delta} \qquad 4.4$$

or upon rearrangement

$$\delta = \left(\frac{3}{2\pi} \cdot \frac{Q\nu}{\omega^2 r^2}\right)^{1/3} \qquad 4.5$$

Reynolds and Taylors numbers for rotational systems have been defined as (3),

$$Re = \frac{Q}{r\nu} \qquad 4.5.1$$

and

$$Ta = \frac{\omega r^2}{\nu} \qquad 4.5.2$$

and thus equation 4.5 can be expressed in terms of these dimensionless parameters as

$$\frac{\delta}{r} = \left(\frac{3}{2\pi}\right)^{1/3} \cdot \left(\frac{Re}{Ta^2}\right)^{1/3} \qquad 4.6$$

Equation 4.6 can therefore be used to calculate the film thickness at any radius from a knowledge of the volumetric flowrate, rotational speed and kinematic viscosity.

The mean residence time of the film on the disc can be obtained by substituting the film thickness (from equation 4.5) into the expression for the average velocity (equation 4.4) to give

$$\bar{V}r = \frac{dr}{dt} = \left(\frac{\omega^2 Q^2}{12\pi^2\nu}\right)^{1/3} r^{-1/3} \qquad 4.7$$

Thus equation 4.7 can be integrated with the boundary conditions

$t = 0$ $\qquad$ $r = ri$
$t = t$ $\qquad$ $r = re$

to give,

$$t = \frac{3}{4}\left(\frac{12\pi^2}{\omega^2 Q^2}\right) \quad (re^{4/3} - ri^{4/3}) \qquad 4.8$$

This expression calculates the mean residence time (t) for liquid to flow between two radial points given by re and ri. Thus the residence time for mass transfer is given when ri = radius of nozzle and re = radius of disc.

4.1.2.3. Other models

The 'centrifugal' model has been modified by a number of workers in an attempt to incorporate the effects of Coriolis, inertial and gravitational forces and hence improve the accuracy of the predicted values. This has resulted in the proposition of two further models; the so called 'Coriolis' model and the more complicated 'general' model. The former of these considers the fact that due to a Coriolis force (which acts in a circumferential direction opposite to the direction of rotation)

the liquid film moves with a lower speed than the disc itself. The 'general' model also takes inertial and gravitational forces into account. As these models have not been used to analyze the mass transfer results of the present investigation details of their development have been omitted. Lim (4) and Bell (7) cover each of these models adequately.

Emslie et al (25) showed that the Coriolis model is equal to the centrifugal model if

$$\omega^2 r >> 2\omega V_r \qquad 4.9$$

if the results for V_r and δ from the centrifugal models are used, a criterion for neglecting the Coriolis acceleration is produced. This expression can be written as

$$\frac{Q^2}{\nu\omega r^4} << 1 \qquad 4.10$$

Using the definitions of the Reynolds and Taylors numbers (equations 4.5.1 and 4.5.2), $Q^2/\nu\omega r^4$ can be rewritten as Re^2/Ta. Hence the limitations of the centrifugal model are controlled by the magnitude of the group Re^2/Ta. The magnitude of this group, and hence the accuracy of the centrifugal model, is considered in section 8.

For rough surfaces, and particularly for the case of a perforated surface, the assumptions upon which the 'centrifugal','Coriolis' and 'general' models are based are unlikely to hold. In these cases it is more accurate to describe the flow conditions with models based upon turbulent flow. Such models have been discussed by Lim (4) and Koerfer (5). To solve the general equations in this case assumptions must be made concerning the velocity distribution and the shear stress. A number of such assumptions have been attempted (4,5), and that of Clare & Jeffs (26) provides the most convenient solution. They showed that if the inertial forces are ignored (justified later by Jones (27)) an expression for the film thickness similar to that for the centrifugal model can be obtained, i.e.

$$\frac{\delta}{r} = \left(\frac{f}{16\pi^3}\right)^{1/3} \cdot \left(\frac{Q^2}{\omega^2 r^6}\right)^{1/3} \qquad 4.11$$

where f is a friction factor equivalent to that of the Fanning friction factor for full tube flow. The friction factor can be determined from (28)

$$f = \frac{\tau\omega}{1/2\rho\bar{V}r^2} \qquad 4.12$$

4.1.3. Experimental hydrodynamic investigations

4.1.3.1. Introduction

This section considers briefly previous work published concerning the experimental investigation of the hydrodynamics of thin films. A detailed study of this topic has previously been presented (4) and therefore this section considers only those areas which were of use during the present hydrodynamic or mass transfer studies.

4.1.3.2. Film thickness measurements

Numerous authors have investigated the thickness of the thin film formed on a smooth rotating disc. The techniques used during these investigations and the ranges of flowrate and rotational speed employed are summarized by Bell (7). Lim (4) compares the results of these investigations with the predictions of the 'Coriolis' and 'centrifugal' models. This comparison indicates that up to values of Re^2/Ta of 1.0(approximately) equation 4.6 can be used with confidence. Above this figure the model based upon the 'Coriolis' force can be used successfully.

Koerfer (5) considered the case of a rough, perforated disc. Due to the leakage, spray and 'flutter' characteristic of this type of surface only one measurement technique was applicable. This method was based upon a high speed photographic technique devised by Watts (6) and involved measuring the radial velocity. From this the film thickness could be determined via continuity considerations. Equipment limitations necessitated the replacement of high speed photography with that available from a normal camera. Thus observations of continuous flowpaths on single photos had to be used to measure the radial velocity. Injections of thick indian ink and immiscible dyes were tested, but in each case the high degree of turbulence dispersed the fluid after only a few centimetres. Eventually the spiral waves formed on the surface of the discs at most speeds were used as an indication of the radial velocity (these waves are described below). To use these waves it had to be assumed that the radial velocity of the waves was equal to the radial surface velocity of the film itself. The results for both perforated and plane discs were plotted as graphs of the dimensionless film thickness δ/r against the ratio Re/Ta^2. Using a least squares fitting method these were correlated to functions of the type

$$\frac{\delta}{r} = A \left(\frac{Re}{Ta^2}\right)^B \qquad 4.13$$

so they could be compared with the 'centrifugal' model (equation 4.6). The results for both discs showed a marked degree of scatter (up to 50% for single values) being mainly due to difficulty in visualizing wave fronts (especially for the perforated disc). The correlation for the plane disc was calculated as;

$$\frac{\delta}{r} = 3.16 \left(\frac{Re}{Ta^2}\right)^{0.39} \qquad 4.14$$

which agrees quite well with the 'centrifugal' model. For the perforated disc the results were correlated as

$$\frac{\delta}{r} = 20.8 \left(\frac{Re}{Ta^2}\right)^{0.50} \qquad 4.15$$

This predicts film thickness's lower than the centrifugal model for values of Re/Ta^2 below 4.1×10^9 and greater for ratios above this figure. This result disagrees with any of the turbulent models presented as these predict greater film thickness's for all flowrate/rotational speed combinations.

It was hoped that the method used by Koerfer could be employed in the present investigation to study the film thickness on mesh discs. However preliminary observations (see 4.2.1.3.2) indicated that the visulisation of spiral waves was even more difficult on these surfaces than it had been on the perforated surface. Therefore the 'centrifugal' model (equation 4.6) was used to predict the film thickness in the analysis of the mass transfer results. The perforated plate was analyzed in terms of the 'centrifugal' model and the correlation presented as equation 4.15.

4.1.3.3. Flow regimes

A number of investigations have been published in which the various flow regimes associated with thin films formed on rotating discs are categorized. These studies have so far been limited to smooth discs. Charwat et al (19) produced a plot of flowrate against rotational speed for the ranges 0-7 cm^3/sec and 6 to 75 radians/sec respectively. On this they indicated the boundaries between the flow regimes observed. Three easily distinguishable regimes were represented. At low speeds and flowrates the film surface was smooth. Increasing the flowrate at a fixed speed led to the formation of 'concentric' waves. These waves moved outward and decayed while the outer part of the film remained smooth. If the speed rather than the flowrate was increased then a pattern of 'spiral' waves developed. These waves appeared to be fixed to the disc and unwound in the direction of rotation. They tended to decay at large radii but, in most cases, they first broke up into a very rough and non-uniform patterm of disconnected wedge-like wavelets. Charwats' flow regime diagram is reproduced in figure 4.1a. In the region above the point of intersection of the boundaries of smooth/concentric and smooth/spiral regimes both types of waves were present, so that their nature was no longer clear. Bell (7) extended such observations for flowrates up to 300 cm^3/sec. The results of this investigation are illustrated in figure 4.1b. This diagram indicates the existance of three zones which are not present on figure 4.1a. At low flowrates the film is broken and liquid flows in the form of rivulets. The diagram does not make it clear how the breakdown varies with radius but it must be assumed that at least part of the disc is wetted at all flowrates for the graph of Charwat to make sense. Increasing the flowrate to beyond 100 cm^3/sec at speeds below approximately 20 radians/sec causes jetting from the inlet. This is caused by the setting of the nozzle being much too small. This therefore gives velocities in excess of the 'natural' value at the exit from the nozzle. At high speeds and high flowrates the film surface

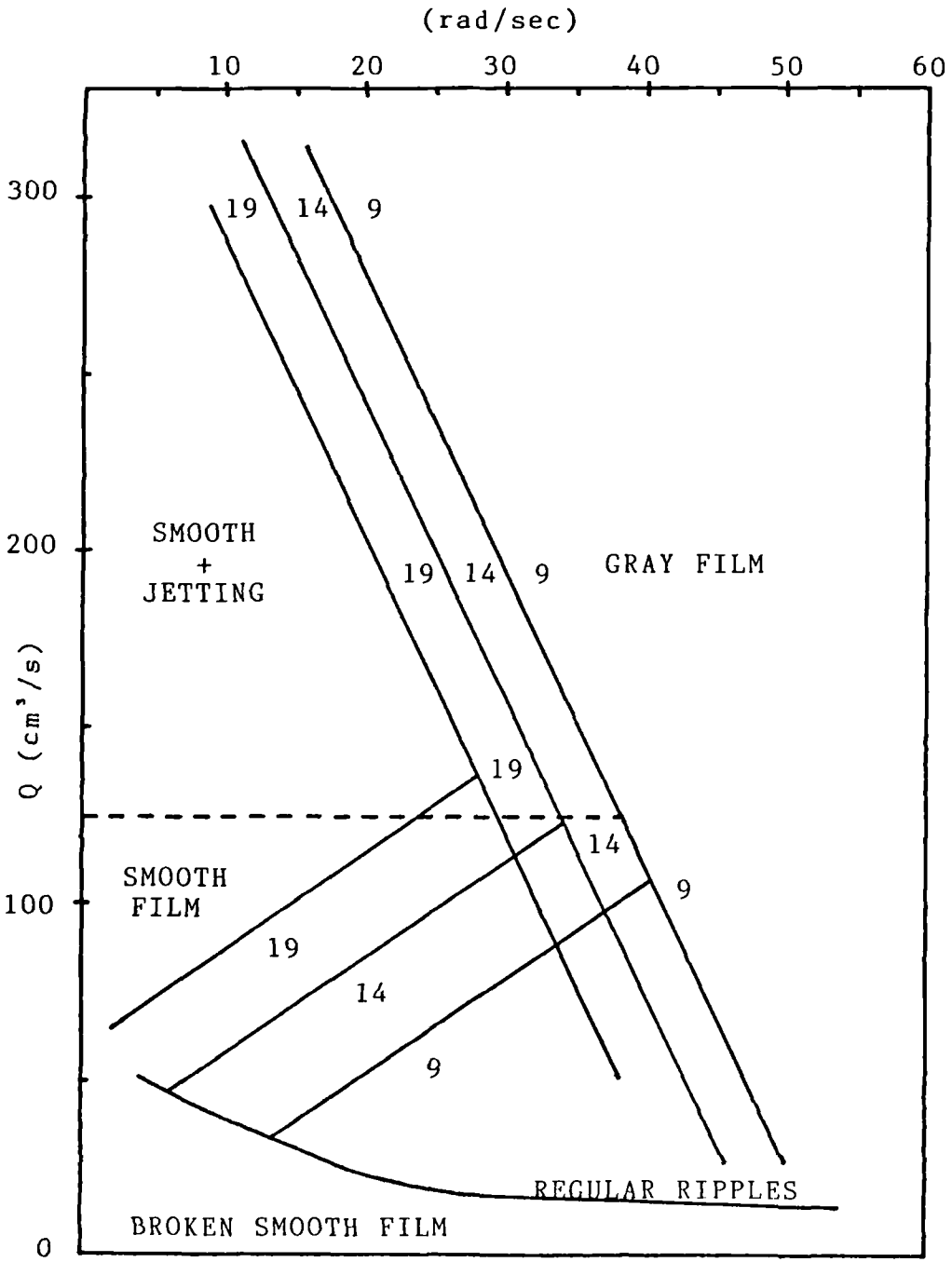

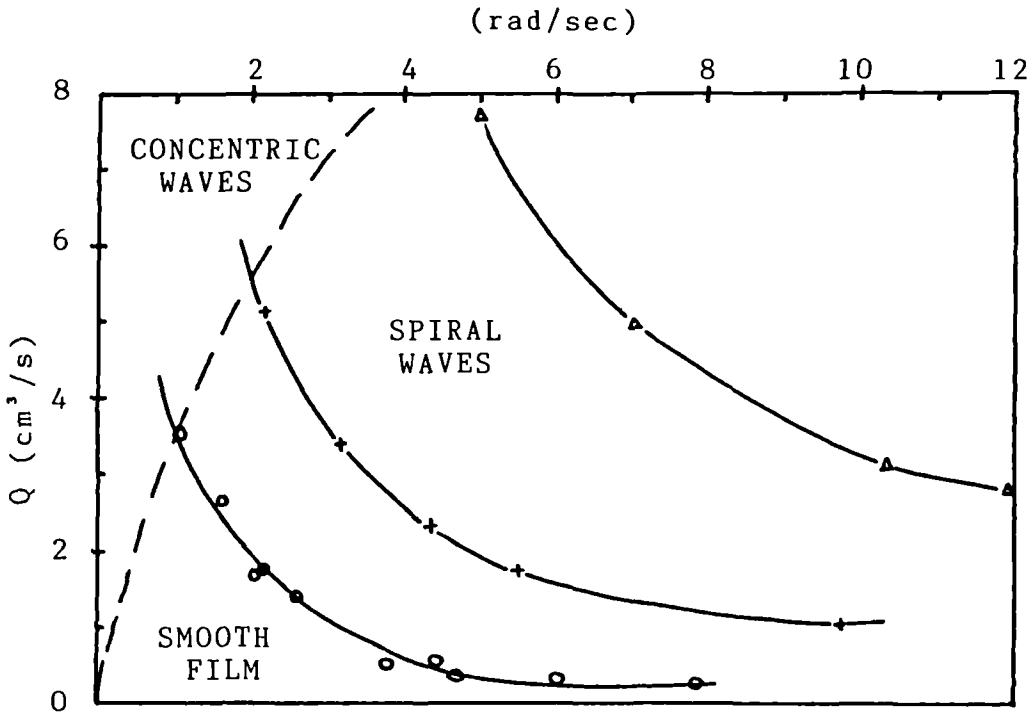

figure 4.1 (a) flow regimes from (19)
0 spiral waves, methyl alcohol
+ spiral waves, ISO-PROPYL alcohol
Δ spiral waves, water with wetting agent
apparent $\sigma^* = 0.96$

figure 4.1 (b) flow regimes from (7)

appears very agitated and reflections from the polished disc surface are not visible. Bell (7) refers to this as a 'gray' film. He theorizes that this phenomenom is a result of centrifugal action causing the crests of ripples or jets to break off and impact upon following fluid.

Bell found the flow regime diagram useful when discussing the results of his heat transfer experiments. A similar diagram was therefore prepared for the coarse mesh disc used in the present investigation. (see section 4.2.1.3.2). The medium and fine meshes could not be analized in this fashion because of the difficulty encountered in observing the film surface.

4.1.3.4. Film breakdown

A number of investigators have studied the breakdown of the thin film formed on a smooth rotating surface. Butuzov and Rifert (29) observed an incomplete film at a flowrate of less than $4cm^3/sec$ in the speed range $95 < \omega < 290rpm$. Clare & Jeffs (26) noted such a breakdown for flowrates of less than $10cm^3/sec$ at a speed of 3000 rpm at low radii. Charwat et al (19) described the process of film breakup in great detail. They noted that as the film began to thin (due to a decrease in liquid flowrate at a constant speed) 'incipient' dry spots were formed. These appeared to be disturbances on the film surface caused by dust particles which had settled on the disc. The film then broke up, usually, but not necessarily immediately downstream of these protruberances. When the film was relatively thick the dry spots were fairly irregular and had a blunt leading edge. When the film was thin and the rotational speed high, they exhibited sharp leading edges and a very regular triangle shape (c.f. 'dry patches' on mesh discs-section 4.2.1.3.2). The authors suggested that two distinct mechanisms were responsible for film breakdown. When the film becomes sufficiently thin (20μm) the breakdown is caused by particles entrained by the liquid which stick to the disc. When the film was thicker breakdown occured'naturally', that is without physical disturbance, as a function of the flow parameters, specifically the Weber number (We), where

$$We = \frac{\sigma / \rho}{\delta \bar{V}r^2} = 9 \left(\frac{2\pi}{3}\right)^{5/3} \left(\frac{\sigma^3 \nu r^4}{\rho^3 Q^5 \omega^2}\right)^{1/3} \qquad 4.16$$

Hartley and Murgatroyd (30) examined the problem of film breakdown and assumed that a critical minimal film thickness is given when the rate of surface energy plus the rate of kinetic energy was a minimum. The two energies are given by

$$\int_0^{\delta} \frac{\rho}{2} . Vr . Vr^2 dy + \sigma Vrs \qquad 4.17$$

Using the centrifugal model velocity profiles, equation 4.17 becomes

$$\frac{1}{35} \frac{\rho \omega^6 r^3 \delta^7}{\nu^3} + \frac{1}{2} \frac{\sigma \omega^2 r \delta^2}{\nu} \qquad 4.18$$

This can then be differentiated with respect to δ and equated to zero to give the minimum condition. On rearranging an expression for the critical flowrate is achieved. i.e.

$$Qc = 5.5 \left(\frac{\nu r^4}{\omega^2}\right)^{1/5} \left(\frac{\sigma}{\rho}\right)^{3/5} \qquad 4.19$$

Bell (7) qualitatively confirmed this result, but found experimental values for Qc some 30% lower than predicted ones.

Koerfer (5) studied the stability of thin films formed on the perforated material described previously (section 2). He noted that at high rotational speeds no film could be observed above the perforations at the edge of the disc. This implied that the liquid flow by-passed the perforations. Insufficient observations were recorded to enable a correlation of this breakdown to be prepared. Barberis (31) recorded photographically the film condition at a radius of approximately 10 cm on a perforated disc constructed from the same material. In this investigation he used flowrates between 40 and 100 cm^3/sec and rotational speeds between 200 and 500 rpm. He noticed that a continuous film was not formed at the lower flowrates at 200 rpm. Increasing the flowrate established a continuous film. At intermediate rotational speeds ($\simeq$ 350 rpm) the perforations appeared to be covered by a liquid film at all flowrates. At 500 rpm this film again disappeared at the lower flowrates. Increasing the flowrate re-established the film.

The breakdown of the thin film formed on a rotating disc is very important as it drastically effects the performance characteristics of a transfer device by reducing the available interfacial area. Therefore a detailed knowledge of the flowrate/speed ranges over which this effect occurs is important when choosing the operational specification of a particular machine. This is discussed with reference to the results of the present investigation in section 8. The breakdown/wetting characteristics of the mesh discs are investigated in section 4.2.1.3.2.

4.1.3.5. Film stability (leakage)

Koerfer (5) outlined the importance of providing a stable film when a perforated surface forms the rotating disc in a transfer device. He investigated film stability by measuring the percentage of the liquid flowrate which leaked through the disc between the inlet nozzle and outer edge. These experiments demonstrated the importance of the 'burrs' surrounding the punched perforations on the so-called 'rough' side. Details of Koerfers experimental technique is presented in section 4.2.2 which is concerned with the leakage characteristics of the mesh surfaces. In addition this section compares the results of his investigation with those determined for the mesh discs.

4.2. Study of films flowing on rotating mesh discs

4.2.1. Preliminary experiments and observations

4.2.1.1. Introduction and description of equipment

Discs fabricated from fine meshes had never been employed as the mass transfer surface in a rotary absorber. Thus it was decided that a series of preliminary experiments should be devised to discover how such discs behaved when running wet and dry over a wide range of liquid flowrates and speeds of rotation. These tests were designed so that the results of the experiments could be used to compare mesh discs with plane, grooved and perforated surfaces operating under the same conditions. Data for these discs had been published by Koerfer (5) and Lim (4).

The equipment used during these preliminary tests was basically the same as that used by the above authors, the main difference being the container within which the discs revolved. This had been changed from a square-brass tank to a cylindrical stainless steel vessel, and thus had to be modified to allow samples to be collected at the periphery of the rotating discs. Such samples were required to enable a series of leakage experiments to be undertaken (see 4.2.2 below).

The flow circuit for the experimental rig is illustrated in figure 4.2. The disc to be studied ran horizontally in a stainless steel cylindrical vessel, lined with a spongy absorbent material so as to minimise backsplashing of liquid from the container walls. It was fixed onto the top of a vertical drive shaft by means of a screw which formed part of the liquid distributor. The distributor was constructed from brass and consisted of two sections. The inner part was cylindrical, threaded at the top to accept a rotary union (into which the feed liquid passed) and at the bottom to fix it, and the relevant disc to the drive shaft. Eight equispaced 4mm diameter holes 11mm from the base enabled liquid passing through the rotary union to be delivered to the disc surface. The height of liquid forming on the disc was controlled by the outer section of the distributor. This fitted flush to the top of the inner section, but formed a 3mm annulus with it at its base. This could be raised and lowered forming different nozzle gaps and fixed in position by two brass grub screws. The vertical shaft extended through the bottom of the container and was driven horizontally (via a 2:1 gear arrangement) by a 220V DC motor equipped with a variable speed controller. A tachogenerator and triggering unit were fixed to the drive. The output signal of the tachogenerator was measured by a digital voltmeter and converted to the appropriate speed by means of a calibration curve. The triggering unit synchronised a stroboscope to allow observations of the disc with frozen images. The whole device was mounted on a rack of some 50cm height.

Liquid was delivered to the disc surface by a Stuart Turner pump capable of delivering a head of up to 20 feet. The liquid flowrate was controlled by a fine needle valve placed after the pump and measured by a calibrated rotameter (metric 18XP). Liquid leaving the edge of the rotating disc collected in

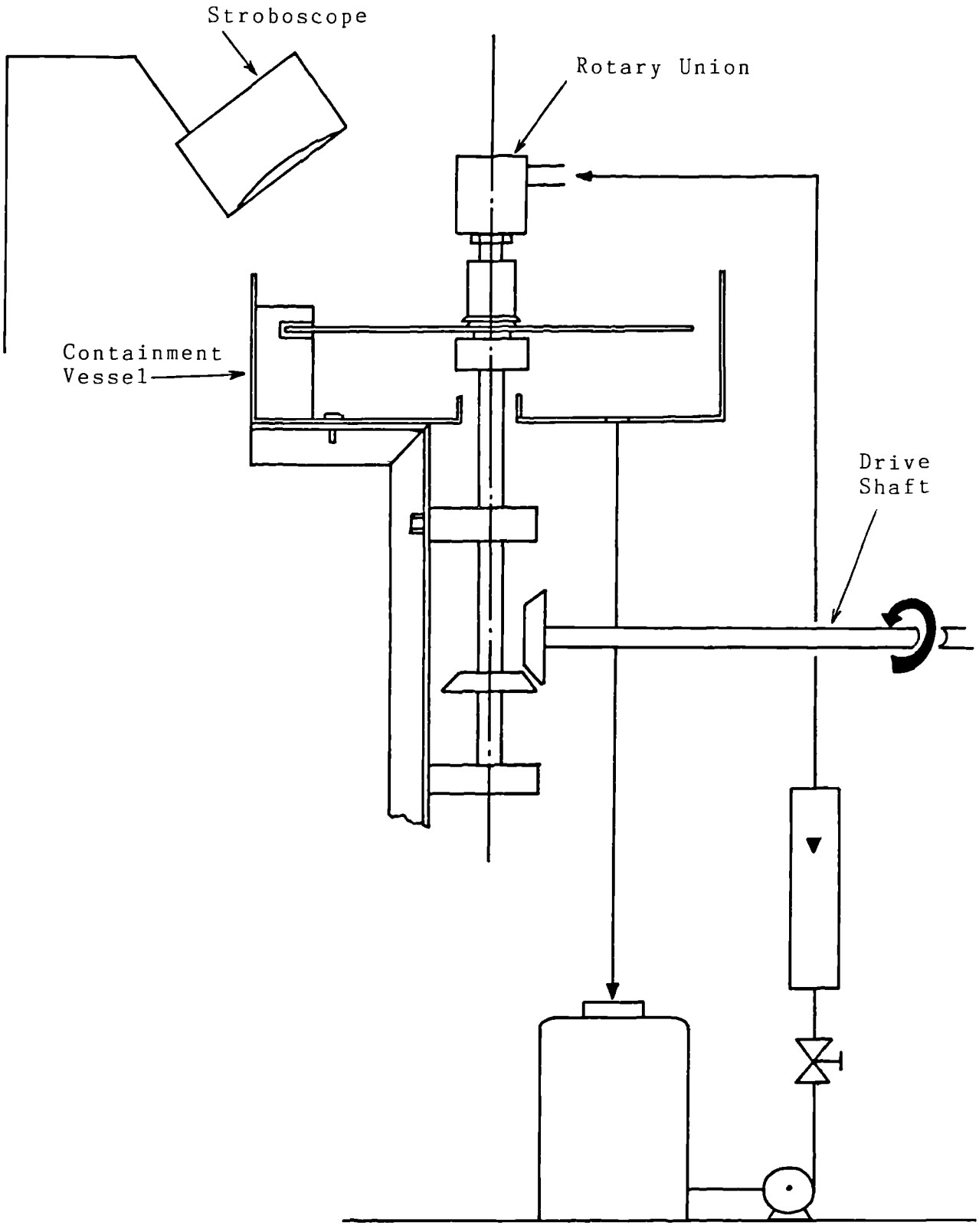

figure 4.2 Test rig for hydrodynamic investigations

the sump of the retaining vessel. From here it returned, under the action of gravity, to the liquid resevoir (which held approximately 40 litres).

4.2.1.2. Description of the disc construction

Three different grades of stainless steel mesh were employed to construct the discs. These meshes were woven from three sizes of wire and the weave produced a surface that was not only rough but which had a large fractional free area. The fractional free area (E) of a disc is defined as that fraction of the surface that consists of void space. Thus;

$$E = \frac{\text{area of holes}}{\text{total active area of disc}}$$

The coarsest mesh (i.e. that which was fabricated from the coarsest wire, woven on the largest pitch to produce holes of the greatest size) consisted of wires of 0.38mm diameter woven on a pitch of 1.25mm. This produced a surface with a fractional free area of 0.49. The second coarsest mesh, the so called medium grade, was constructed from 0.27mm wire on a 0.9mm pitch to give a value of E equal to 0.48. Finally, the finest mesh had wires of 0.23mm diameter woven on a 0.62mm pitch. This gave a value of E of 0.40.

Therefore each mesh provided a surface with a higher fractional free area than the perforated material first studied by Koerfer (5). The fact that the coarse and medium meshes had approximately the same fractional free area meant that the influence of wire size on disc performance could be determined seperately.

In order to make the flimsy meshes more rigid and to minimise the 'fraying' of the weave at any cut edges the discs had to be reinforced. This was achieved by forcing 'Davids' Isopon' into the holes in a band around the circumference and centre of the discs. This rigid but rough support was then filed down to give a smooth surface flush to the top of the wires. The reinforced areas were then painted with two coats of a rubberised paint to give a smooth water resistant finish. Samples of reinforced mesh were covered with a 2M aqueous diethanolamine solution to determine whether the chemical solvent caused the reinforcement to break down. Such tests showed that no such degeneration would occur. The central reinforcement covered an area approximately 50mm in diameter. A 25mm hole was punched in the centre of this to enable it to be fixed to the drive shaft. The outer diameter of each disc measured 305mm and the reinforcement was 7.5mm wide. This produced an active perforated diameter of 290mm. The discs constructed for use in the mass transfer experiments were slightly smaller than those used in the preliminary experiments. These differences are discussed in section 7.2.2. The reinforcement technique however, was identical.

4.2.1.3. Experimental work

No work had been published concerning the operation of flexible rotating discs and so to begin with the discs were observed running first dry and then wet over a wide range of rotational speeds. The qualitative results of these observations are presented below.

4.2.1.3.1. Discs running dry

The first experiments undertaken studied the discs running dry. The aim of these was to observe how a flexible surface behaved when it was rotated. While the discs were at rest they sagged around their circumference. At low speeds of rotation this effect could still be observed and in addition any imperfection in the disc surface was clearly visible. As the speed was slowly increased the edge of the disc began to rise due to the effect of centrifugal forces. This effect eventually produced a virtually level surface. However, at all speeds, the small imperfections present on the discs caused a degree of vertical movement. It was thought that this would possibly lead to liquid being thrown from the disc surface. When the speed of rotation was increased beyond the normal operational range (>1500 RPM) a regular, apparently sinusoidal oscilation developed on top of these random movements. This oscillation increased in magnitude with further increases in speed. Beyond a critical value the oscilations became unstable. To restore stability the speed had to be cut dramatically.

The following table presents the speeds at which each disc became level and where the sinusoidal oscillation first appeared. All speeds are in revolutions per minute.

Table 4.1 Speed boundaries for mesh plates

coarse-mesh	medium-mesh	fine-mesh	
1420	800	1020	flatness obtained
1830	1500	1520	oscilation begins

4.2.1.3.2. Discs running wet

It was hoped that observations of the discs running wet would be useful in analysing their mass transfer performance. The proposed operational ranges of liquid flowrate and speed of rotation were 40 to 100 cm^3/sec and 500 to 1500 RPM respectively. Thus, to begin with, an intermediate flowrate of 60 cm^3/sec was chosen and the speed of rotation varied from zero to 2000 RPM. The coarse mesh was used during these observations.

With the disc at rest liquid entering the system quickly drained through the first few rows of holes adjacent to the distributor. As the speed was slowly increased a film of liquid gradually began to spread across the surface of the disc. It was difficult to observe with the naked eye exactly what proportion of the disc was wet at a particular speed. Due to the high fractional free area of the surface and the transparency of the fluid used (water) the surface appeared remarkably similar to when it was at rest. The spread of the liquid was observed by stopping the disc suddenly after it had been running at the speed of interest.

Due to the high surface tension of water, liquid remained in the holes over which the film had been present. This area gradually increased with speed until the whole of the surface was wetted. The mesh was wet preferentially in the direction which was termed 'with' the weave. (As the meshes were woven of perpendicular strands the resultant disc did not present a uniform surface in all radial directions. 'With' the weave was therefore the direction where flow was along the channels formed between consecutive wires. Similarily 'against' the weave was 45° removed from this position when flow was over the wires forming such channels). Once the surface had been completely wetted a further increase in the speed of rotation produced feint, spiral waves close to the centre of the disc. These waves were similar in appearance to those observed on plane discs by Charwat and Kelley (19) and Bell (7).

If the speed was reduced once the disc had been completely wetted the sequence described above was not reversed. As the disc slowed the liquid film became more visible and the waves present across the whole radius of the disc. These waves remained until very low speeds. Once they had vanished the film appeared smooth. However at even lower speeds ripples flowing in an opposite direction to the spiral waves were formed on the surface. Additionally liquid was seen dripping from the disc below these ripples. The film could be maintained even when the surface was brought to rest.

On re-increasing the rotational speed the above sequence of events was reversed. That is, leaking ripples gave way to a smooth surface which was in turn replaced by the pattern of spiral waves. These waves were visible up to speeds of approximately 1000 RPM. Beyond this they became too feint to observe. Once the waves had vanished the surface resembled the 'gray' regime described by Bell (7) for plane discs. When the synchronized stroboscope was used to freeze the image the film surface showed a great deal of turbulence (similar to that photographed on perforated discs by Koerfer (5)).

In order that a flow-regime diagram for a coarse-mesh disc could be prepared similar observations using flowrates between 20 and 100 cm^3/sec were recorded. Such observations indicated the parameter ranges over which the thin film was smooth or 'gray' and where leaking ripples or spiral waves were present. The transitional speeds between these regimes at each flowrate used are presented in Appendix G. This data was used to prepare the flow regime diagram presented in figure 4.3.

During these experiments the stroboscope was often used to 'freeze' the disc surface allowing the thin film to be observed easily. Whilst using this technique it was observed that the surface around the edge of the disc appeared darker than that in the centre. Additionally no turbulence could be seen in these areas. When the disc was brought suddenly to rest, from the speed of interest, these areas were dry, i.e. no liquid was present in the mesh holes. If such dry spots were formed, during the operation of a mass transfer device fitted with mesh discs, the efficiency of the machine would be dramatically reduced (due to the decrease in interfacial area). Thus knowledge pertaining to the formation of

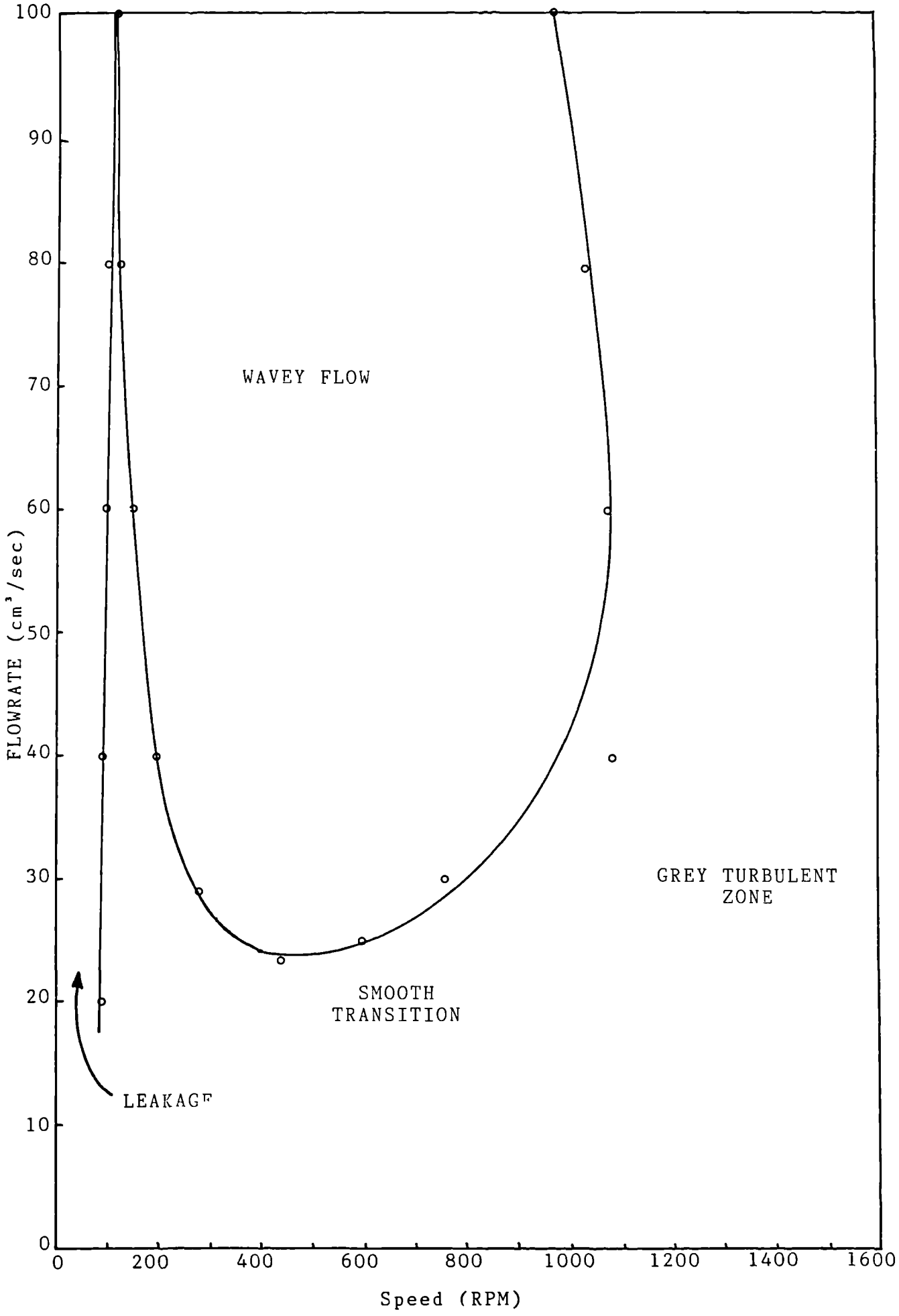

figure 4.3 flow regimes for a coarse mesh

such dry areas was needed in the analysis of the mass transfer data collected from the rotary test rig. Therefore a series of observations was undertaken to determine how the development of these dry spots was influenced by the speed of rotation and the liquid flowrate. These observations were difficult to achieve due to the problems associated with visualising the rotating film (as outlined above). The stroboscope helped at high rotational speeds but even under these circumstances it was impossible to determine an accurate value of the fraction of surface area which was dry. In an attempt to improve the ease with which these observations could be taken, dye was added to the water. It was hoped that the coloured (wet) areas would then be clearly visible against the dry areas. In reality the dye tended to colour everything, effectively masking the regions of interest. More success was achieved when the inside of the retaining vessel was covered with a layer of matt black paint. This reduced the intensity of light reflected from the vessel and thus increased the contrast between the light and dark (wet and dry) areas. Up to 400 RPM observations using the naked eye were the most successful. Above 1000 RPM the stroboscope method produced the most reliable observations. At intermediate speeds the discs rotated too slowly for the stroboscope to produce steady (unflickering) images and too quickly to allow observations with the naked eye. In this range the dry areas were analysed by stopping the disc and noting at which speeds dry patches were formed. Using this method a certain fraction of the actual dry area was rewetted as the disc slowed down. However tests at speeds where the stroboscope method could be used indicated that this inaccuracy was negligable.

Using a flowrate of 60 cm^3/sec on the coarse mesh dry patches began to form between 650 and 750 RPM. These took the form of four equispaced triangles, 20mm high and 10mm broad, in the positions where flow was 'with' the weave. An increase in speed caused these dry patches to enlarge, although this enlargement was largely restricted to the circumferential direction. By 1000 RPM the four triangles were approximately 35mm tall and 90mm broad. Above this speed similar areas began to develop in the four directions where flow was 'against' the weave. As these grew the original dry patches decreased slightly. As the areas formed 'against' the weave were of similar size to those 'with' the weave the overall dry area increased. A further increase in speed caused the original areas to re-increase so that by 1500 RPM the height of these triangles was approximately 80mm while the breadth remained approximately 90mm. The dry patches at these high speeds were different than those originally formed as they were constantly crossed by thin rivulets. These rivulets crossed at random points and lasted for random durations.

Observations such as these were repeated at other flowrates between 40 and 100 cm^3/sec to determine the influence of liquid flowrate on the wetting characteristics of the coarse mesh. A similar sequence to that described above was noticed at each flowrate. However the speed at which each regime started increased with increasing flowrate. Thus at 100 cm^3/sec dry areas began to develop only when the speed reached approximately 1000 RPM, whilst at 40 cm^3/sec dry patches were already present at 500 RPM. It was not possible to repeat these observations as thoroughly for the

fine and medium meshes due to the inability in observing the disc surfaces. Limited observations indicated that these meshes behaved similarily and that the film breakdown was most pronounced for the fine mesh.

4.2.2. Leakage measurements

4.2.2.1. Introduction

The formation of a stable film on a perforated surface is dependent on the condition that there is no leakage of liquid through the perforations. Koerfer (5) carried out a series of experiments investigating the leakage behaviour of a number of perforated surfaces. He recommended that similar tests should be applied to discs fabricated from fine meshes in order to determine the suitability of such surfaces. This section describes how such experiments were undertaken and considers the significance of the results. These tests employed the equipment described in section 4.2.1.1, modified as shown below. The three mesh discs used in the preliminary measurements (section 4.2.1.2) formed the perforated surfaces. The range of experimental parameters was chosen so that the results could be compared with those of the perforated plate used in Koerfer's (5) mass transfer work.

4.2.2.2. Experimental procedure

In order that the liquid leakage could be measured the equipment described (and used) previously had to be modified. A simple, box-like structure was welded onto the inside wall of the cylindrical retaining vessel. This was designed so that the edge of the spinning disc passed through a slot cut across its inner face. The slot had to be wide enough to allow for the sagging of the disc encountered at low speeds of revolution. Therefore water leaving the edge of the disc at the section covered by the box was collected and measured by draining it through a pipe into a 1000 cm^3 graduated cylinder.

Liquid leakage was measured using the technique described by Koerfer. This involved an initial calibration of the collector using a plane disc as the rotating surface. For a plane surface the amount of liquid leaving the edge of the disc is equal to the volume pumped to the centre, i.e., no leakage occurs. Therefore if the rate of liquid collection is measured for known inlet flowrates the 'angle' over which the collector operates can be determined as;

$$\text{'angle' of collection} = \frac{\text{flowrate from collector}}{\text{inlet flowrate to the disc}} \times 360°$$

Therefore such a calibration was determined over the range of flowrates and rotational speeds of interest.

To calculate the flowrate at the edge of the mesh discs and hence the leakage between the centre and periphery, similar measurements were taken for each disc. Therefore the 'edge' flowrate could be calculated from

$$\text{'edge' flowrate} = \frac{360}{\text{'angle'}} \times \text{flowrate from collector}$$

The value of 'angle' used is that corresponding to the same combination of flowrate and rotational speed. The difference between the inlet and edge flowrates is therefore the amount of liquid leaking through the disc.

The results of these experiments showed a large amount of scatter and it was decided that the cause of this was the calibration method used. (This is discussed below). Therefore the collector was re-calibrated using what was thought to be a more accurate technique. This involved calibrating each disc individually using a modified version of the method described above. In this, the plane disc employed during the calibration was replaced by the mesh disc of interest. This was covered by a sheet of thin, sticky backed plastic on its lower surface. The film prevented leakage but maintained all other properties of the disc. Using the data collected previously the leakage properties of each mesh was determined from the results of its individual calibration. These leakage results are presented in Appendix G, along with those calculated from the original calibration. Figures 4.4 to 4.6 present these results graphically.

4.2.2.3. Discussion of results

As noted above, when the results using the initial calibration method were plotted they showed an unacceptable degree of scatter especially at the higher flowrates. Tests showed that on average the measurements of collected volume were reproducable to within 2%. In addition it seemed unlikely that the scatter could be attributed to inaccurate readings of the inlet rotameter or graduated cylinder. From observations noted during the experiments a more likely cause of error seemed to be the nature of the discs themselves. The flexible nature of the mesh resulted in a degree of peripheral sag even though the disc edges had been reinforced. Such sagging was in evidence at the lower speeds. At high speeds the centrifugal forces produced an approximately horizontal surface, but imperfections in the disc caused a degree of vertical movement. The result of these effects was to alter the disc/collector profile from that characteristic of the rigid disc used in the calibration. Such an alteration could have caused the 'splashing' encountered in the collector to have been increased or decreased thus effecting the calibrated value of the 'angle' of collection. In addition the 'rough' surface of the mesh disc produced far more spray than that which had been associated with the plane disc. The result of this would have been an increase in the apparent leakage from the surface under investigation.

The method used to recalibrate the collector reduced the errors associated with these effects by using the actual mesh discs covered with a film of sticky backed plastic. Being positioned on the underside of the disc this stopped liquid leakage but still allowed the same volume of spray to be produced. As the film was thin, flexible and light no significant change in the physical properties of the surface was observed.

The results of the leakage experiments using the improved calibration technique are presented in figures 4.4 to 4.6. These plots show the edge flowrate as a function of speed for particular values of the inlet flowrate. Figure 4.7 presents an analagous graph for the perforated material used during the mass transfer studies (5).

The graphs show that a significant loss only ocurrs below speeds of approximately 200 RPM. This is the regime that

corresponds to the 'leaking ripple' zone shown on figure 4.3. A number of points show negative leakage (particularly with the coarse mesh). This indicates that a degree of inaccuracy is still associated with the experimental method. However this inaccuracy is quite insignificant. The results are very similar to those for the perforated surface, although these do not show the large leakage at low speeds.

The results of this study lead to the conclusion that a stable film can be formed on each of the mesh discs over the parameter ranges of interest. Therefore the discs are suitable for use in the rotary test rig described in section 7.

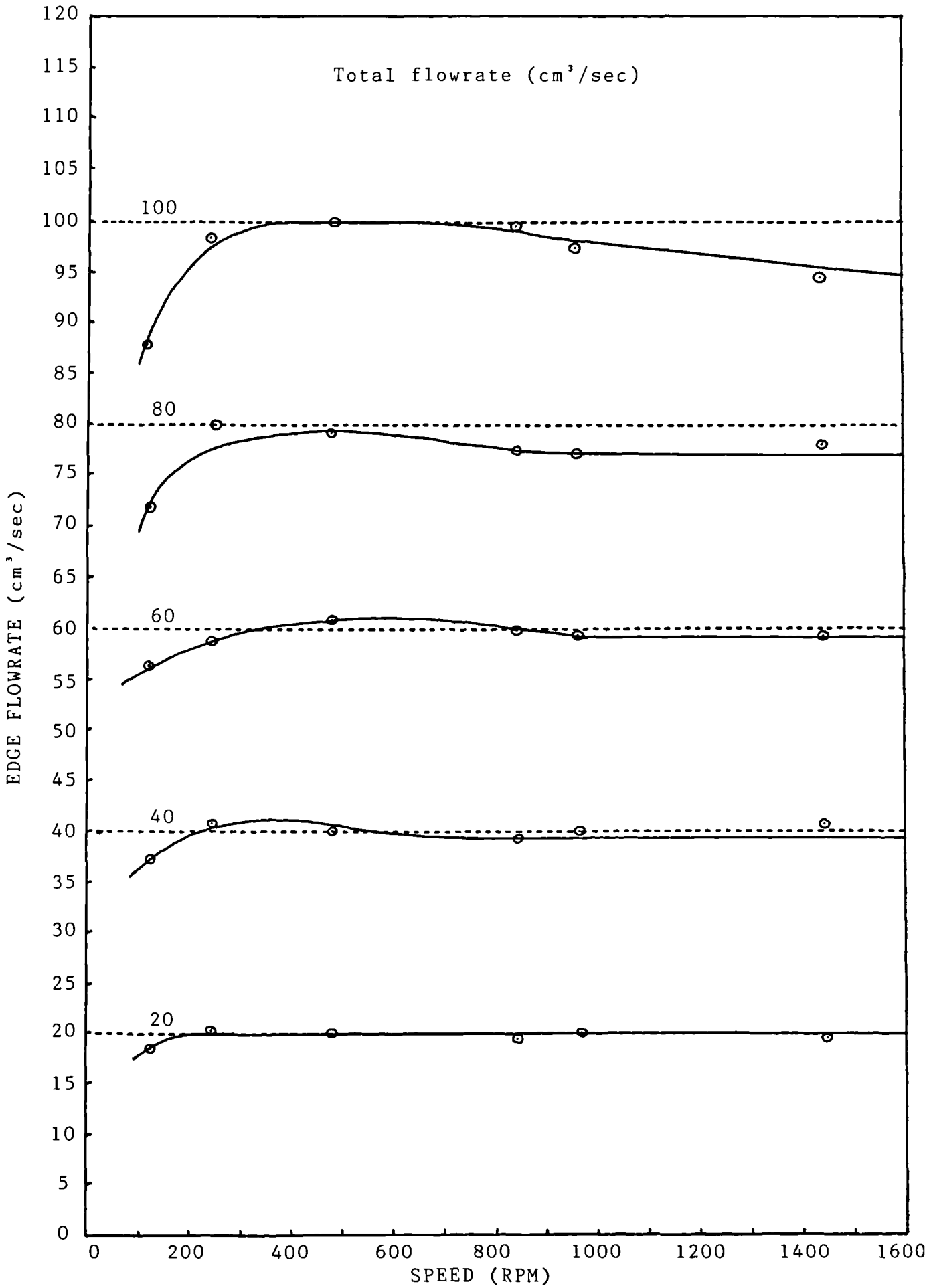

figure 4.4 leakage on the stainless steel mesh: coarse

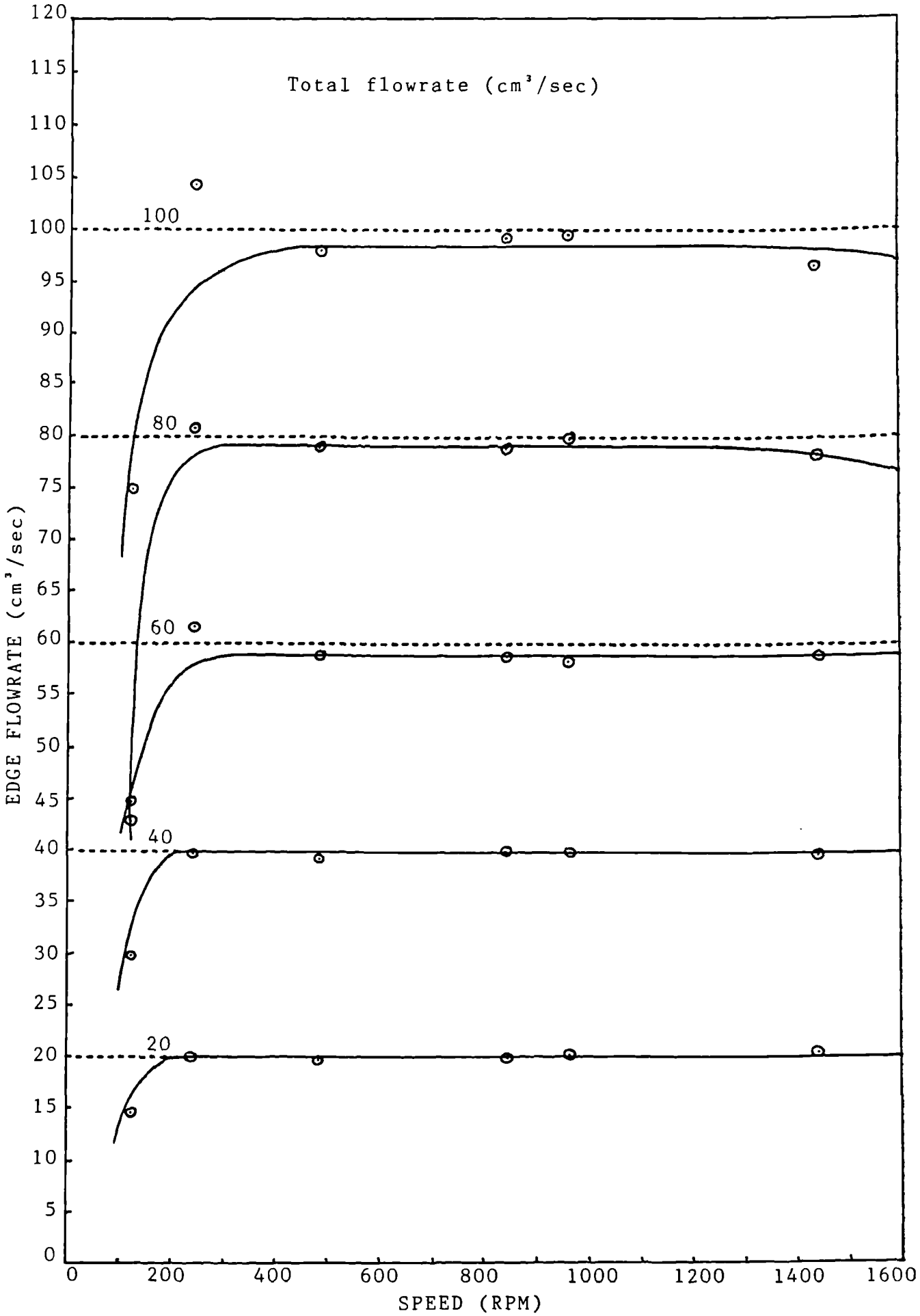

Figure 4.5 leakage on the stainless steel mesh: medium

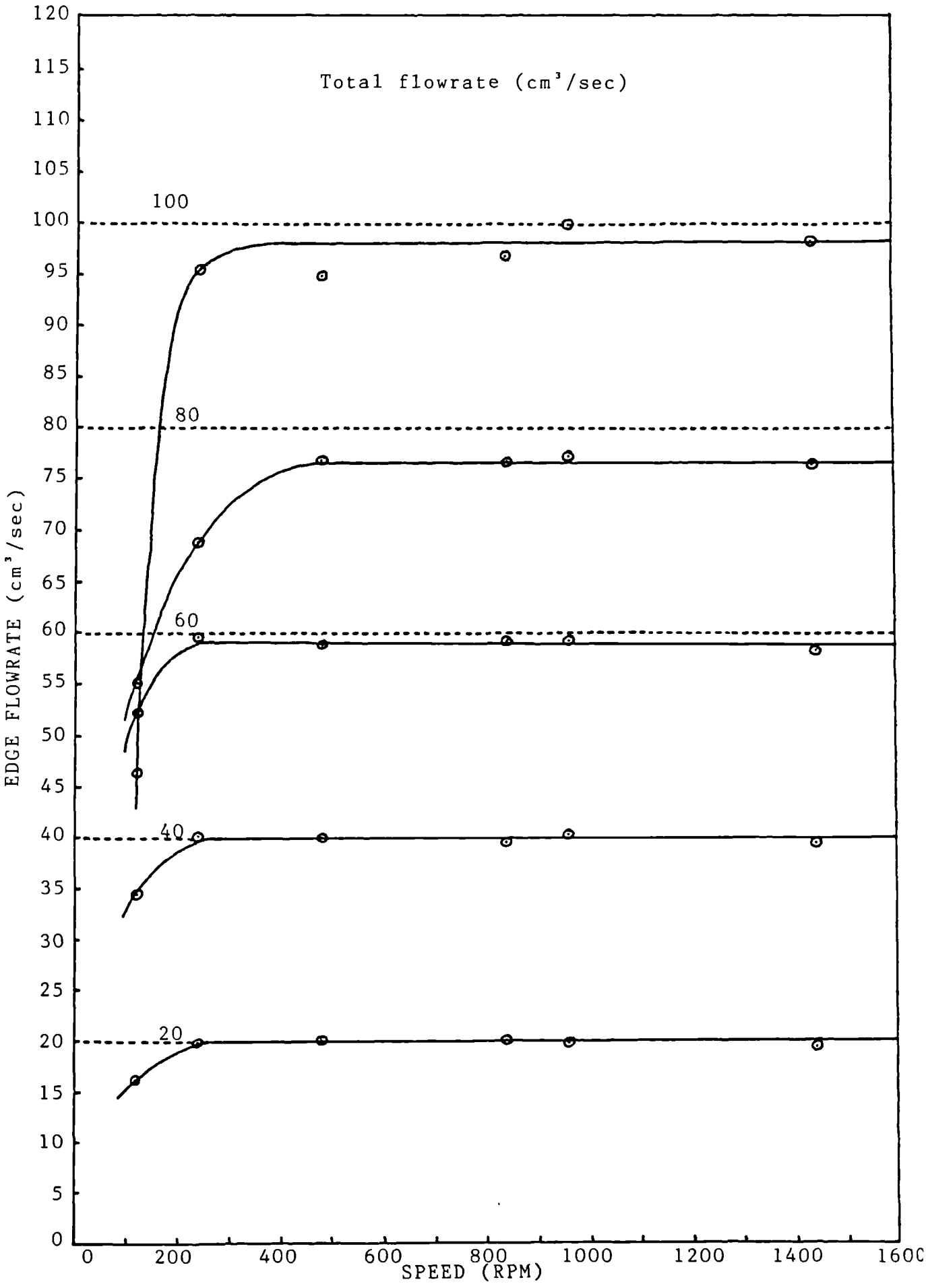

figure 4.6 leakage on the stainless steel mesh: fine

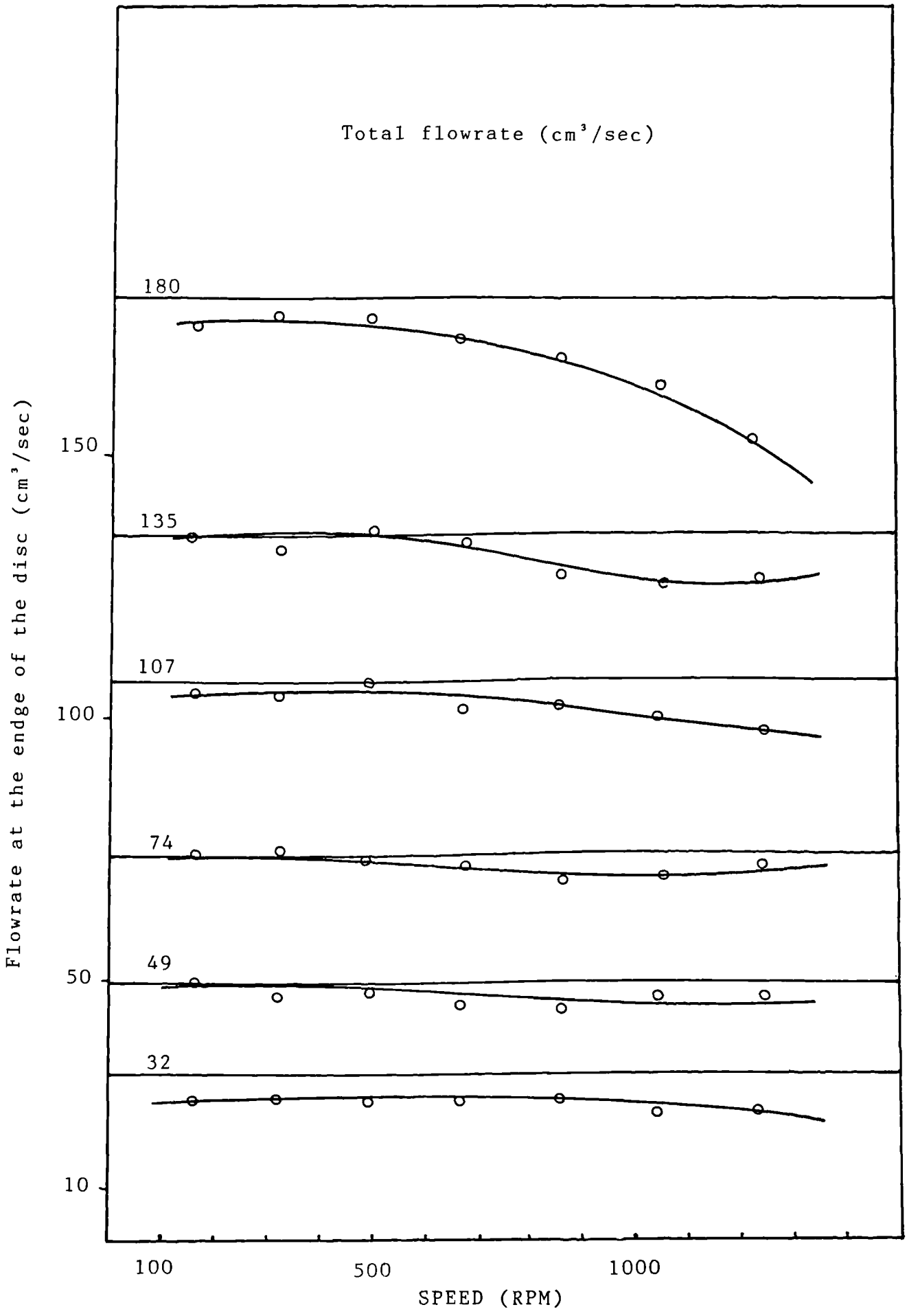

figure 4.7 leakage results for perforated disc (Koerfer)

5.0. MASS TRANSFER PROCESSES (WITH AND WITHOUT AN ASSOCIATED CHEMICAL REACTION)

5.1. Physical mass transfer processes

5.1.1. Introduction

This section outlines the general concepts associated with mass transfer and illustrates how a number of theoretical models, designed to represent real systems have been developed. In addition the practical value of such models is discussed with particular reference to their use in rotational geometries.

5.1.2. General concepts

The removal of unwanted, gaseous contaminants by gas absorption is a process widely used in the chemical industry. This is achieved by bringing the gas into contact with a liquid in which the impurities alone are soluble. The component, or components to be absorbed have to be transferred from the bulk of the gas to the bulk of the liquid. The force which produces the movement of the molecules of the soluble component is refered to as the 'driving force'. This is an effect which is caused by the non-equilibrium of the concentration of the component in the gas-phase with that in the liquid-phase. The rate of mass transfer is thus proportional to this driving force.

The gas and liquid phases can be regarded as offering a resistance to the passage of the component to be absorbed, thus reducing the effectiveness of the driving force provided. The magnitude of this resistance is expressed as a 'mass transfer coefficient' in the basic mass transfer equation. This coefficient is a function of the flow conditions prevailing in the transfer equipment and the physical properties of the substances involved.

The basic mass transfer equation is written as,

$$N = K_L.A.(\Delta C) \qquad 5.1$$

where N = rate of mass transfer
A = interfacial area
ΔC = concentration driving force
and K_L = overall mass transfer coefficient.

The overall resistance to mass transfer is given by $\frac{1}{K_L}$. This consists of a resistance due to the liquid phase, an interfacial resistance and a resistance due to the gas phase. The existance of an interfacial resistance is a controversial topic. A number of investigators (22,32-4) state that interfacial resistance is a possible cause of low absorption rates associated with a number of systems. Others (8,35-6) however, have pointed out that only in the case of very high absorption rates or very low gas pressures will this resistance be a determining factor in gas absorption. In most common situations, and for the purpose of the present investigation, it can be assumed that the interfacial resistance is negligible.

This implies that there is a physical equilibrium between the gas and liquid phases.

The overall resistance to mass transfer can be thus written as,

$$\frac{1}{K_L} = \frac{1}{k_L} + \frac{H}{k_g} \qquad 5.2$$

where $1/k_L$ = liquid phase resistance

$1/k_g$ = gas phase resistance

and H = Henry's law constant

The Henry's law coefficient express's the physical equilibrium between the liquid and gaseous phases and is defined as,

$$H = \frac{C_1^i}{P_g^i} \qquad 5.3$$

where C_1^i = concentration of the component in the liquid at the interface

P_g^i = pressure of the component in the gas, at the interface.

In many mass transfer processes the resistance associated with one phase is considerably greater than that due to the other. In these cases the phase which contributes the major resistance to mass transfer is said to be controlling. For sparingly soluble gases the value of H is very small and thus the gas phase term in equation 5.2 becomes negligable compared with the liquid phase term. The overall resistance to mass transfer is therefore approximately equal to the resistance due to the liquid phase only. Kwanten and Huiskamp (37) present a formula, derived from the penetration theory concept which can be used to estimate the importance of the gas-phase resistance. This is reproduced below (equation 5.4).

$$\frac{\text{rate of absorption without gas-phase resistance}}{\text{rate of absorption with gas-phase resistance}} = 1 + H.R.T. \left(\frac{D_L}{D_g}\right)^{1/2} \qquad 5.4$$

Using this equation it can be shown that the rate of mass transfer in practically all gas-liquid contacting systems is controlled by the liquid phase resistance. This is the case for the carbon dioxide-water system used in the present investigation.

Mass transfer coefficients can be determined for a particular system from experimental measurements which allow a mass balance to be calculated. These provide a measurement of the rate of mass transfer. Assuming that a value of the Henry's law coefficient is available they also provide a value of the concentration driving force. Therefore the mass transfer coefficient representing the system at the particular set of conditions can be calculated

provided the interfacial area is known. In many cases, particularly those where random packing elements are used (for example the various types of rings) the actual interfacial area is not known. In such cases the resistance to mass transfer is expressed as a product of the area and the mass transfer coefficient i.e. $K_L.A$. For a mass transfer system, which employs rotating discs as the active transfer surface such problems do not arise provided that the discs are completely wetted. Assuming this condition is satisfied the interfacial area is equal to the surface area of the disc.

In most design situations it is not practical to measure experimentally the mass transfer coefficients for the system of interest. Additionally it is possible that such values will not be available in the literature. Therefore there is a need to develop theoretical models of the mass transfer process from which mass transfer coefficients can be calculated. These can then be used to estimate the size of equipment required to perform a particular duty under specified conditions (driving force) or alternatively calculate the performance available from a device of a specific size. To be of use these models have to take account of the various mechanisms by which the concentration driving force can move matter, i.e.,

- molecular diffusion, which is a result of the thermal motion of the molecules
- turbulent diffusion, where eddies remove matter from the gas/liquid interface.

The type of mechanism which provides the dominant effect in a particular system is,to a large extent, a function of the conditions present at the phase boundary. The following section outlines a number of the more important models developed to predict mass transfer coefficients. These vary in the way that they represent the surface condition.

5.1.3. Mass transfer models

Three major models have been proposed for the physical absorption of a gas in a laminar liquid. These are due to Whitman (38), Higbie (22) and Dankwerts (39). In these cases the mechanism of mass transfer is essentially controlled by molecular diffusion.

In the film model Whitman assumes that the total resistance to mass transfer in the liquid phase is located in a stationary thin-film (thickness δ) adjacent to the phase boundary. Similarily the gas phase resistance is concentrated in a thin-film of thickness δ'. The soluble component is assumed to traverse the liquid film under the action of steady-state molecular diffusion before macroscopic mixing distributes it throughout the bulk of the liquid. Thus Fick's second law for stationary, one dimensional diffusion can be integrated with the appropriate boundary conditions to give,

$$R = \frac{D}{\delta} (C_1^i - C_1^b) \qquad 5.5$$

and thus the liquid phase mass transfer coefficient is given by,

$$k_L = \frac{D_L}{\delta} \qquad 5.6$$

where D_L = the diffusivity of the soluble component in the liquid.

Higbie, in his penetration model, assumed that a liquid element absorbs by molecular diffusion until it hits a discontinuity at which point it is mixed with the bulk of the liquid and replaced at the surface with a fresh liquid-element. He assumes that the time between consecutive discontinuities (the so called exposure time) is constant (θ). In his analysis he considers the liquid element as having a semi-infinite depth (i.e. the gas never reaches the lower boundary before being mixed with the liquid bulk) and thus molecular diffusion is represented by a non-steady state model. This analysis produces an expression for the rate of mass transfer per unit area of,

$$R = 2\sqrt{\frac{D_L}{\pi\theta}}\,(C_1^i - C_1^b) \qquad 5.7$$

and thus

$$k_L = 2\sqrt{\frac{D_L}{\pi\theta}} \qquad 5.8$$

Dankwerts outlines a similar non-steady state model though he assumes that individual liquid elements remain at the phase boundary for a random duration. He defines a term, S which represents the fraction of the surface which is renewed in unit time. This is independant of the time of exposure. The surface renewal model produces an expression for the mass transfer coefficient of,

$$k_L = \sqrt{D_L . S} \qquad 5.9$$

Numerous other models have been developed which attempt to produce a more accurate representation of the effect of the phase boundary condition. These are basically modifications of the three models outlined above. The calculation of mass transfer coefficients using these methods is discussed in many texts dealing with the process of mass transfer and a useful summary of their relevance to rotary geometries is presented by Lim (4). The usefulness of these models is limited by the requirement that in each case a system parameter has to be known (either δ, θ or S in the above examples). Values of these are, however, in general unknown and in most cases very difficult to determine experimentally. This limits the ability of these methods to predict mass transfer coefficients.

Theoretical models are of most use when the process of mass transfer is designed in such a way that it fulfills the requirements inherant in the development of the model. The grooved discs employed by Lim (21) were an attempt to produce a liquid

surface that would conform to Higbies' penetration model. In this case it was assumed that the laminar film formed was completely mixed when it passed over the discontinuities seperating consecutive grooves. Thus, the time taken for liquid to flow across a groove was equal to the 'exposure-time', defined by Higbie and required in equation 5.8.

Although the practical use of theoretical models is limited , they provide a convenient method of representing the effect that a change in diffusivity has on the mass transfer coefficient associated with a particular system. Dankwerts and Higbies' models vary from that of Whitman in this respect. The thin film model predicts that the mass transfer coefficient is proportional to the diffusivity. Both surface renewal models however, conclude that it is actually proportional to the square root of the diffusivity. It has been demonstrated, that surface renewal models are most suited to systems where the liquid phase is flowing and the thin film theory is best applied to systems in which there is a quiescent liquid phase. Therefore the variation of a system mass transfer coefficient due to a change of temperature or alternatively as an effect of using a different gas phase, can be estimated for the system of interest. The use of this procedure in the present investigation is outlined in section 5.2 below.

A number of other models attempt to represent mass transfer into a turbulent film, i.e. where the mechanism is essentially eddy controlled. These are adequately reviewed by Lim (4). In general these require a knowledge of the eddy diffusivity in addition to a system parameter. As it is again very difficult to predict turbulent diffusion coefficients experimentally these methods are of only limited use in practical situations. Methods which attempt to remove the eddy diffusivity from the calculation by modelling it in terms of other system parameters have also been presented. Davies (40) showed that these tend to underestimate mass transfer coefficients (by up to a factor of 10) due to an inability to represent the complicated flow. The presence of surface waves makes these models particularly prone to error.

In general it can be concluded that turbulent mass transfer processes do not lend themselves to theoretical modelling. However, although these models are of only limited use they do demonstrate that the mass transfer characteristics of a particular system are enhanced by inducing turbulence.

5.1.4. Mass transfer to a liquid film on a rotating disc

Several models have been developed to predict the mass transfer properties of thin films formed on rotating surfaces (3,4,5). Each of these is based upon Higbie's penetration theory. The models for different disc surfaces vary in the way that they define the 'exposure time'.

Venkataraman (3) limited his study to smooth laminar films and developed a number of models which he compared with his experimental results. In his basic model, the so called 'crude' theory, he assumed that a surface element is neither stretched nor contracted as it grows older.

Thus the rate of absorption can be described by,

$$dN = (\Delta C)\sqrt{\frac{D}{\pi t}}.\ dA(t) \qquad 5.10$$

For the exposure time, t, he used the residence time of the film on the disc which is given for the centrifugal model by equation 4.8. . After substituting,

$$dA(t) = 2\pi r.Vr.dt \qquad 5.11$$

where the surface velocity at any particular radius (Vr) was again calculated from the centrifugal model (equation 4.3) he finally had to integrate,

$$dN = 4\Delta C \cdot \sqrt{\frac{\pi . D_L . B}{3}} \quad \left(\frac{r}{r^{4/3} - r_o^{4/3}}\right) dr \qquad 5.12$$

where
$$B = 0.306 \frac{\omega^{2/3} Q^{2/3}}{\nu^{2/3}} \qquad 5.13$$

between the radius of the distributor (r_o) and the outer radius of the disc (r). This was achieved by the substitution of a standard integral which resulted in the expression,

$$N = 6\Delta C\sqrt{\frac{\pi DB}{3}}\left[\frac{r_i^{2/3}}{2}\sqrt{(r_i^{4/3} - r_o^{4/3})} + \frac{r_o^{4/3}}{2}\ \text{loge}\ (r_i^{2/3} + \sqrt{(r_i^{4/3} - r_o^{4/3})} - \frac{r_o^{4/3}}{2}\ \text{loge}\ r_o^{2/3}\right] \qquad 5.14$$

This equation predicted values some 23% lower than his experimental results. In further models Venkataraman took into consideration a velocity component normal to the interface which develops as the surface element changes with age. He restricted this analysis originally to small depths of penetration in order that he could assume the normal velocity component was proportional to the distance from the interface. Again the penetration theory was adopted and the residence time and velocity distributions of the centrifugal model were utilised. The resulting diffusion equation was solved by a method outlined by Beek and Kramers ( ). This produced an expression for the rate of mass transfer of,

$$N = 4.\Delta C\sqrt{\pi D_L B.}\ \left(\frac{3}{8}(r_i^{8/3} - r_o^{8/3})\right)^{1/2} \qquad 5.15$$

This expression produced values which were approximately 7% greater than his experimental results. When this model was refined to take into account the influence of inertia and the effect of the Coriolis acceleration the agreement between theoretical and measured values was within the experimental error. Details of this 'refined' model are not reproduced in the present work as only the 'approximate' model was used to produce theoretical values which could be compared with the experimental results.

Lim (4) modified Venkataraman's 'approximate model' by assuming exposure and mixing take place in a series of concentric rings with a width equal to the wave length of the waves on the disc. He used the 'approximate' model to describe the mass transfer process and calculated the exposure time equal to one wave length from the centrifugal model. Because the wave length data was limited he had to assume an average value which was then used for all speeds and flowrates. For low rotational speeds (227 RPM) this method over-estimated the rate of mass transfer by up to 30%. This was because the waves present on the disc were of a much larger wave length than that used in the model. Good agreement was found at higher speeds (1100 RPM). Although this model can predict values which agree closely with experimental results, Lim warns against its adoption until further work concerning the wave length of the spiral waves has been completed. He states that an accurate fit could have been obtained for vitually any set of data provided the correct wavelength had been chosen.

Koerfer (5) adopted a similar method when preparing an equation to model mass transfer on a perforated disc. He again assumed that mass transfer took place in a continuous step-by-step exposing and mixing process, the width of a transfer element being equal to the average distance between consecutive holes. Thus using the 'approximate' theory with an exposure time calculated from the centrifugal model he obtained an expression which could be integrated step-wise from the distributor to the outer edge of the disc. To simplify the complicated expression obtained he reworked the model using the penetration theory. Values obtained from each of these models are compared with his experimental results between 100 and 600 RPM. This shows that at the lowest speeds the model based upon the 'approximate' theory can be used quite successfully. At higher speeds the values predicted are up to 15% less than the experimental results. Values based upon the penetration model are up to 50% less than the experimental results at all rotational speeds. He assumed that these discrepancies were a result of using a molecular diffusivity rather than a combined eddy and molecular diffusivity as proposed by Kishinevsky (42). That is at the higher speeds the liquid flow during the time of exposure is no longer laminar but involves a degree of turbulence.

The following section outlines how the models and general concepts presented in this section were used to prepare and analyse the mass transfer results of the present investigation.

5.2. Physical mass transfer in relation to the present investigation

5.2.1. Introduction

This section outlines how the general concepts and theoretical models, presented in the previous section, were used in the preparation and analysis of the mass transfer results of the present investigation. This topic contains three distinct areas and these are discussed individually in the following subsections. Section 5.2.2 shows how the mass transfer coefficients of the present investigation were calculated from the measured data. Section 5.2.3 shows how the data of other investigations was re-analysed so that it could be compared with the results of the present work. This is seperated into a description of data gained from the carbon dioxide/water system and results obtained from systems with a different gas phase (i.e. oxygen and ozone). The final sub-section considers how the theoretical models (e.g. the 'approximate' model) were used to compare the results of the present investigation with theoretically derived values.

5.2.2. Calculation of mass transfer coefficients in the present investigation

The mass transfer coefficient for the physical absorption of carbon dioxide into water is calculated from a measurement of the dissolved gas concentration at the outlet of the rotary rig. This is obtained from the analysis technique described in detail in section 6.2. This technique provides a 'raw' (mV) measurement of the concentration. This is converted to an actual value (C_b°) from a calibration curve (concentration in g/cm^3). The flowrate (Q) and temperature (T) of the liquid phase, corresponding to this outlet concentration are also recorded. The flowrate is measured by a set of rotameters and converted to cm^3/sec by an appropriate calibration. The liquid phase temperature is measured by a copper/constantan thermocouple placed in the inlet liquid feed just before the rotary rig. The mV reading is converted to degrees centrigrade by a multiplication factor. These measurement techniques are described in section 7.

Thus, the measurements of outlet concentration and liquid flowrate can be used to calculate the rate of mass transfer (N), i.e.

$$N = QC_b^\circ \quad (g/sec) \qquad 5.16$$

This assumes that the carbon dioxide concentration at the inlet is negligible. A simple analysis of the feed liquid using the carbon dioxide eletrode justified this assumption.

The mass transfer coefficient representing the particular hydrodynamic and physical system of interest is calculated from a rearranged form of the basic mass transfer equation (equation 5.1) i.e.

$$k_L = \frac{N}{A.\Delta C} \quad (cm/sec) \qquad 5.17$$

The mass transfer area (A) is assumed to be equal to the surface area of the thin film. This is therefore calculated from

$$A = \pi(re^2-ri^2) \qquad 5.18$$

where re = the radius to which the absorption chamber is flooded (section 7.2.3) and ri = the nozzle radius.

Although it has been shown in section 4 that at particular liquid flowrates and rotational speeds areas of the mesh and perforated discs are dry, insufficient work has been completed to allow the mass transfer area to be modified with respect to this effect. Dry areas will cause the mass transfer coefficient calculated to be less than that its true value. This reduction will be proportional to the percentage of the disc which is dry. It was hoped that by not allowing for this potential source of error in the above calculation the mass transfer results would reflect the conditions where dry areas are formed.

A logmean concentration driving force was used to represent the force moving molecules of carbon dioxide from the gas/liquid interface into the bulk of the water. This was chosen because at the operational conditions used the bulk carbon dioxide concentration was significant. Again assuming the inlet concentration is zero (in the liquid phase) and that the interfacial concentration is a constant (C_L^i) the driving force for a co-current process, can be caluclated from

$$\Delta C = \frac{(C_L^i-0)-(C_L^i-C_b^o)}{\log_e\left[\frac{(C_L^i-0)}{(C_L^i-C_b^o)}\right]} \qquad 5.19$$

or

$$\Delta C = \frac{C_b^o}{\log_e \frac{C_L^i}{(C_L^i-C_b^o)}} \qquad 5.20$$

When carbon dioxide is absorbed from gas mixtures its partial pressure, and hence its inter-facial concentration, decreases from inlet to outlet. The value of C_L^i is therefore not constant. To avoid this complication in the present investigation a high gas flowrate was used. Thus, even of the outlet liquid had been saturated the amount of carbon dioxide transfered would have reduced the partial pressure by a negligible amount. This is demonstrated in Appendix K. Measurements of the inlet total pressure, using a water manometer, showed that over the operational ranges of flowrate and rotational speed this was approximately constant at just over one atmosphere (up to +4cm water). To allow for the pressure drop through the absorption chamber and to simplify the calculation a total pressure of one atmosphere was used. As the inlet gas supply is dry a certain amount of humidification occurs as it passes through the absorption chamber. Simple calculations show that even if the outlet gas is saturated the change

in gas partial pressure and liquid flowrate is insignificant.

With the above assumptions the interfacial concentration of carbon dioxide can be calculated from a knowledge of the Henry's law coefficient (H). Dankwerts (43) recommends the following correlation.

$$\log_{10} H = \frac{1140}{T} - 5.30 \qquad 5.21$$

where T is in Kelvin
and H is given in (mole/l.atm)

This can therefore be used to predict H at the measured liquid temperature (T). The interfacial concentration is therefore found from

$$C_L^i = \text{partial pressure of } CO_2 . H . \frac{44}{1000} \qquad 5.22$$

The logmean driving force can thus be calculated and from this a value of the system mass transfer coefficient determined. This mass transfer coefficient refers to the specific hydrodynamic conditions present in the rotational device at the relevant liquid phase temperature. So that the results could be compared with those from other investigations the mass transfer coefficients had to be altered so that they refered to a standard temperature. Twenty degrees centigrade was chosen as this had been used in the majority of the previous investigations. The mass transfer coefficients calculated were for temperatures in the range 14 to 22°C. As the maximum temperature modification was small it was assumed that the hydrodynamic properties of the liquid (i.e. density, surface tension and viscosity) would be the same at the measured and modified temperatures. Assuming mass transfer takes place in accordance with Higbies' 'penetration' theory the mass transfer coefficient representing the system is proportional to the square root of the diffusivity. Thomas and Adams (45) present values of the diffusivity of carbon dioxide in water (D) and thus the modified mass transfer coefficient can be calculated from

$$k_{L_{20}} = k_L \sqrt{\frac{1.7 \times 10^{-5}}{D}} \ (\text{cm/sec}) \qquad 5.23$$

The values tabulated in Appendicies D-F and plotted in section 8 are the temperature modified mass transfer coefficients.

The procedure outlined in this section formed the basis of the computer programme 'DATA-AN' listed in Appendix I.

5.2.3. Analysis of previous mass transfer results

Results of a number of previous investigations where mass transfer is studied on a rotary surface are available. Some of these report mass transfer coefficients while others present overall rates of mass transfer. Systems studied are water/

carbon dioxide, water/oxygen and water/ozone. Results of these investigations are presented for a temperature of 20°C. A wide variety of disc surfaces, liquid flowrates and rotational speeds are represented by this data. It was thus hoped that the results could be re-analysed to allow a direct comparison with the results of the present investigation. This section shows how this was achieved using the data of the investigations mentioned in section 2.

·Venkataraman (3) measured the mass transfer performance of the system carbon dioxide/water on smooth discs. The maximum liquid flowrate used was only 7.6 cm^3/sec. As this was much smaller than the flowrates used in all other investigations, the data contained within this report was not re-analysed.

·Watts (6) was also concerned with the absorption of carbon dioxide in water on smooth discs. The results of these investigations are presented as mass transfer rates. To be of use in a comparison these have to be transformed into mass transfer coefficients. This is achieved by using the disc dimensions and gas conditions stated. Watts used a 34.3cm diameter disc with an inlet nozzle of 9.85cm diameter. Therefore the active area available for mass transfer is $853cm^2$. Pure water was used as the inlet feed and the gas phase consisted of carbon dioxide at one atmosphere. Using equation 5.21 and 5.22 the interfacial carbon dioxide concentration can be calculated as $1.75 \times 10^{-3} g/cm^3$. Thus combining equations 5.16, 5.17 and 5.20 the mass transfer coefficient can be expressed as

$$k_L = \frac{1}{853Q}\left[\log_e \frac{1.715\times10^{-3}}{(1.715\times10^{-3}-\frac{N}{Q})}\right] \text{ (cm/sec)} \qquad 5.24$$

·Lim (4) published mass transfer coefficients for the system oxygen/water. These can be changed into values for carbon dioxide/water by allowing for the difference in the diffusivities of oxygen and carbon dioxide. Higbie's 'penetration' theory is again used. The diffusivities of oxygen and carbon dioxide in water at 20°C are $2.4\times10^{-5} cm^2/sec$ (4) and $1.7\times10^{-5} cm^2$ sec (5) respectively. Thus

$$k_L = k_{LO_2}\sqrt{\frac{2.4}{1.7}} \quad \text{(cm/sec)} \qquad 5.25$$

·Koerfer (5) published mass transfer data for the oxygen/water system. These are transformed using equation 5.25.

·Barberis (31) studied the system ozone/water. Because ozone and carbon dioxide have approximately the same diffusivity at 20°C the mass transfer results can be compared directly.

5.2.4. Use of mass transfer models

The 'approximate' model (section 5.1.2) was used to predict the performance of a smooth rotating disc at conditions corresponding to those used in the present investigation. The enhancement of mass transfer coefficients associated with the mesh disc could thus be calculated. The 'approximate' theory was used as it has been shown in previous investigations to be capable of predicting the performance of 'laminar' films accurately. The rate of mass transfer is predicted using equation 5.15. The mass transfer coefficient is then calculated in the same way as Watts' data was re-analysed (section 5.2.3). Because the bulk concentration of carbon dioxide significantly effects the driving force this calculation proceeds iteratively. This is demonstrated below.

Using equation 5.15 a value of the rate of mass transfer can be calculated assuming that the bulk concentration of carbon dioxide is zero, i.e. $\Delta C = C_i^i$. This forms a first approximation, which can be used to calculate C_b° from equation 5.16. Thus a second approximation of ΔC can be calculated from equation 5.20 and used to predict a new value of N. This procedure is repeated until successive iterations produce the same value of N. This is then used with the corresponding values of A and ΔC to calculate the mass transfer coefficient from equation 5.17.

5.3. Mass transfer accompanied by chemical reaction

5.3.1. Introduction

In order to enhance the rate of mass transfer attained in a particular piece of equipment a solvent which reacts chemically with the gas to be absorbed can be employed in place of one that physically absorbs the gas. The degree of enhancement is called the 'chemical acceleration factor' and is defined so that:

$$R = \phi.k_L.C^* \qquad (5.26)$$

where R = rate of mass transfer/unit surface area
ϕ = chemical acceleration factor
k_L = mass trnsfer coefficient attained under the same hydrodynamic conditions using a solvent of similar physical properties where no reaction occurs
C^* = concentration of free gas at the surface

Thus a knowledge of the acceleration factor is needed to determine the ability of a particular solvent to absorb a gas when accompanaied by a chemical reaction. Although most publications dealing with absorption accompanied by a chemical reaction are theoretical, many can be used to predict the chemical acceleration factor from a knowledge of the microkinetics of the reaction and the rate of physical absorption in the relevant equipment. This section discusses work published on this topic and outlines its applicability to the absorption of carbon dioxide into aqueous solutions of diethanolamine.

The effect of a simultaneous chemical reaction on the rate of absorption is often studied by adopting a simplified model of the liquid flow pattern. This is then treated mathematically. Of the many mass transfer theories much of the published work has made use of Whitman's film theory, Higbie's penetration model and Dankwerts' surface renewal theory. The latter does not lend itself to the calculation of the rate of mass transfer easily but is very useful in predicting when a particular kind of transfer process occurs. Consequently these models have been developed further than have others, and lend themselves more readily than most do. Which of these models represents the actual physical/chemical process is a question of less importance than whether one of them is found, to produce accurate predictions of the effect of a chemical reaction.

Dankwerts (45) explores the field of mass transfer accompanied by chemical reaction in some depth. He considers the theory associated with the absorption processes of quiescent and agitated liquids and also the equipment in which empirical studies can be undertaken. Sherwood and Pigford (46) present an extensive review of the use of the film and penetration models in this field. A number of the papers mentioned therein present the fundamentals of chemical absorption. Pioneering work in this area was published by Hatta (47) who used the film theory to analyse the effect of an infinitely fast irreversible first order reaction. A second order irreversible reaction in the liquid phase was studied by van Krevelan and Hoftyzer (48) again using the film theory. The accuracy of this method was demonstrated by Peaceman (49) who measured rates of mass transfer with and without chemical reaction and compared his results with the model. The applicability of the penetration theory

was first studied by Dankwerts (50) who considered a first order reaction. This was applied to a second order reaction over a limited range of variables by Perry and Pigford (51) and later over a much wider range by Brian, Hurley and Hasseltini (52). The penetration theory was generalized with respect to the order of reaction by Brian (53) and Astarita (54).

It has been shown (34,55) that in many cases the difference in values predicted by the various models is less than the variation in the physical quantities needed for their calculation. The choice of model on which to base the predictions is therefore mainly a matter of convenience.

The type of chemical process which has received the most theoretical attention is that in which the dissolved gas undergoes an irreversible second order reaction with a non-volatile reactant in the liquid phase. The interest in this scheme is not accidental since this type of reaction is encountered when carrying out a number of important technological processes. Until recently the reaction of carbon dioxide with aqueous solutions of diethanolamine was thought to undergo such a mechanism. However recent work including that by Hikita, Asai, Ishikawa and Honda (56) has led to the proposition that the reaction is actually third order. The order and mechanism of this important reaction is discussed in section 3.3.6. Brian (53) indicated that the reaction order did not effect the acceleration factor greatly especially at low values of ϕ. The effect of a chemical reaction on this system is studied by a number of authors including Dankwerts (43) Babak et al (57), Sada et al (58), Coldrey and Harris (59) and Nunge and Gill (60).

5.3.2. Calculation of acceleration factors for the case of a second order irreversible reaction

When mass transfer is accompanied by a second order irreversible reaction the concentration profiles of dissolved gas and reactant, in the region of the surface are dependent on a number of circumstances. In general the reaction occurs entirely within the boundary layer, in a rather narrow reaction zone, and thus the reactant has to diffuse from the bulk of the liquid and the gas from the interface. However, when certain conditions are met the reaction simplifies so that it becomes either psuedo first order, fast psuedo first order or instantaneous. The calculation of the chemical acceleration factor in such situations is simplified. Figure 5.1 shows the concentration profiles of unreacted gas and reactant according to the thin-film theory for each of the above situations. Dankwerts (43) presents formulae for determining when the particular conditions are achieved, and indicates how the acceleration factor can be calculated in such cases using the surface renewal model. Brian et al (52) consider these simplifications in their analysis of the penetration theory.

5.3.2.1. Pseudo first order reaction

Under certain circumstances the concentration of reactant in the neighbourhood of the surface is very little different from that in the bulk of the liquid, and the dissolved gas undergoes a pseudo first order reaction. This condition is satisfied if (43):

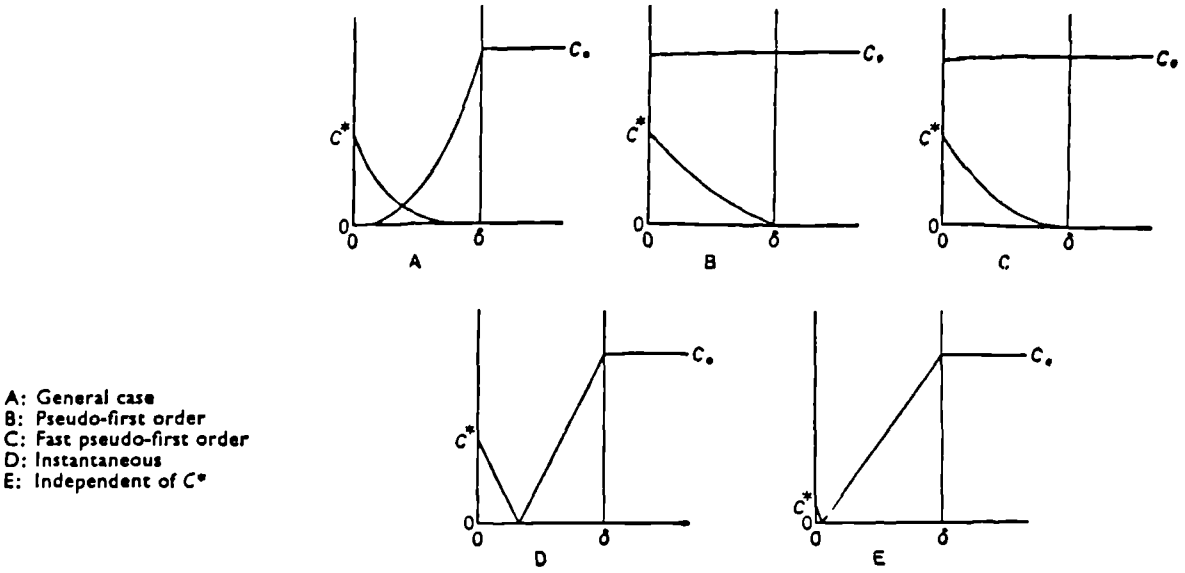

figure 5.1 Concentrations of carbon dioxide at the surface of a reactive solution

figure 5.4 Correction to equation 5.32 $\phi a = 3$

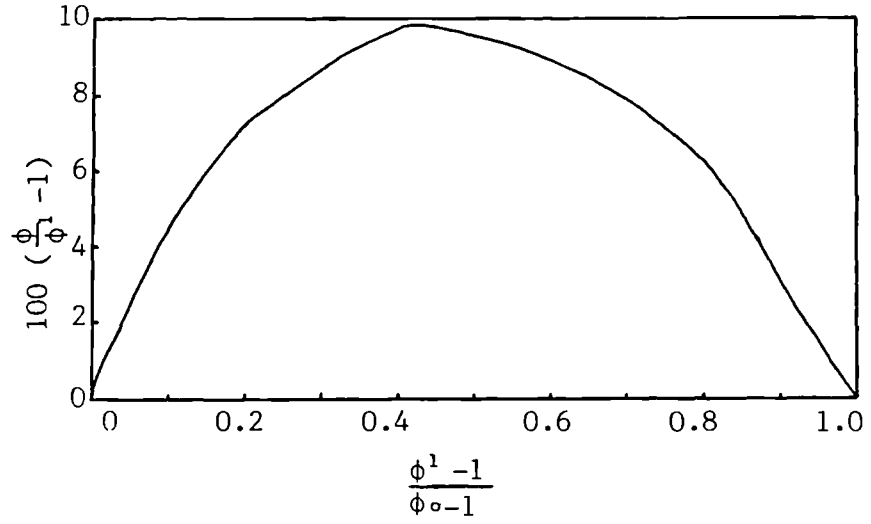

figure 5.5 Correction to equation 5.32 $\phi a = 6$

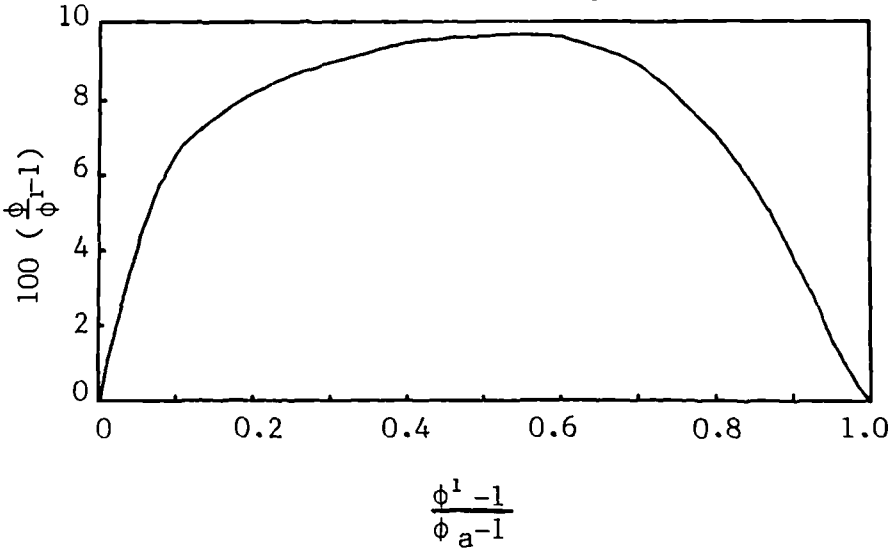

$$(D\ k_2 C_0)^{1/2} \leq 1/2\ k_L (1 + [C_0 / (Z.C^*)]) \qquad (5.27)$$

where D = diffusivity of gas in the solution
k_2 = second order rate constant
C_0 = concentration of reactant in the bulk of the liquid
Z = number of moles of reactant reacting with one mole of gas

The factor 1/2 in this equation is arbitrary but it ensures that equation 5.28 below is accurate to within 10%. If this condition is satisfied then the acceleration factor for the penetration and surface renewal models (43,52) is:

$$\phi = (1 + [D\ k_2 C_0 / k_L^2])^{1/2} \qquad (5.28)$$

Peaceman (49) has shown that this agrees with values predicted by the film theory to within 7%.

5.3.2.2. Fast pseudo first order

If condition 5.27 is satisfied and when (43):

$$(D\ k_2 C_0)^{1/2} \geq 5 k_L \qquad (5.29)$$

then the chemical acceleration factor is given by:

$$\phi = \frac{(D\ k_2 C_0)^{1/2}}{k_L} \qquad (5.30)$$

where again the factor five in the inequality 5.29 is arbitrary but ensures that equation 5.30 is accurate to within a few per cent.

5.3.2.3. Instantaneous

Under some conditions the reaction between dissolved gas and reactant can be treated as instantaneous; the two diffusing to a reaction zone close to the surface where the concentration of both is zero. The condition for this is (43):

$$(D\ k_2 C_0)^{1/2} \geq 10 k_L\ (1 + [C_0/(Z.C^*)]) \qquad (5.31)$$

The acceleration factor predicted by the penetration theory can then be calculated by the use of figure 1 in reference (52) However an approximate value (ϕ_a) can be found (52) by using:

$$\phi_a = 1 + (D_0/D)^{1/2} (C_0/Z.C^*) \qquad (5.32)$$

where D_0 = diffusivity of the reactant,

which is better at high values of ϕ_a and where the diffusivity ratio is near to 1.0. If the film theory is used then the acceleration factor can be calculated (52) from:

$$\phi_a = 1 + (D_0/D).(C_0/Z.C^*) \qquad (5.33)$$

Thus for an infinitely rapid chemical reaction, the film and penetration theories agree when the ratio of diffusivities is equal to unity. The more this ratio differs from unity the larger the disparity between predicted values will be. The choice of model in such cases must be based on experimental observations. Equation 5.32 can also be used to calculate an approximate solution to Dankwerts surface renewal model (54).

5.3.2.4. General case

For conditions intermediate between those of equations 5.27 and 5.31, that is where reactant is depleted near the surface, but the reaction is not fast enough to be treated as instantaneous, a number of solutions have been proposed. Each of these methods relies on the use of charts presented in the original references. Those which are relevant to the present work have been reproduced here (figures 5.2 to 5.7). Van Krevelen and Hoftyzer (48) have given a numerical solution for the film model, the accuracy of which has been demonstrated by Peaceman (49). They define two dimensionless quantities and show that the acceleration factor can be expressed as a funtion of these. They express this function mathematically as:

$$\phi = \frac{Ha(1-(\phi-1).P)^{1/2}}{\tanh[Ha(1-(\phi-1).P)^{1/2}]} \qquad (5.34)$$

$$\text{where Ha = Hatta No.} = \frac{(k_2 D\, C_o)^{1/2}}{K_L} \qquad (5.35)$$

$$\text{and P = concentration-diffusion parameter} = Z.\frac{D}{D_0}.\frac{C^*}{C_0} \qquad (5.36)$$

and as a graph with Ha as the ordinate, ϕ as the absisca and P as the variable (figure 5.2). Brian et al (52) report that this equation can be used to represent the penetration theory with errors of up to 17%. Dankwerts (43) improved this disparity to approximately 10% by re-defining the concentration diffusion parameter as:

$$P' = (C_0/Z.C^*).(D_0/D)^{1/2} \qquad (5.37)$$

and by replotting figure 5.2 to give 5.3.

Brian et al (52) present a method with which values within 3% of the actual penetration model can be calculated. This uses equation 5.38 below along with figures 5.4 to 5.7. They re-defined equation 5.34 above to give:

$$\phi' = \frac{Ha(1-[(\phi'-1)/(\phi_a-1)])^{1/2}}{\tanh[Ha(1-[(\phi'-1)/(\phi_a-1)])^{1/2}]} \qquad (5.38)$$

where ϕ_a is the value of the acceleration factor assuming the reaction is instantaneous, and which is calculated from equation 5.32. This first approximation of the acceleration factor, ϕ', is

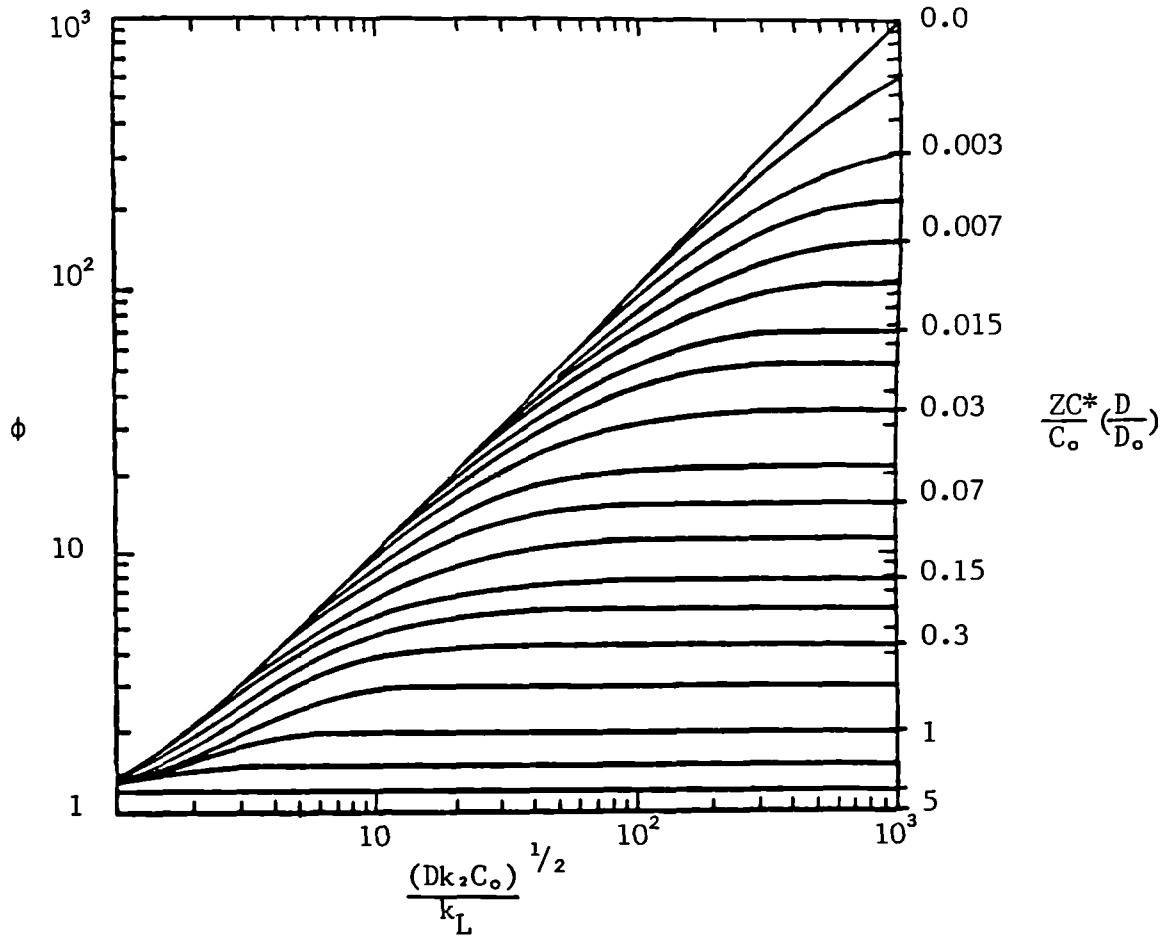

figure 5.2 chemical acceleration factor for 2nd order reaction (film theory)

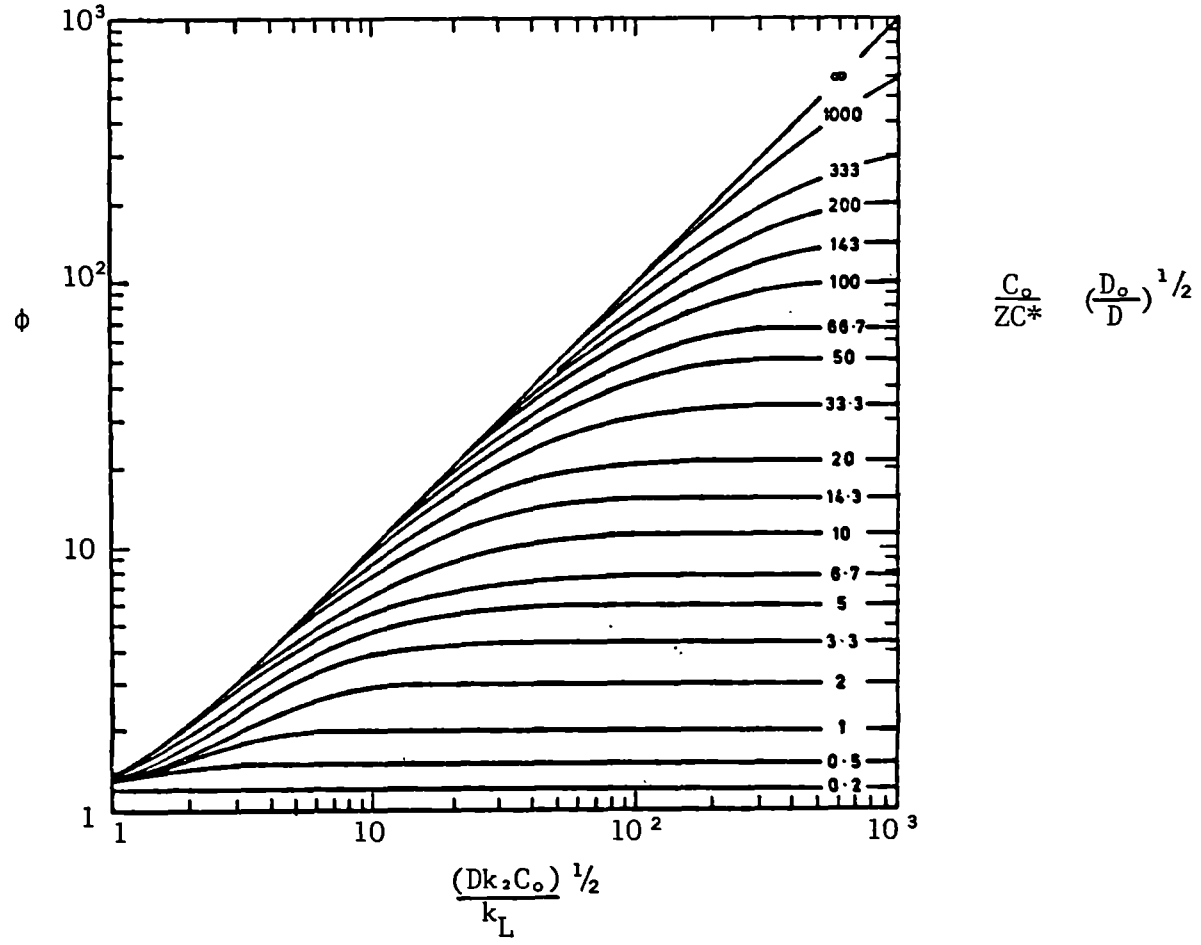

figure 5.3 Chemical acceleration factor for 2nd order reaction (penetration theory)

then used, together with ϕ_a and the diffusivity ratio D_o/D to obtain a second value, ϕ, by interpolation of the data within figures 5.4 to 5.7. The figures presented in the original reference contain values of the diffusivity ratio between 0.02 and 10 but these have been replotted for $D_o/D = 0.37$ which is the value of the diffusivity ratio for carbon dioxide in a 2M aqueous solution of diethanolamine at 25°C. (See section 5.4).

5.3.3. Calculation of acceleration factors for the absorption of carbon dioxide by aqueous diethanolamine when the reaction proceeds reversibly.

Under certain conditions during the absorption of carbon dioxide by aqueous solutions of DEA the reverse reaction and the back pressure of carbon dioxide may become appreciable. This is most likely to occur when the degree of carbonation of the solution is high. The use of the following expressions to predict the chemical acceleration factor under such circumstances has been demonstrated by Dankwerts (43). The applicability of this method to a certain situation can be judged by comparing the interfacial concentration of carbon dioxide to the concentration of free carbon dioxide in the bulk of the solution which is calculated from:

$$C_b = K_c \cdot \frac{\alpha^2}{(1-2\alpha)^2} \qquad (5.39)$$

where C_b = the bulk concentration of free carbon dioxide
K_c = the stoichiometric equilibrium constant for the primary reaction between carbon dioxide and DEA see(section 5.4)
α = the degree of carbonation i.e. the number moles of carbon dioxide asborbed per mole of DEA

Again, as in the case of irreversible second order reactions, under certain conditions the reaction can either be approximated by a pseudo first order or an instantaneous reaction.

5.3.3.1. Pseudo first order reaction

For the reaction to proceed as a pseudo first order reaction the following condition must be satisfied:

$$2. \frac{((C^*-Cb)/Co).(1-\tanh(Ha)/Ha)}{((2.Cb/\alpha.Co)+\tanh(Ha)/Ha)} << 1.0 \qquad (5.40)$$

This condition assumes that no hydrolysis of the carbamate has occured (see section 3.3.6). In such a case the chemical acceleration factor is calculated from:

$$\phi = \frac{(C^*-Cb).(k_L^2+D.k_2.Co)^{1/2}}{k_2 C^*} \qquad (5.41)$$

figure 5.6 Correction to equation 5.32 $\phi_a = 11$

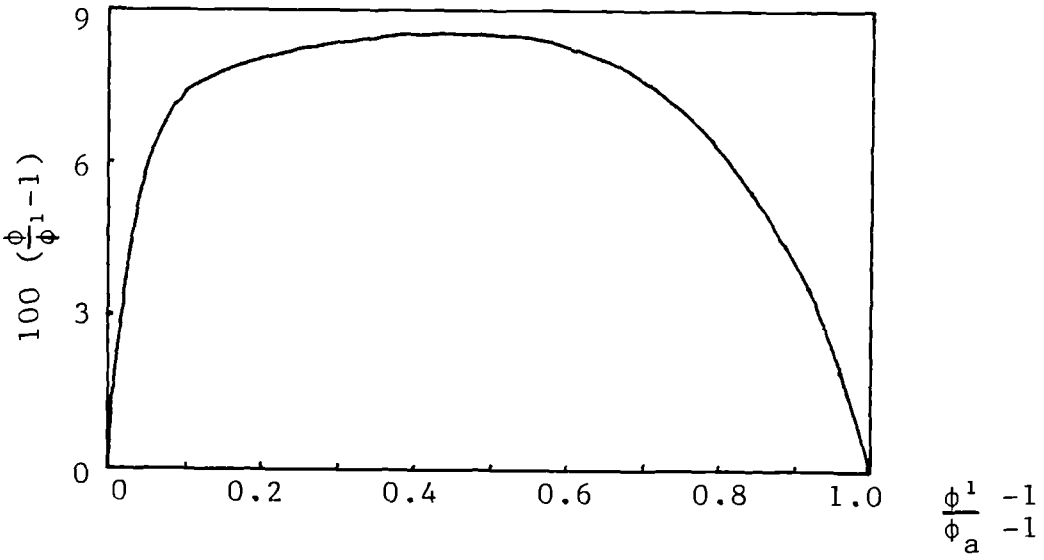

figure 5.7 Correction to equation 5.32 $\phi_a = 21$

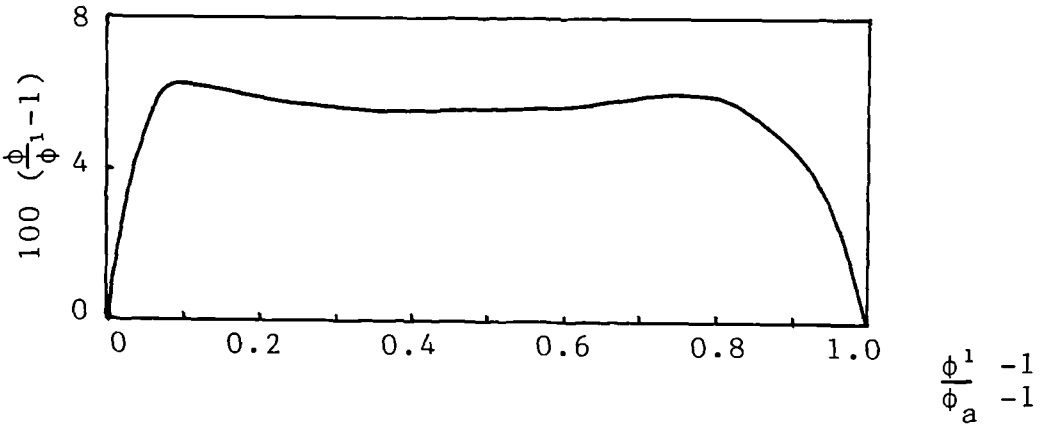

figure 5.8 Suggested method of interpolation between 'psuedo first order' and 'instantaneous' regimes

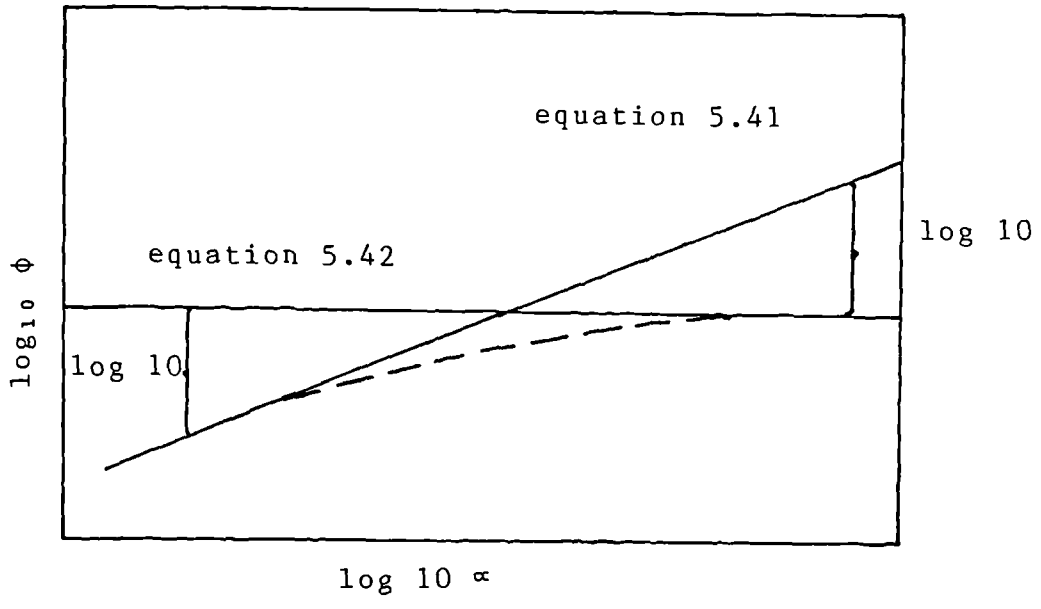

5.3.3.2. Instantaneous reaction

If the right and left hand sides of criterion 5.40 are exchanged it indicates that the reaction is fast enough to proceed instantaneously to equilibrium. In this case the expression for the acceleration factor is:

$$\phi = (1+\delta)\left[\frac{(1+\delta)\ (C^*-Cb)+\frac{M}{2}(\delta[1-2\alpha]-\alpha)}{(1+\delta).C^*+\delta\frac{M}{4}(1-\alpha)}\right] \qquad (5.42)$$

where $\delta = (C^*/K_c)^{1/2}$

M= concentration of DEA before carbonation

This equation was derived by a method similar to that used by Olander (61) and it assumes that the diffusivities of all species are equal. Babak et al (57) state that for diffusivity ratios (D/D_o) in the range 0.3 to 3.0 a value of unity is an acceptable simplification. Thus this method is applicable for a carbon dioxide/DEA system as $D/D_o \simeq 0.37$.

5.3.3.3. General case

When the reaction is intermediate between a pseudo first order and an instantaneous reaction the acceleration factor has to be calculated by a completely graphical method. This involves plotting out equations 5.41 and 5.42 with α as the independant and ϕ as the dependent variable so that a rough interpolation can be made in the manner of figure 5.8.

5.4. Physio-chemical data for mass transfer calculations

5.4.1. Introduction

This section outlines the properties needed to calculate the rates of mass transfer for the absorption of carbon dioxide into water and various amines. Although the only amine solution studied in the present work is an aqueous solution of diethanolamine, the properties of other amines are required so that a comparison of their performance can be made. Such a comparison is useful in indicating the relative merits of the various amines commercially available when used to absorb carbon dioxide. The calculation of the chemical acceleration factors for each amine using the physical mass transfer coefficients obtained for water in the rotary contact machine will suffice as a method of comparison. The methods available for calculating chemical acceleration factors are presented in detail in section 5.3.

5.4.2. Solubility of carbon dioxide in water

The solubility of carbon dioxide in pure water can be calculated by using the following formula to estimate the Henrys law constant H (mole/l.atm) (43)

$$\log_{10} H = \frac{1140}{T} - 5.30 \qquad 5.43$$

This formula is for pressures up to approximately three atmoshperes and thus can be used with confidence in the present work. The temperature (T) is absolute (K).

5.4.3. Solubility of carbon dioxide in amine solutions

To calculate the chemical acceleration factor under a given set of conditions the physical solubility of carbon dioxide in the aq-amine solution is required. Obviously it is not possible to measure by conventional methods the solubility of carbon dioxide in solutions with which it reacts. A first estimation could be its solubility in water at the same temperature and pressure. However the presence of ions in the solution tends to lower the solubility and therefore if reasonably accurate figures are required this must be allowed for. The available information on the solubility of carbon dioxide, oxygen, nitrogen, hydrogen, nitrous oxide etc. in neutral salt solutions, and also theoretical considerations indicate that it may be possible to infer the solubility of carbon dioxide in solutions with which it reacts (62,63). It has been found that the solubility of gases in non-reacting electrolyte solutions can be estimated to within about 10% by the expression:

$$\log_{10}(H/Hw) = -K_s I \qquad 5.44$$

where:

$$K_s = i_+ + i_- + i_g \qquad 5.45$$

and: H = solubility in given electrolyte solution
Hw= solubility in water

I = ionic strength of the solution = half the sum of the quantity obtained by multiplying the concentration of each species by the square of its electric charge (gion/l).
i_+, i_-, i_g = contributions due to cation, anion and gas respectively.

The values of i for carbon dioxide and for various ions at 25°C are reported by van Krevelen and Hoftyner (62). These are reproduced here in table 5.1. The value for the HCO_3^- ion is due to Kothari and Sharma (64). The effect of temperature on K_s is slight and thus the value at any practical temperature may be taken as approximately equal to that at 25°C. For estimating the solubility of carbon dioxide in carbonated amine solutions it can be assumed that the carbamate salt has the same effect as a solution of ammonium bicarbonate of equal molarity and same total N_2 content. Therefore the value of K_s will be due to NH_4^+, HCO_3^- and CO_2 and will thus be 0.031+0.021-0.017 = 0.035. The ionic strength will vary with the degree of carbonation. As two moles of amine react with one mole of carbon dioxide to form one mole of carbamate and if the degree of carbonation is α and the original amine concentration M then the concentration of carbamate (and hence the concentrations of NH_4^+ and HCO_3^-) will be αM. Thus the ionic strength can be calculated as:

$$I_s = 1/2\ ([NH_4^+].1+[HCO_3^-].1) \qquad 5.46$$

$$I_s = 1/2\ (2\alpha M) \qquad 5.47$$

$$I_s = \alpha M \qquad 5.48$$

Therefore the solubility of carbon dioxide in an aqueous solution of diethanolamine is a function of the degree of carbonation and will decrease as the edge of the rotating disc is approached. This method will estimate the solubility to within 30% (43)

5.4.4. Diffusivity of carbon dioxide in pure water

A considerable amount of information is available on the diffusivities of dissolved carbon dioxide in water. For the purpose of this work a graph of diffusivity against temperature for the range 10-45°C prooved convenient (44). This is reproduced as figure 5.9.

5.4.5. Diffusivities of amines in pure water and aqueous solutions

The diffusion coefficients of ethanolamines in aqueous solutions have been measured at 25°C by Thomas and Furzer (65. Figure 5.10 shows their results for mono-, di- and tri-ethanolamine. At temperatures other than 25°C Dankwerts (43) suggests that values can be calculated with reasonable accuracy if it is assumed that the variation is approximately the same as that of carbon dioxide in water. Therefore figure 5.9 can be used to calculate the magnitude of the temperature dependence.

figure 5.9 The diffusivity of carbon dioxide in water at various temperatures

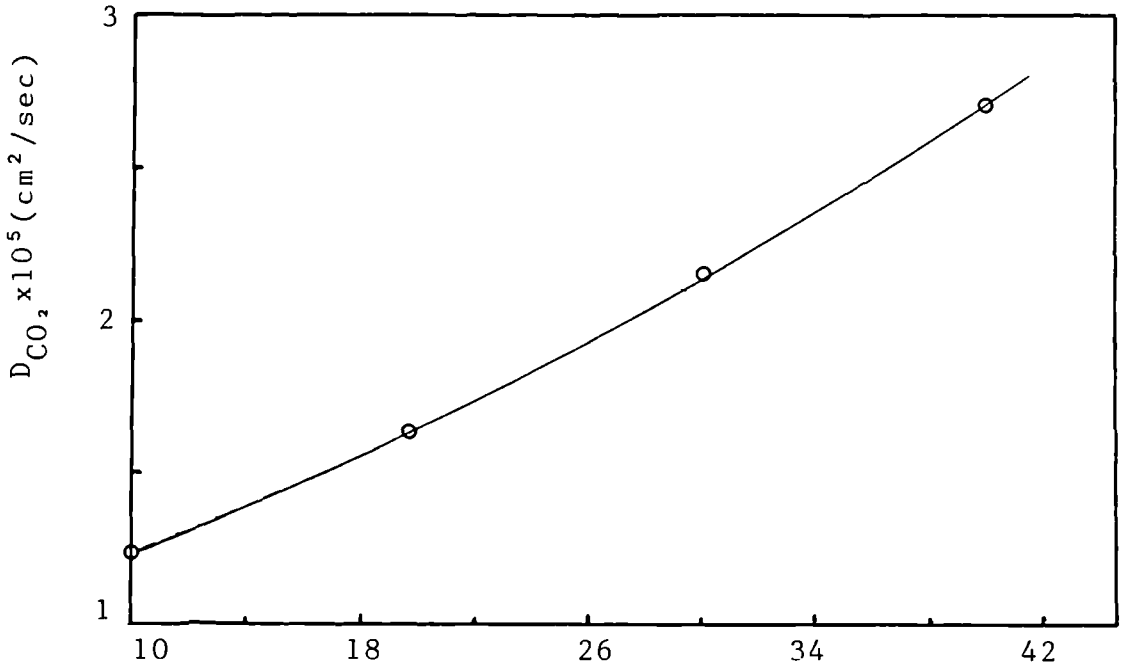

figure 5.10 Diffusivities of amines in water (25°C)

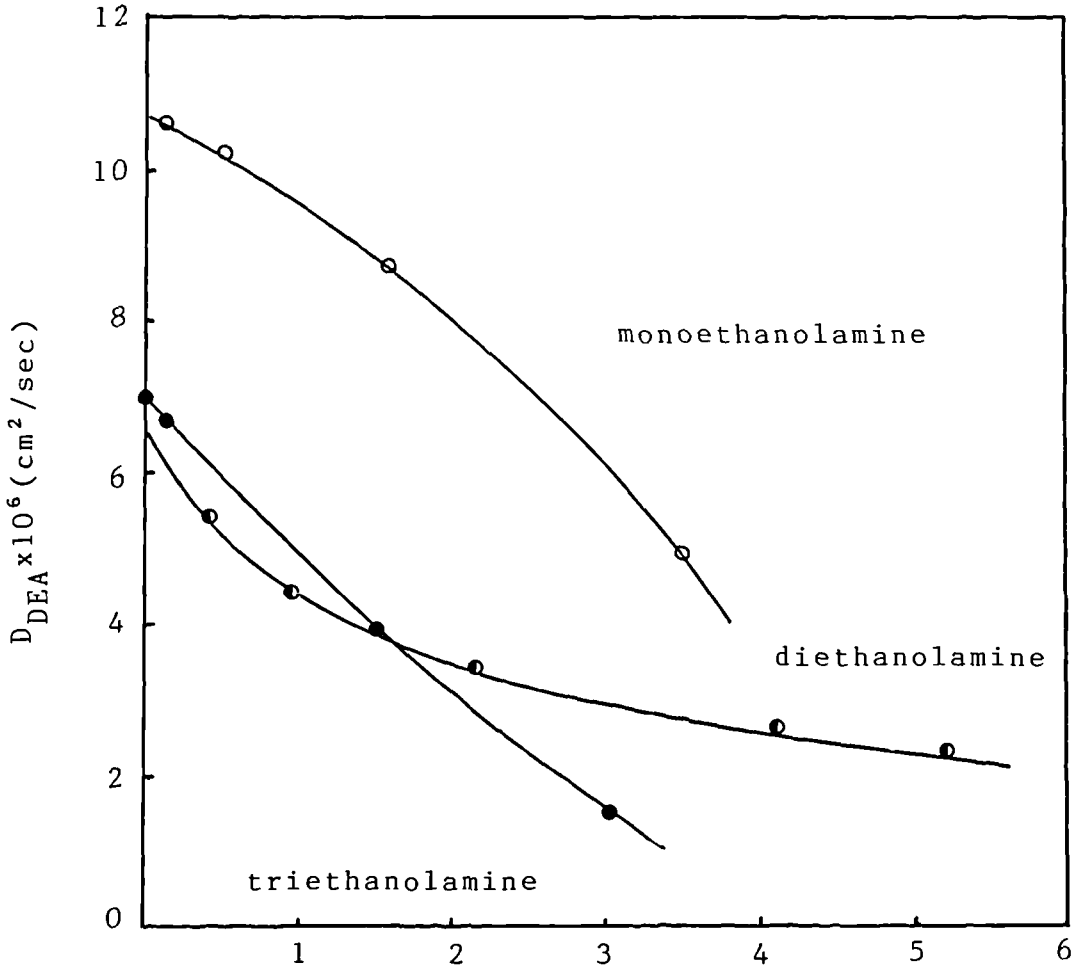

5.4.6. Diffusivity of carbon dioxide in aqueous solutions of ethanolamines

It is impossible to measure the rate of diffusion of carbon dioxide through solutions with which it reacts. However the diffusion coefficient can be estimated if it is assumed that the degree of reduction is equal to the proportional ratio of the diffusivities of the relevant ethanolamine in the appropriate aqueous solution to that in pure water (43). This ratio can be calculated by using figure 5.10 and applied to the value of the diffusivity of carbon dioxide in pure water taken from figure 5.9.

5.4.7. Reaction rate constants

The reaction of carbon dioxide and amines (including diethanolamine and aqueous solutions of diethanolamine) is discussed in detail in section 3. . As stated, there is some disagreement whether the reaction of DEA + carbon dioxide is second or third order. Before 1977 it was generally accepted that the reaction was second order as MEA, that is first order in carbon dioxide and first order in the ethanolamine, thus

$$\text{rate of reaction (mol/l.s)} = k_2[Am][CO_2] \qquad 5.49$$

where k_2 is the second order rate constant for the amine (l/mols) and [Am] is the concentration of the ethanolamine (mol/l). ([Am] is equivalent to the term C_b^0 used to denote the bulk concentration of reactant used in section 5.1). Sharma (66,68) and Jenson, Jorgensen and Faurholt (67) have reported rate constants for MEA and DEA assuming the reaction to be second order. The values are presented in table 5.2. The data for MEA agree reasonably well. However, the value for DEA obtained by Sharma is much less than that reported by Jensen et al. The reason for this discrepancy is not clear. The available information in the literature (43) on the absorption of carbon dioxide into aq. DEA solutions indicates values nearer to those of Sharma. Values for the ethanolamines MEA, DEA, MIPA and DIPA are reported in table 5.3. Hikita et al (56) in 1977 measured the homogeneous reaction rate of carbon dioxide with DEA and found that the reaction was third order; that is first order with respect to carbon dioxide and second order with respect to DEA, thus

$$\text{rate of reaction (mol/ls)} = k_3 [Am]^2 [CO_2] \qquad 5.50$$

where k_3 is the third order rate constant. Hikita et al reported a value of 1270 ($l^2/mol^2 sec$) at 25°C.

5.4.8. Stoichiometric equilibrium constants

A value of the equilibrium constant of the fast reaction (see chapter 3) is required so that the concentration of free CO_2 in the bulk of the solution can be calculated. Values of K_c where

$$K_c = \frac{[R_2NH]^2[CO_2]}{[R_2NCOO^-][R_2NH_2^+]} \qquad 5.60$$

are given in table 5.4 below (69).

Table 5.1 Data for the computation of Ks (equation 3)

Species	i(ℓ/gion)
Na^+	0.094
K^+	0.071
NH_4^+	0.031
$CO_{3=}$	0.021
SO_4	0.021
OH^-	0.061
HCO_3^-	0.021
CO_2	-0.017

Table 5.2 2nd order reaction rate constants at 18°C

k_{MEA}	4700	5100	(ℓ/mol sec)
k_{DEA}	5800	1000	(ℓ/mol sec)

Table 5.3 Rate constants for the reaction between carbon dioxide and some amines used industrially (from 7,8,9,11) (k_2 = ℓ/mol.sec)

Amine	Temperature (deg)C					
	15	20	25	30	35	45
MIPA	3500	4750	6620	7950		19500
DIPA	230		400		680	
MEA		5100*	7600		13000	
DEA		1000*	1500		2500	

(* 18°C rather than 20°C)

Table 5.4 Stoichiometric equilibrium constants for various amines

Amine	k_c (mole/ℓ) at 20°C
Ammonia	1.5×10^{-4}
MEA	9.0×10^{-6}
DEA	2.3×10^{-4}

6.0. METHODS OF ANALYSIS

6.1. General introduction

The operating characteristics of a mass transfer device are determined by constructing a mass balance around the system. This section outlines the analytical techniques used, during the present investigation, to enable such a balance to be calculated.

A mass balance can be calculated by measuring the concentrations of the component in the gas or liquid phases. Ideally both should be prepared as a check of the analytical techniques used, and, assuming they are within an acceptable margin of each other, the average taken. In general it is more difficult to collect and analyse gas samples accurately than it is to consider the liquid phase. This is particularly true in a system which employs a rotating surface. In the present investigation the feed gas enters at the centre of the device and leaves at the periphery. Hence it is difficult to collect a representative sample without having to install some form of complicated seal around the central drive shaft. An insitu, on-line measurement technique would have been suitable for the cases where the feed gas did not consist of pure carbon dioxide (i.e. carbon dioxide/nitrogen mixtures) but the space available for such a device was limited. Therefore the mass balance for the present investigation was prepared from liquid side measurements only.

Three individual analysis methods were needed to prepare mass balances for the systems in the experimental rig. The following sections discuss these in detail. The first of these deals with a technique associated with the water/carbon dioxide system while the other two consider the DEA/carbon dioxide system. Section 6.2 considers the methods available for measuring the concentration of dissolved carbon dioxide in water. Section 6.3 discusses similar techniques where water is replaced by aqueous DEA solutions. The same analysis method could not be used as carbon dioxide is chemically rather than physically combined in the latter system. Section 6.4 outlines methods of calculating the DEA concentration of an aqueous ethanolamine solution. Each of these subsections contains a review of methods used by previous investigators concerned with the relevant system, followed by comprehensive details of the method chosen. In each case the effect of solution regeneration on the chosen analysis technique, is discussed.

6.2. Determination of the concentration of carbon dioxide in water

6.2.1. Introduction

In order to calculate a mass balance for the system carbon dioxide/water the concentration of dissolved gas in the outlet liquid stream had to be measured. This section discusses the analytical techniques available and indicates why the method chosen was the most suitable. Details of this prefered technique are then presented.

Numerous methods have been published in the literature, and these can be divided into four main categories, i.e.

-graviometric methods
-titrative techniques
-pH/alakalinity measurements
-gas sensing electrodes

This section compares and considers the merits of each type of technique by discussing specific examples as well as the results of comparative investigations. This discussion is not intended to form a comprehensive review of this extensive topic but rather to act as a guide to the methods available and to their usefulness with respect to the present investigation.

6.2.2. Review of methods available

The most commonly used method of measuring the carbon dioxide concentration of water has been titration to the phenolphalein end-point with NaOH or Na_2CO_3, while the alkalinity is determined by titration to the methyl orange end-point with dilute HCl. The alkalinity of the sample is required so that the fraction of carbon dioxide present as the carbonate can be calculated. The end-points of both titrations are sensitive to the concentration of other solutes (75) and thus numerous attemps have been made to modify this method in order to obtain more accurate results (76-79). Hammerton and Garner (80) and Rogers (81) found that these methods were unsatisfactory, the measured results being subject to high systematic errors. These errors were generally due to the low hydrolysis of carbon dioxide.

For low concentrations of carbon dioxide, the solution can be stripped of gas which is then reabsorbed into a smaller volume of an absorbent liquid. Stripping is achieved by the acidifcation of the sample and Barium hydroxide is frequently used to absorb the evolved gas. The residual hydroxide is then estimated by titration (82,83). British standard method 1 (84) recommends that evolved carbon dioxide is re-absorbed in a solution of sodium hydroxide which is then titrated to methyl-orange and phenophthalein end points with dilute sulphuric acid. This graviometric method has found some popularity but its use is limited by the length of time required for a single analysis ($\simeq$ 1 hour) and the high risk of contamination which is a result of the amount of handling needed (85).

The same general principle is employed in a method in which the dissolved carbon dioxide was extracted from a sample of water and the gas then introduced in suitable quantity and concentration for analysis by a gas chromatograph. Gaunt and Shanks (86) acidified with sulphuric acid and boiled for 20 minutes under reduced pressure to evolve carbon dioxide which, after drying, was carried into a chromatograph by hydrogen which acted as the carrier gas. The quantity of gas was thus estimated directly. Warner (87) injected 0.2cm^3 of aqueous solution into a pre-column packed with pre-dried, 8-12 mesh calcium sulphate which evaporated the solution and released the absorbed carbon dioxide. The gaseous sample was then carried into a seperation column packed with silica gel by a stream of helium. The concentration of carbon dioxide was calculated from a measurement of the 'peak'height recorded by a D.C.L. microkatharometer.

Rogers (81) warns that these methods are only suitable for solutions which have a negligible alkalinity. Park et al (88) compared a gas chromatographic method for measuring the carbon dioxide content of sea water with the pH/alkalinity method. The gas chromatographic method was based upon a technique described by Swinnerton et al (89) and used a single silica gel column. They reported a good reproductability (0.7%) in five consecutive readings.

The pH method is described in detail by Harvey (90) and relies on measurement of pH alkalinity, salinity, inorganic boron concentration and the temperature of the sea water, together with a knowledge of the dissociation constants of carbonic and boric acid in sea water. Under ideal conditions a standard deviation of ±1% was obtainable from this method. The authors concluded that the former method was more convenient and should proove more useful than pH/alkalinity methods in routine oceanographic, limnological and water polution works.

Other pH/alkalinity methods have been published (91,92, 17) and the reliability of this general technique has been discussed by Rogers (81). He concludes that provided a good quality glass electrode is employed and the dissociation constants used are correct, the method should produce accurate results. Any errors that are found tend to be caused by small amounts of carbon dioxide escaping from the sample before it can be analysed. The method developed by Perciful (17) and used by Watts (6) in his mass transfer investigations is one which is based upon pH/alkalinity measurements. This employs an equation developed by Perciful to calculate the total carbon dioxide content and which relies on a knowledge of the volume of acid used in the pH titration, the volume of base added to the sample to absorb all free CO_2 in solution the pH of the sample and the analysis temperature. These were read into an IBM1620 computer along with polynomial descriptions of the equilibrium constants (as functions of the temperature) and the carbon dioxide concentration was thus calculated. Perciful found that this method could be used with confidence and as it is very similar to those considered by Rogers (81), it has to be concluded that the discrepancies in Watts' results (see section 2) cannot be linked with the experimental method. It is possible that the errors could be associated with the sampling method used if this allowed some, or all, of the free carbon dioxide in solution

to escape. The sampling method used by Watts is not discussed in sufficient detail to allow the formation of any definite conclusions.

The most convenient method for measuring the carbon dioxide content would be one which required a small volume of sample and where the time required to analyse the sample was a minimum. Obviously, an on-line, insitu measurement technique would be ideally suited. A simple and elegant method which meets these specifications is one based upon the measurement of the pH of the solution, a technique commonly used in blood analysis for dissolved carbon dioxide. Venkataraman (3) found that it was possible to modify this method so that he could estimate the dissolved carbon dioxide in water rather than in blood. The method, as outlined in Venkataraman's thesis, makes use of a Severinghaus (93) carbon dioxide electrode which is primarily a pH glass electrode arranged to measure the pH of a very thin film of aqueous sodium bicarbonate solution. This is seperated from the sample solution by a Teflon membrane which is only permeable to carbon dioxide molecules. The result of carbon dioxide diffusing through the membrane is a lowering of the solution pH due to the formation of carbonic acid. A calomel reference electrode is in contact with the electrolyte and the pH of the bicarbonate layer is determined by measuring the potenetial between the electrodes. There is a logarithmic relationship between the pH and the partial pressure (or concentration) of the carbon dioxide. It was found necessary to regulate the temperature of the system by circulating water from a thermostatic bath through an enveloping jacket. This temperature control was essential because of the large temperature dependancy of the electrode potential.

Since Venkataraman's investigation a number of gas sensing electrodes have become available commercially. These include an electrode for determining the concentration of carbon dioxide in aqueous solutions. The performance characteristics of these gas-sensing membrane probes has been studied by Bailey and Riley (94). They paid attention to the calibration and detection limits, the response speed, the osmotic effect associated with the concentration gradient across the membrane, the selectivity of the probes to other ionic species and the effect of temperature on the response. In addition they considered methods of using probes in continuous flow analysis and recommended ways in which a standard analytical procedure could be developed. They concluded that gas-sensing membrane probes offered a much faster analysis technique than older methods and one which could be used as accurately as pH/alkalinity measurements. Midgley (85) investigated the use of gas-sensing membrane electrodes in the determination of carbon dioxide in power station waters. He concluded that the best of these devices can be used to provide accurate measurements of dissolved carbon dioxide concentration in an on-line situation with only infrequent calibration. He compared the probes with pH/alkalinity, gas chromatographic and graviometric methods to demonstrate the convenience of a method based upon gas-sensing electrodes.

Considering the convenience, reliability and accuracy of the above methods it was decided that a gas-sensing electrode would provide the basis of the analysis technique used in the

present investigation. The following section describes the construction, theory and operation of the carbon dioxide sensing probe chosen. Details of how the probe was installed in the rotary test rig can be found in Chapter 7.

6.2.3. The application of gas sensing, membrane probes

The electrode used to measure the concentration of dissolved gas in the outlet liquid stream was a carbon dioxide gas sensing membrane probe manufactured by EDT Research. The operation of this is identical to the 'Severinghaus' electrode adapted by Venkataraman (3). This was described in detail in the preceeding section. It is a combination electrode and thus consists of an electrode pair. The sensing membrane is a flat faced glass pH electrode and the reference electrode is a silver/silver chloride wire. The electrode pair is sperated from the sample solution by a gas permeable membrane. The junction between the two electrodes is completed with a filling solution containing carbonate ions. When the membrane (which is fixed into a detachable cap) is tightened against the glass electrode, a thin layer is produced and this thin layer acts as a sensor responding to changes in the partial pressure of carbon dioxide in the sample solution.

The electrode was supplied with a flow-through cell which could be screwed onto the membrane cap to facilitate on-line measurements. Since the probe had a temperature coefficient of 1-2mV/°C it, and the attached flow-cell were immersed in a constant temperature bath to avoid any errors associated with this effect. Using standard solutions to calibrate the device, steady consistent readings could not be obtained with the electrode contained in this set-up. The response of the electrode itself was checked by removing it from the flow cell and dipping it in a volume of solution. As a steady reading was attained it was concluded that the electrode was functioning correctly and that the membrane was not leaking. Thus as the liquid bath removed all temperature effects it seemed likely that the inaccuracies were a result of using the flow cell. Inspection of the flow cell revealed that with the electrode in position the membrane touched the back of the cell. Tests showed that this caused the membrane to leak which resulted in a steady drift of the mV reading This screw on flow cell was therefore not used during the mass transfer experiments. An alternative flow cell was designed and constructed from perspex. This is described in detail in section 7.

The electrode was calibrated by measuring the response associated with solutions of known carbon dioxide concentration. These were formed by delivering equal flowrates of a standard sodium bicarbonate solution and a 0.1M solution of sulphuric acid to the flow cell. The acid caused the carbonate ions to oxidise, thus forming a known concentration of free carbon dioxide. The electrode response corresponding to this concentration was noted. The Nernstian range of operation of the probe is with solutions with a dissolved carbon dioxide concentration of between 10^{-4} and 10^{-2} moles/litre (i.e. 4.4 to 440 ppm) and thus the calibration was prepared with solutions in this range. Since the response over this range is Nernstian, only two points are required to determine the calibration curve. In practice three solutions were employed to reduce the possibility of error. These sodium

bicarbonate solutions had concentrations of 2×10^{-2}, 2×10^{-3} and 2×10^{-4}M, thus when mixed with equal volumes of acid formed 10^{-2}, 10^{-3} and 10^{-4}M solutions of free carbon dioxide respectively.

Midgley (85) recommended that gas sensing probes should be re-calibrated at regular intervals and concluded that when they are in constant use this duration should be no greater than six hours. During the mass transfer experiments one run was completed each day and it was decided that the calibration should be repeated before the start of each new run. After a number of runs it became apparent that the gradient of the calibration curve remained constant although the position of the calibration points varied. Thus only one standard solution had to be analysed to determine the calibration chart. The 2×10^{-2}M solution was chosen since, this was the nearest to the concentration of the outlet liquid stream, therefore the accuracy of this point was the most crucial.

The outlet carbon dioxide concentration corresponding to the liquid flowrate, rotational speed, radial position and disc surface used was calculated from the associated mV reading and calibration by the computer programme DATA-AN. This is listed in Appendix I.

Once the design of the liquid flow cell had been improved the performance of the gas sensing probe was very satisfactory. On average a steady, (mV) reading was obtained in less than 5 minutes following the change of a system parameter. The dependancy of the probe response on the liquid flow rate through the cell was investigated by varying the delivery rate from 3 to 100 ml/min. This had no effect on the output mV signal, thus a high flow rate was used since this minimised the response time of the probe (by reducing the time required to flush out the flow cell). The accuracy of the probe was demonstrated by Swanson (95). He used the analysis technique and apparatus developed in the present investigation to measure the concentration of carbon dioxide in an electrolyte solution containing sodium carbonate. The results of these tests were within 5% of accurate theoretical predictions.

6.3. Determination of the concentration of carbon dioxide in an aqueous ethanol amine solution

6.3.1. Introduction

The methods outlined in the previous section can not be used to measure the outlet carbon dioxide concentration when the liquid phase is changed from water to aqueous solutions of diethanolamine, since these methods rely on the physical presence of carbon dioxide molecules in solution. When carbon dioxide is absorbed into aqueous diethanolamine solutions it reacts with the ethanolamine to form the carbamate. This reaction scheme was discussed in chapter 3. Therefore, in order that the liquid-phase mass balance can be calculated, a technique is required to measure the acid-gas loading of an ethanolamine solution. In addition, as the amount of DEA available is limited, such a technique cannot use large samples which are destroyed during the analysis. Again, an on-line technique, if available, would provide the most convenient method of analysis.

This section reviews methods presented in the literature to calculate the acid gas loading of various ethanolamine solutions. In addition it shows how these were used in the development of an analysis technique applicable to the present research. This technique is then described in detail.

The analysis techniques considered can be conveniently seperated into two categories. The first deals with methods which remove the absorbed carbon dioxide from the solution by reversing the absorption reaction. The volume, or weight of the gas evolved is then measured to calculate the acid gas loading. These methods vary in the way that the carbon dioxide is evolved and in the way that the evolved gas is monitored. Such techniques are considered in the section dealing with 'physical methods'. The second category contains 'indirect' methods of measuring the acid-gas loading of a solution. In such techniques a property of the solution that is affected by the amount of carbon-dioxide absorbed is measured. This is then used to infer the acid-gas loading from calibration curves prepared by using samples of known carbon dioxide concentration. These methods are only practical if the measured property is a function of the loading throughout the whole range of interest. Additionally, the variation of the property must be significantly greater than the inaccuracy inherent in its measurement.

6.3.2. Physical methods

A considerable amount of work has been published concerning the use of a titration method to measure the acid-gas loading of carbon dioxide/ethanolamine solutions. Much of this is due to Mason and Dodge(70), who studied the equilibrium solubility of carbon dioxide in various ethanolamines. They considered a number of methods. These included those involving differential titration (where two indicators were used) and methods where the carbamate ion was precipitated as barium carbonate. They came to the conclusion that accurate, consistent results could not be obtained by any of these methods. A number of other researchers, working in the same field, reached similar conclusions. These include Reed and Wood (71) and Lee, Otto and Mather (72). However a number of other papers concluded that methods involving titrations could be used accurately. Fournier and Philbert (96) prepared equations for the absorption of carbon dioxide by three ethanolamines including DEA. They measured the concentration of carbon dioxide by a method which involved the precipitation of barium carbonate via the addition of barium acetate. This, they reported, gave results within 0.5% of the theoretical value. Jones et al (74) also used a technique involving the precipitation of the carbamate ion as the barium salt, although they used barium chloride to achieve this effect. They reported that this method could be used with reasonable success. However, they expressed a preference for a method which was first outlined by Mason and Dodge (70).

This method is a slight modification of an analytical technique for determining the concentration of carbonate ions in natural, solid carbonates such as chalk, limestone and feldspar. This standard technique is described in most texts dealing with analytical tests (e.g. (97)) briefly outlined in Appendix B. Mason and Dodge (70) showed that with only slight modifications to the apparatus, carbonated solutions of ethanolamines could be used instead of solid samples. The basic principle of the method is to evolve the carbon dioxide absorbed in the solution by addition of a concentrated acid to the sample. The gas evolved is then forced to flow through a suitable absorption train during which all pollutants are removed. Thus all that remains is pure carbon dioxide. This is then re-absorbed into a known weight of a suitable solution. Therefore the change in weight of absorbent is equal to the amount of carbon dioxide evolved from the acidified sample. If the volume and normality of the sample are known then its carbonation ratio (i.e. mols of carbon dioxide/mols of diethanolamine) can be calculated.

This general technique has been widely adopted, especially by research groups measuring the equilibrium solubility of carbon dioxide in aqueous ethanolamine solutions. However, the ways in which it has been modified to produce a practical analytical method vary between individual groups. Such variations are probably due to the use of different original source texts and the availability of materials and equipment. A selection of these methods are presented below.

•Mason and Dodge (70) used sulphuric acid to acidify the ethanolamine and ascarite to absorb the evolved carbon dioxide.

To insure against any change in weight of the ascarite tubes due to moisture, tubes containing calcium chloride and phosphorus pentoxide were placed ahead of the ascarite. Phosphorus pentoxide was also placed in one limb of the ascarite tube itself. They showed that by paying careful attention to small details, accurate results could be obtained. The method was tested by absorbing a known amount of carbon dioxide in a standard solution of DEA. This was then acidified to check that the same weight of gas was evolved.

•Reed and Wood (71) also used suplhuric acid but rather than measure the change in weight of a carbon dioxide absorbent they collected the evolved gas in a burette. After correcting the volume to standard conditions they reported their results as the volume of carbon dioxide per volume of solution.

•Jones et al (74) swept the liberated carbon dioxide from the reaction flask with nitrogen and passed it in series through a drying tube and a tarred absorption tube containing Caroxite. They reported that this method gave more consistent results than using barium carbonate precipitation.

•Jeffrey and Kipping (73) acidified their samples with concentrated phosphoric acid and boiled the mixed solutions. The amount of gas evolved was measured using a gas chromatograph containing a 2ft activated charcoal column with helium as the carrier gas.

•Layan and Lelong (98) used concentrated sulphuric acid and detected the carbon dioxide evolved by ultra-violet and infra-red photometry. They noted that the second detection system provided the most consistent results.

•Carmasi et al (99) described an apparatus for detecting acid gasses, especially hydrogen sulphide and carbon dioxide, in basic solutions such as aqueous ethanolamines. The equipment worked by super heating a constant volume of solution at a constant temperature and pressure. The volatized acid gas was seperated from any water vapour or gasses volatized from the basic components of the sample, by condensation. It was then measured by using either a flow meter or a katharometer (hot wire detector).

•Koci and Jelinek (100) used sodium hydroxide to absorb carbon dioxide liberated by sulphuric acid. Any pollutant gasses evolved were removed by a suspension of chromium oxide in concentrated sulphuric acid. The operations were performed in a modified Orsat apparatus.

•The dow gas conditioning handbook (101) outlined a method that involved the acidification of the sample but measured the evolved gasses by titration of the absorbent solution with known standards. Again this titration method was one which relied on the precipitation of barium carbonate from a soluble barium salt (in this case the hydroxide). The apparatus could also be used to measure the concentration of DEA in the aqueous solution and determine the quantity of hydrogen sulphide present. This paper gave more details concerning the apparatus and reagents used

than those mentioned above and was therefore more useful when constructing such equipment. In addition it outlined a step-by-step experimental procedure to be used with the apparatus.

These analytical techniques can be used to produce accurate measurements of the acid gas loading of aqueous ethanolamine solutions. However, in general, they require large samples (which are destroyed during analysis), are very time consuming (taking approximately one hour per reading), can produce large errors if the experimental method is slightly inaccurate, and can not be used on-line. In these respects they do not conform to the requirements of the present investigation outlined as above.

The technique of evolving chemically combined carbon dioxide by acidifying the solution is also used by Pearce et al (102). They outlined a method for determining the acid gas loading of ethanolamine solutions using a gas chromatograph. This is based on a similar technique discussed in the Dow gas conditioning handbook (101). The authors used a Hewlett-Packard model 5880 chromatograph fitted with a thermol conductivity detector. The seperation column consisted of a 10ft long, 1/8" diameter thin walled stainless steel tube packed with Teflon substrate which had been coated with Oronite NI-W. This was held at 120°C to insure the quantitative release of carbon dioxide from the injected sample. The authors found it necessary to pretreat the column with an injection of 1:1 hydrochloric acid between every fourth sample. This insured that sufficient acid was absorbed on the column inert carrier to neutralize the ethanolamine. The output signal from the hot-wire detector was plotted by a chart recorder. The trace produced was used to determine the carbonation ratio of the injected sample. In order to analyse the trace the area below the peak associated with the acid gas had to be calibrated. This was done by determining the peak area produced for samples of known carbonation ratio. The authors used an apparatus similar to that described above (101) to determine the carbonation ratio of these standard solutions. Using this technique reliable results could be obtained. This method uses very small samples and once the initial calibration has been performed does not take a great deal of time to perform. In these respects it is more attractive than the previous technique. However it still can not be used to produce on-line readings and if many samples are to be analysied the need to pretreat the column causes the operation to be quite time consuming.

6.3.3. Indirect methods

When carbon dioxide is absorbed by an aqueous ethanolamine solution it reacts to form the appropriate carbamate. If, as a result of this, a measureable property of the solution is changed, its magnitude can be used to infer the amount of carbon dioxide absorbed. This is refered to as an 'indirect' method of analysis. The applicability of such a method to a particular system is dependent on it successfully fulfiling a number of criteria. Firstly, the property of the solution measured must be a function of the gas loading throughout the operational range of the system. Secondly, the variation of the property with a small change in the carbonation ratio must be significantly greater than the inaccuracies inherent in the measurement technique used. Finally, a method must be available to measure the actual acid-gas loading of a series of specially prepared standard solutions so that a calibration curve can be produced. If these criteria can be met then an 'indirect' method can form an ideal on-line analysis technique provided the relevant solution property can be recorded continuously. Properties particularly suitable for this purpose are temperature, refractive index and pH. This section considers each of these properties with respect to the system carbon dioxide/aqueous diethanolamine.

The reaction of diethanolamine and carbon dioxide is exothermic thus the temperature of the reaction mixture is a function of the amount of gas absorbed. Therefore in principle, if the change in temperature is measured and the enthalpy of the reaction known, the acid gas loading can be calculated. However this only applies to a closed system. In a real system a certain fraction of the heat of the reaction will be lost, either to the gas phase, the equipment or the atmosphere. Thus a measurement technique based upon temperature would be difficult to calibrate accurately. No reference to such a technique could be located in the literature.

To investigate how the refractive index of the ethanolamine/water solution changed as a function of the gas loading a number of test solutions were prepared. Carbon dioxide was bubbled through a measured weight of a standard DEA solution for a certain length of time. Its new weight was measured and the approximate gas loading calculated. The refractive index of the sample was measured and recorded. The sample was analysed as soon as it had been prepared to minimise the amount of gas rediffusing from solution. This investigation was undertaken using fresh diethanolamine as well as a solution which had been regenerated in the equipment described in Appendix A. The results showed that the change of refractive index with carbonation ratio was small. Additionally they indicated that the process of regeneration altered the refractive index significantly. Therefore in order that this property could be used to measure the degree of carbonation a new calibration curve would have to be produced after each regeneration. Again no reference to an 'indirect' method based upon refractive index could be found in the literature.

Ethanolamines are basic and therefore the reaction with carbon dioxide (an acid gas) tends to neutralise the solution. Kohl and Risenfeld (103) discuss the pH of various ethanolamines,

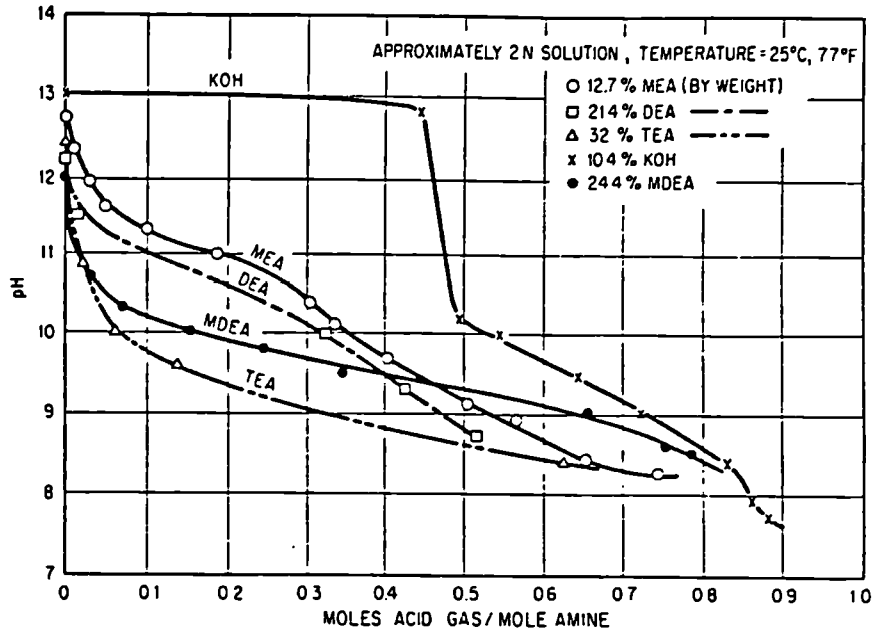

figure 6.1 Titration curves showing pH during neutralization of ethanolamine and KOH solutions with CO_2 (7)

figure 6.2 pH values of aqueous mono- and diethanolamine solutions (6)

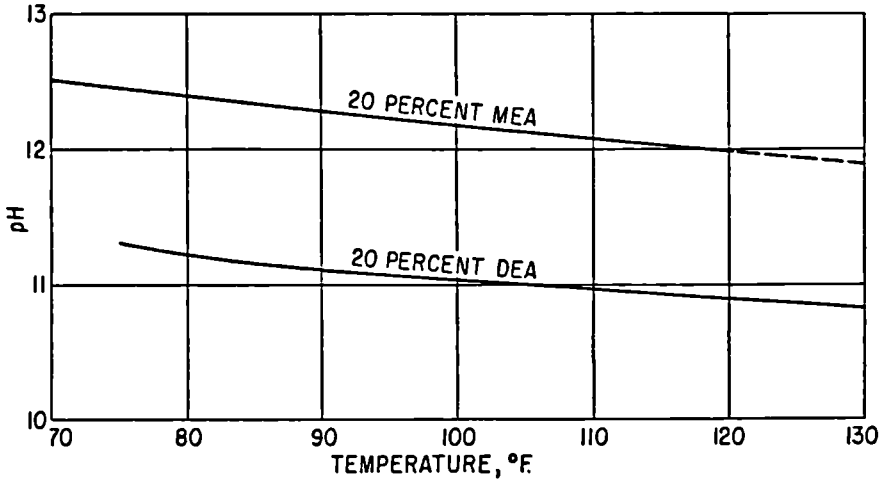

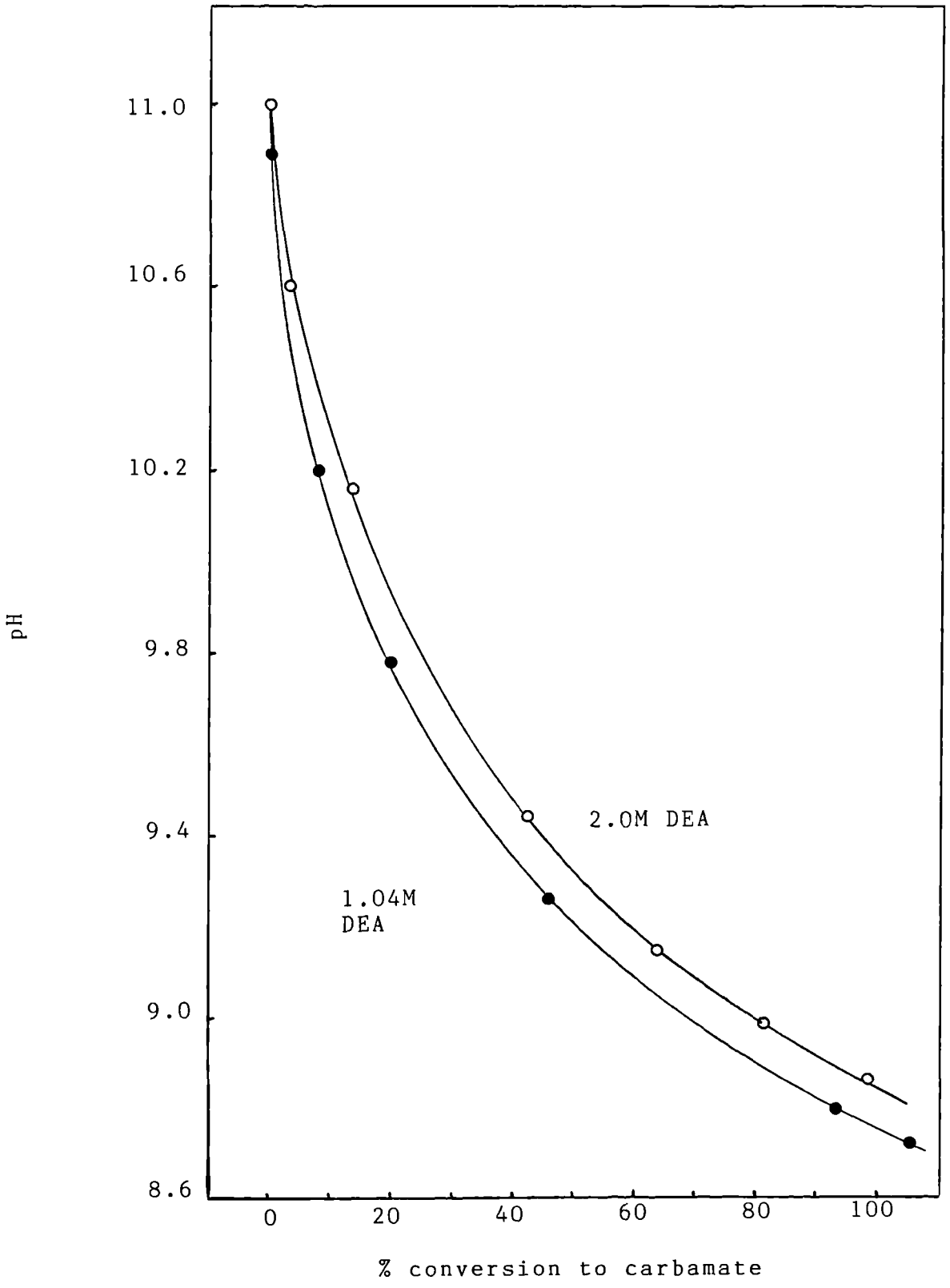

figure 6.3 pH vs per cent conversion for 1 and 2 Molar DEA

including DEA. They showed that the pH of an ethanolamine solution was a function of the degree of carbonation and presented a graph of pH against carbonation ratio for a 2N solution (see figure 6.1). This graph was produced from measurements made by bubbling pure carbon dioxide through the aqueous solution. Periodically the pH and carbonation ratio were determined. The curve produced did not show a sudden end-point characteristic of neutralization reactions involving inorganic bases. The authors interpreted this behaviour as an indication of the presence of non-ionized species during neutralization. Over the range of carbonation ratios of interest (0 to 0.5) the pH of the DEA solution varied from approximately 12.0 to slightly less than 9.0. Also included was a graph showing the temperature dependance of a 20wt% DEA solution (see figure 6.2). The pH of such a solution varied from 11.3 at 75°F to 10.8 at 130°F. Cryder and Maloney (104) studied the rate of absorption of carbon dioxide in aqueous diethanolamine solutions. They found it desirable to use an on-line technique to monitor the concentration of carbon dioxide in solution. The method they adopted was to measure the pH of the solution and produce a calibration curve using the method outlined by Mason and Dodge (70) (as discussed in section 6.3.2). They found that it was necessary to alter this calibration curve to allow for the change in solution pH caused by the regeneration process. The calibration curve for pure solutions is presented in figure 6.3. A number of other papers, discussing an analysis technique based upon pH measurement, have been published in the Soviet Union. Translations of these, are not available. A limited amount of information, however, was extracted from the relevant abstracts. Kovalenk et al (105) studied the effect of various factors on the pH of aqueous solutions of ethanolamines. These included temperature, initial ethanolamine concentration, the degree of carbonation and the presence of impurities caused when regenerating the solution. They reported that the pH was a linear function of temperature between 20 and 90°C. More importantly they concluded that resinous substances formed during the regeneration of the solution had a pronounced effect on the pH. The effects found for the other factors were not reported in the abstract. Volodin et al (106) developed this research by preparing a polynomial description and nomogram for determining the pH values of carbonated solutions. They used a method involving mathematical experimental planning and obtained the dependancy of pH on temperature and solution carbonation. Although the polynomial was reproduced in the abstract it did not state to which ethanolamine it applied nor provide values for two constants contained in the equation.

Measurement of solution pH provides the most suitable indirect method for determining the concentration of absorbed carbon dioxide. However its use is, limited by the need to recalibrate each time the diethanolamine solution is regenerated. This reduces the convenience of this method by necessitating regular measurements using a physical method.

In essence the gas-sensing membrane probe used during the water experiments provides a further indirect method for use with the aqueous diethanolamine system. For alkaline solutions (re. where the dissolved carbon dioxide is in the form of carbonate ions), acid can be delivered to the flow cel during the analysis of the sample as well as during the calibration process. Therefore the

absorbed carbon dioxide is released, and its partial pressure is measured as described previously. This technique therefore destroys the samples delivered to the flow cell and thus was considered impractical in the present investigation.

6.3.4. The application of gas chromatography to the measurement of the concentration of absorped carbon dioxide in aqueous diethanolamine solutions.

6.3.4.1. Introduction

As a result of the preceeding investigation a gas chromatographic method was chosen as the analysis technique for measuring the concentration of absorbed carbon dioxide in the aqueous DEA solutions. Although this method does not conform to all the requirements outlined in section 6.1 it was considered to be the most suitable. The time required for the analysis of a sample was relatively short and the results were found to be accurate and repeatable. Although the method requires samples which are destroyed during the analysis the magnitude of these is negligible compared to the volume of the solution as a whole. In addition the majority of the equipment required was available in the department and, with only minor modifications, could be used for the measurement of the diethanolamine concentration of the solutions (section 6.4).

This section describes the conditions and procedures used during the operation of the gas chromatograph and explains the reasons why they were chosen. The method used to analyse the measured output is then described in detail.

6.3.4.2. Operating conditions

The gas chromatograph used was a Pye 'Model 44' heated Katharometer programmed chromatograph. This has an operational temperature range of 35-420°C although a maximum temperature of 350°C is recommended as this removes the possibility of having an oven temperature in excess of the detector. The heated katharometer head forms the roof of the oven compartment and provides mounting for the katharometer and injection heads. The katharometer itself is enclosed in a seperate oven, the temperature of which can be controlled independently. This enables the columns to be temperature programmed without affecting the detector temperature. The coiled seperation columns are suspended from the head unit and connected between the injection heads and the katharometer inlet pipes.

The operating conditions chosen were based upon those outlined by Pearce et al (102) and upon the results of trial runs using a series of standard solutions. The seperation column used was 10 feet long and constructed from 1/8 inch diameter, thin walled, stainless steel tubing. It was packed with Teflon (substrate) which had been coated with 10% Oronite N1-W. The column temperature was held constant at 120°C which was high enough to insure the quantitative release of the absorbed carbon dioxide. 99.9% pure helium was used as the carrier gas so as to attain the maximum possible sensitivity from the katharometer. A flow rate of 30 ml/min was used as this produced a reasonable retention time. Higher flowrates were employed to determine whether this would reduce the tailing demonstrated by the carbon dioxide peaks. However it was found that the effect of this was only minimal. The katharometer bridge current was set at 270mA. This was slightly higher than the value recommended in the operating manual (though

less than the maximum permisable value) as this increased the sensitivity of the detector. High bridge currents tend to reduce the filament life but since the chromatograph was to be used infrequently it was felt that this reduction would be negligible. A sample size of 1.0μℓ was used as this produced a good peak area without removing too much of the acid absorbed on the inert packing (see below). The detector oven temperature (150°C) was set slightly above the column temperature to avoid condensation within the katharometer. A higher set point was not chosen as this would have sacrificed sensitivity. The chromatograph itself was placed away from drafts, air conditioning, heat vents, poorly insulated outside walls and direct sunlight as all of these can lead to fluctuations of temperature in the detector and column ovens. The effect of such fluctuations on the output signal are discussed below.

6.3.4.3. Operating procedure

To remove the absorbed carbon dioxide from the aqueous solution effectively the solumn was run in what is termed 'tandem chromatographic operation'. This involves the use of chemical reactions in conjunction with the chromatographic analysis. These reactions can occur ahead of the injection port, in a pre-column reactor, within the column, or in a post-column reactor. In the present investigation the inert packing was chosen so that it could be saturated with acid prior to the analysis of a batch of samples. Thus an injected sample reacts with the absorbed acid effectively reversing the absorption reaction and releasing the carbon dioxide. This is achieved by pre-treating the column with a 50μl injection of 1:1 hydrochloric acid. Tests with standard solutions showed that this was a sufficient volume to ensure that enough HCl was absorbed to neutralize the amine for at least five samples (the actual number of samples which could be analysed before the column needed resaturating varied with the concentration of carbon dioxide in the injected samples). After the pre-injection of hydrochloric acid the column was left for approximately 45 minutes to allow any acid not absorbed by the packing to be exhausted. The reattainment of a steady base output signified when the column was ready for use.

A 1μℓ glass syringe fitted with an 11.5cm needle was used to deliver the sample to the seperation column. Using this length of needle ensured that the sample was discharged beyond the region at the front end of the column where temperature gradients exist. Once the needle had penetrated the injection head the sample was discharged as quickly as possible and the needle immediately removed. This minimised the amount of air allowed into the column at the time of injection.

A second sample was delivered to the column once all the peaks corresponding to the first sample had been detected and a steady base voltage reattained. This took approximately fifteen minutes. Five sample were delivered in this fashion before the packing was re-saturated with a further injection of acid.

Since all of the chromatograph analysis was to be completed in a short period of time the detector oven was left at the operating temperature overnight. This removed the need to wait

for up to three hours the following morning for a steady base line to be obtained. The operating manual recommends that for a long filament life the detector current should be turned off overnight but for the highest stability the next morning it should be left on, along with the oven heater and the carrier gas. The current was therefore left on throughout the duration of the chromatographic analysis.

6.3.4.4. Analysis of the output of the heated katharometer

The size of a chromatographic peak is proportional to the amount of material contributing to that peak and the peak size can be determined in a number of ways. This section considers the methods available and explains why computer integration was used in the present investigation.

The simplest and easiest measurement technique is one involving the measurement of the peak height (that is the distance from the base line to its apex). As long as none of the system parameters are altered this height is proportional to the amount of the relevant material in the sample. If any of a number of factors are changed (even slightly) then the peak height can be crucially effected. For the peak height to remain constant the peak width (that is the width at half the peak height) must also be unaltered. If the peak is broadened (for some reason) the peak height will decrease even if the same sample is used. The temperature of the column effects the retention time of a peak by approximately 3% per degree Celsius. Thus a 1°C change in column temperature between the standard and unknown chromatographs can cause a 3% change in the peak width. This will be accompanied by a compensating change in the peak height such that the product of height and width remains constant. The carrier gas flow rate also effects the retention time and thus the peak height. A 1% change in the flow rate causes a 1% change in the height. In general however this effect is less crucial because as the detector itself is flow sensitive most chromatographs are fitted with a good flow control system. For the carbon dioxide/diethanolamine solution the factor which has the most effect on the peak height is the speed of the injection. The reason for this is that for peaks (like that of carbon dioxide) with retention volumes between one and two times the hold up of the column the retention time is more a function of the injection time than the chromatographic process. Thus a fraction of a second change in the injection time can double the width of these peaks. 'Sharp' peaks, such as that associated with carbon dioxide are particularly susceptible to this effect. Tests with standard solutions showed that the peak height varied by up to approximately 20% for the system used in the present investigation.

The factors which alter the peak height of successive injections do not effect the area of the peak and thus a measurement of peak area is of more value than that of peak height. A variety of methods are available for calculating the area under a peak. Methods involving triangulation and the multiplication of the height and the width at half the height provide good estimates for symmetrical (gaussian) peaks. However when the peak of interest exhibits tailing (as does that of carbon dioxide) these methods

can not be employed. A rather time consuming method involves the cutting out and weighing of the peak which is then compared with the weight of a known area. This can be quite accurate, as can a method which involves the use of a draftman's planimeter, but again both have only limited use in situations where the peak tails. In such cases the area can only be accurately determined by an electric integrator or by a computer/data logger system equipped with a suitable interface. The latter of these options was used in the present investigation.

An Oasis MADC12LB data acquisition instrument module was connected via an instrument grade electronic amplifier (with gain of 100) to the output of the chromatograph. This machine was capable of recording up to 1818 voltage measurements at time intervals between 0.1msec and 999 seconds. The amplifier was required because the output from the katharometer was in mV while the smallest measurement range available was 0-1.0V. The Oasis data logger uses a 32K BBC micro computer to set the characteristics of each input channel used and to store the measured data. The data logger is connected to the 1MHZ bus of the computer. The data collected by the logger is therefore readily available for analysis using programs written for the BBC computer. Figure 6.4 illustrates the computer/data logger system used in the present investigation. The capacitor/resistor combination at the input of the electrical amplifier was required to dampen extraneous A.C. signals generated by the katharometer element. This interference could not be removed completely and a compromise was achieved between a.c. suppresion and response times.

A program 'PLOTER' was written for the BBC machine to enable the recorded data to be plotted in a graphical form. This program also automatically integrated the resultant plot thus providing a measurement of the area of the carbon dioxide peak. 'PLOTER' is listed in Appendix I , along with an example of its output.

Chromatograms were produced for a number of specially prepared solutions with known carbon dioxide concentration. These were integrated using the program 'PLOTER' and the calulated peak areas used to calibrate the detector. Trials had indicated that the peak due to carbon dioxide began approximately 15 seconds after a sample was injected and that the output took 80 seconds to return to the base voltage. The Oasis was therefore programmed for 1800 scans with an inter scan delay of 50 msecs. The machine was activated 10 seconds after a sample had been injected, and any data collected for 90 seconds. A base voltage of 0.1mV was used so that when the data was integrated the effect of the sinusoidal interference was removed. This calibration indicated that the peak area was linearily proportional to the carbon dioxide concentration and that a unit area (V.msecs) was equal to 3.9×10^{-5} g/cm^3 at an output attenuation of 20.

The samples collected were also analysed using this method. The carbon dioxide concentration could therefore be calculated from the product of the measured area (corrected to an attenuation of 20) and the above proportionating factor. These concentrations could therefore be used to calculate the rate of mass transfer and thus the enhancement due to the chemical reactions. These results are presented in Appendix H, and discussed in Section 8.

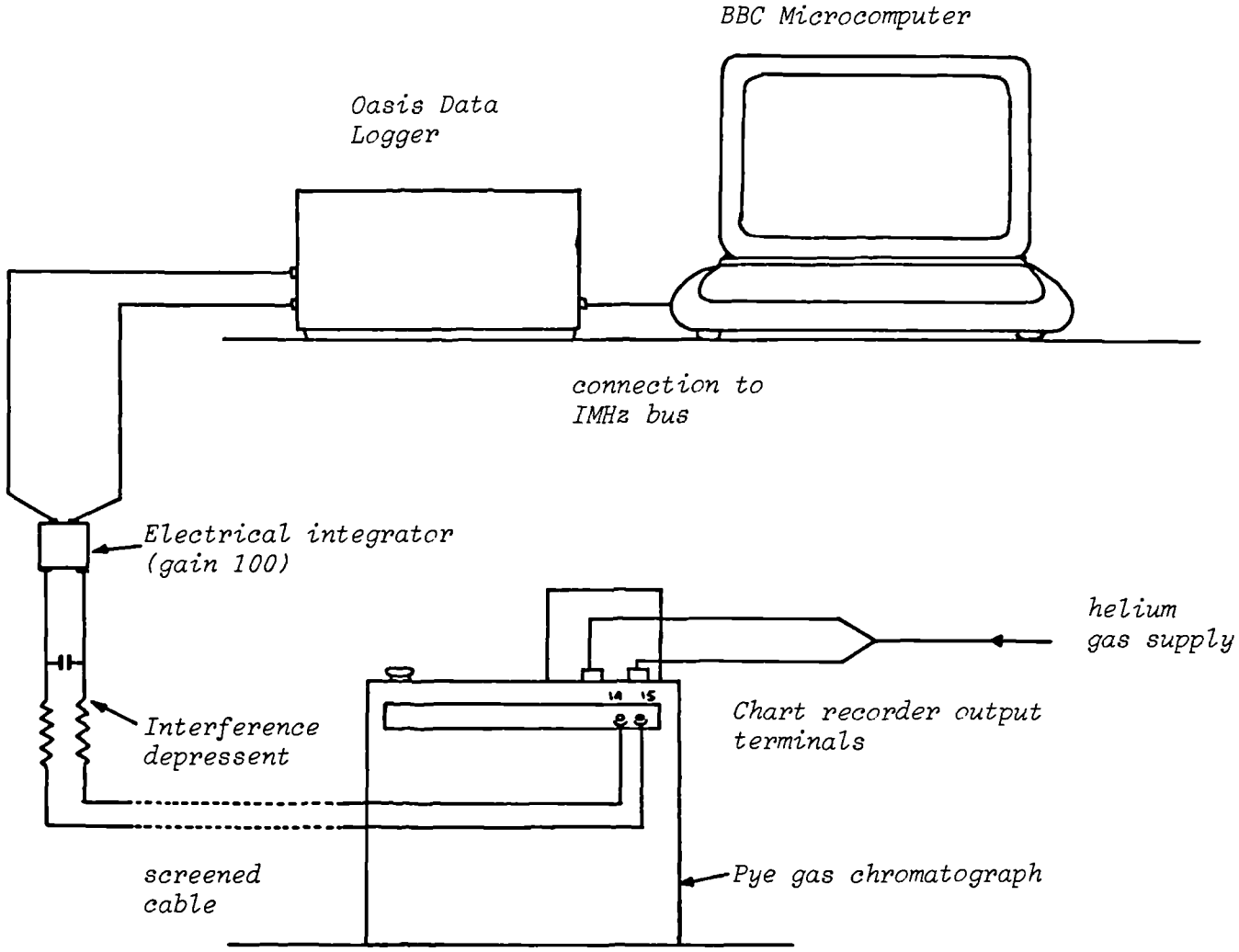

figure 6.4 Chromatographic analysis system

6.4. Determination of amine strength

6.4.1. Introduction

In order to determine the degree of carbonation of a particular sample (i.e. mols of carbon dioxide/mol of diethanolamine) from the measured carbon dioxide concentration (section6 3.4) a technique for determining the amine strength is required. For fresh solutions (i.e. those which have not been regenerated or allowed to oxidise) an alkalinity titration is sufficient. A used solution is likely to contain caustic, or soda ash, or other non-regenerable basic materials that will be titrated as amine giving erroneous results. These solutions can be analysed in a number of ways. If the alkalinity titration is run potentiometrically many of the complications can be removed. The resulting curves will accurately depict the presence of certain acids. Weak acids such as carbon dioxide or hydrogen sulphide will be evolved and will have only a minor effect on the slope of the titration curve. These acids may not be determined accurately due to the gradual break in the curve, and will not be shown in the back titration. In like manner the amine salts of such weak acids, for example, amine carbonates, borates, hydrosulfides and cyanates will be detected in the alkalinity titration for free amine but not determined accurately. A gas chromatographic method can be used to determine the amine strength and also produce accurate measurements of the concentration of heat stable regeneration products. Such a gas chromatographic technique was developed to calculate the carbon dioxide concentration this latter method was chosen. The following sections describe the analysis techniques developed for fresh and regenerated solutions.

6.4.2. Alkalinity titration

The amine concentration of fresh solutions can be determined from an alkalinity titration. 0.1N hydrochloric acid is titrated against a 1ml sample of amine measured with a 1ml glass syringe. The end point of the titration can be determined with bromophenol blue indicator, which turns from lavender to yellow. The amine concentration is determined from

$$\frac{(\text{ml of HCl}) \cdot (\text{Normality of HCl}) \cdot (\text{milliequivalent weight})}{(\text{sample size in ml})\ (\text{specific gravity of approx \% amine})} = \text{mol fraction amine} \qquad 6.1$$

where the milliequivalent weights of commonly uses ethanolamines are-

MEA	0.061
DEA	0.105
MDEA	0.119
DIPA	0.133

6.4.3. Chromatographic analysis

A chromatographic technique was developed to allow the ethanolamine strength of regenerated solutions to be determined. The gas chromatograph used is described in section 6.3.4. The operating conditions used were based upon those suggested by

Pearce et al (102), the limitations of the machine and the results of an extensive series of trails. These are described below.

The seperation columns used were constructed from 3ft long sections of 1/8 inch diameter, thin walled, stainless steel tubing. These were packed with 60-80 mesh, Tenax gas chromatograph porus polymer. They were fixed in the column oven in parallel between the injection heads and the katharometer detector. Two identical columns were needed as they were to be used interchangeably thus minimising the effect that the diethanolamine had on the resistance of the detector (see below). The column oven was temperature programmed so that after being held for 5 minutes it rose at a rate of 24°C/min to 300°C where it was held for a further 5 minutes. This allowed the peaks due to the heavier (heat stable compounds) to be produced with a reasonable retention time. Pearce et al (102) recommended that a temperature of 275°C should be used for the detector oven. However, as this is below the maximum column temperature (300°C) the possibility of condensation within the detector is increased. As this is to be avoided (if possible) then a detector temperature of at least 300°C should be used. Helium with a flow rate of 30 ml/min and pressure of 40 psif was used as the carrier gas. This pressure was high enough to ensure that the flow controllers would accurately control the flowrate over the whole of the temperature programme. The katharometer bridge current was set at 170 mA which is the recommended value for a detector oven temperature of 300°C.

The seperation column had to be pretreated before reproducable results could be obtained. This was done by making succesive injections of sample (between three and five). One microlitre of solution being used per injection. This saturated the column packing and brought it to adsorptive-desorptive equilibrium. The diethanolamine peak (which had a retention time of 8 mins 30 seconds) was calibrated by standarisation (using 1,3-butanediol as an internal standard). This involved preparing solutions with a known diethanolamine and internal standard concentration and measuring the ratio of their peak areas (1,3-butanediol has a retention time of 6 minutes). Thus if a known amount of standard is added to a sample of unknown DEA concentration the measured ratio can be used to calculate the concentration from a measurement of the peak areas.

Oxidising, halogenated or strongly reducing components, particularly if they are present in large amounts can change the resistance of the filaments in the detector. One indication that this problem is present is if there is a permanent or slowly changing shift in the baseline following a large peak. Such a shift was found to accompany the peak associated with DEA. To equalise the changes occuring in the detector the sample and reference columns were periodically reversed. This shift in base line was allowed for in the calculation of peak area by integrating from a line drawn between the start and end voltages.

Peak areas were calculated by the program 'PLOTER' using values collected by the Oasis data acquisition module. (See section 6.3.4.4). 'PLOTER' is reproduced in Appendix I. The time delay between the peaks due to the standard and DEA was sufficient to allow the module to be reset. Thus a full 1818 scans could be used for each peak.

7.0. EXPERIMENTAL FACILITY

7.1. General introduction

This section contains a detailed description of the experimental facility used to collect mass transfer data for the systems carbon dioxide/water and carbon dioxide/aqueous diethanolamine. The description is divided into three sub-sections. The first deals with the design, construction and operation of the rotary test rig showing how it was modified when changing from the physical mass transfer system to the chemical system. This sub-section also shows how the conclusions of the proceeding chapter on analysis techniques were applied to the actual machine. The second sub-section describes in detail the apparatus built to regenerate diethanolamine solutions, 'loaded' with carbon dioxide. The design of this area was based upon the investigation of regenerable mass transfer processes presented in Chapter 3. Any conclusions taken from that chapter and used in the design consideration are noted here. Finally the section of the experimental facility used to deliver the feed liquid to the rotary apparatus and regeneration system is described. Details of how this facilty was modified to allow Nitrogen blanketing of the storage tanks while DEA experiments were in progress are also included.

7.2. The design and construction of the rotary test rig

7.2.1. Basic Design considerations

This section of the experimental facility was designed to allow the mass transfer properties of the systems carbon dioxide/water and carbon dioxide/aqueous diethanolamine to be measured. The choice of solvents influenced the materials of construction and the methods used to collect liquid samples needed to form a mass balance around the apparatus. The basic requirement of such a device was the ability to deliver a known liquid flowrate to the centre of a rotating surface. Mass transfer then occurs by exposing the thin film formed by the centrifugal forces, to the gaseous phase of interest. In equipment used in previous investigations (see Chapter 2) the active mass transfer surface revolved in a large, gas filled, vessel. A continuous flow of gas was maintained through this vessel. Therefore, the gas pressure above the film surface remained constant over the whole of the disc. This then implied that the interfacial concentration of dissolved gas would also be constant. The gas phase in the present investigation was forced to flow over the liquid surface by rotating the disc in a confined space. This flow could have effectively been co or counter current. To simplify the equipment design co - current flow was selected, thus the rotary absorber design had to allow gas to enter at the centre of the machine.

A secondary aim of the experimental investigation was to measure the variation of the mass transfer coefficients with radius. Such measurements had only previously been completed for smooth discs where a probe was used to remove liquid samples from the surface. A device such as this could not be used in the present investigation due to the space restrictions above the rotating disc, and in any respect was useless for perforated or mesh discs due to their roughened surfaces. The method adopted in the designed equipment also removed the additional stage of mass transfer caused by the spray zone at the edge of the discs. Furthermore samples could be taken without disturbing the film as probes were prone to do. Unfortunately, the method devised made the removal of gas from the annulus of the absorption chamber a problem. This was solved by providing a series of vents in the main support plate of the rotary absorber.

The proposed investigation required that smooth, perforated and various mesh discs were used as the active mass transfer surface. Therefore the rotary absorber had to be designed so that the discs could be changed without disrupting the rest of the apparatus. Results were required when these discs were mounted flush to a solid base plate as well when suspended. Any variation in the mass transfer properties of the plane disc due to a change in its position, would indicate the effect that a change in the hydrodynamics of the gas phase had on the mass transfer process. These measurements could be used to determine whether, as predicted, the absorption process for these systems was liquid phase controlled. The measurements with perforated and mesh discs could be used to study the effect that a solid surface had on the type of thin film formed. Due to the confined nature of the absorption chamber it was not possible to design the rotary absorber so that both

sides of a suspended disc were exposed to the gas phase. Therefore the type of film formed on a mesh disc (as discussed in Chapter 2) could not be determined.

The test rig was designed so that the plane of the rotating disc could be positioned both horizontally and vertically. Therefore the variation of performance of a rotary absorber with respect to inclination could be determined. These results were required to ascertain whether such technology could be applied to the design of a scrubber for a closed-cycle nitro diesel engine. Additionally, such information was useful when evaluating the data of Watts (6). (Discussed in Chapter 2).

7.2.2. Design of the rotating surfaces

Four different disc surfaces were used in the mass transfer experiments. These consisted of a plane disc, a perforated disc and two discs constructed from the stainless steel meshes described in Chapter 4. The meshes used were the so-called 'fine' and 'coarse' grades. The 'plane' disc was fabricated from a sheet of 1mm stainless steel plate. The material first employed by Koerfer (5) (see Chapter 2) was used to construct the perforated disc. This was used with its 'rough' side up.

The dimensions of the four discs were identical, thus they could be used interchangeably in the rotary absorber. Each disc had a diameter of 300mm and a centrally punched 35mm hole. Twelve equispaced 3mm holes were drilled through the plates at a radius of 145mm. These were used to locate the discs in the absorption chamber of the rotary test rig.

The edge of the mesh discs were reinforced by the method described in section 4.2.2. This reinforcement was 10mm wide around the disc circumference and 6mm around the edge of the central hole. The central reinforcement was covered by the inlet liquid nozzle and helped to form a stable film. A similar area was created on the perforated disc by filling the holes with araldite once the burrs had been removed.

7.2.3. The rotary absorber

This section describes the individual components which form the rotary absorber. It details how these were assembled and outlines how, through careful design, they met the requirements of the investigation. These requirements were discussed in a previous section. Additionally it indicates how the various discs were mounted in fixed and suspended positions in the absorption chamber.

The rotary absorber is constructed from six major components and a number of minor items. The major components were fabricated from high quality stainless steel due to the corrosive nature of aqueous diethanolamine solutions (see Chapter 3). These items are shown assembled in figure 7.1. Figures 7.2 to 7.6 contain the engineering drawings of each of these pieces. The smaller components are detailed in figures

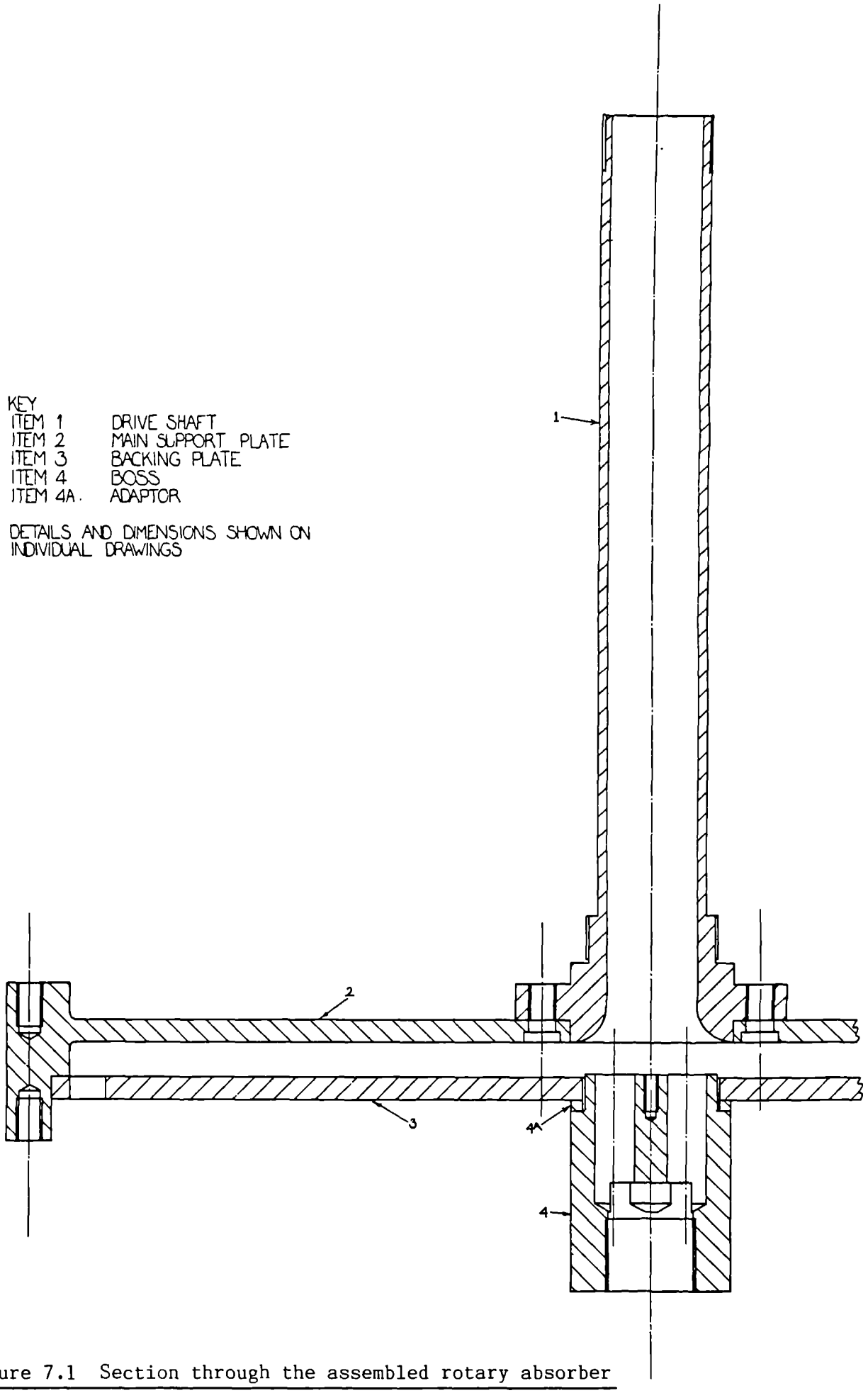

figure 7.1 Section through the assembled rotary absorber

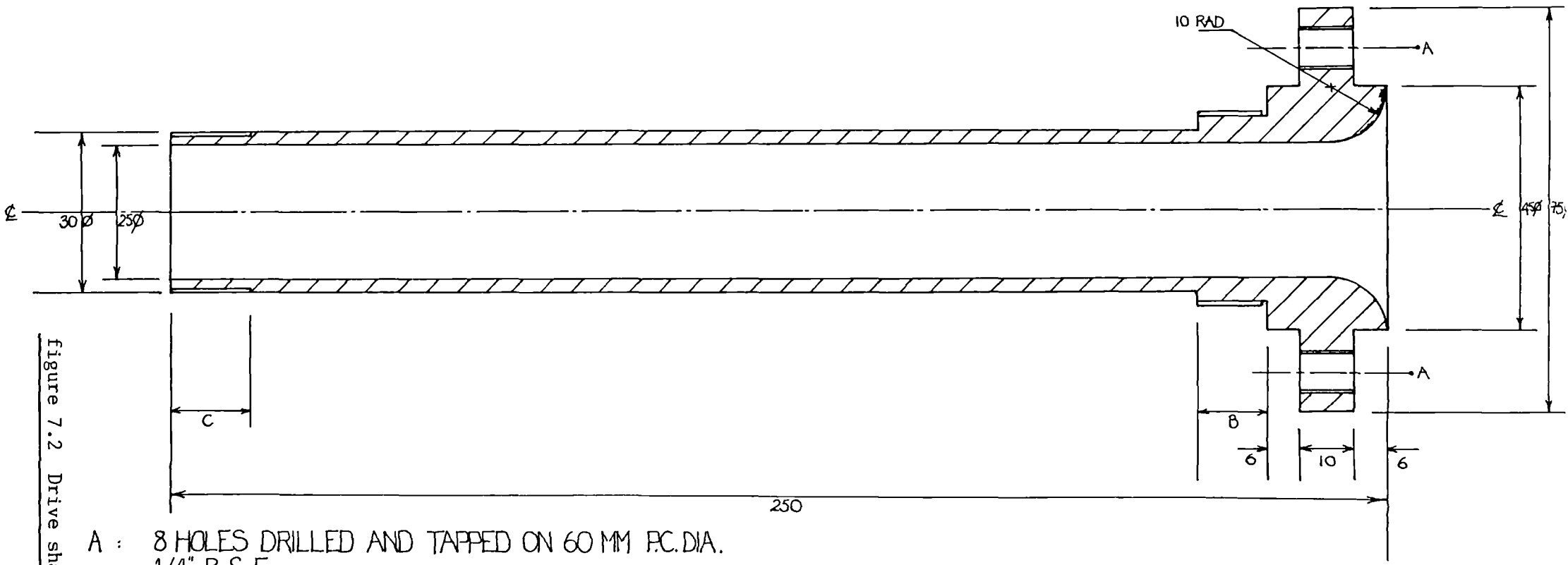

figure 7.2 Drive shaft (item 1)

A : 8 HOLES DRILLED AND TAPPED ON 60 MM P.C. DIA. 1/4" B.S.F.

B : 12 MM THREAD 36 MM O.D. 20 T.P.I. WHITFORM

C : 15 MM THREAD 30 MM O.D 20 T.P.I. WHITFORM

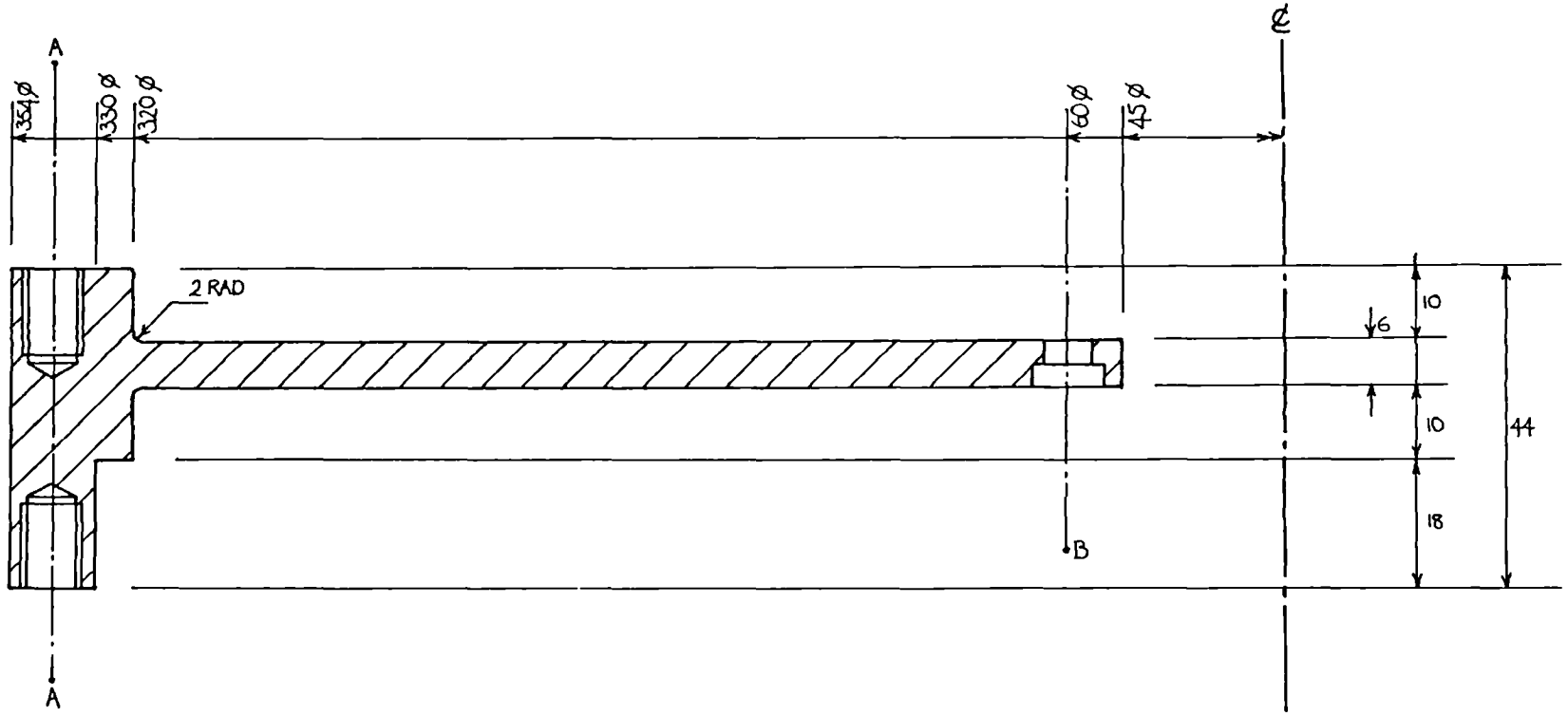

figure 7.3 Absorber main support plate (item 2)

A : 12 HOLES EQUISPACED ON 342 MM
P.C. DIA.. DRILL AND TAP 1/4" B.S.F. X 12 MM DEEP

B : 8 HOLES ON 60MM P.C. DIA.
DRILL 9/32"
COUNTERBORE 10MM DIA. X 3MM DEEP

figure 7.4 Absorber backing plate (item 3)

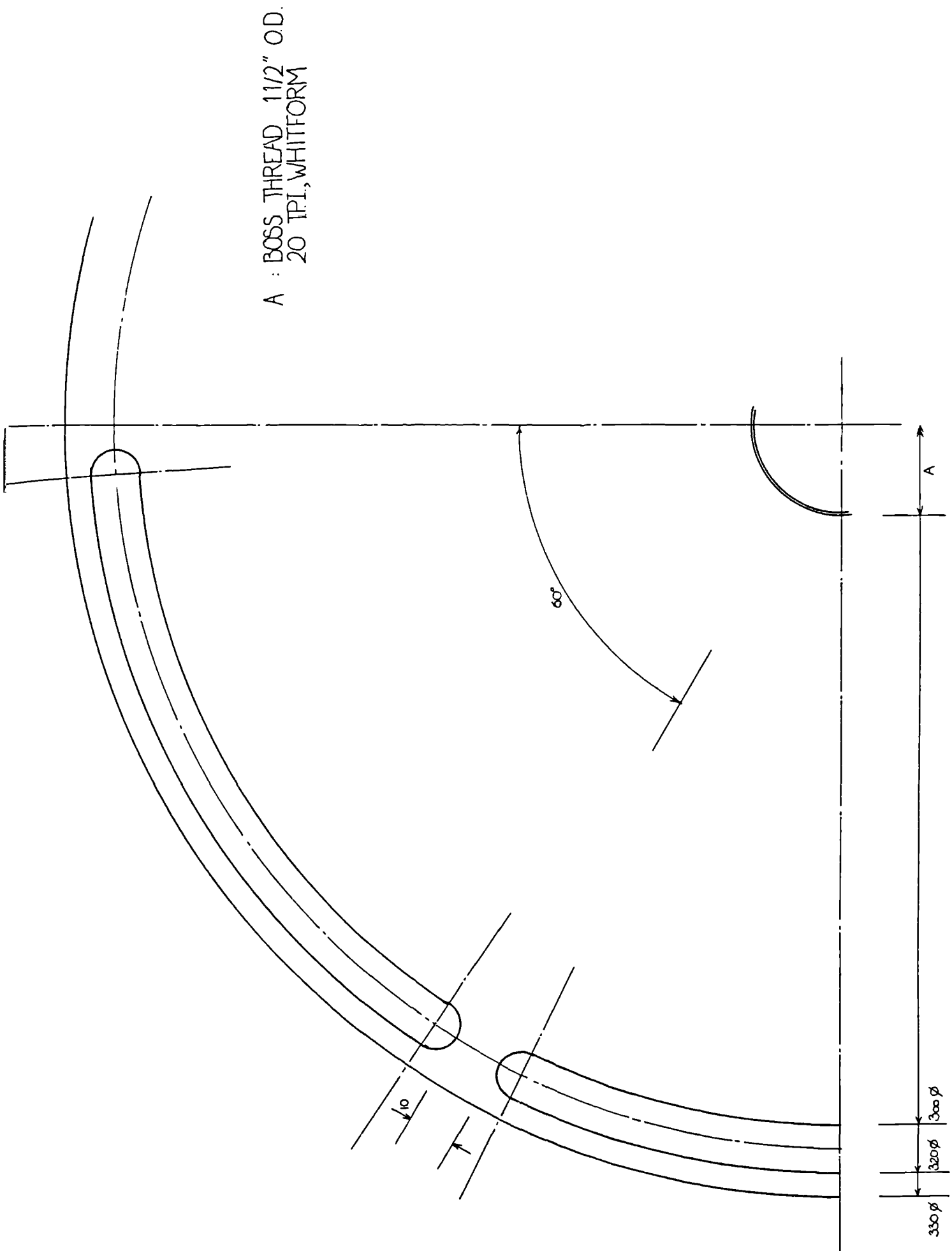

The liquid and gas streams, which constitute the mass transfer system, are fed to the centre of an absorption chamber which is formed between two smooth, stainless steel plates held 10mm apart. The liquid stream enters the chamber from below through a boss (item 4) which is screwed centrally into the 6mm thick backing plate (item 3). Liquid enters the boss via a brass rotary union (manufactured by Deublin: serial no. 6075-001-124), which is screwed into the end of the boss furthest from the backing plate. A right handed thread was used so that the rotation of the absorber did not unscrew the union. Liquid enters the absorption chamber after passing through one of the four cylindrical channels drilled lengthwise through the boss. These channels were designed so that they presented the maximum cross-sectional area for fluid flow, while retaining the material strength of the internal end of the component. The boss is used in conjunction with an adaptor (item 4A). This item allows the length of the threaded shoulder to be reduced from 10mm to 7mm. When the boss and adaptor are assembled, before being screwed into the backing plate (as in figure 7.1), a 1mm deep, unthreaded step, is the only part of the boss which protrudes into the absorption chamber. This stub mates with the hole punched centrally, in the requisite disc. The disc is held securely at its centre and around its periphery so that it can neither lift away from the baseplate or rotate independantly of it. It is fixed to the base plate at its outer edge by 12 equispaced 1/8" flat-headed stainless steel screws that pass through matching holes in the base plate and disc and are secured in position by specially fabricated nuts (see figure 7.8). The holes in the base plate are countersunk so that the screw heads are flush with its outer surface. Four teeth, equispaced around the edge of the liquid nozzle (item 5) which is screwed into the centre of the boss, grip the disc at its centre. Additionally the teeth maintain a 1mm nozzle gap which has been shown, in Chapter 4, to be suitable over the operational range of flowrates and speeds. The nozzle forces the liquid emerging from the boss to spread across the disc. The design of the nozzle was based as closely as possible on that used in the preliminary experiments. Thus, although this could not be observed while the absorber was in operation, it was felt, that its performance would be satisfactory. Discs can be suspended in the absorption chamber if the adaptor is screwed onto the boss after this has been screwed into the base plate. In this case the nozzle grips the disc against the upper surface of the adaptor. The outer edge is secured by using the special nuts mentioned above as spacers. The flat headed screws are then held in place by normal 1/8" nuts and washers.

Gas approaches the absorption chamber by passing down the centre of a stainless steel tube which doubles as the drive shaft of the absorber (see section 7.2.4 below). The drive shaft (item 1) mates with a centrally located, 45mm diameter, hole formed in the 6mm thick main support plate (item 2). It is held in position by eight 1/4" BSF bolts which pass from the absorption chamber through matching holes drilled in the support plate and the collar of the drive shaft. The holes in the support plate are countersunk so that with the bolts in position the heads do not protrude into the absorption chamber. A gas tight seal was provided between the two components by running a bead of 'Silica-set' around the inside of each of the counter-bored holes and upon the

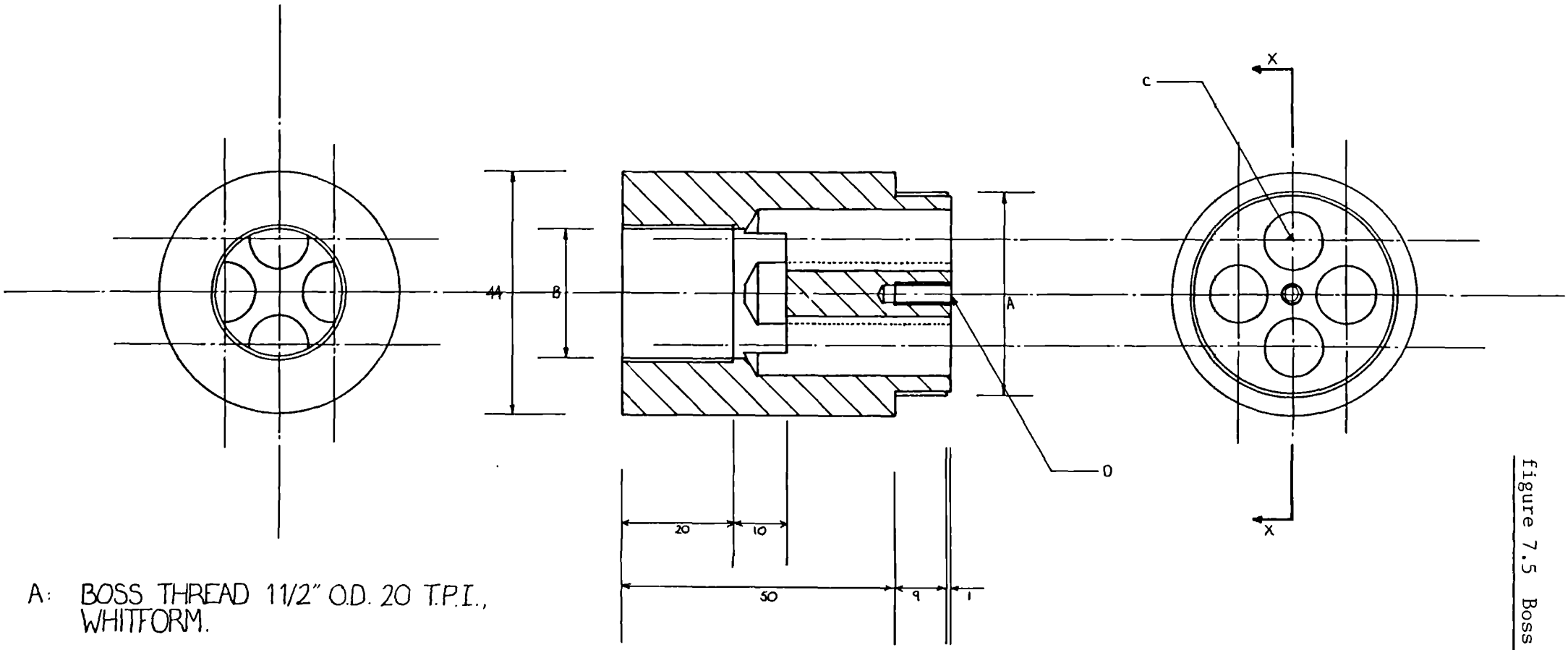

figure 7.5 Boss (item 4)

A: BOSS THREAD 1 1/2" O.D. 20 T.P.I., WHITFORM.

B: BOSS THREAD 1" 14 UNS R.H. TO SUIT ROTARY UNION 6075-001-124.

C: 4 HOLES 11 M.M. DIA. EQUISPACED ON 10 MM RADIUS CIRCLE, 35 MM. DEEP.

D: 4 MM O.D DRILLED AND TAPPED HOLE, 10 MM DEEP, TO SUIT NOZZLE.

figure 7.7 Inlet nozzle (item 5)

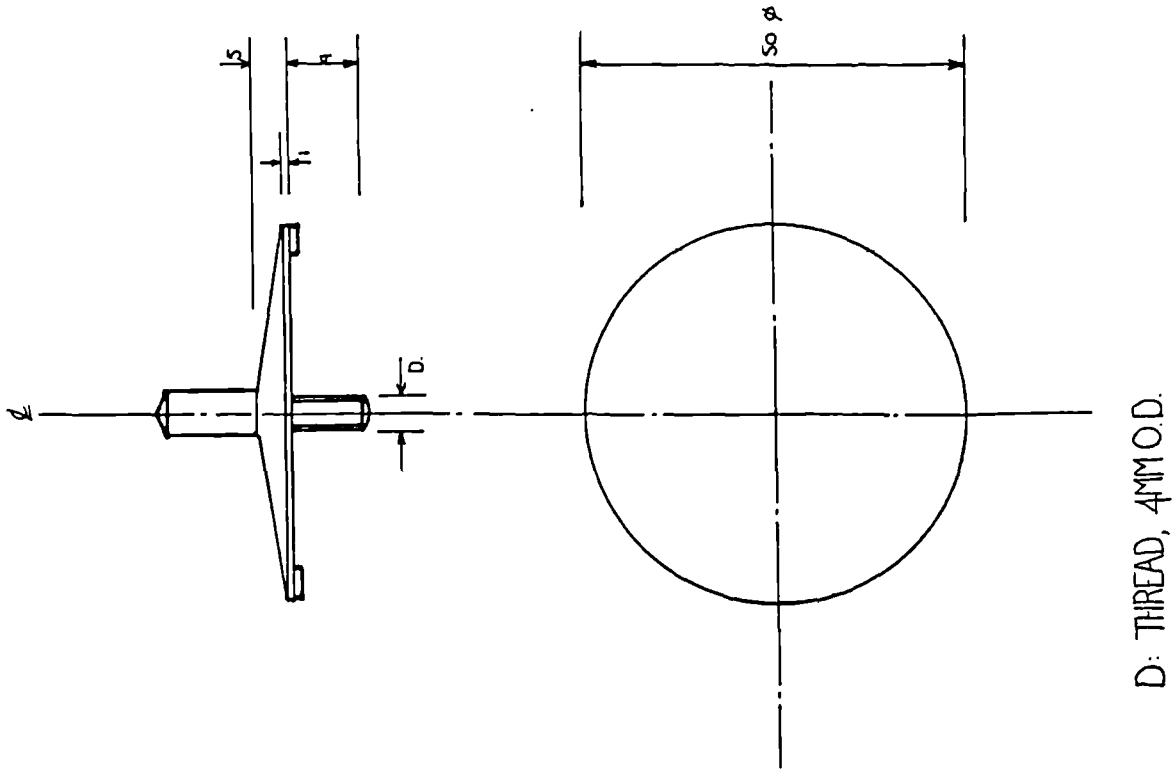

figure 7.6 Boss adaptor (item 4A)

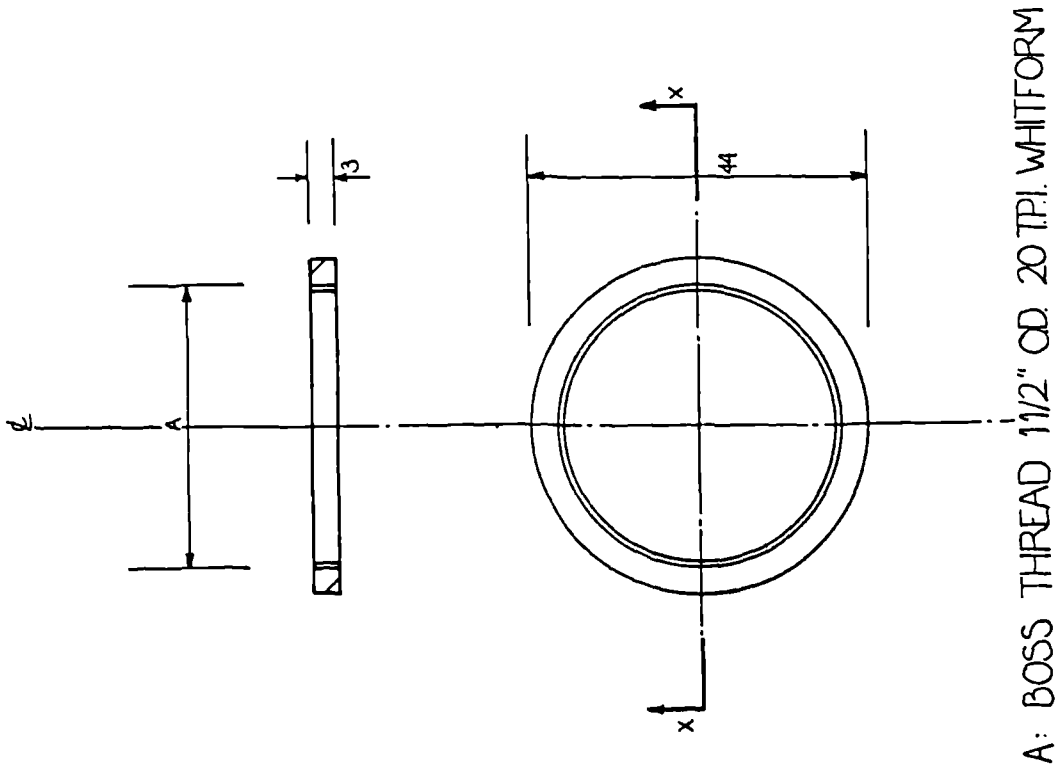

inner face of the drive shafts' 75mm diameter collar. Gas enters the 250mm long drive shaft through an aluminium rotating-union (manufactured by Deublin: serial number: 2200-000-027). This is connected to the drive shaft via a specially fabricated stainless steel nut (item 6) which rests on a thrust bearing located in the base plate block (item 11). This is part of the sub-assembly used to support the rotary absorber, details of which are presented in section 7.2.4 below. Gas emerges into the absorption chamber through a tapered orifice located above the liquid nozzle. The gas is thus forced to flow radially outwards through the narrow chamber formed between the disc surface and the main support plate. The upper surface of the liquid nozzle and the tapering around the gas entrance were designed to smooth the transition of gas passing from the drive shaft to the absorption chamber.

The rotary absorber is assembled from the drive shaft/main support plate and backing plate/boss/disc sub-assemblies described in the preceeding paragraphs. The latter is connected to the former by six 1/8" diameter flat headed stainless steel screws which pass through counter-sunk holes, equispaced around the periphery of the backing plate. These locate in holes that are drilled and tapped in the centre of a 5mm wide step cut into the inside edge of the outer section of the main support plate. This therefore forms a cylindrical chamber, 10mm deep and 320mm diameter in which various discs can be located. The main support plate was designed so that it formed a 10mm deep rim around the circumference of the absorber above and below the absorption chamber. Twelve holes, drilled and tapped to take 1/4" BSF screws, were equispaced around each of the rims. These were required so that specially designed perspex lids could be connected to the body of the absorber so forming secondary chambers above and below the absorption chamber. These chambers were required so the gas and liquid streams respectively, could be removed from the absorber.

A series of 10mm wide slots cut around the outside edge of the backing plate forced liquid leaving the disc surface to flow from the absorption chamber into the liquid-side sub-chamber below. A rubber O-ring, compressed between the main support plate and the liquid-side perspex plate (item 7), formed a liquid-tight seal around the rim of the sub-chamber. Thus, liquid arriving at the edge of the absorber is forced to flow back towards the centre. As the machine is rotating at high speeds this effect causes a liquid layer to form in the annulus which gradually floods the absorption and liquid side chambers. Liquid is scooped from this layer by a stationary pick up tube and pumped from the absorber by the rotational energy it gains while passing through the machine. This method of removing liquid from the rotary absorber meant that the variation of mass transfer coefficients with radius could be determined for any kind of disc. In addition the formation of a spray effect due to film breakdown at the disc edge was avoided. Unfortunately this complicated the removal of gas from the absorption chamber. The surface area available for mass transfer depends on the thickness of the liquid layer formed around the edge of the absorption chamber. This is controlled by the position of the pick up tube. The pick up tube assembly was designed so that the nozzle inlet could be set over a wide range of radii. The nozzle itself was designed to operate effectively at all radii over the operational ranges of flowrate and speed of rotation.

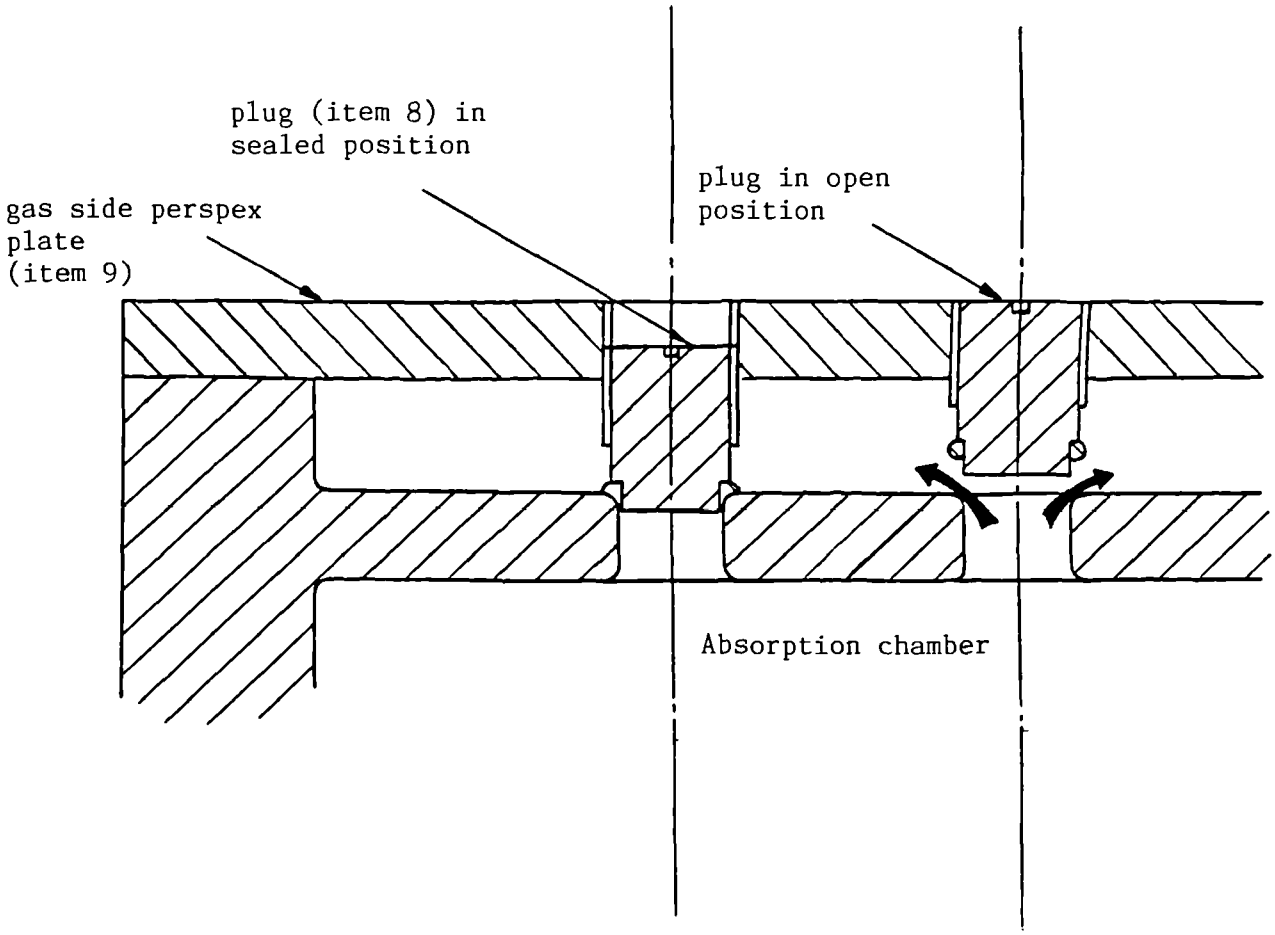

figure 7.10 Position and operation of gas sub-chamber sealent plugs

figure 7.8 Securement of discs in suspended position

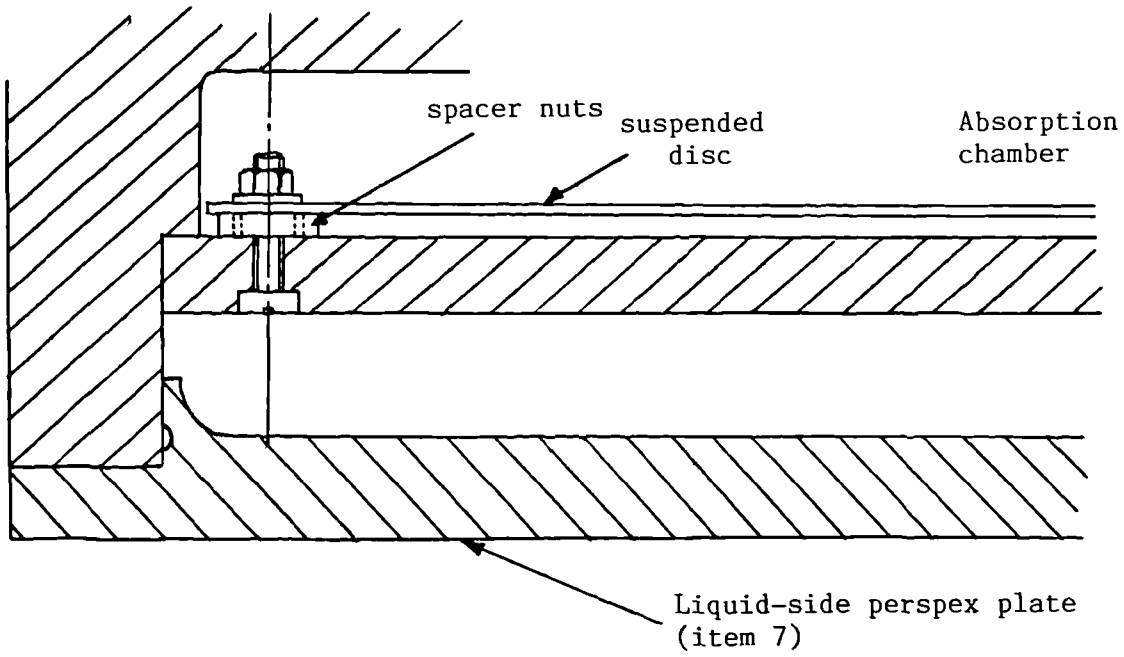

To measure the mass transfer properties of a disc, from the edge of the liquid nozzle to a particular radius, the pick up tube is set at a corresponding position in the liquid sub-chamber. The absorber then fills with liquid from its outer edge to that radius. Liquid flowing across the disc surface is thus only exposed to the gas phase-over a limited path length before entering a wall of liquid.

Gas is removed from the absorption chamber via a series of vents drilled through the main support plate. These were designed so that mass transfer coefficients could be measured at four radial positions. The vent system at each of these radii consisted of six 10mm diameter holes drilled on a radius 10mm less than that to which the absorber is to be flooded. The inlet and outlet of each hole was tapered. Each hole could be sealed by winding down a plug (item 8) located in the gas-side perspex-plate (item 9) directly above the requisite hole. Figure 7.10 shows the operation of these plugs. Therefore when measuring mass transfer properties at a particular radius all vents were closed, apart from those corresponding to that radius. Gas passing from the absorption chamber into the gas-side sub chamber was discharged to the atmosphere through a slot cut around the centre of the perspex plate.

7.2.4. Support plate sub-assembly

The sub assembly described in this section was designed to support the rotary absorber and secure it to a rigid frame (detailed in section 7.2.5 below). The assembly consists of six pieces. Two of these, the base plate (figure 7.11) and the base plate block (figure 7.12), were fabricated in the department while the rest were bought in. Each item was again constructed from high quality stainless steel.

The base plate (item 10) and the base plate block (item 11) form the main supporting element of the sub-assembly. The block sits in a groove, 3/16" deep and 3/4" wide cut in the face of the support plate. The plates are secured at right angles by two 1/4" stainless steel set screws. A 32mm diameter hole is drilled through the centre of the block. This was counterbored to a depth of 1/2" and a diameter of 47mm. The block was positioned in the groove so that the counter-sunk side of the hole was adjacent to the short side of the base plate. A stainless steel thrust bearing (made by RHP cat. no. 51106) sat in the recess formed by the counterboring. This had a diameter of 47mm, a depth of 15mm and was designed for a shaft of 30mm diameter. It was located in the recess after immersing it in liquid nitrogen so that upon reattaining room temperature it was locked in position. The upper surface of the thrust bearing stood slightly proud of the face of the support block, and it is upon this that the stainless steel nut (item 6 see 7.2.3 above) sat. The drive shaft (item 1) passes through the fixed thrust bearing and two self lubricating cast iron pillow block bearing units (made by Asahi cat. LP206) fitted with taper blocks. These were fixed to the base plate by bolts passing through 9/16" diameter holes drilled in the base plate (see figure 7.13). A pulley block was fixed onto the drive

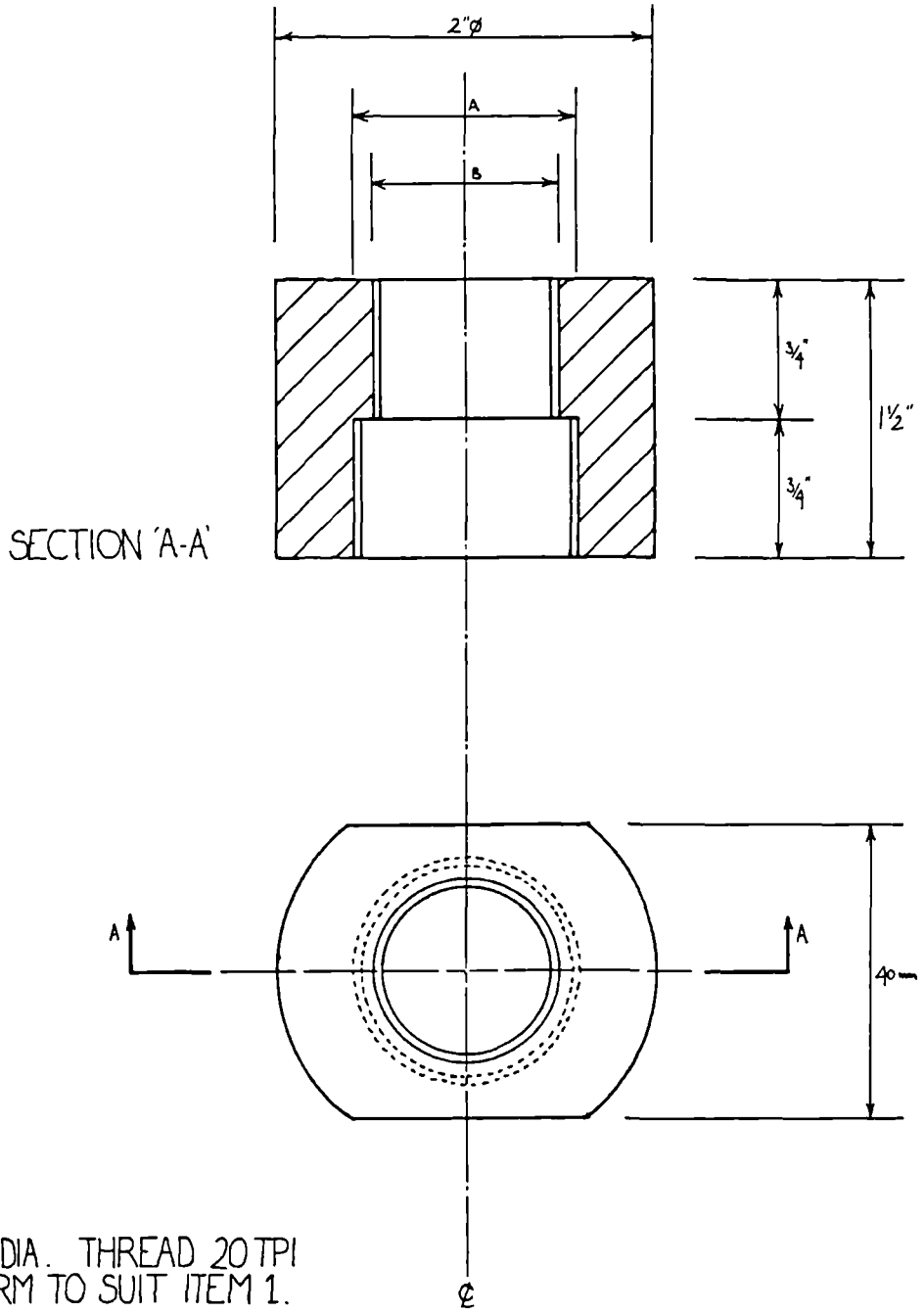

A : 30 MM DIA. THREAD 20 TPI WHITFORM TO SUIT ITEM 1.

B : 1" DIA. THREAD 14 UNS. LH. TO SUIT ROTARY UNION 2200-000-027

figure 7.9 Drive shaft nut (item 6)

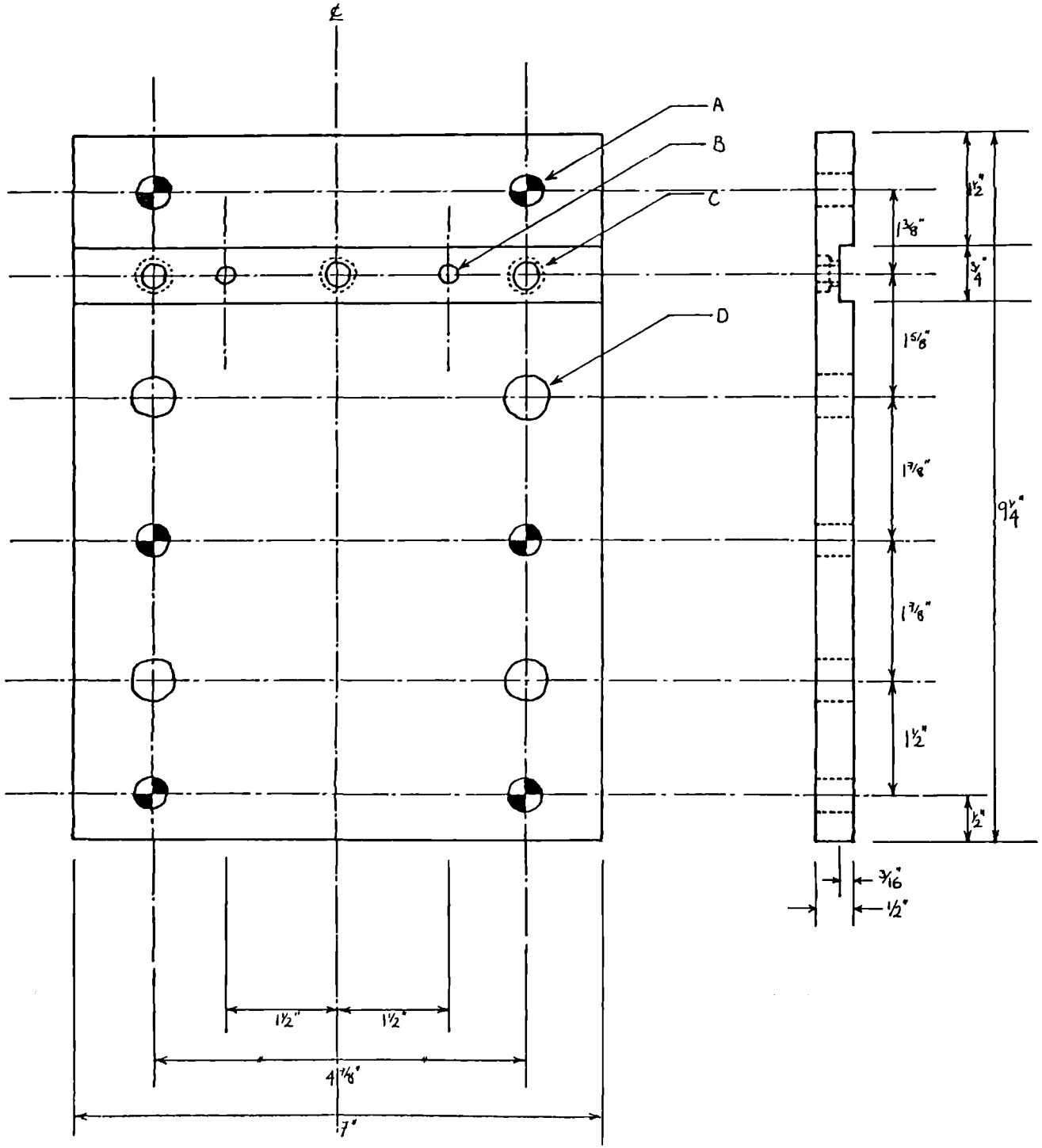

A: 6 HOLES DRILL 7/16" DIA.

B: 2 HOLES DRILL 1/4" FIT WITH 1/4" DOWELS 3/4" LONG

C: 3 HOLES DRILL 5/16" COUNTER-SINK FOR 1/4" DIA B.S.W. SETSCREWS

D: 4 HOLES DRILL 9/16" DIA.

figure 7.11 Base plate (item 10)

A : 2 HOLES DRILL 1/4" DIA. FOR DOWELS X 3/4" DEEP

B : 3 HOLES DRILL AND TAP FOR 1/4" B.S.F. X 3/4" DEEP.

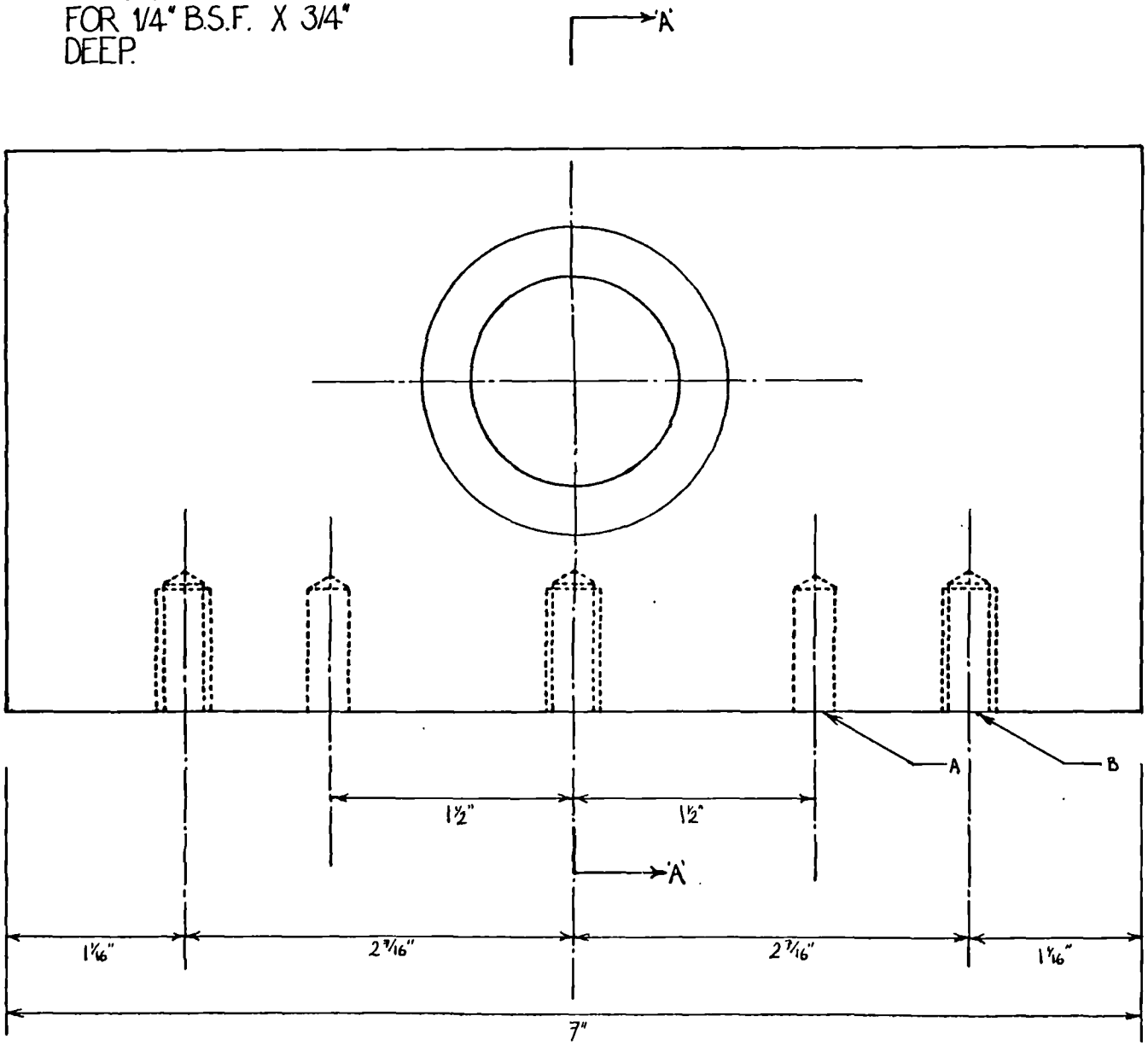

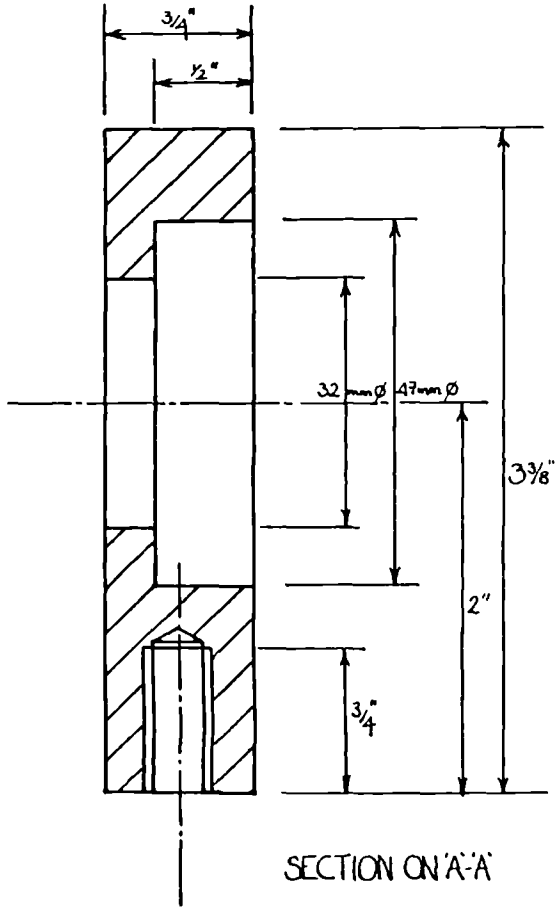

SECTION ON 'A'-'A'

figure 7.12 Base plate block (item 11)

7.2.5 Support frame

The support plate sub assembly, holding the rotary absorber, is fixed to a rigid support frame made from 2 inch wide, 1/4 inch thich mild steel angle iron. The frame also provides support for a number of ancillary items required in the operation of the rotary absorber. An isometric sketch of the frame is provided in figure 7.15. Three carbon steel support plates are fixed to the frame in the positions shown. These were skimmed to produce a true surface onto which the support plate sub-assembly, the dc motor and the measuring device were mounted. These plates are detailed in figures 7.16 to 7.18.

The rigid frame was painted to protect the carbon steel from corrosion due to spillages of either water or diethanolamine. Four casters were fixed to the base of the frame and to the side holding the support plate sub-assembly. This allowed the test rig to be moved if necessary when the rotary absorber was aligned either vertically or horizontally. Three legs were also attached to these sides. These could be wound down to raise the casters off the ground thus avoiding any movement while the rig was in operation. The legs also allowed the rig to be levelled. The frame also provided support for the inlet and outlet liquid pipes, the inlet gas line, the variable speed controller, guards around the rotary absorber, and a splash tray to catch any liquid escaping from the liquid side sub-chamber. These items were attached in such a fashion that the rig could be easily transformed from vertical to horizonatal operation.

The whole rig was mounted on a 1/2 inch thick cast iron plate which rested in turn on a 1/2 inch thick soft rubber mat. This helped spread the load evenly over the floor and provided a level surface to operate from. The cast iron plate was painted in a similar manner to the support frame. Both the frame and cast iron plate were electrically earthed.

Photograph 7.1 shows the rig set up for vertical operation.

7.2.6 Ancillary items

This section describes any items used on the rotary test rig that do not form part of the rotary absorber, support plate sub assembly or support frame. These include the D.C. Motor, the variable speed controller, the liquid pick-up nozzle arrangement and the minature jacuator. These components are shown assembled in figures 7.13 and 7.14.

7.2.6.1 D.C. Motor

An 'Anyspeed' 112130M, 1.50KW D.C. Motor was used to drive the rotary absorber. This motor had a top speed of 3000 RPM. It was mounted on a support plate which was fixed to the rigid support frame in the position shown on figures 7.13 and 7.14.

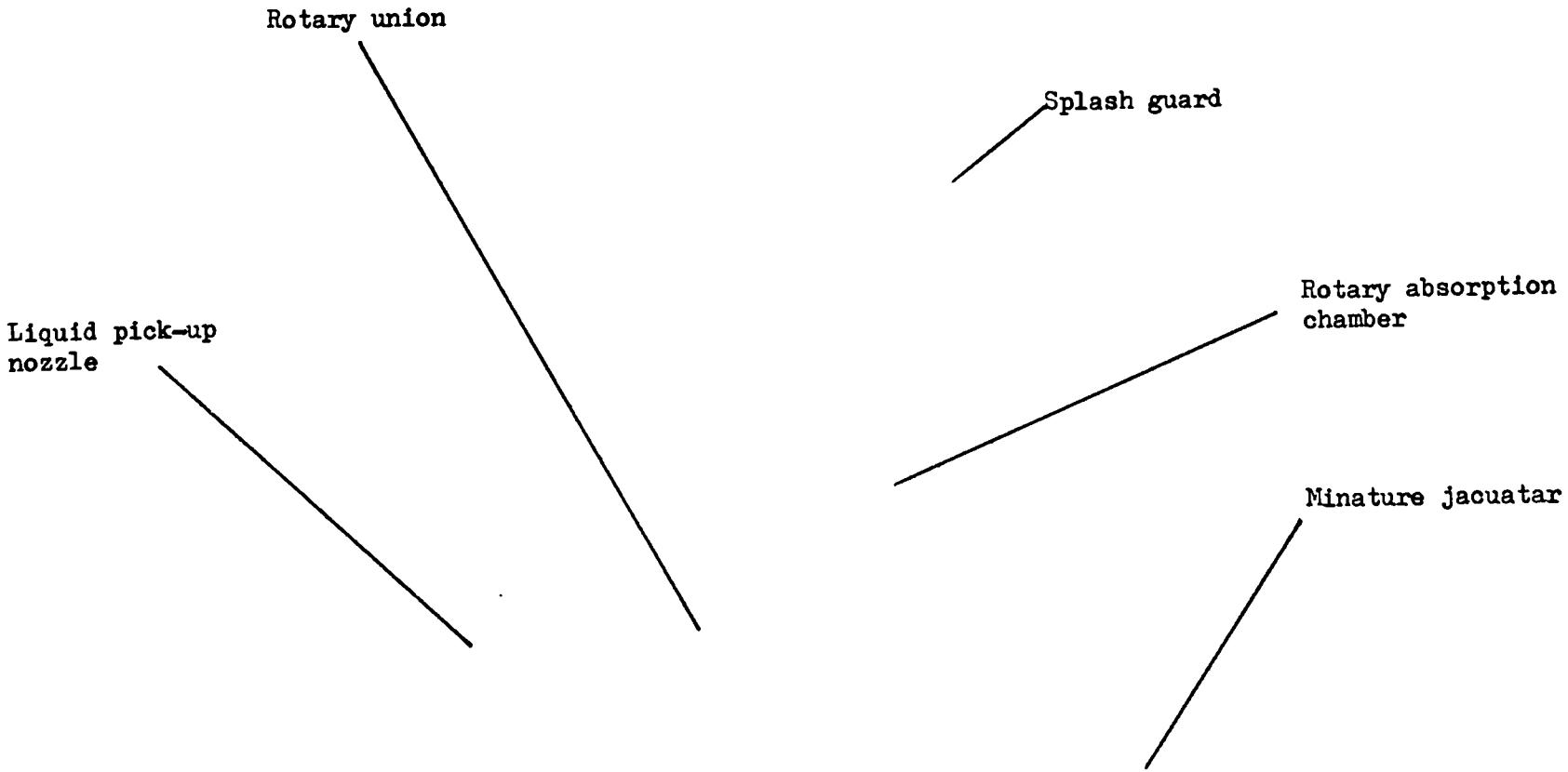

Photograph 7.1

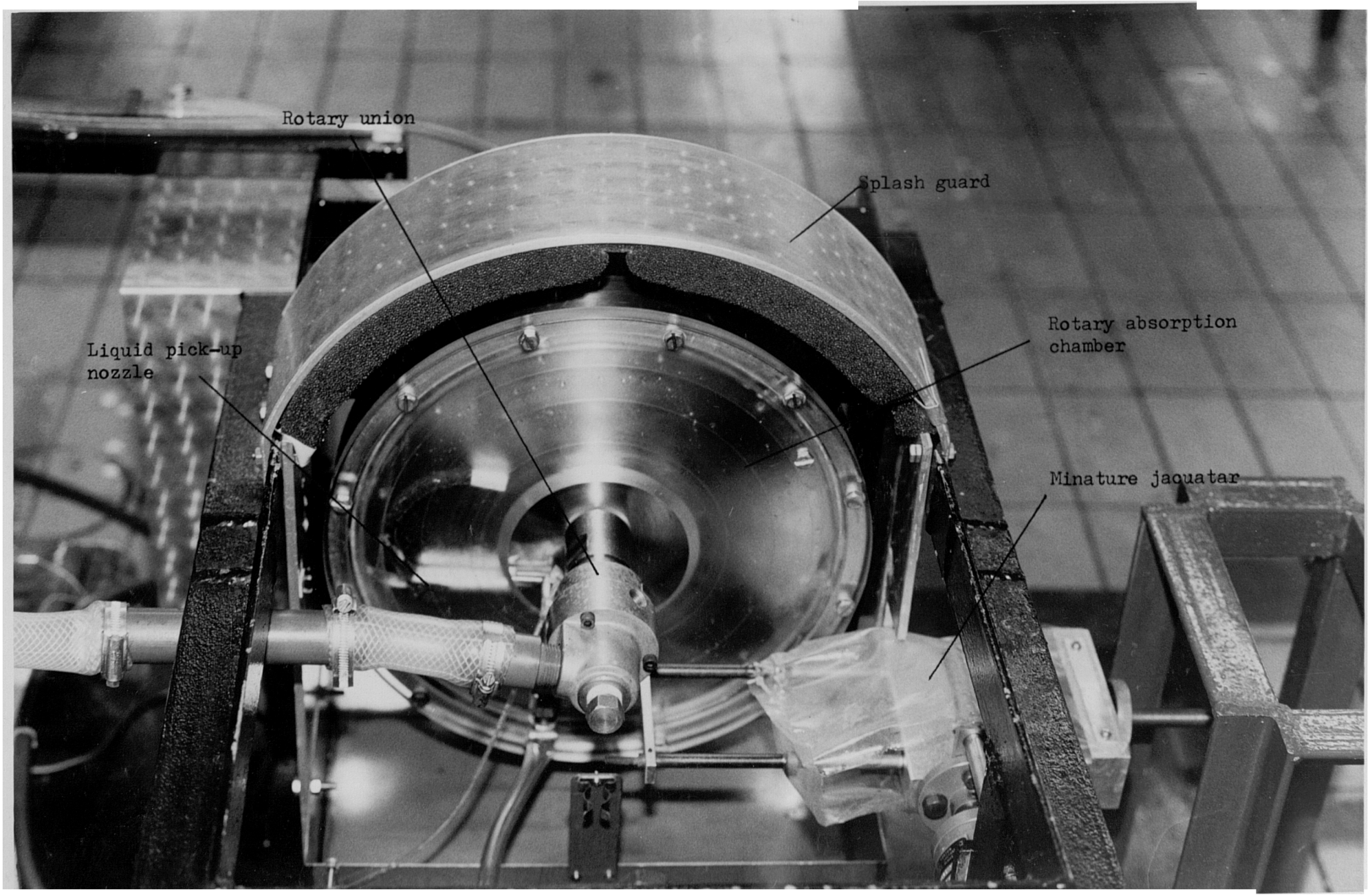

Photograph 7.1

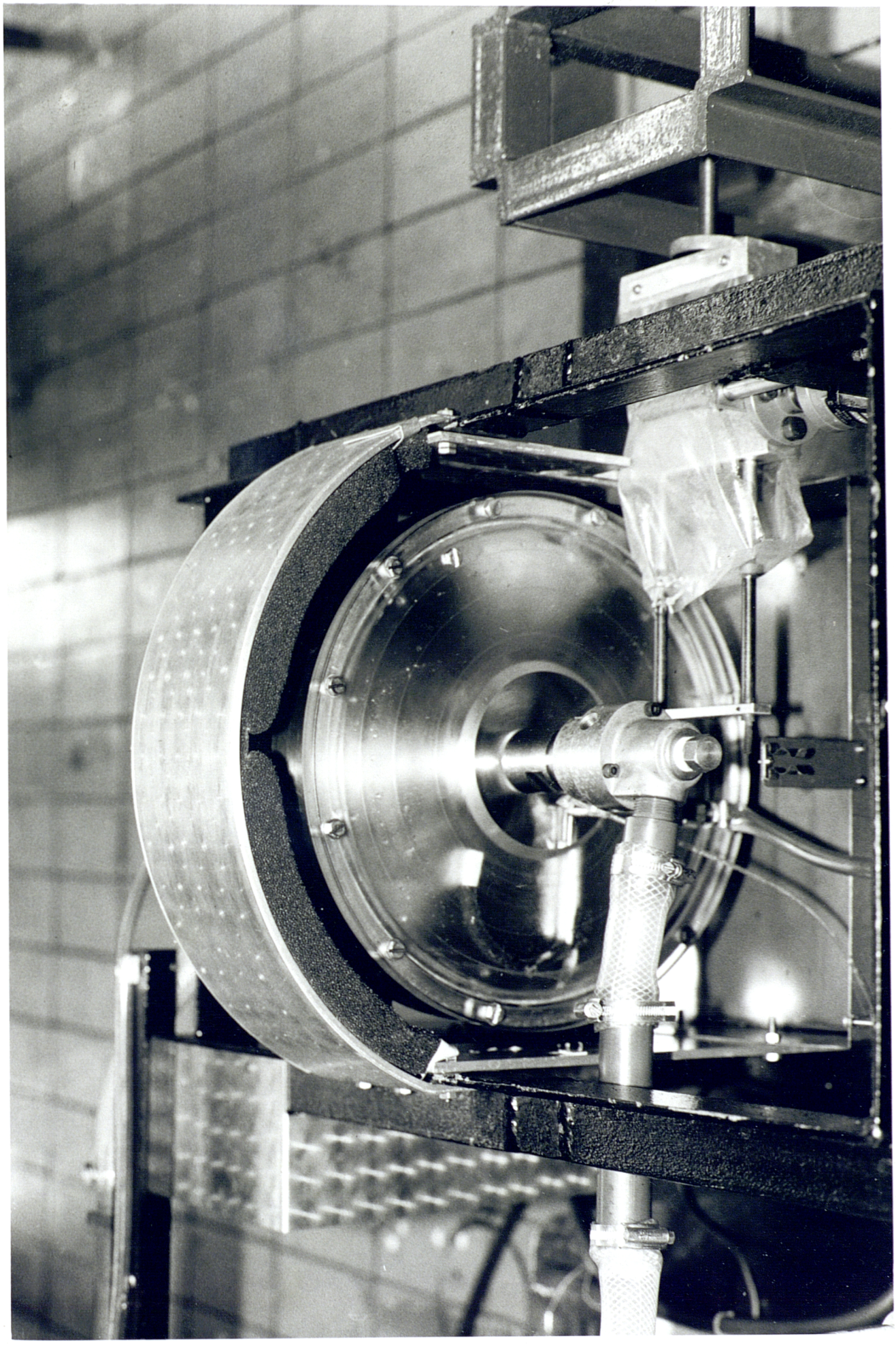

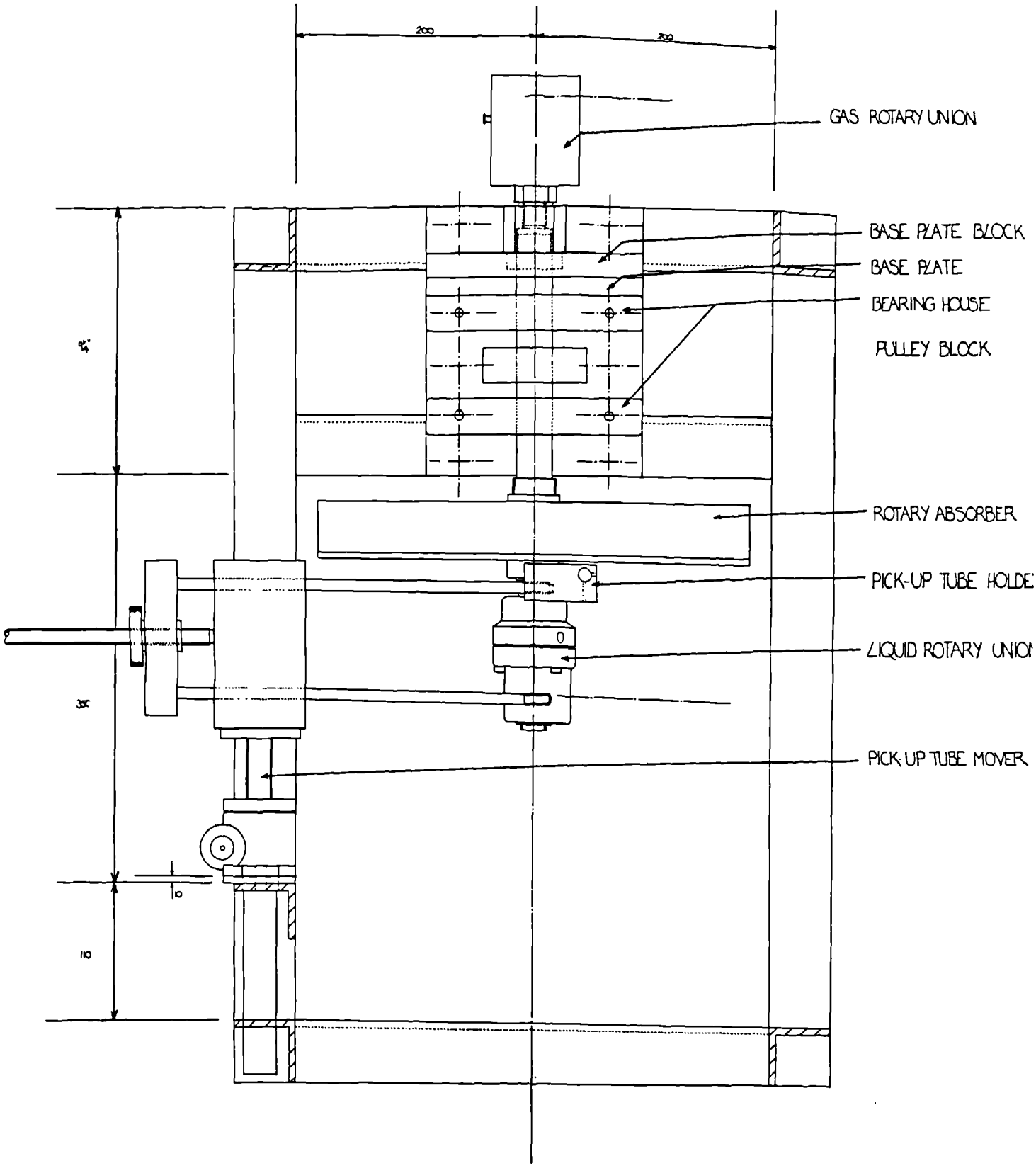

7.13 Front elevation of the rotary absorber and support frame

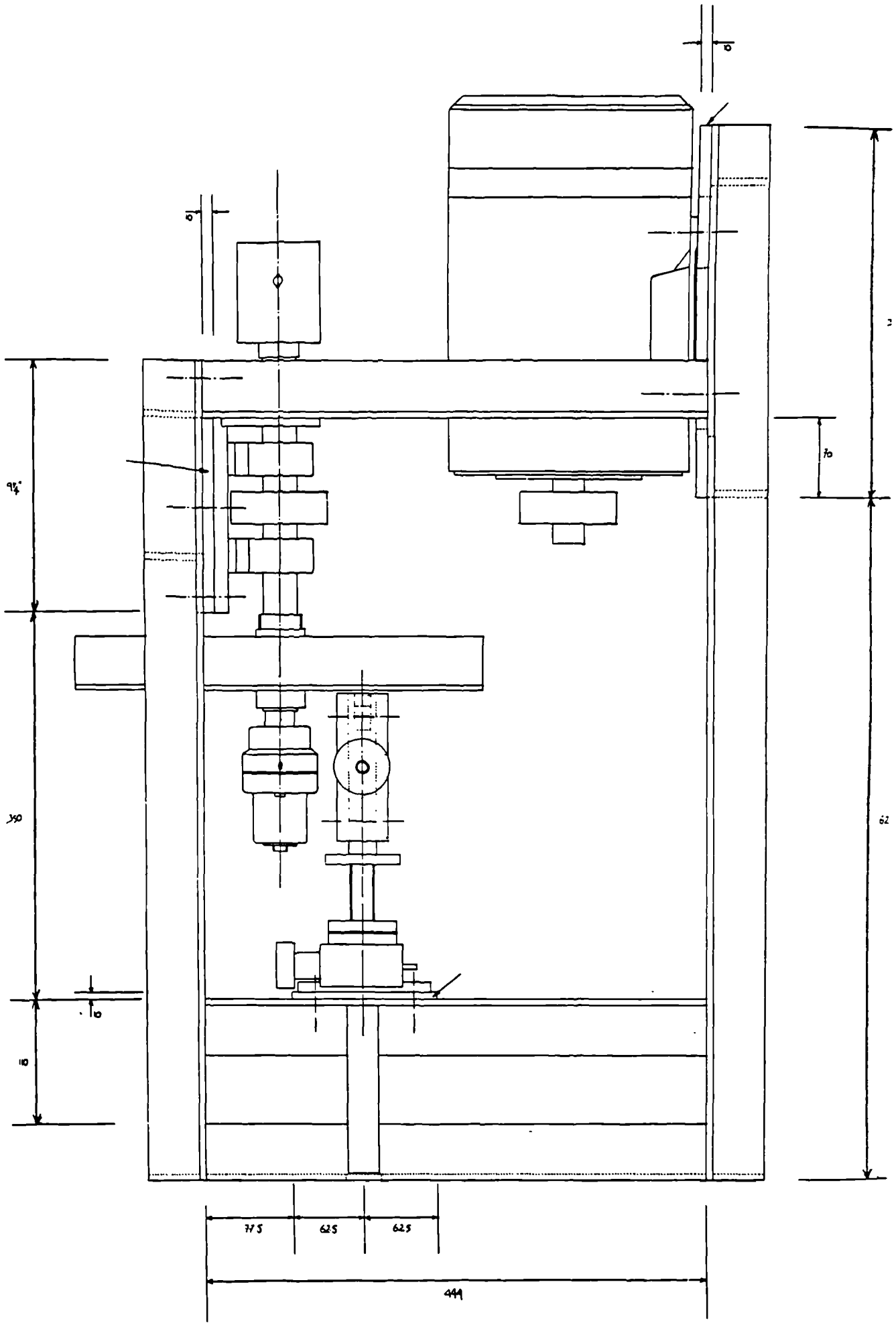

figure 7.14 Side elevation of rotary absorber, ancillary items and support frame

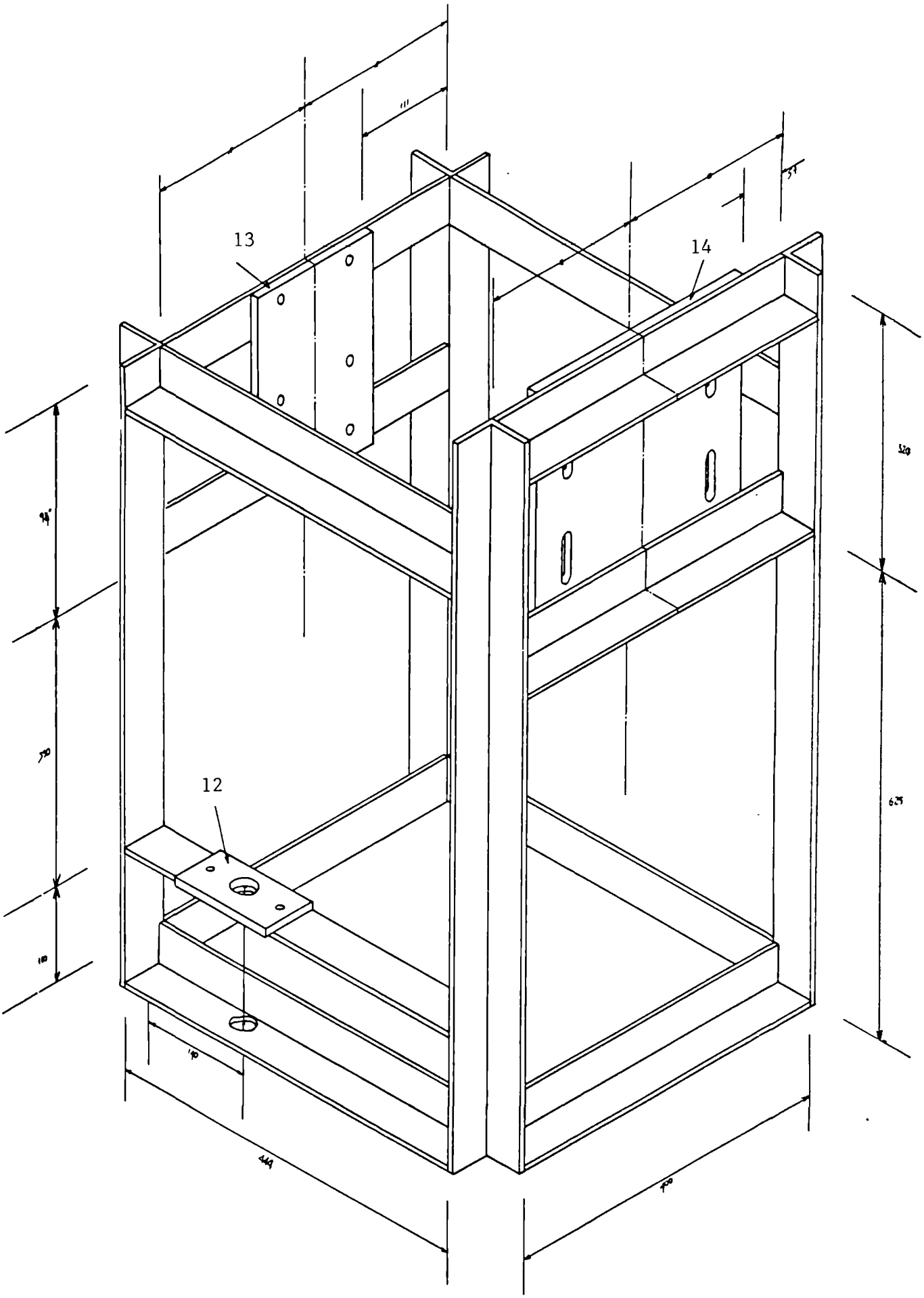

figure 7.15 Isometric sketch of the absorber support frame

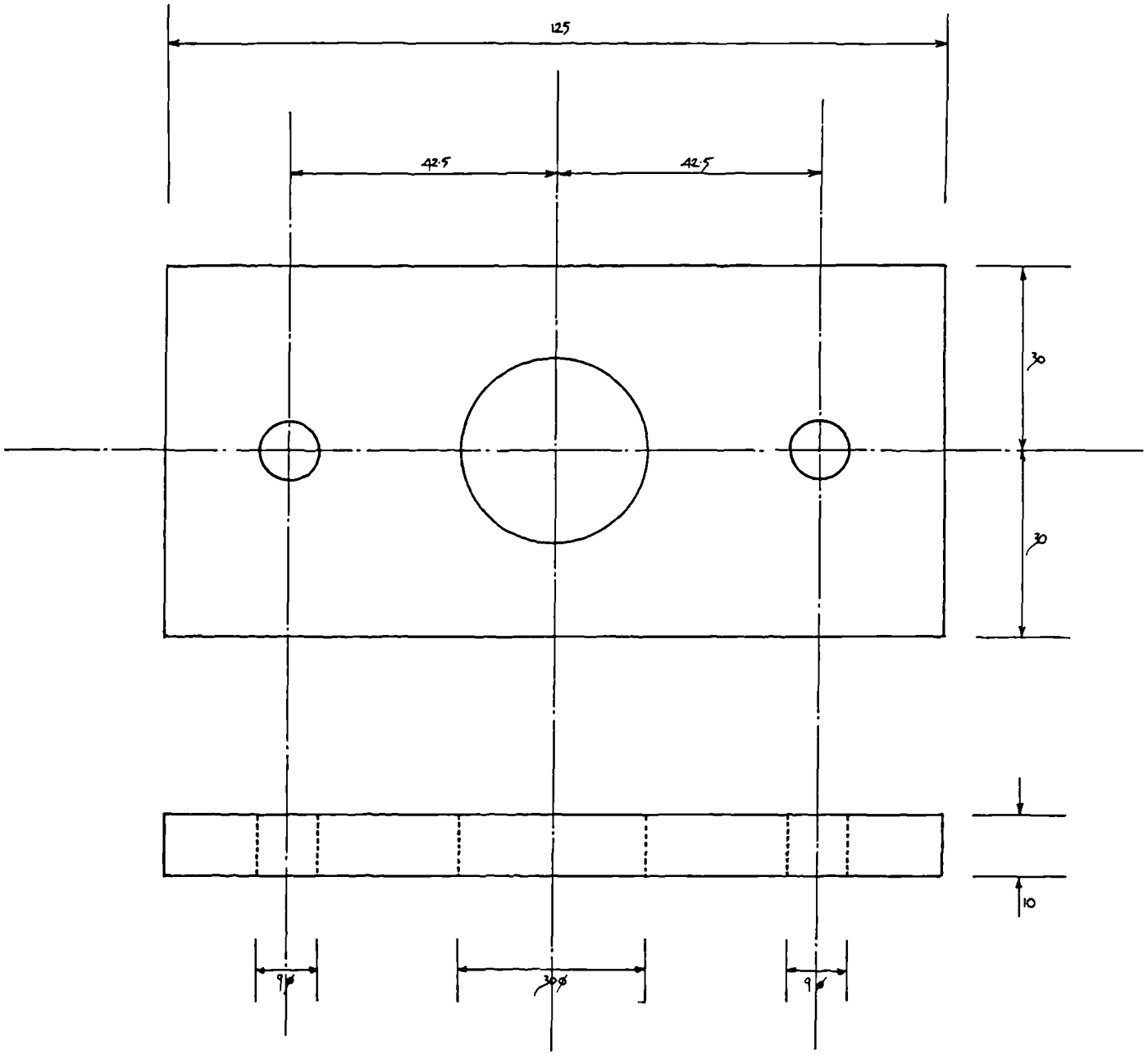

figure 7.16 Minature jaculator support plate (item 12)

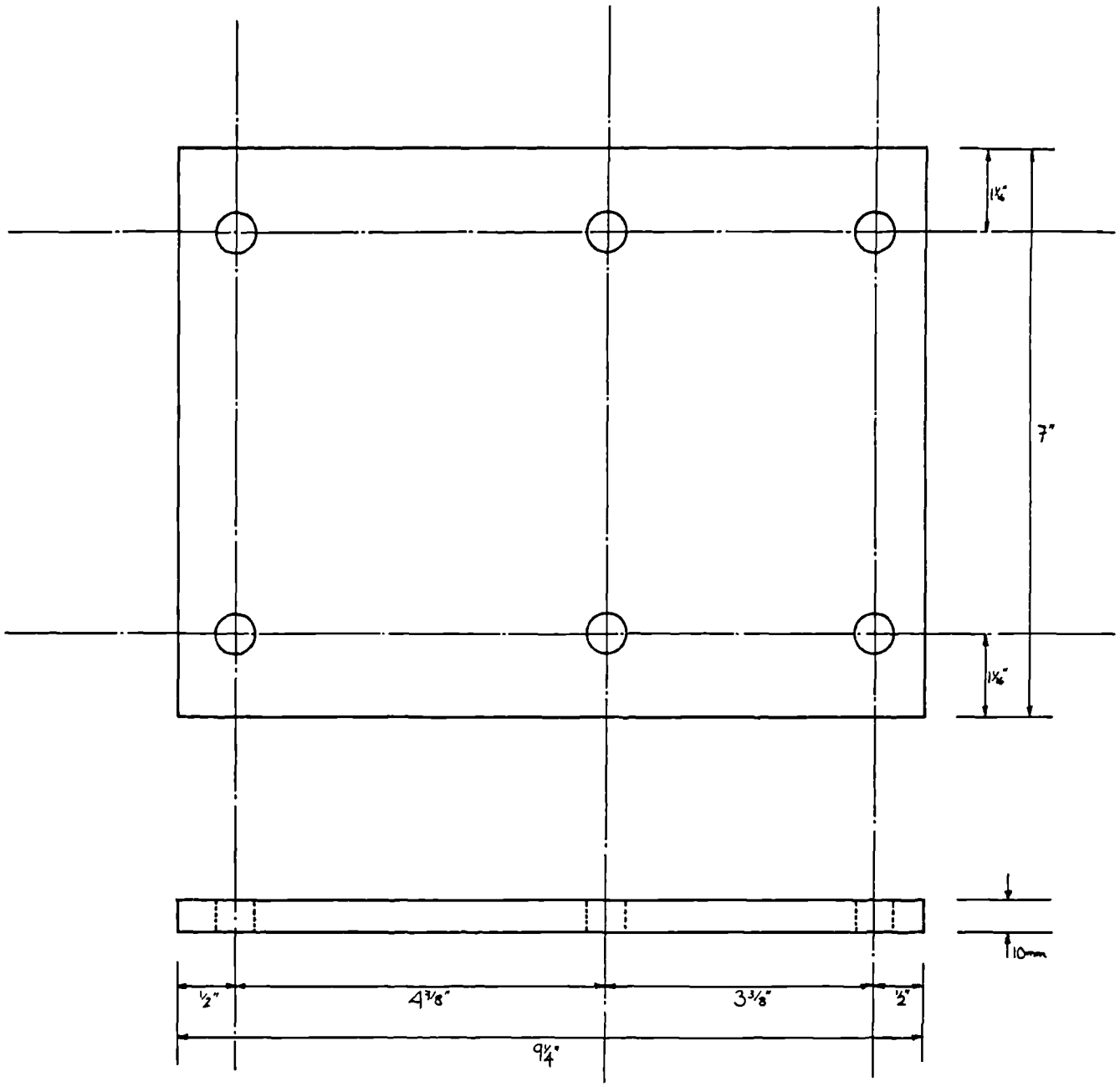

'ES DRILL 7/16" DIA.

figure 7.17 Absorber support plate (item 13)

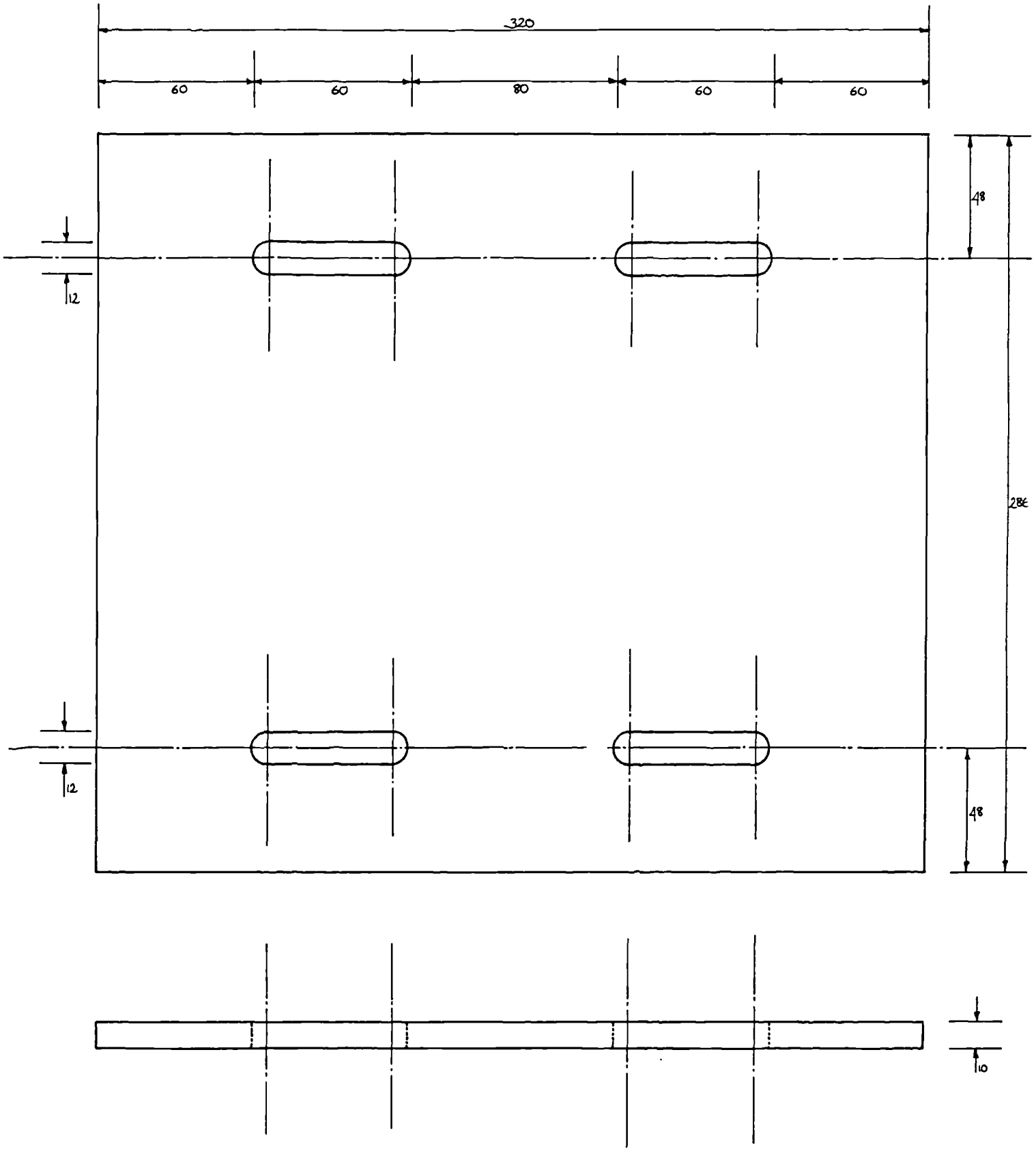

figure 7.18 Motor support plate (item 14)

7.2.6.2 Variable speed controller

An 'Anyspeed' Cheetah C5, 12 amp variable speed controller was used to control the D.C. Motor. This was mounted on the rigid support frame behind a fabricated aluminium gaurd to minimise the chance of water splashing onto it. The controller was set so that the maximum speed available was 1600 RPM. It was calibrated with reference to a tachometer so that any rotational speed of interest could be set from the numbered scale. This calibration was checked to ensure that the additional loading associated with liquid flowing through the absorber has a negligible effect.

7.2.6.3 Liquid pick-up nozzle arrangement

Liquid was removed from the liquid side sub chamber of the rotary absorber by a stationary stainless steel pick-up nozzle. This arrangment was supported by a screw jack (described below). The pick-up tube arrangemnt was designed so that the orifice of the nozzle could be moved to any radial position of interest via operation of the jack.

The pick-up tube assembly consisted of four short sections of 10mm diameter, 1mm thick stainless steel tubing,(i.e. the pick-up nozzle, the collection tube, the down tube and the removal tube). The nozzle was fixed at an angle of 30° to the collection tube which was in turn fixed at 90° to the down and removal tubes. Figures 7.19 and 7.20 show these sections assembled. The removal tube was held in an aluminium pick-up tube holder (shown in figure 7.21) by two 2mm grub screws. The pick-up tube holder was designed so that it could be screwed onto the end of the upper arm of the minature jacuator. Figures 7.13 and 7.14 show the pick-up tube holder in position.

The outside of the nozzle orifice was tapered for 5mm so that the leading edge caused minimum disturbance in the annular liquid layer. This produced a nozzle diameter of fractionally less than 10mm. Calulation showed that this should have been capable of accepting the maximum flowrate (100 cm^3/sec) at the lowest speed (500 RPM) and smallest radius (84mm). However, the nozzle tended to choke at the lowest speeds and higher flowrates. These conditions were therefore avoided in the mass transfer experiments.

7.2.6.4 Miniature Jacuator

A miniature jacuator manufactured by Duff Norton (model number: ME2625-150) was mounted on the rigid support frame in the position shown in figures 7.13 and 7.14. The rotational movement of the jacuator was limited by two restraining bars which passed through its base and which were fixed to its main body. The aluminium pick-up tube holder screwed onto the devices upper arm and was held in position by a lock nut. The pick-up tube assembly was carefully positioned in the holder so that the nozzle orifice could be moved radially through the liquid-side sub-chamber without the 'down-tube' interfering with the liquid rotary union.

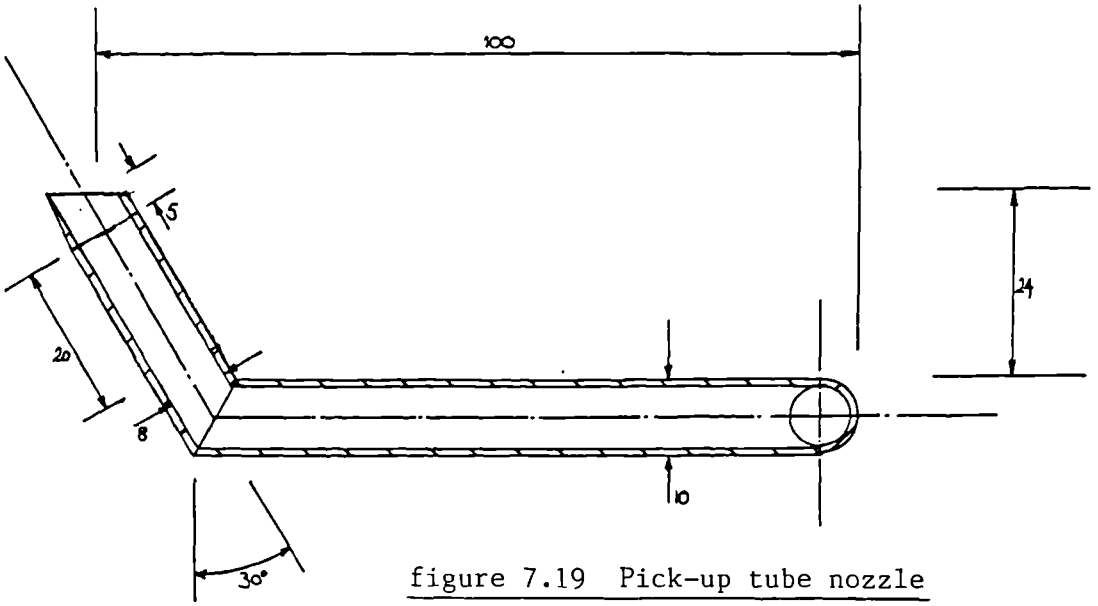

figure 7.19 Pick-up tube nozzle

figure 7.20 Pick-up tube collection tubes

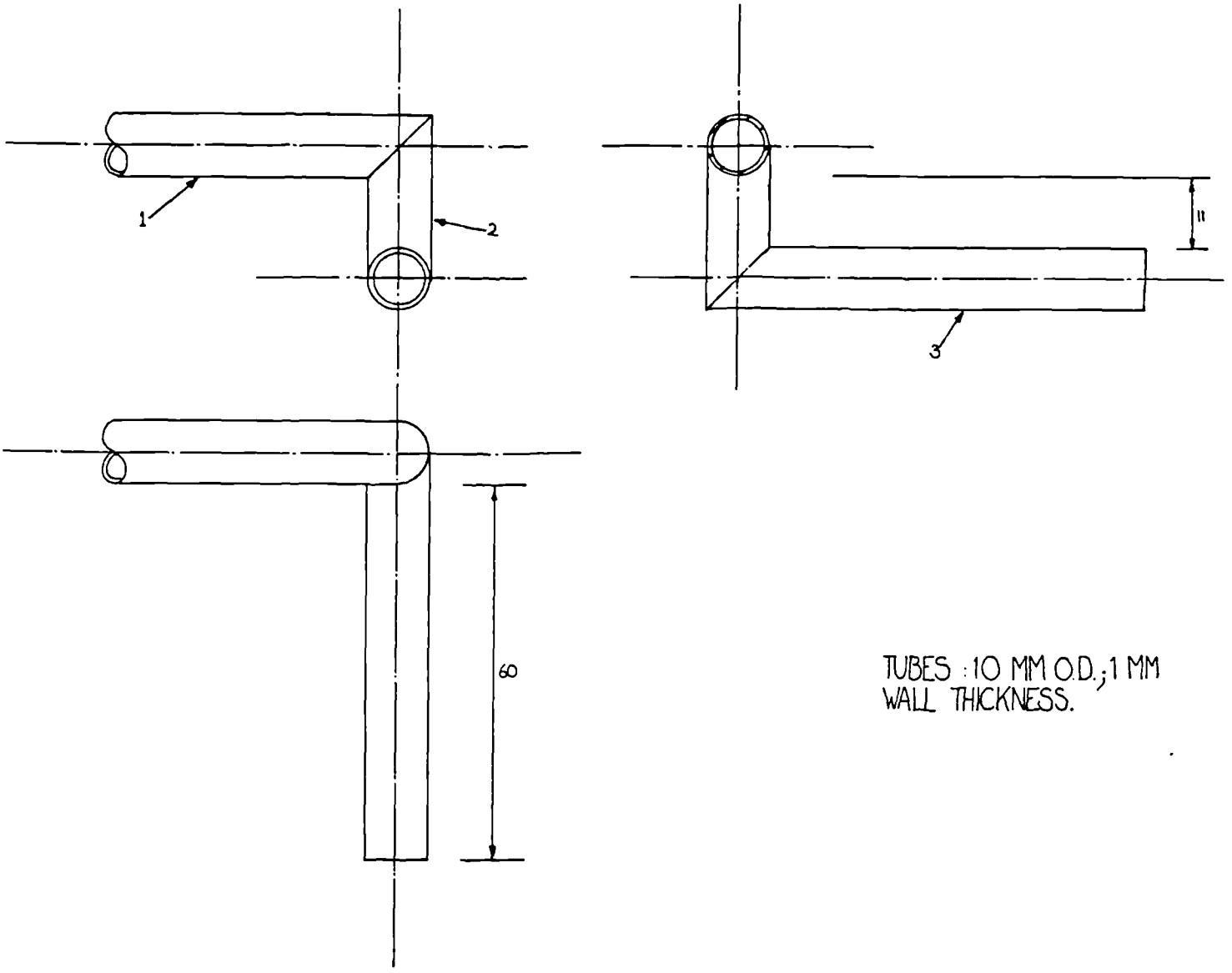

TUBES : 10 MM O.D.; 1 MM WALL THICKNESS.

1 : COLLECTION TUBE (NOT SHOWING END DETAIL)
2 : DOWN TUBE
3 : REMOVAL TUBE (GRIPPED BY PICK-UP TUBE HOLDER)

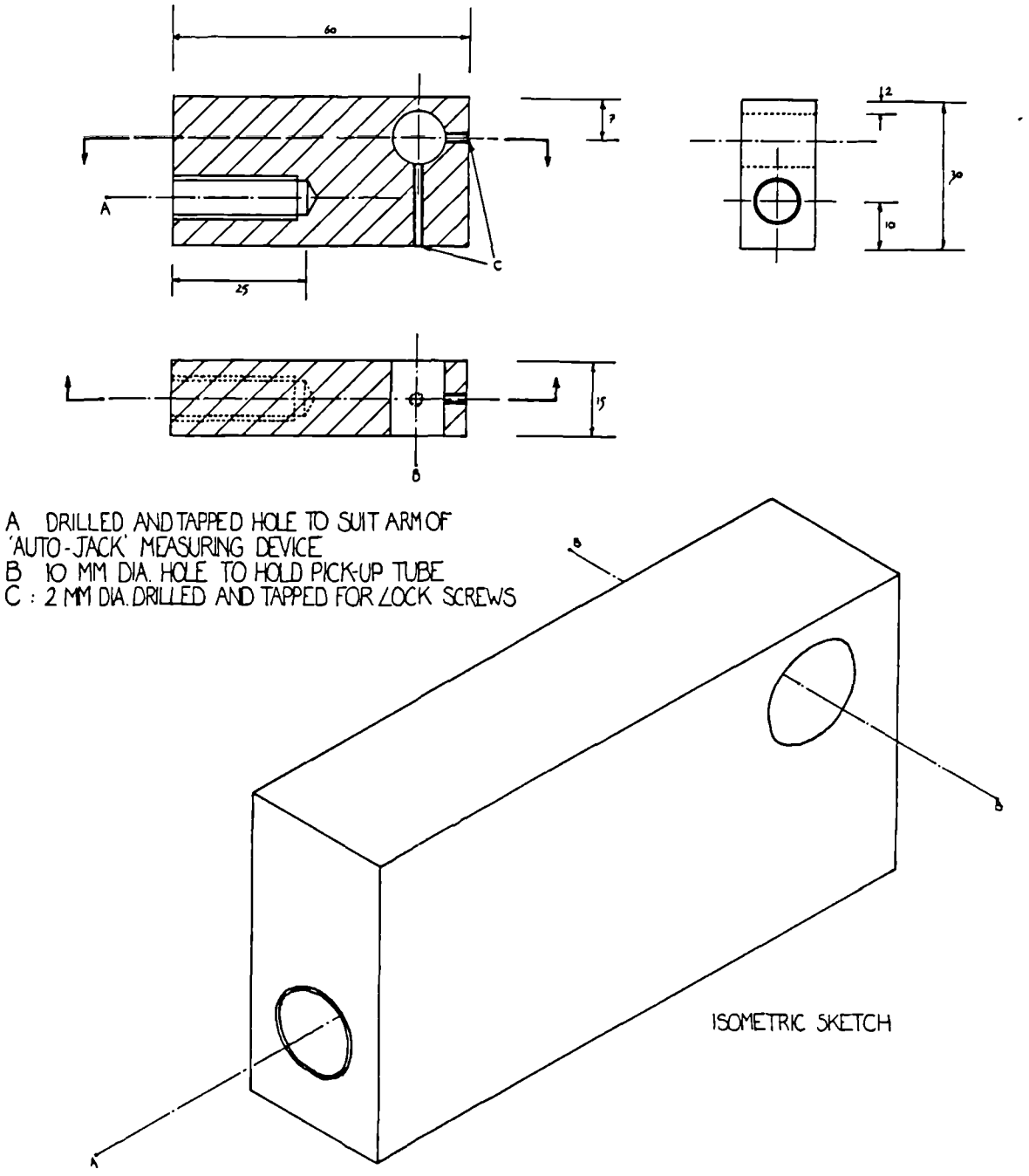

figure 7.21 Pick-up tube holder

7.2.6.5. Shroud

Due to the design of the pick-up system an annular liquid layer is formed in the absorption chamber. This will, to a certain extent, contribute to the overall rate of mass transfer. In order to quantify this a 'shroud' was designed to fit above the rotary disc so that mass transfer could only occur into the face of this layer. This shroud was formed from a sheet of 1mm stainless steel plate and had a diameter equal to that of the discs. It was fixed to the base plate using the peripheral screws and held 1mm away by the special spacer nuts described previously.

7.2.7. Pipework associated with the rotary absorber

Figure 7.22 shows the arrangement of pipes used to deliver and remove the gaseous and liquid phases from the rotary test rig. All connections to the absorber were made with flexible piping, thus enabling the inclination of the absorption chamber to be altered easily from vertical to horizontal position. As well as showing inlet and outlet gas and liquid lines figure 7.22 shows the positions from which samples were extracted.

7.2.8. Sample withdrawal and analysis system

Figure 7.23 illustrates schematically the system used to withdraw samples from the rotary absorber and deliver them to the electrode flow cell for analysis. In addition it shows the connections which were required so that the electrode could be calibrated. The operation of this system is described in detail in section 8.2 where the experimental procedure used during the mass transfer investigations is outlined. Photograph 7.2 shows the sampling system connected to the rotary absorber positioned for vertical operation.

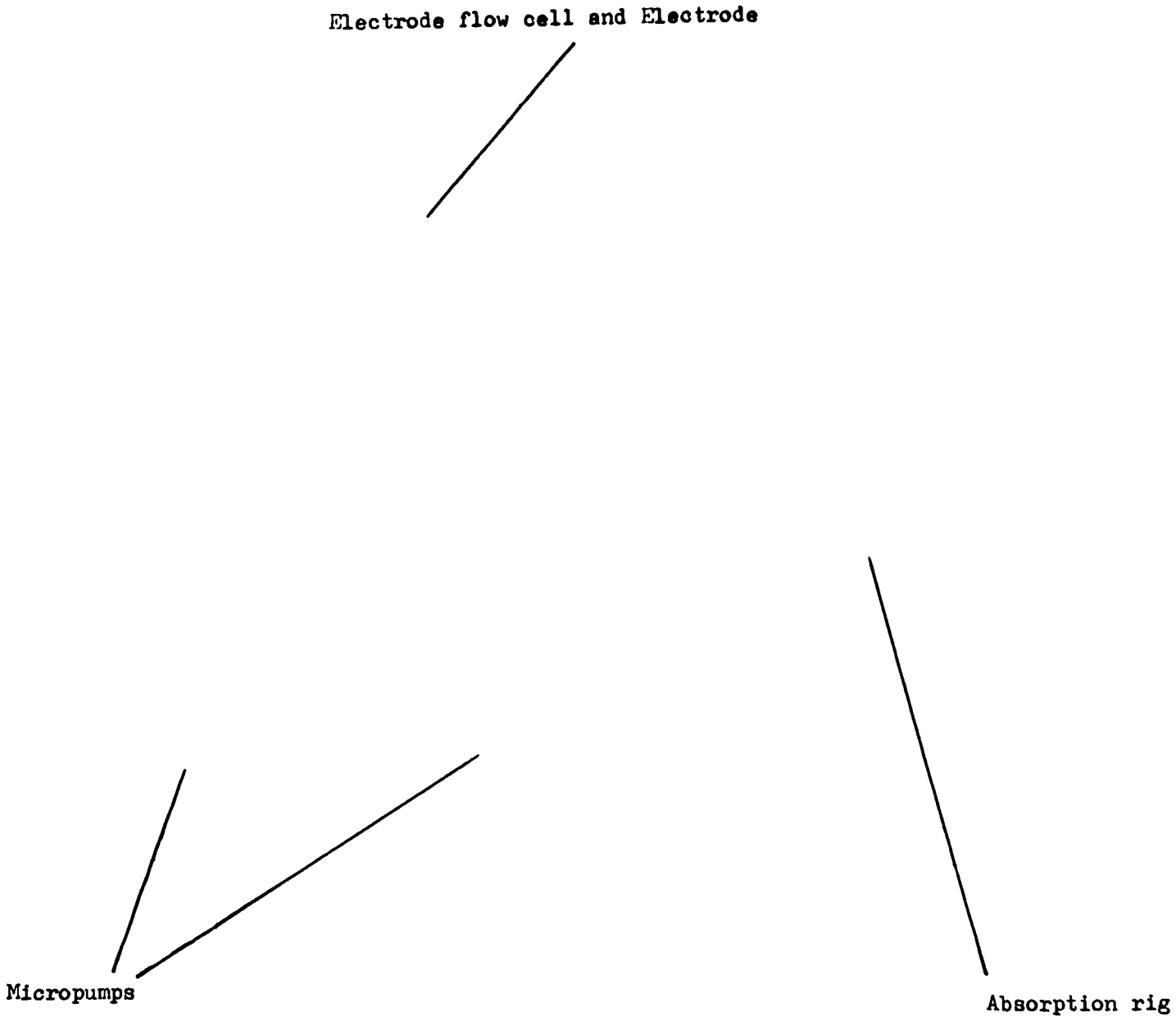

Photograph 7.2

Electrode flow cell and Electrode

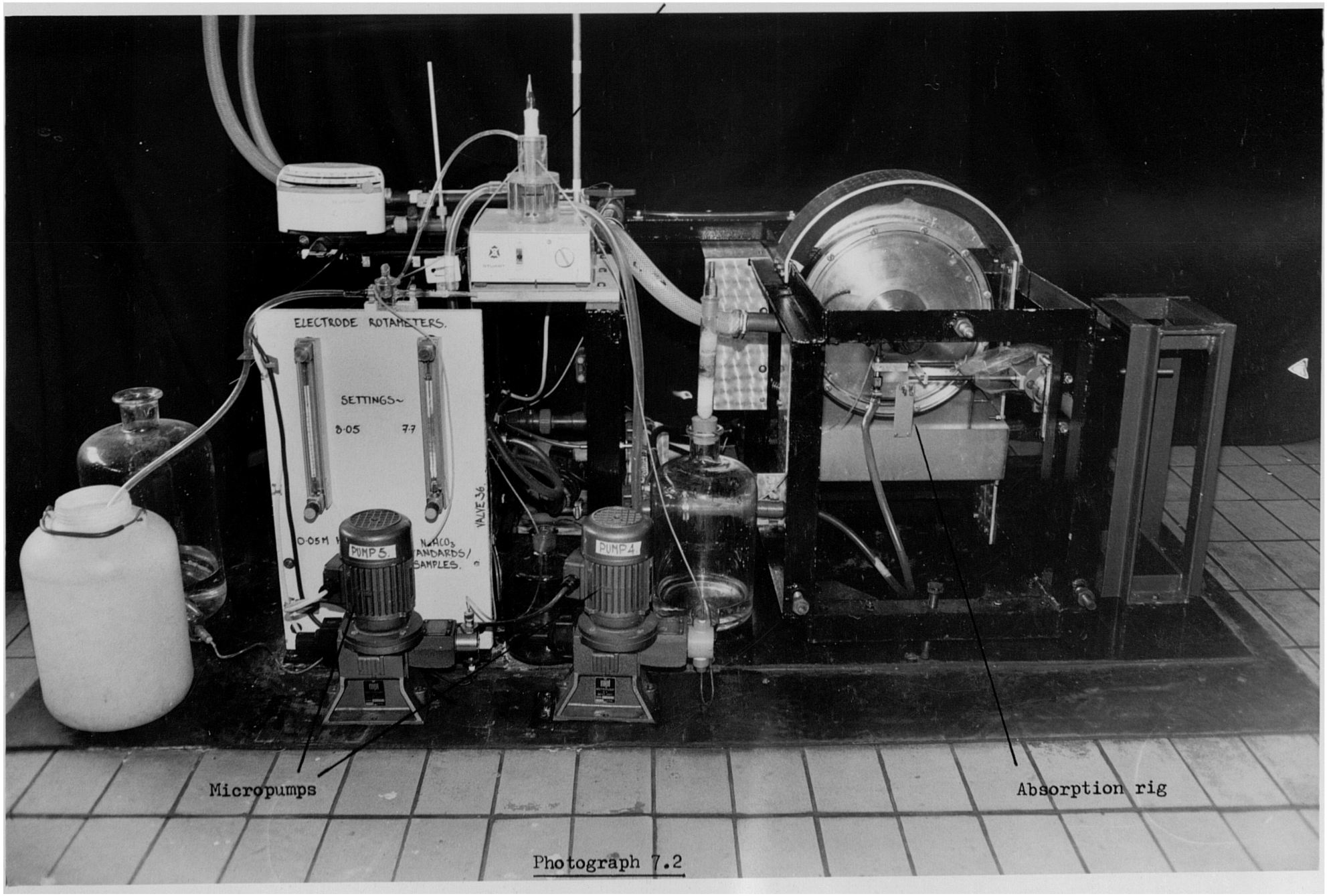

Photograph 7.2

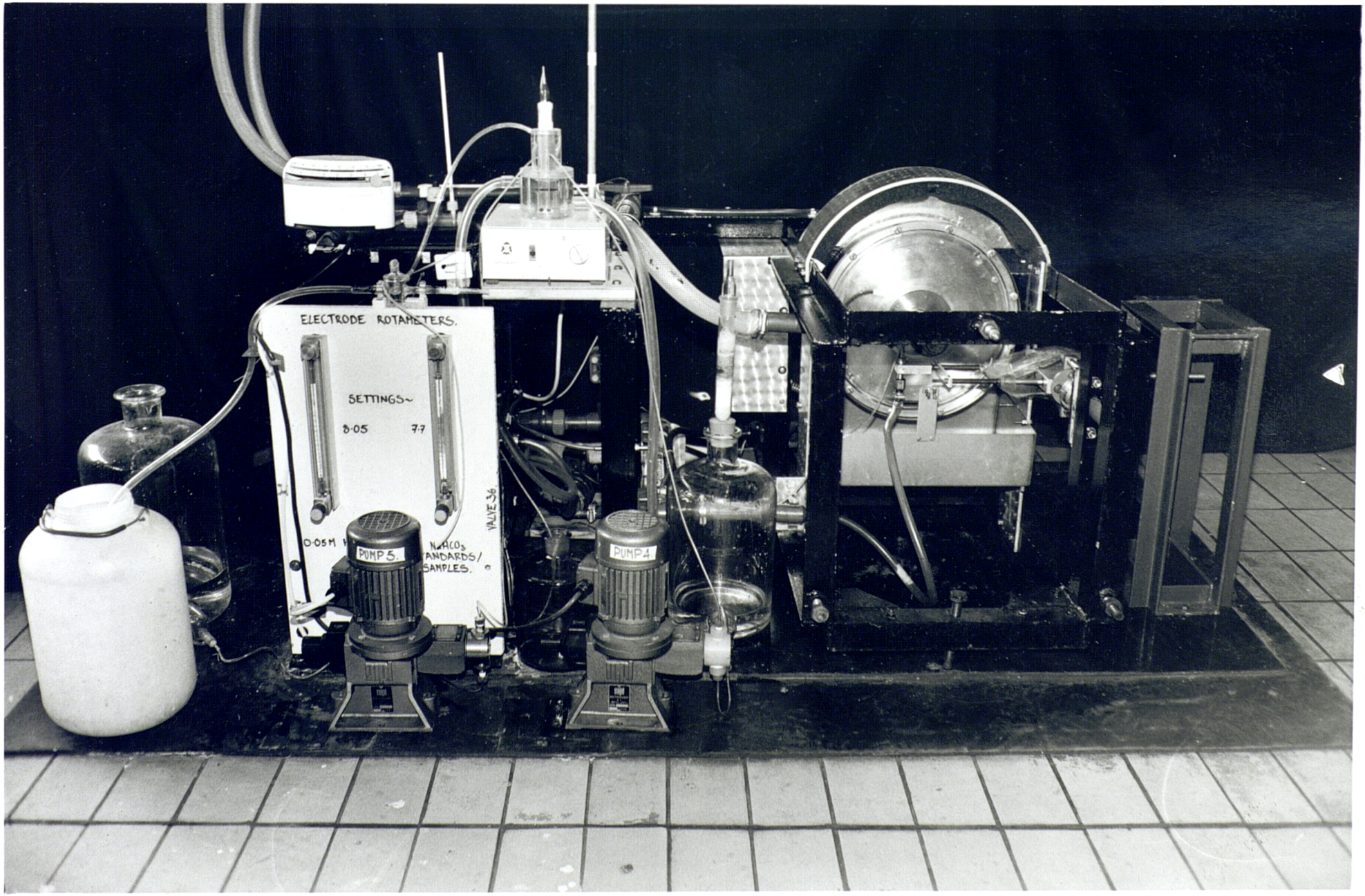
ELECTRODE ROTAMETERS.
SETTINGS~
8·05
7·7
VALVE 36
0·05M
PUMP 5.
NaHCO3 STANDARDS/ SAMPLES.
PUMP 4

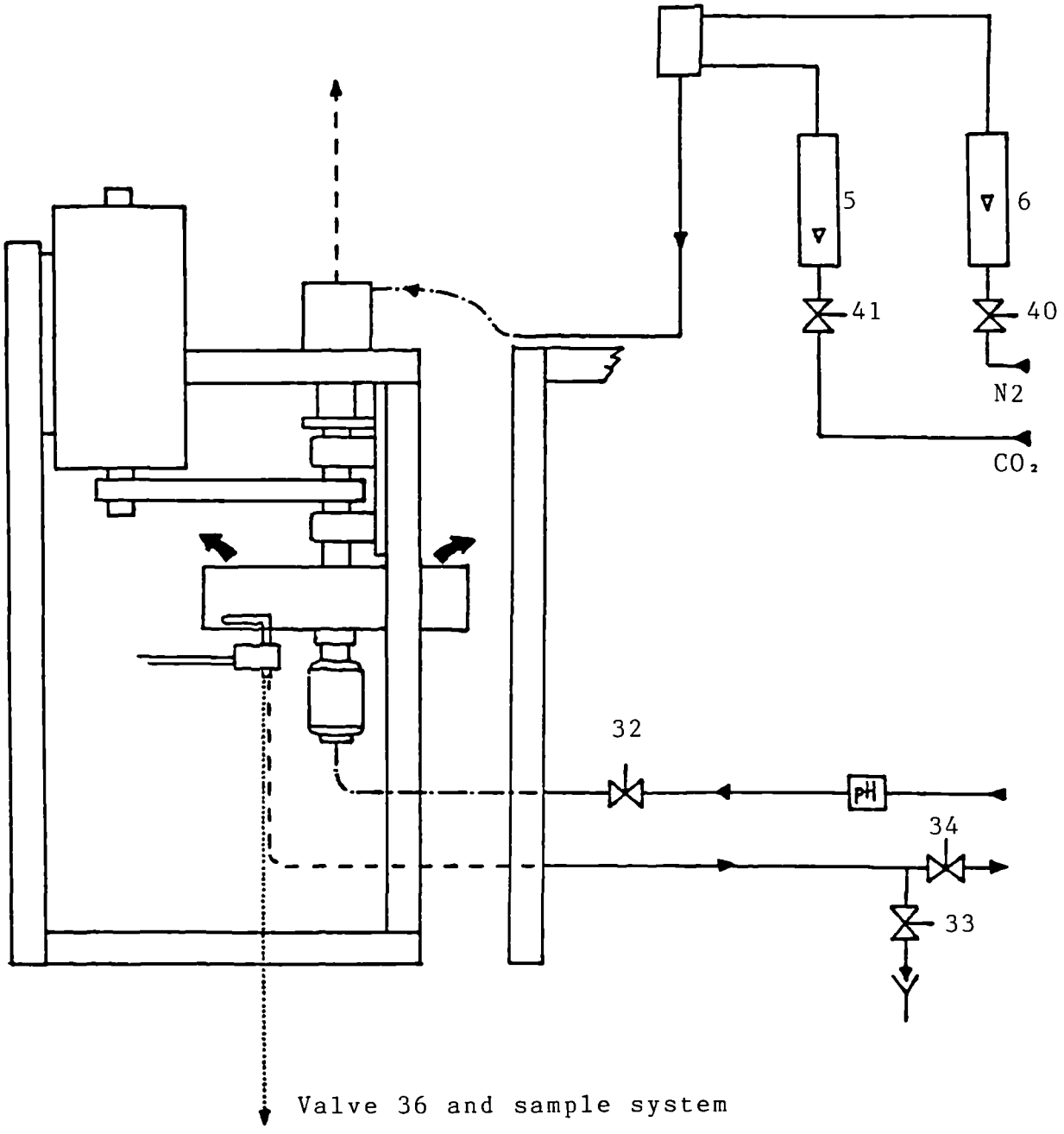

figure 7.22 Pipework associated with the rotary absorber

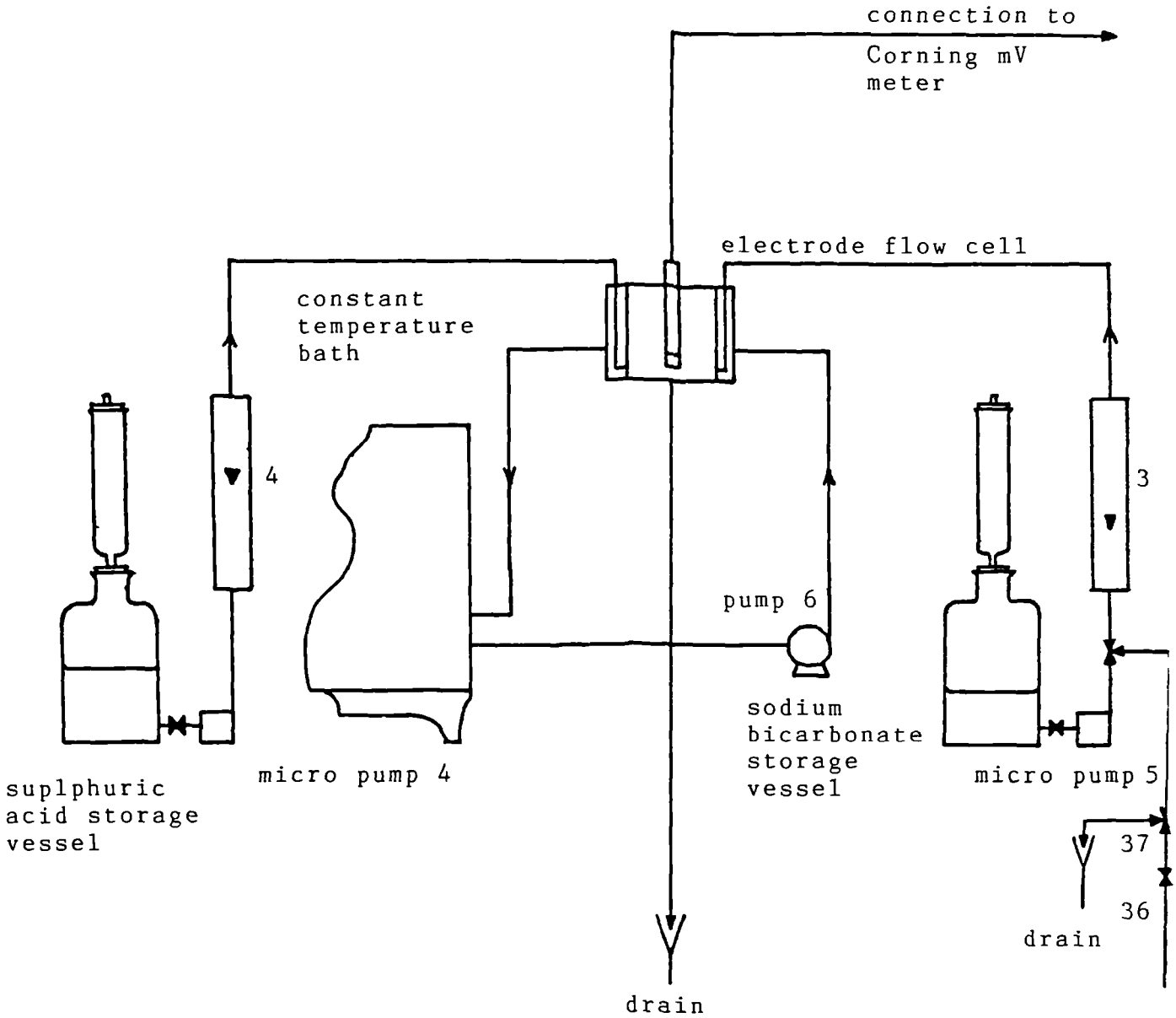

figure 7.23 Sample withdrawal and analysis system

7.3. Regeneration system

7.3.1. Introduction

A regeneration system was designed and constructed to allow 'loaded' solutions of aqueous diethanolamine to be 'scrubbed' of absorbed carbon dioxide. This consisted of a packed column, a liquid cooled condensor, a steam heated, kettle-type reboiler, and a liquid-cooled holding vessel. Feed to the system could be withdrawn from any of the 3 plastic storage tanks and metered by rotameters no 1 and no 2. At the end of the regeneration process the de-gassed solution could be pumped from either the brass holding tank or the brass reboiler to tank no 3 or no 1 by pump no 2. Figure 7.24 illustrates the regeneration system and storage tankage. All process pipework in this section of the facility was constructed from 1" O.D. P.V.C. tubing apart from that which was connected to the reboiler. As this had to withstand temperatures up to 120°C, PVDF tubing was utilised. This was connected to the tanks and the PVC pipework by short lengths of steel-braced flexible rubber tubing which was tested for heat stability up to temperatures of 150°C.

Photograph 7.3 illustrates the regeneration system.

7.3.2. Regeneration column

The regeneration column was constructed from a 2m length of 8" I.D. stainless steel pipe. This was flanged at each end to allow it to be fixed to the reboiler and condensor. The column was packed in two sections with 1" diameter high temperature plastic pall rings. These were used as they allowed proper wetting at the design liquid flowrates. Figure 7.25 provides a cross-section through the column showing the distribution of packing and the position of the feed tubes, distribution plates and support plates.

Feed to the column (CO_2 'loaded' diethanolamine at approximately 70°C) is distributed over a sieve tray positioned between the two packed beds. It is fed to the distributor down four identical feed tubes which pass through the top of the column and double as support rods for the upper packed section. Liquid passing down through the lower packed bed is stripped of CO_2 by a counter-current flow of steam which is generated in the reboiler. The steam and stripped carbon dioxide pass out of a 4" vent in the top of the column where the steam is condensed and returned to the column. This returning liquid is distributed over the top of the upper packed section by a wear type distributor. The upper bed of packing strips any DEA entrained within the steam into the liquid stream returning from the condensor.

The feed distribution system, the support plates and the condensate distributor were all constructed from stainless steel as evidence suggested that under these conditions the vapour/liquid mixture was highly corrosive. Figures 7.26 to 7.32 present detailed engineering drawings of these items.

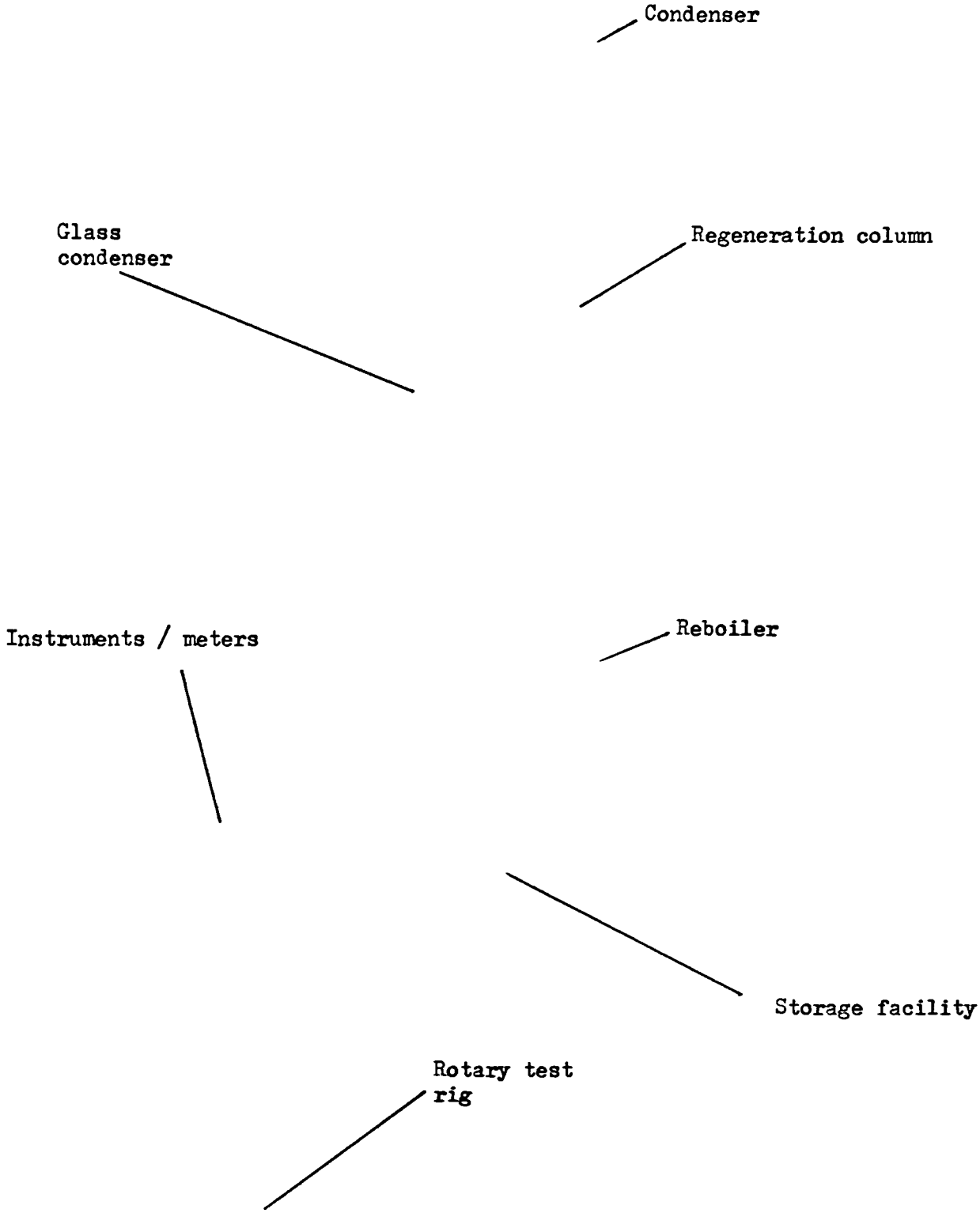

Photograph 7.3

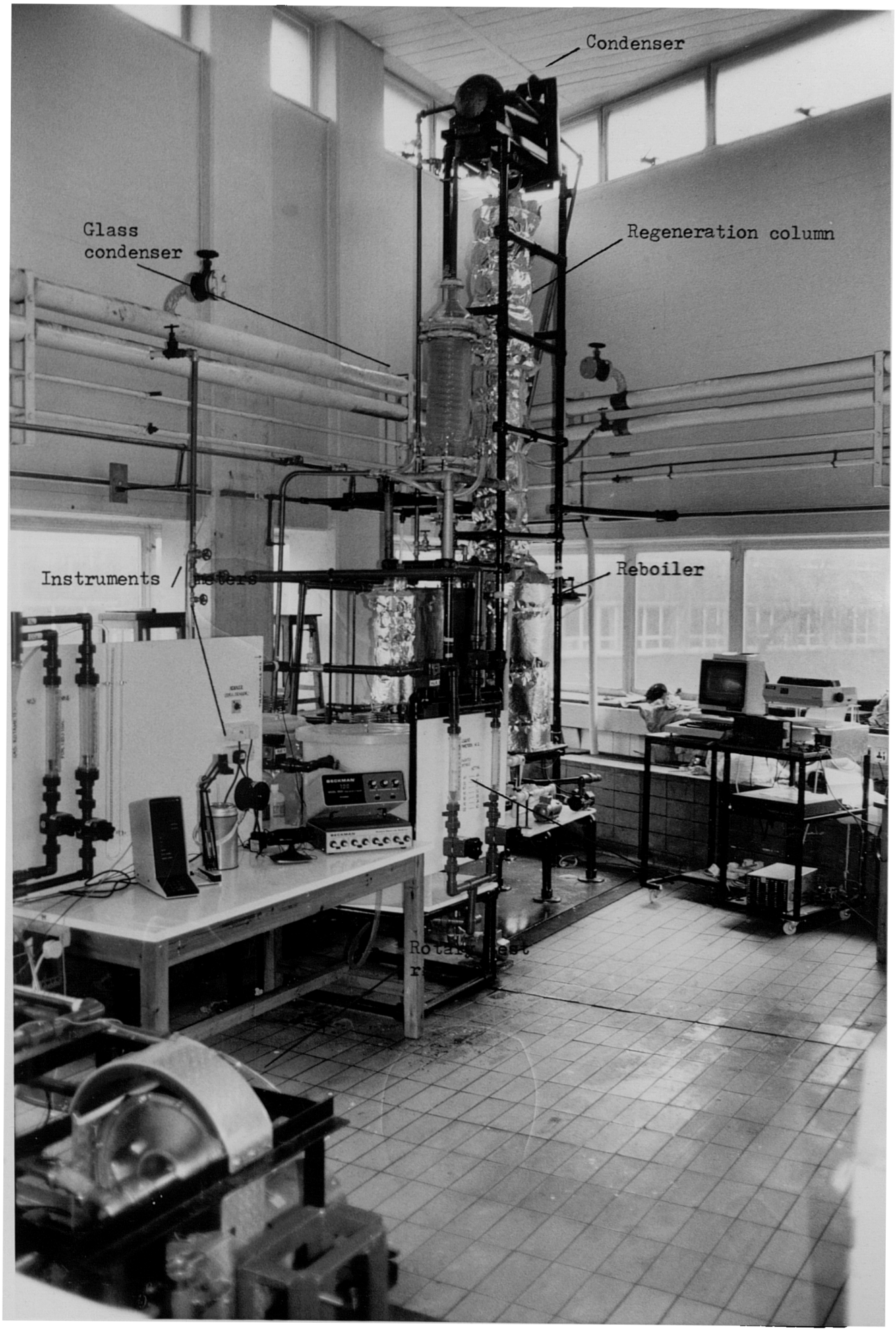

Photograph 7.3

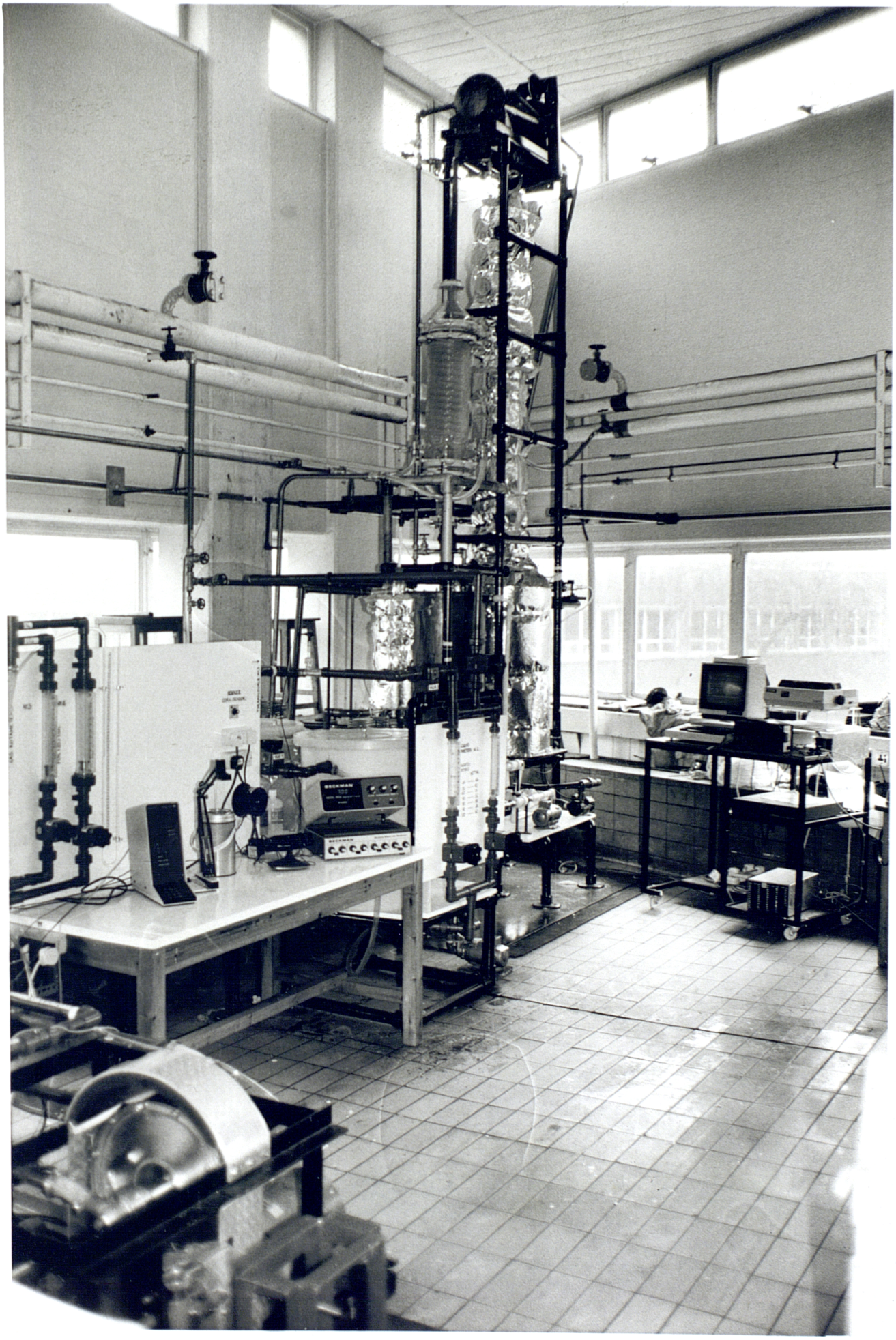
BECKMAN

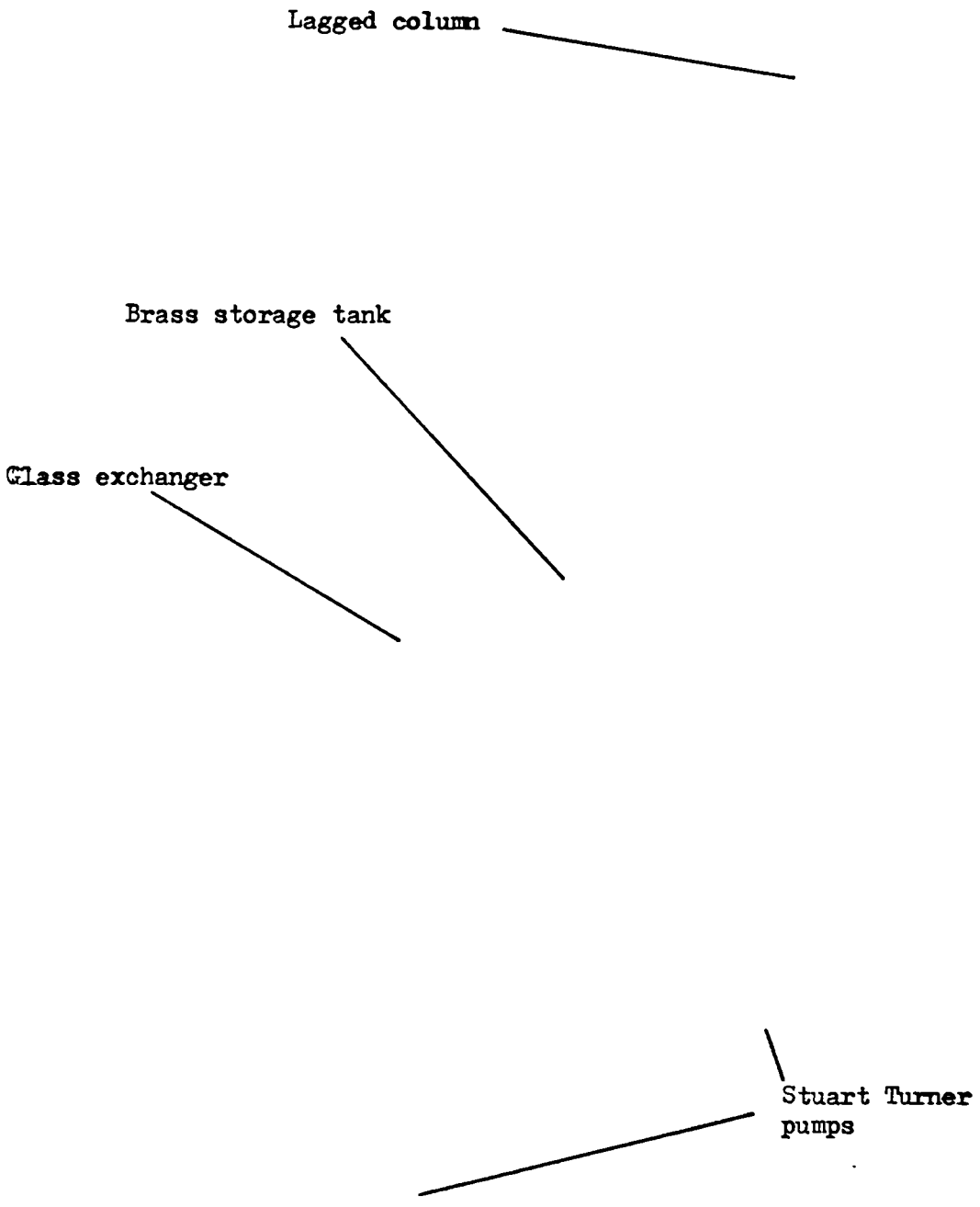

Photograph 7.4

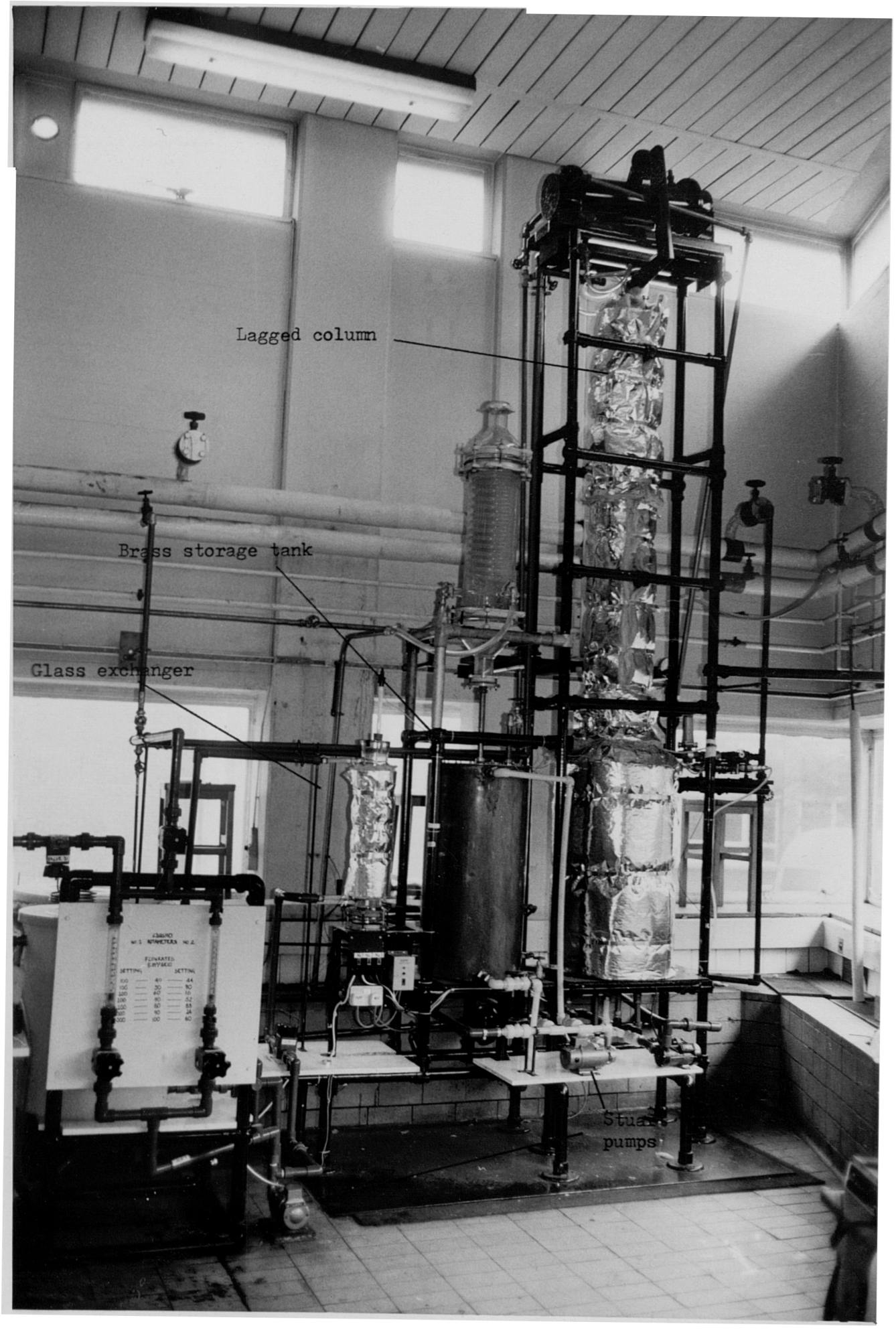

Photograph 7.4

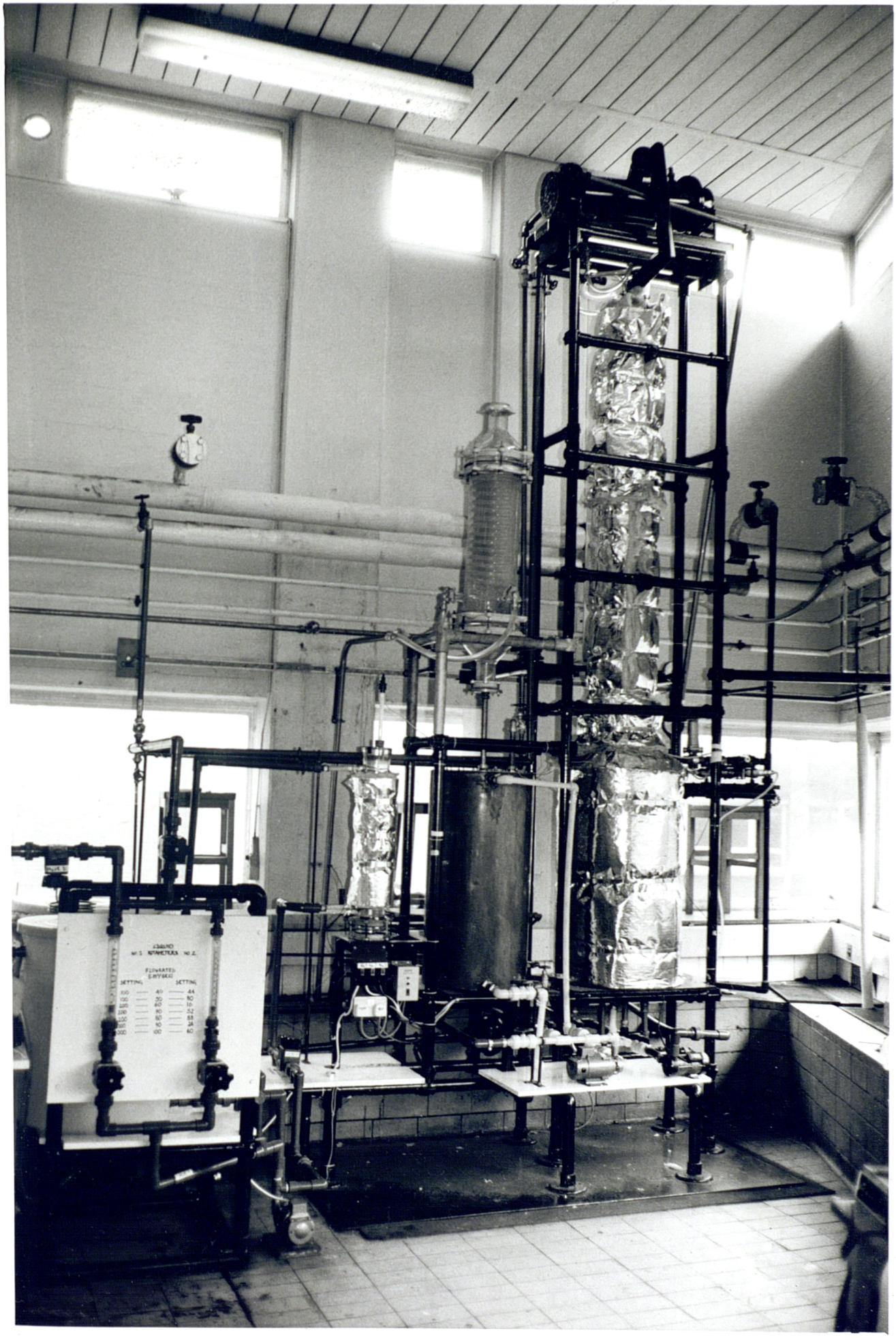

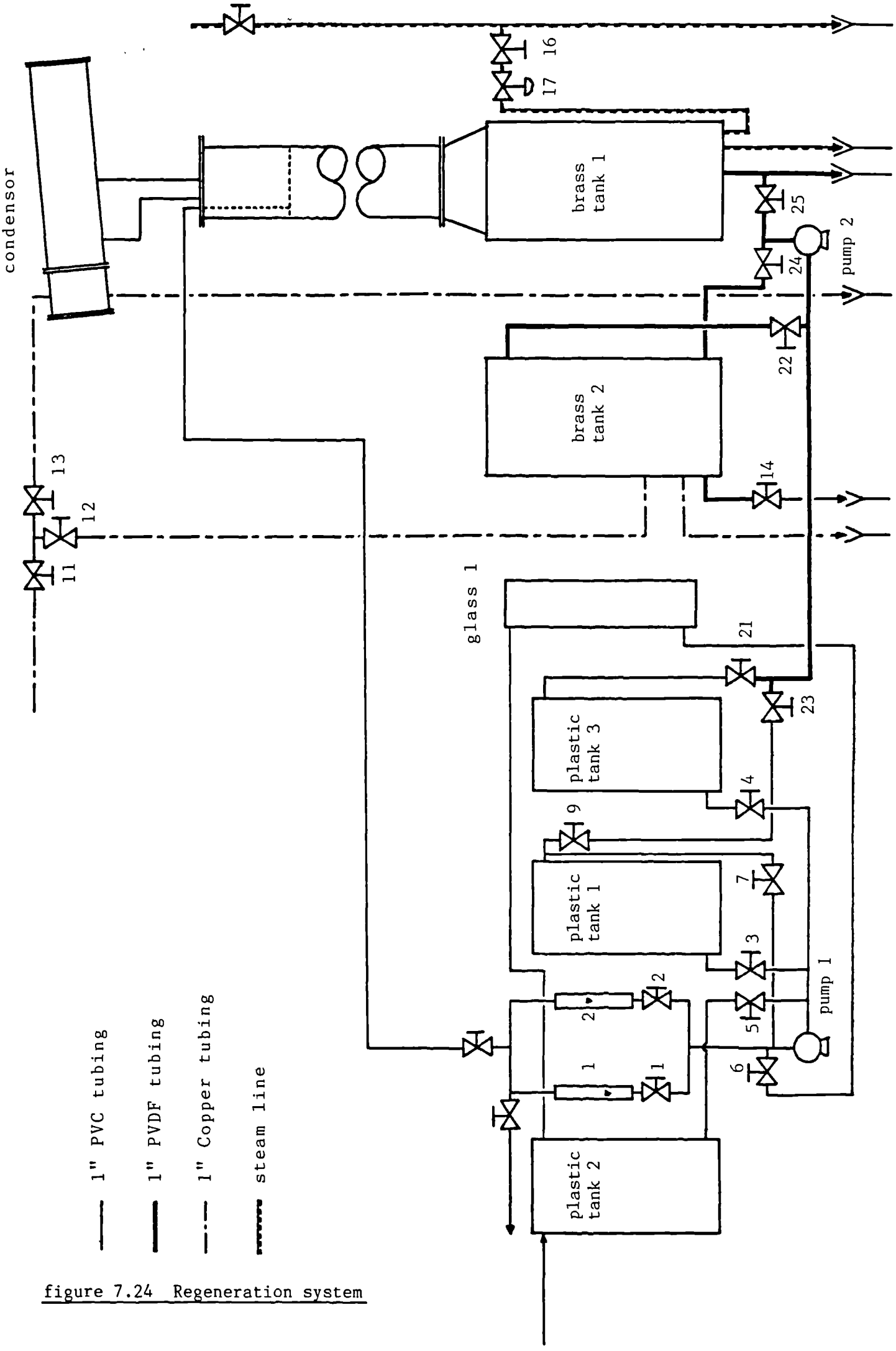

figure 7.24 Regeneration system

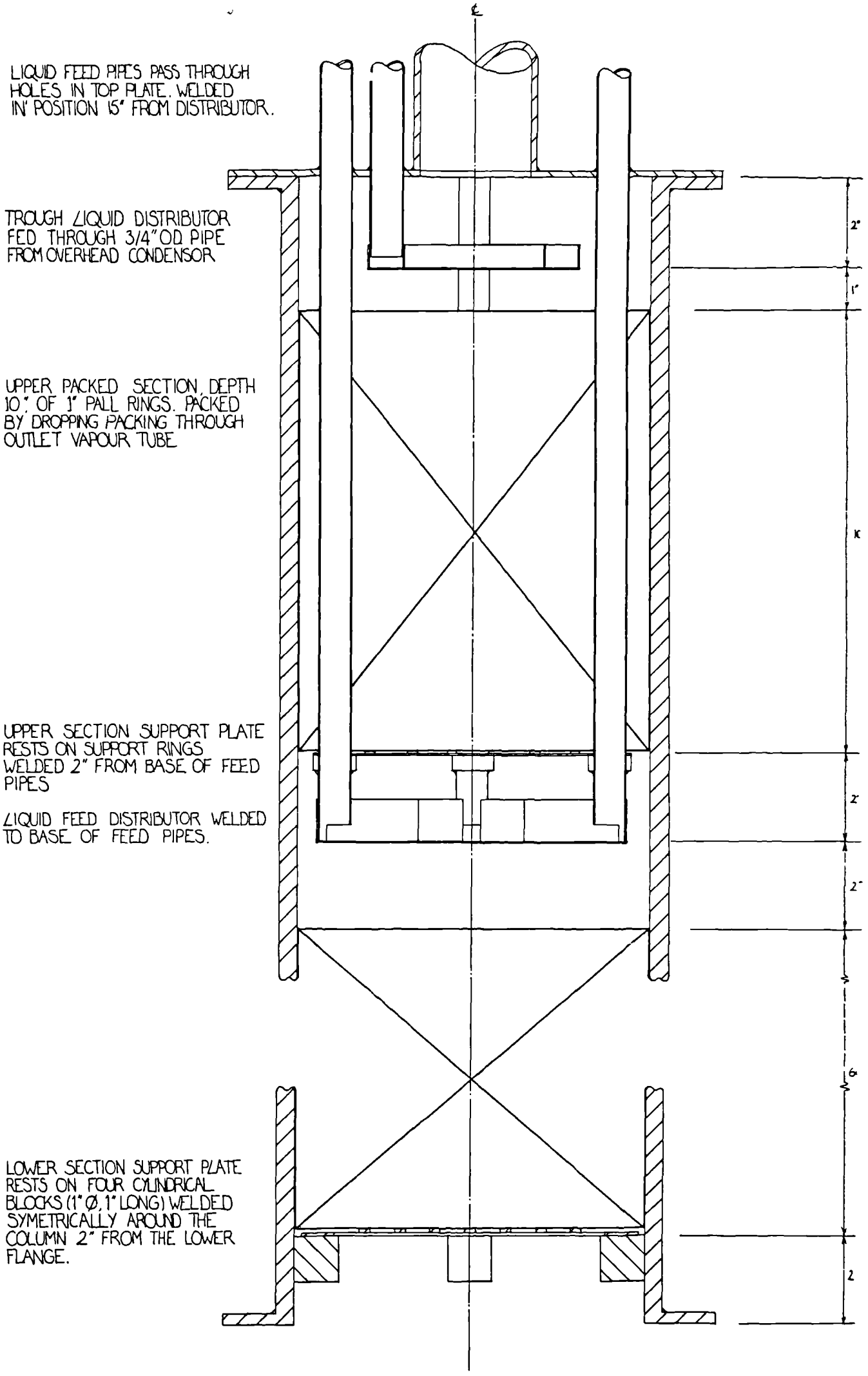

figure 7.25 Crossection through the regeneration column

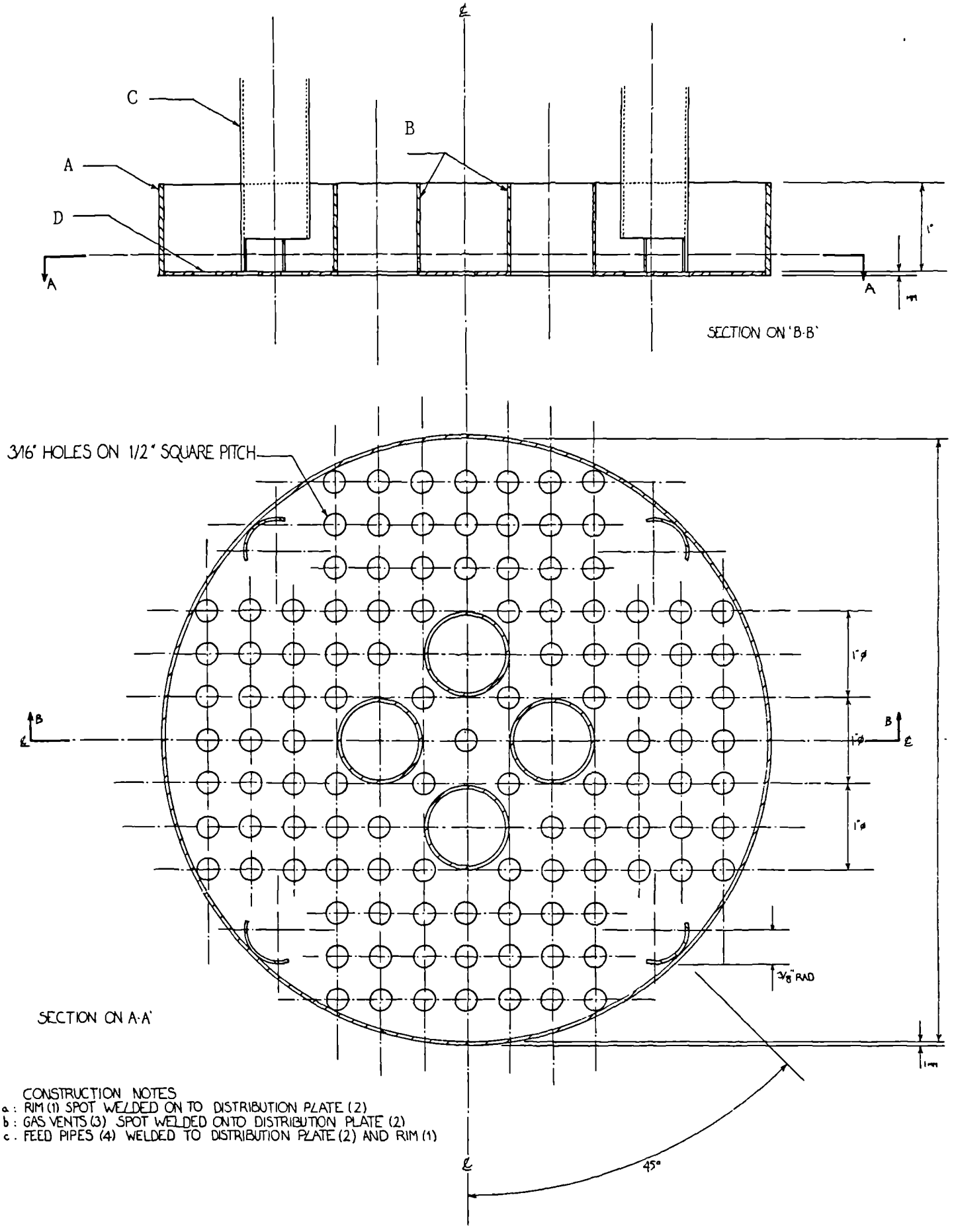

figure 7.26 Sieve plate distribution (item D)

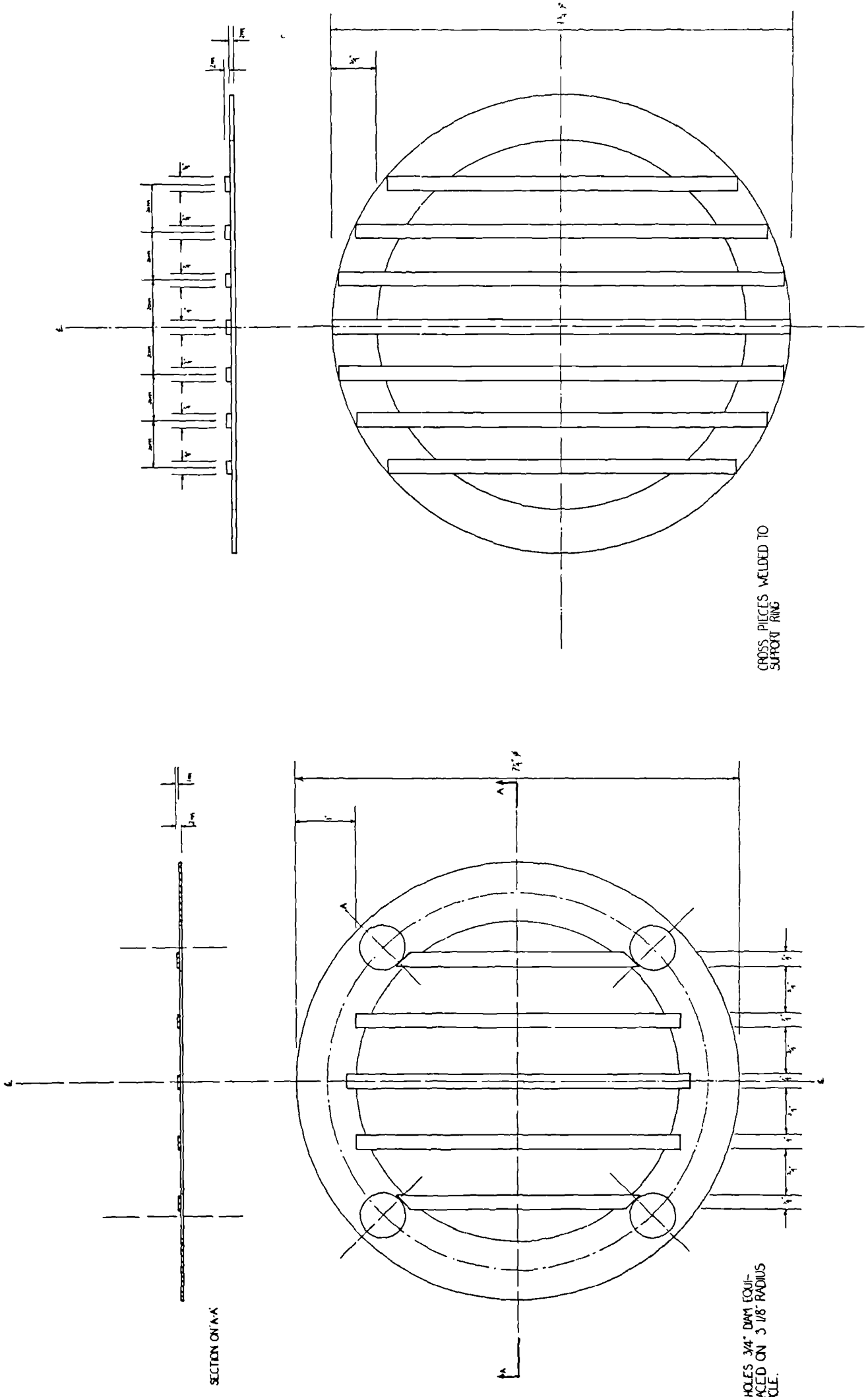

figure 7.27 Packing support plates

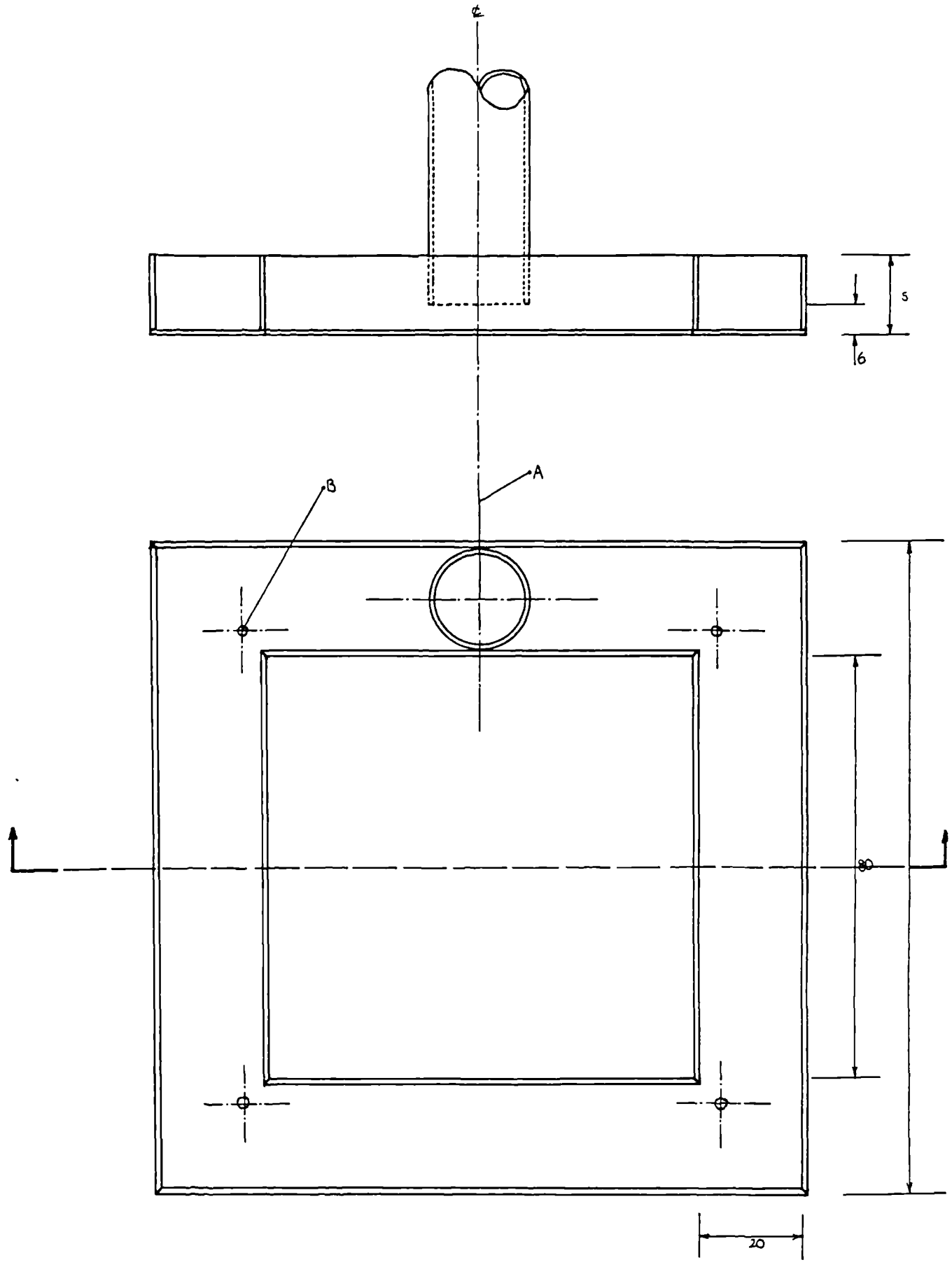

A : LIQUID FEED PIPE. 3/4" O.D. SPOT WELDED TO TROUGH PLATE
B : 4 x 2MM DRAINAGE HOLES
ALL PLATE THICKNESS 1MM

figure 7.28 Weir distribution

figure 7.29 Feed distribution tubes (item B)

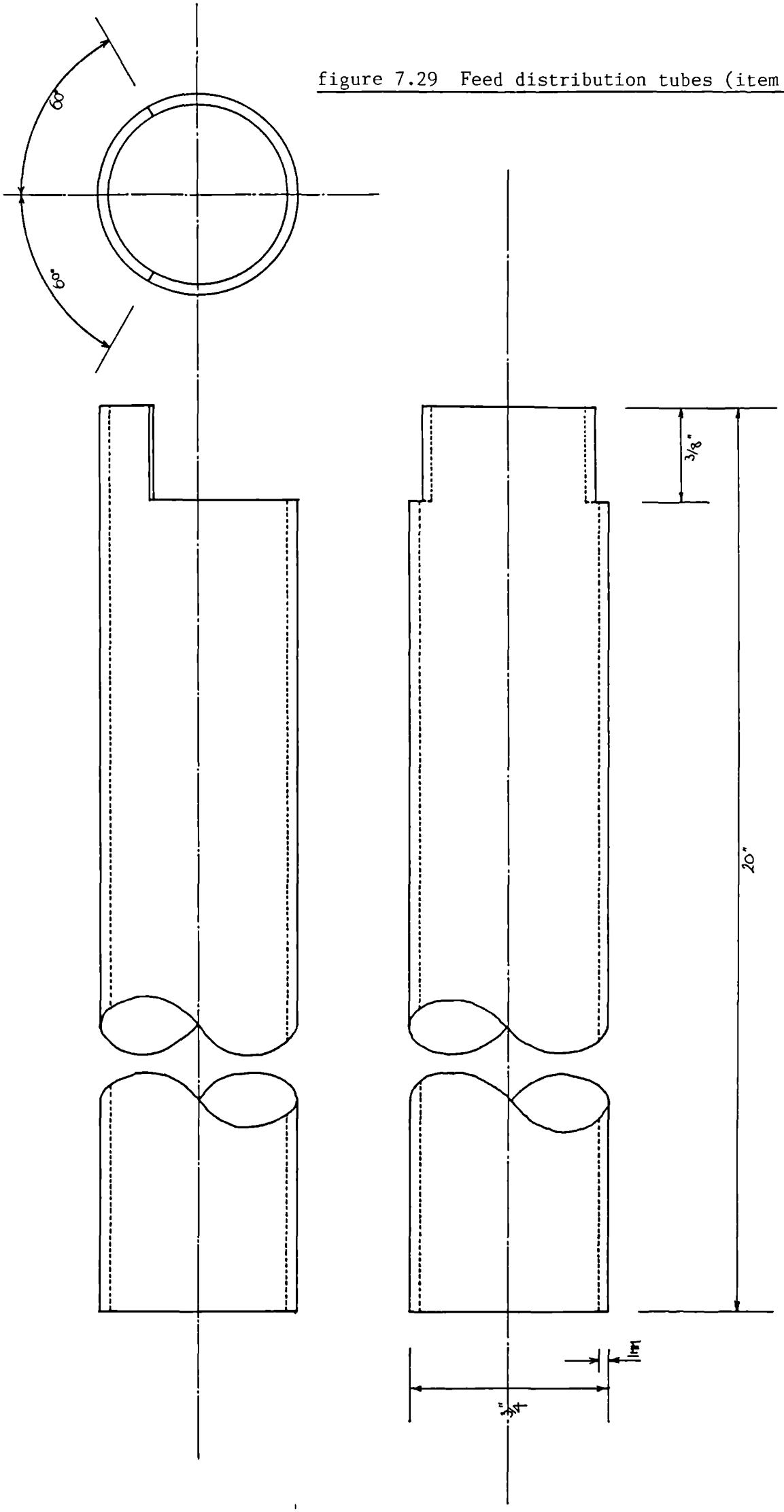

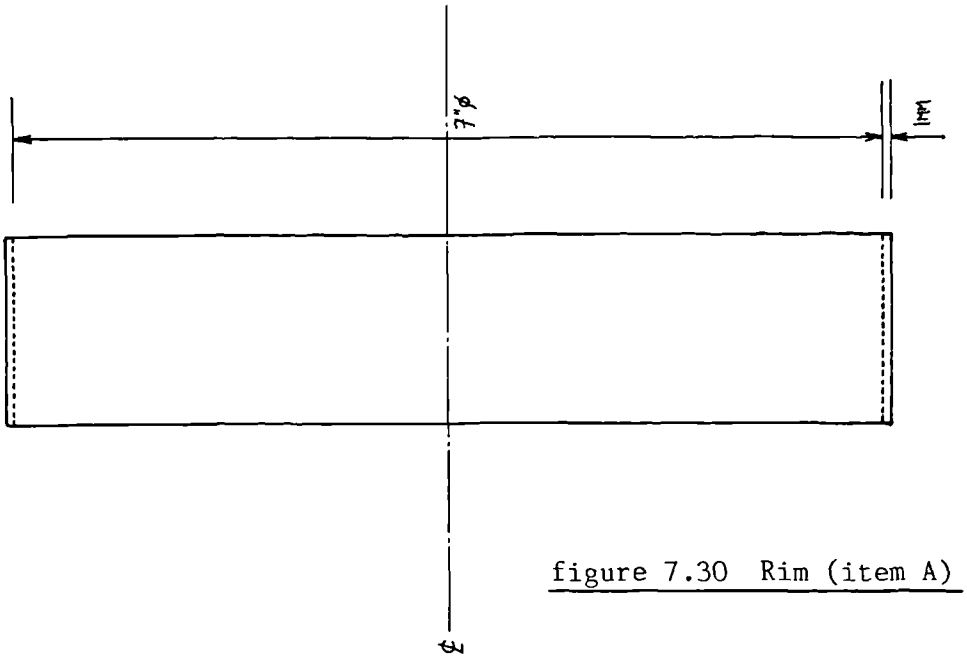

figure 7.30 Rim (item A)

figure 7.31 Gas vents (item B)

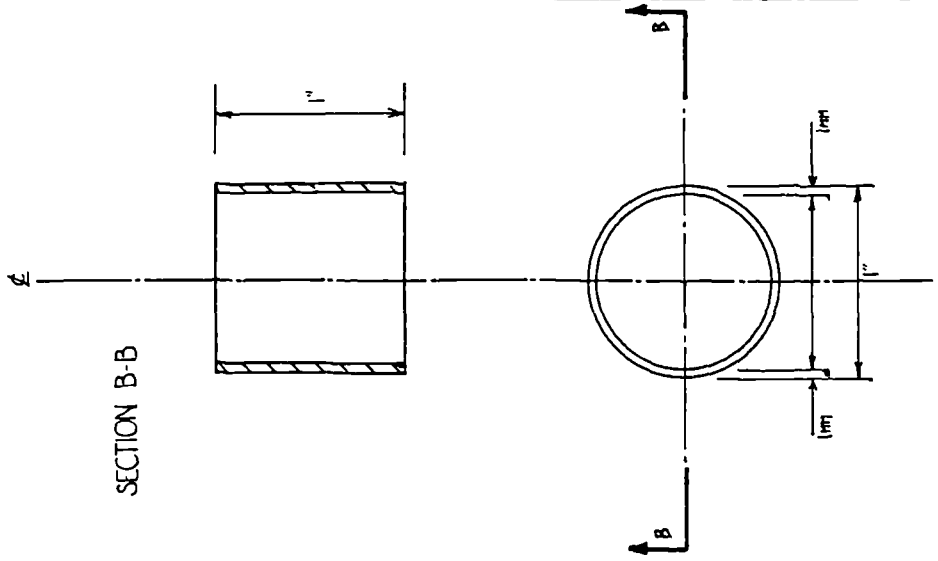

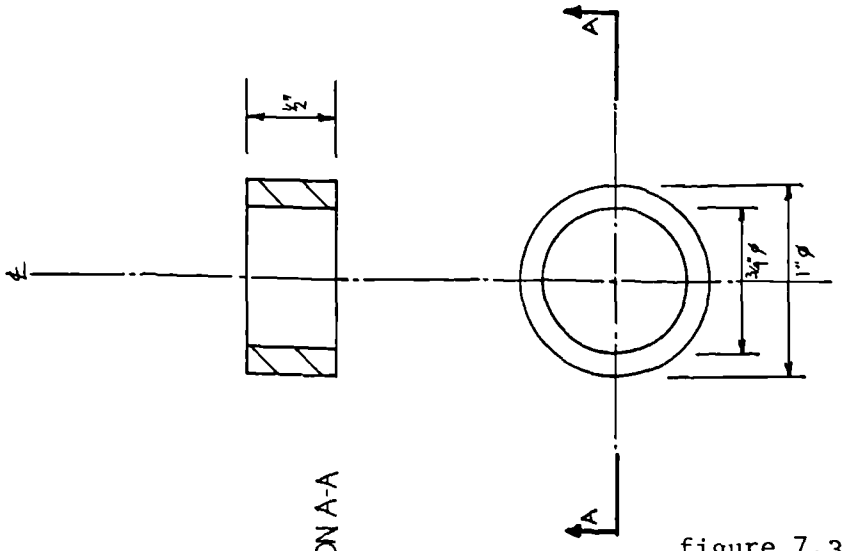

figure 7.32 Support plate rings

7.3.3. Reboiler

A large cylindrical brass tank was adapted to form the basis of the steam heated kettle-type reboiler. This had an internal diameter of 450mm and a depth of approximately 680mm. As mentioned in section 3 there is some evidence to suggest that aqueous solutions of diethanolamine corrode brass, expecially when they contain free carbon dioxide. Therefore, although the choice of a brass vessel was not ideal, financial limitations precluded the acquisition of a stainless steel tank. Similarily copper tubing was used to construct the steam heating coils even though this material was also corrosible. In order to determine the useful life of these items a series of corrosion tests was carried out. These tests indicated, as suspected, that a corrosive environment was formed, however they also showed that if free carbon dioxide could be precluded from the reboiler the rate of corrosion was manageable. The method of operation of the regeneration system was therefore adapted to take account of this conclusion (see Appendix L). Appendix A describes the corrosion tests.

In order to process 200 cm^3/sec of fully loaded diethanolamine solution a reboiler duty of approximately 60KW was required. Approximately half of the heat supplied was necessary to raise the feed from an inlet temperature of 70°C to the boiling point of the solution (approximately 105°C at just over atmospheric pressure). The rest of the energy was required both to reverse the absorption reaction and produce the necessary flow rate of steam to effect this regeneration. In order to avoid thermal degradation of the diethanolamine the heating medium had to be at a temperature below 150°C. An electric element could therefore not be employed, as the surface temperature of such a device is well in excess of this limit. Steam heating was therefore chosen, The size of heating coil required was designed assuming a condensing steam temperature of 130°C so that the temperature could be increased if the resultant duty proved insufficient. Assuming an overall heat transfer coefficient of 1400 $W/m^2.°C$ the area of steam coil required was $1.65m^2$, it was thus designed to provide an area of $1.8m^2$. A double wound helical coil was fabricated from 1" O.D. copper tubing. The outer coil had a diameter of 405mm while that of the inner was 334mm, there was thus a 10mm gap between the tank wall and the outer edge of the outside coil and 10mm between the coils themselves. Ten turns of each coil were necessary to provide the required transfer area. The inlet and outlet of each coil was positioned so that they passed through the base of the reboiler which was mounted on a wooden platform supported by scaffolding poles. The inlets of each coil (i.e. the bottom turns) were connected to the departmental high pressure steam supply via a pressure regulating control valve and a shut off valve. The outlets (i.e. the top turns) were routed to the drainage system via a thermodynamic steam trap. It was felt that the steam pressure would be sufficient to blow condensed steam from the coils.

The reboiler was positioned below the packed column as shown in figure 7. 24. They were connected by a stainless steel conical reducer which was flanged at both ends. Liquid delivered to the column therefore perculated through the packing before cascading into the reboiler. The steam generated in the reboiler passed through the conical connection and then up through the column.

The level in the reboiler was controlled so that a depth of liquid between 550 and 600mm was always maintained. The steam coils were therefore never exposed to the more corrosive vapour phase and the liquid was prevented from rising up the column and flooding the lower packed bed. This was achieved by installing three metal probes through 1/4" boiler fittings at depths of 500, 550 and 600mm. These were connected to an electric relay which was in turn connected to pump 2. The relay was tuned so that when the level rose beyond the top probe (i.e. a circuit was 'made' between this and the bottom (reference) probe), pump number 2 was activated and liquid was pumped into the brass storage tank. When the level had fallen so it was below the middle probe (i.e. the circuit between this and the reference probe was broken) the pump was switched off. The sensing probes were constructed from 10cm pieces of 1/4" diameter stainless rod and protruded 8cm into the reboiler. The reference probe was fabricated from a 10cm length of 1/8" O.D. stainless steel tubing welded shut at one end. This end protruded 8cm into the reboiler. A copper/constantan thermocouple (coated with heat shrink plastic tubing) was placed inside the reference probe and the outer end sealed with araldite. The thermocouple was extended to the relay mounted on the main control panel/board where the mV reading could be displayed. Each of the probes was electrically insulated from the brass tank so that a circuit could not be formed through the vessel walls by wrapping insulating tape around three centimeters of the outside ends of the probes. Valve 24 was opened sufficiently so that a flowrate of 300 cm^3/sec was attained when the pump was activated. It thus took 1 minute 20 seconds to reduce the liquid level from 600 to 550mm and 40 seconds for it to refill.

7.3.4. Condenser

A two pass, mild steel, shell and tube heat exchanger was employed as the steam condenser in the regeneration system. This was mounted 800mm above the top of the packed column on a specially fabricated cradle which in turn was mounted on the column-support frame. The 4" vent hole was connected to the inlet of the shell side by a length of 4" I.D. rubber hosing. Condensed steam was returned to the column through a 3/4" tube connecting a vent on the lower end of the exchanger with the wear distributor mounted above the top bed of packing. Carbon dioxide entering the condenser was exhausted through a 1/2" vent installed on the upper surface of the exchanger. Water from the departmental cold water supply was used as the condensing medium on the tube side of the exchanger. The flow rate of this could be controlled by valve 13. The exit water stream was sent to drain.

In order to process 200 cm^3/sec of loaded diethanolamine it was estimated that the condenser would need a duty of approximately 17kW. Assuming an overall heat transfer coefficient of 400 W/m^2k and a minimum log mean temperature of 80°C a tube surface area of 0.53m^2 was required. The heat exchanger available contained 30, 1cm diameter 1m long tubes and thus was well capable of performing this required duty.

7.3.5. Brass storage tank

Regenerated diethanolamine automatically removed from the reboiler by the action of the level controlling relay was

pumped into a brass storage tank. This tank had exactly the same dimensions as that used for the reboiler. To facilitate cooling of the liquid the tank was fitted with a copper cooling coil which was fed from the same supply as the column overhead condenser. Because the diethanolamine fed to the storage tank was at its boiling point a condenser was needed to prevent hot vapours escaping from its vent. A large double coil water cooled glass condenser was employed. This was held in a support frame which was positioned above the storage tank and vapours fed to the shell side through a length of steel braced rubber tubing. Unlike the reboiler this tank was left unlagged so that the regenerated liquid could cool to a temperature at which it could be pumped to the storage tanks as soon as possible. This minimised the corrosion experienced by the tank.

7.4. Storage facility

7.4.1. General description

Three, interlinked, plastic storage vessels were utilised as the storage facility for the solutions required in the mass transfer experiments. Each of these had a capacity of 500 litres. The system was organised so that during the water/carbon dioxide experiments any of the three storage vessels could be used as the feed tank. This allowed a considerable number of experimental runs to be completed before it was necessary to refill the tanks. During the experiments where aqueous solutions of diethanolamine were employed as the liquid phase, tank 1 (see figure 7. 24) was used for the feed, tank 2 to receive the liquid returning from the absorption chamber while tank 3 was used to store freshly regenerated DEA (a full tank of un-loaded DEA was required to fill the reboiler of the regeneration system prior to its use). During the period where DEA was being studied the storage tank lids were sealed and a blanket of oxygen free nitrogen maintained above the liquid. This helped to prevent oxidative degeneration of the solutions.

Liquid could be pumped from the storage facility to either the regeneration system or the rotary absorption rig by pump 1. In each case the liquid flowrate could be measured (and controlled) by rotameters number 1 and 2. These measured flowrates between 20 and 200 and 2 and 20 cm^3/sec respectively.

A further feature of the storage facility was the ability to preheat the contents of tank 1 to any required temperature. This was achieved by cycling the contents of the tank through an insulated glass heat exchanger positioned adjacent to the vessels. The heating medium in this exchanger was water, held at 95°C by an on-off controller linked to a 2kW immersion heater. This facility was necessary so that the feed to the regeneration column could be preheated to 70°C. The temperature of the liquid was monitored by a thermocouple placed in the line immediately before the exchanger.

8.0. Experimental mass transfer investigation using carbon dioxide/water system

8.1. Introduction

This section describes the mass transfer experiments undertaken during the course of the present investigation using a carbon dioxide/water system. This description is divided into three sub-sections. Section 8.2 presents the procedures used to calibrate the gas sensing membrane probe, providing sufficient data to calculate the required mass transfer coefficients. The calculated results are presented and discussed in section 8.3. This description is sub-divided into a number of shorter sections each of which deals with a discrete set of experiments. Mechanisms to describe the observed behaviour are expounded therin. Section 8.4 compares the results of the present investigation with corresponding data taken from previous studies. In order that the results could be directly compared, the methods described in section 5.2.3 were used to re-analyse the data previously presented.

8.2. Experimental procedure

8.2.1. Introduction

This section outlines the procedure adopted for obtaining experimental mass transfer data from the rotary test rig whilst using a carbon dioxide/water system. The description is divided into two seperate parts, these being covered in the following sub-sections. At the beginning of each day it was necessary to re-calibrate the carbon dioxide gas sensing membrane probe (described in section 5.2.3), used to measure the outlet acid gas loading of the liquid phase. Although the calculated calibration curve varied only slightly from one day to the next, the change over a period of days could be critical. Originally it was planned to recalibrate the electrode after each set of experimental runs, however, the results of preliminary trials demonstrated that this was unnecessary, the change being negligible over this short period of time. Calibration took approximately $1\frac{1}{2}$ hours to perform, one hour of this being necessary to allow the thermostatic bath to attain a constant temperature. Once calibration had been completed the experimental mass transfer runs could be initiated. Due to the limited volume of the storage tanks available only a small amount of data could be collected during a single run. The number of runs which could be completed each day was a function of the availability of carbon dioxide, and in some experiments, nitrogen.

An experimental run is classified as the measurement of outlet concentration and solution temperature at a particular rotational speed over the range of flowrates of interest. Flowrate was varied at a constant speed because the system stabilized more rapidly than when a step change was applied to rotational speed. Measurements at five rotational speeds (500, 750, 1000, 1250, and 1500 RPM) and four flowrates (50.0, 66.7, 83.3 and 100.0 cm^3/sec) comprised a standard set of experimental data for a given surface held in a given position and at a given inclination.

8.2.2. Calibration of the gas sensing electrode

The gas sensing membrane probe was recalibrated before each experimental run. This was achieved by delivering known amounts of a standard $2x10^{-2}M$ sodium hydrogencarbonate solution and a standard solution of $1 x10^{-2}M$ hydrochloric acid at a set rate to the electrode flow cell. This thus formed a solution of known carbon dioxide concentration ($1x10^{-2}M$ if the flow rates of acid and carbonate were equal) and the associated mV reading could be used as one point on the calibration curve. Originally a second point was measured at the lower end of the probe's Nernstian range (i.e. $1x10^{-4}M$ CO_2) to fix the curves gradient. However experience indicated that this was constant at -55.5mV/decade, and thus only one calibration point was required.

At the beginning of a calibration run the heater of the thermostatic bath was switched on and the temperature allowed to rise to its controlled point of 25°C. The level of water in the bath was increased during this period to the marked maximum level, thus replacing liquid which had evaporated between runs. Once the controlled temperature had been attained pump 6 was activated. Water was thus circulated from the base of the

tank through the outer sleeve of the electrode cell and then back to the tank. The stop taps on the exits of the reservoirs containing carbonate and hydrochloric acid were removed, as were the bungs in the entrainment tubes placed before the reservoirs. The valves in the sample lines (see figure 7.23) were positioned so that flow to the flow cell was from the reservoirs rather than from the rotary test rig. With the valve at the exit of the flow cell open micropump number 5 (carbonate) was switched on followed 15 seconds later by micropump number 4 (acid). This order was used so that the initial concentration of carbon dioxide in the flowcell was greater than the required value of $1x10^{-2}$M. This was found to help the electrode reach a stable value in a short length of time. The flowrate of carbonate and acid were controlled by the set points (piston lengths) of the relevant micropump. These were fixed before the first calibration run at 3ml/min (as per the instructions for the electrode) and checked occasionally to make sure no drift was occuring. Once the level of liquid in the flow cell had risen so that it covered the membrane of the electrode the magnetic stirrer was switched on. Refraining from activating the stirrer till this time helped avoid bubbles being trapped beneath the electrode tip. The formation of such bubbles during the initial test runs was found to cause 'noise' in the output mV signal, and was thus to be avoided. Once the electrode had been immersed it took approximately 10 minutes to attain a steady reading. This was of the order of -23mV. Before this was recorded as the calibration value it was observed for five minutes to ensure that no drift was occuring. If the reading did show a degree of drift the membrane was first checked for bubbles. These were removed if found. If no bubbles could be located or if their removal did not stop the drift, filling solution was injected into the electrode. If the drift was due to a low filling solution level causing an 'open' circuit between the reference and sensing sections of the electrode this action would stop the drift. If after this attention the mV signal continued to drift the micropumps were switched off, the electrode removed and the membrane changed. This would solve the problem if it were caused by a leaking membrane, which apart from electrode failure would be the only possible cause of this instability.

The mV reading attained was used in the computer programme 'DATA-AN' (listed in Appendix I), to locate the position of the calibration graph.

8.2.3. Mass transfer measurements

The procedure for collecting experimental data using the purpose built rotary test rig is most conveniently presented when considered in three seperate sections, i.e. apparatus preparation and start-up, collection of data and apparatus run-down and draining. These are discussed in the following paragraphs.

To prepare the rotary test rig for an experimental run it was necessary to check that the valves on the inlet and outlet liquid lines, the inlet gas line and on the sample lines were in the correct position. In addition the plugs used to close the vent holes in the upper surface of the absorption chamber had to be set correctly. The procedure presented here was developed during the preliminary test runs and, if implemented exactly

allowed measurements to be taken after only a minimal 'settling' period (i.e. the time where the mV reading was unsteady). Valve numbers used during the following description refer to those marked on figures 7.22, 7.23 and 7.24.

Liquid was directed towards the rotary test rig and away from the regeneration section by closing valve 8 and opening valve 31. Valve 7, on the recycle loop around pump 1 was opened so that although valves 1 and 2 were closed, once the pump was activated a flowrate greater than the minimum required could be attained. Depending on which tank was used for the feed tank, valves 3, 4 or 5 were opened. Valve 32 on the inlet liquid line directly before the rotary rig was initially closed. On the outlet liquid line valve 33 was opened and valve 34 closed so that flow was from the test rig to the drain. The valves on the sample line were positioned so that flow was from the rotary test rig through the electrode flow cell and then to drain. Flow was directed through rotameter 3 and controlled by valves 36 and 37.

To prepare the apparatus for an experimental run the D.C. electric motor was activated and the variable speed controller used to attain the required rotational speed. The absorber was then allowed to run for up to fifteen minutes to let the bearings reach the operational temperature. The rotational speed was then checked using a tachometer and any adjustments required made. Preliminary tests had indicated that the set speed was changed by only a negligible amount once liquid was introduced. The pick-up nozzle was then set so that it was at the outside radius. Whilst the rotary absorber was being run up to the operational temperature valve 40 (and 41 in the runs where a 50/50 nitrogen/carbon dioxide mixture was required) was opened thus allowing the absorption chamber to be purged. Simultaneously valve 2 was fractionally opened once the pH electrode in the feed line had been removed. The feed line (up to valve 32) was therefore slowly filled with liquid, the displaced gas being vented through the electrode socket.

Once the absorber bearings had reached the operational temperature, the inlet liquid feed line had been vented and the pH electrode replaced, valve 32 was opended allowing liquid to enter the absorption chamber. Simultaneously valve 1 was opened and the flowrate set at the required value (usually 50 cm^3/sec). As the annular liquid layer formed, the pick up nozzle was positioned so that its inner liquid surface was at the required radius. The etched marks on the liquid side PVC screen were used for this purpose. The flowrate to the electode flow cell was controlled by operation of valves 36 (coarse) and 37 (fine) and measured by rotameter 3.

Once the gas sensing membrane probe was providing a steady mV signal this and the corresponding temperature (given in mV by thermocouple 2) were recorded, these data along with the corresponding rotational speed, liquid flowrate, gas pressure (which was approximately constant at 1 atmosphere) and radial position were used to calculate the associated mass transfer coefficient. Once the necessary readings had been taken, the inlet flowrate was increased to the next value of interest. This necessesitated a slight alteration in the position of the pick-up nozzle

so that the correct radial position was re-attained. On average it took approximately 10 minutes to attain a steady mV reading with the initial flowrate. With successive changes a steady reading was attained in approximately 3 minutes. In all cases a constant reading was taken to be one that did not change over a period of one minute. Once all flowrates of interest had been analysed the rotational speed was altered. The above procedure was then repeated. The mV reading took on average 5 minutes to re-attain a steady value following a step change in the rotational speed.

Once the required rotational speeds and liquid flowrates had been analysed, or the feed tanks emptied the following procedure was used to run down and drain the rotary test rig. Valve 1 was closed followed by valve 32, thus stopping the flow of liquid to the absorption chamber. Pump 1 was then switched off. The speed of rotation was increased to 1500 RPM and the pick-up nozzle positioned at the largest radius available. This allowed a large proportion of the annular liquid layer to be removed. Valve 33 was then closed to prevent liquid flowing back to the absorption chamber once it was brought to rest. The remaining liquid was then removed via the drain cut in the edge of the liquid side polycarbonate sheet. Finally valves 40 and 41 were closed stopping the flow of gas to the absorption chamber.

8.3 EXPERIMENTAL RESULTS

8.3.1. Introduction

The experimental mass transfer results for the system carbon dioxide/water can be conveniently considered as eight distinct sets of data. This section considers each set in a seperate sub-section. These present the results tabulated in Appendicies D, E and F in a graphical form and discuss their relevance individually, as well as with respect to the experimental investigation as a whole.

Section 8.3.2 is concerned with data collected from smooth, perforated, coarse-mesh and fine-mesh discs fixed to the base plate of the absorption chamber with the plane of the disc vertical. Pure carbon dioxide at an approximate pressure of 1.0 atm was used as the gas phase during these experiments. Data for these experiments is contained with tables D.1, D.2, D.3 and D.4. Section 8.3.3 compares the results using the coarse mesh disc with those of a similar run where the gas phase consisted of a carbon dioxide/nitrogen mixture with a carbon dioxide partial pressure of approximately 0.5 atm. This comparison was required to determine whether, as assumed, the resistance due to the gas phase could be ignored and the system modelled as though it were liquid phase controlled. The data for this is presented in Table D.7.

Section 8.3.4 examines the effect of using the perforated and mesh discs in a position where they were suspended away from the base plate of the rotary absorber. This was achieved by conducting experimental runs for the coarse mesh and perforated surfaces using the same flow conditions as used in the previous section. The fine mesh was not used during this section of the experimental examination since the results of the previous section indicated that the coarse mesh produced higher mass transfer performance. Data for this set of experiments is presented in tables D.5 and D.6.

With the rotary absorber positioned for horizontal surface operation,runs with the smooth, perforated and coarse mesh discs were undertaken using a flowrate of 83.3 cm^3/sec and a gas pressure of 0.5 atm. These runs used the discs in a suspended position. Section 8.3.5 compares the results of these experiments with the corresponding data from plates with a vertical inclination (i.e. the data discussed in section 8.3.3). This permitted the effect of disc inclination on the mass transfer characteristics to be determined. As well as providing important information regarding the applicability of rotary technology, to the proposed nitro-diesel engine scheme, it was hoped that this investigation would allow the data of Watts (6) to be compared with that of other researchers (see section 2). Data for this set of experiments is contained within tables D.8, D.9 and D.10.

Section 8.3.6 examines the mass transfer characteristics of smooth, perforated and coarse mesh discs using flowrates greater than 100 cm^3/sec (the maximum flowrate used in the previous investigation), at a speed of 1500 RPM. This speed was chosen to correspond to the proposed operational speed of the closed-cycle nitro-diesel engine. Tables D.11, D.12, D.13, D.14 and D.15 contain the

data collected during this section of the investigation. Runs were completed with the coarse-mesh and perforated surfaces for fixed/vertical and suspended/horizontal combinations of position and inclination. The smooth disc was used with its surface horizontal.

The characteristics of the coarse mesh disc at flowrates in excess of 100 cm^3/sec are further examined in section 8.3.7. These experiments were required to determine whether the observed dependancy of the mass transfer characteristics with respect to the rotational speed were present at the higher flowrates. The results of this section of the experimental investigation were useful when considering the phenomenom of film breakdown. The coarse-mesh disc was used in a suspended, vertical position at speeds between 1250 and 1500 RPM, and at flowrates up to 266.7 cm^3/sec. The range of speeds was limited by the performance of the pick-up nozzle. Data for these experiments is contained in Table D.16.

In order to determine the degree to which the liquid layer in the annulus of the absorption chamber contributes to the mass transfer of the discs, a series of runs was completed in which the disc surface was 'shrouded' from the gas phase. The measured mass transfer rate was therefore due solely to the annular layer. Section 8.3.8 considers the data tabulated in table E.1, and shows how these measurements were used in the calculation of a correction factor to be applied to the data discussed in previous sections.

Due to the limitations of the pick-up tube nozzle only a small amount of data, concerned with the variation of the liquid phase mass transfer coefficient with radius, was collected. This is discussed in section 8.3.9. The fine mesh and smooth discs were employed as the active mass transfer surfaces during this section of the investigation. A fixed, vertical position was chosen thus enabling the relevant data discussed in section 8.3.2 to be used for the largest radius (141mm). Tables F.1, F.2, F.3 and F.4 contain the collected data for radii of 116 and 84mm. The fine mesh was chosen to represent the 'perforated' surfaces as the results of the initial section of the investigation (and the observations of section 4.2.1.3.2) had indicated that this surface was most prone to film breakdown. It was hoped that these measurments would be useful in calculating the performance of the disc in the absence of film breakdown (i.e. at a smaller radius).

8.3.2. Smooth, perforated, coarse mesh and fine mesh discs in a vertical, fixed position

The results discussed in this sub-section form the basis of the whole experimental investigation as they are used in the succeeding sections as a means of comparison. The data collected represents the mass transfer coefficient (as outlined in section 5.2.2) of the thin film formed at flowrates of 50.0, 66.7, 83.3 and 100.0 cm^3/sec and speeds of 500, 750, 1000, 1250 and 1500 RPM.

This data is presented in figures 8.1 to 8.4 as graphs of the measured mass transfer coefficient (corrected to 20°C) against the rotational speed, at various flowrates. Salient features of

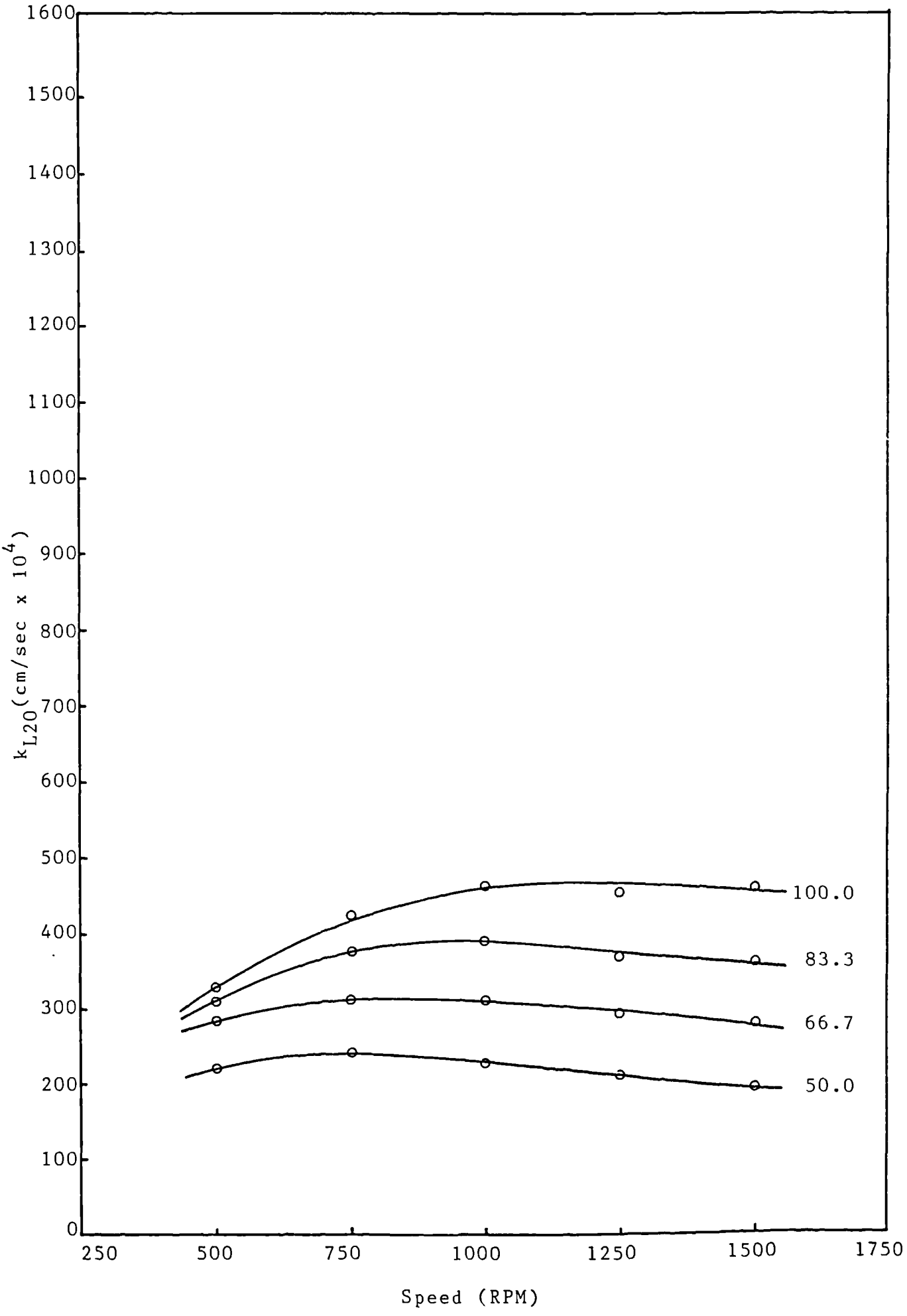

figure 8.1 smooth disc in a vertical, fixed position

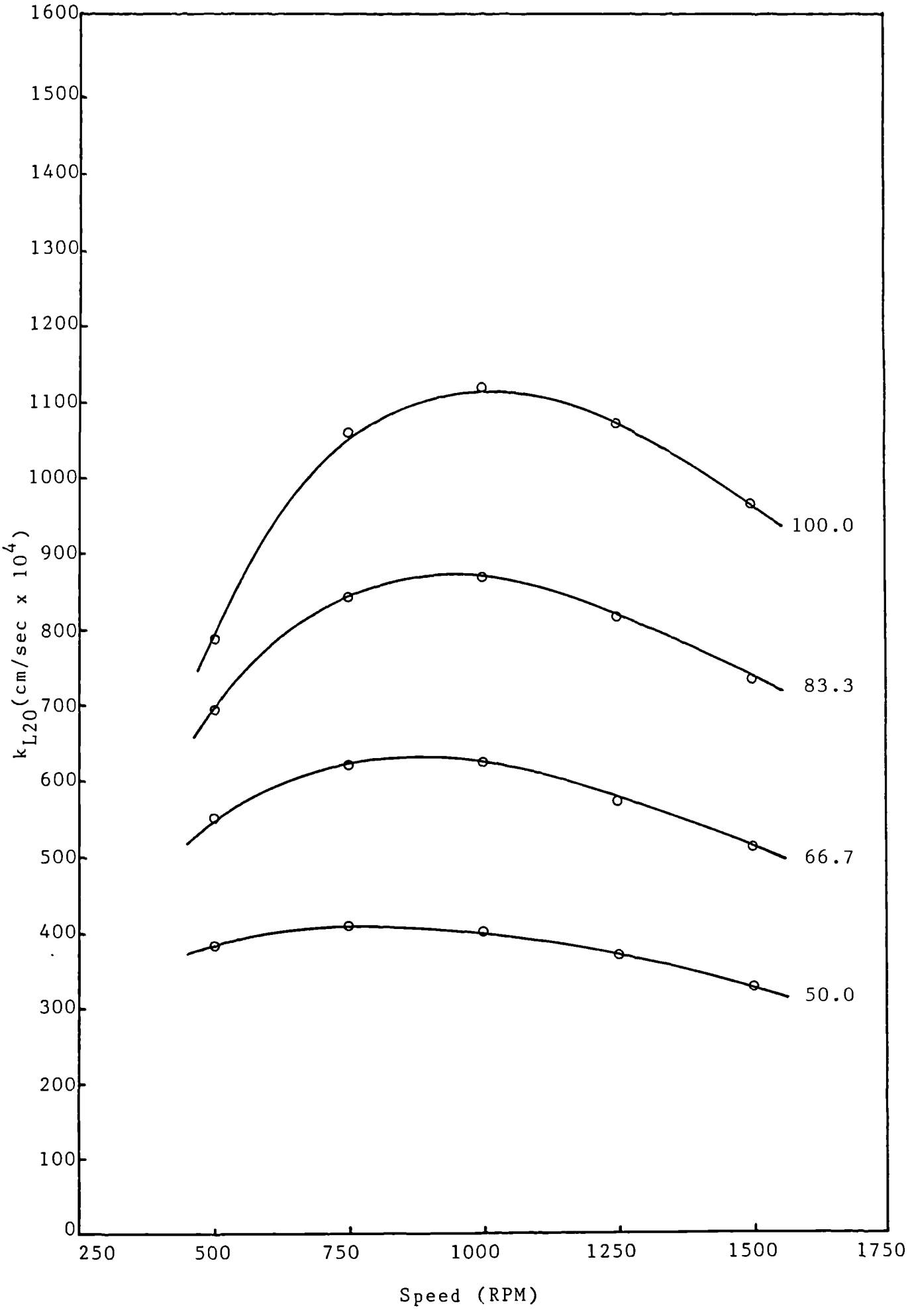

figure 8.2 perforated disc in a vertical, fixed position

these figures are discussed below.

For each of the four surfaces used an increase in the flowrate from 50.0 to 100.0 cm^3/sec, at a fixed speed, resulted in an increase in the mass transfer coefficient. This increase was greatest for the three 'perforated' plates. At the lower speeds it was observed for all the surfaces used, this increase was most pronounced at the lower end of the range of flowrates. For example, at 500 RPM with the smooth plate, increasing the flowrate from 50.0 to 66.7 cm^3/sec (a proportional increase of 33%) raised the mass transfer coefficient by 28%. However when the flowrate was doubled then the transfer coefficient was increased by only 50%. At 1500 RPM identical changes in the flowrate caused a 43% and a 130% increase in the mass tranfer coefficients respectively.

Figures 8.1 to 8.4 were also useful for examining how the performance of the various surfaces was effected by changing the rotational speed at a fixed flowrate. The speed was increased from 500 to 1500 RPM. At all flowrates used, and for each of the surfaces employed, increasing the rotational speed from 500 RPM caused a corresponding increase in the mass transfer coefficients. However once a certain critical speed had been exceeded a further increase caused the mass transfer performance to be reduced. The magnitude of this limiting speed and the degree of the corresponding decrease in performance were shown to be functions of the flowrate and the disc surface. For all but the fine-mesh disc the speed at which this maximum mass transfer coefficient occurs increases with increasing flowrate. For example, when using the coarse-mesh disc at 50.0 cm^3/sec the maximum performance was attained at 750 RPM, while at 100.0 cm^3/sec this was increased to approximately 1110 RPM. The critical speed for the fine-mesh disc was constant at approximately 750 RPM. Figure 8.4 showed that the performance of the fine mesh was affected most by an increase in the rotational speed beyond the critical point. At 83.3 cm^3/sec. for example, an increase in speed from 750 to 1500 RPM caused the associated mass transfer coefficient to decrease by nearly 30%. Of the three 'perforated' plates the coarse-mesh disc was the least affected, suffering a decrease of only 6% at 100.0 cm^3/sec. Although the smooth disc demonstrated a behaviour similar to that of the 'perforated' surfaces the magnitude of the maximum was far less pronounced.

In previous investigations rotational speeds greater than 1000 RPM have seldom been employed. It is thus not surprising that the critical speed characteristic demonstrated by the results of the present investigation, has not been reported. This characteristic of the mass transfer performance is important as it apparently limits the efficiency of a rotational system which operates at a high speed. This is of particular importance in the development of a stripper for a closed cycle nitro-diesel engine where the engine rotates at a speed of 1500 RPM. The following paragraphs discuss possible reasons for this characteristic, for each of the disc surfaces in turn.

In section 4.1.3.4 it was shown that at a combination of high speeds and low flowrates (where the film is at its thinnest), incipient dry spots tend to form on smooth plates. These can be

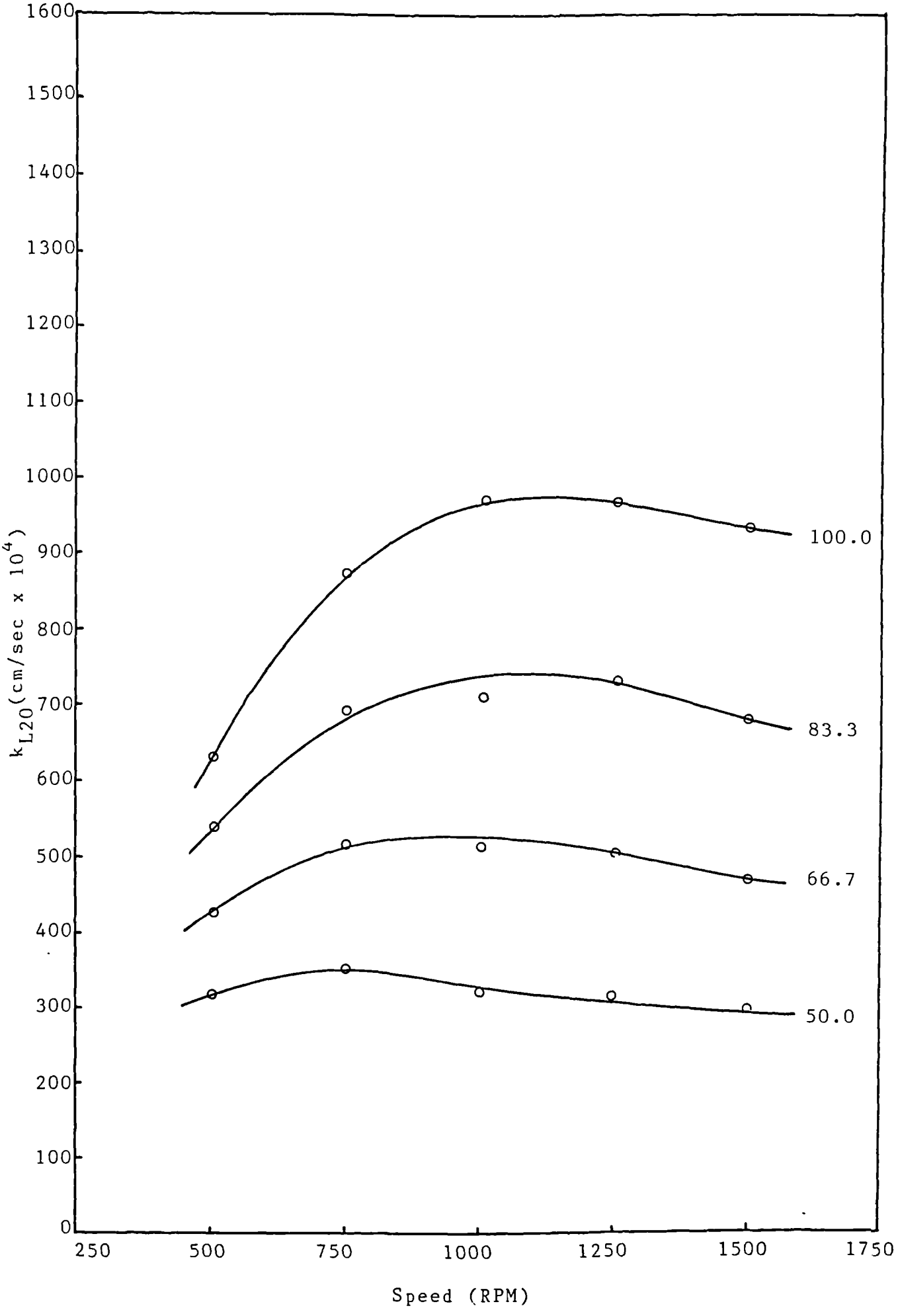

figure 8.3 Coarse-mesh disc in a vertical, fixed position

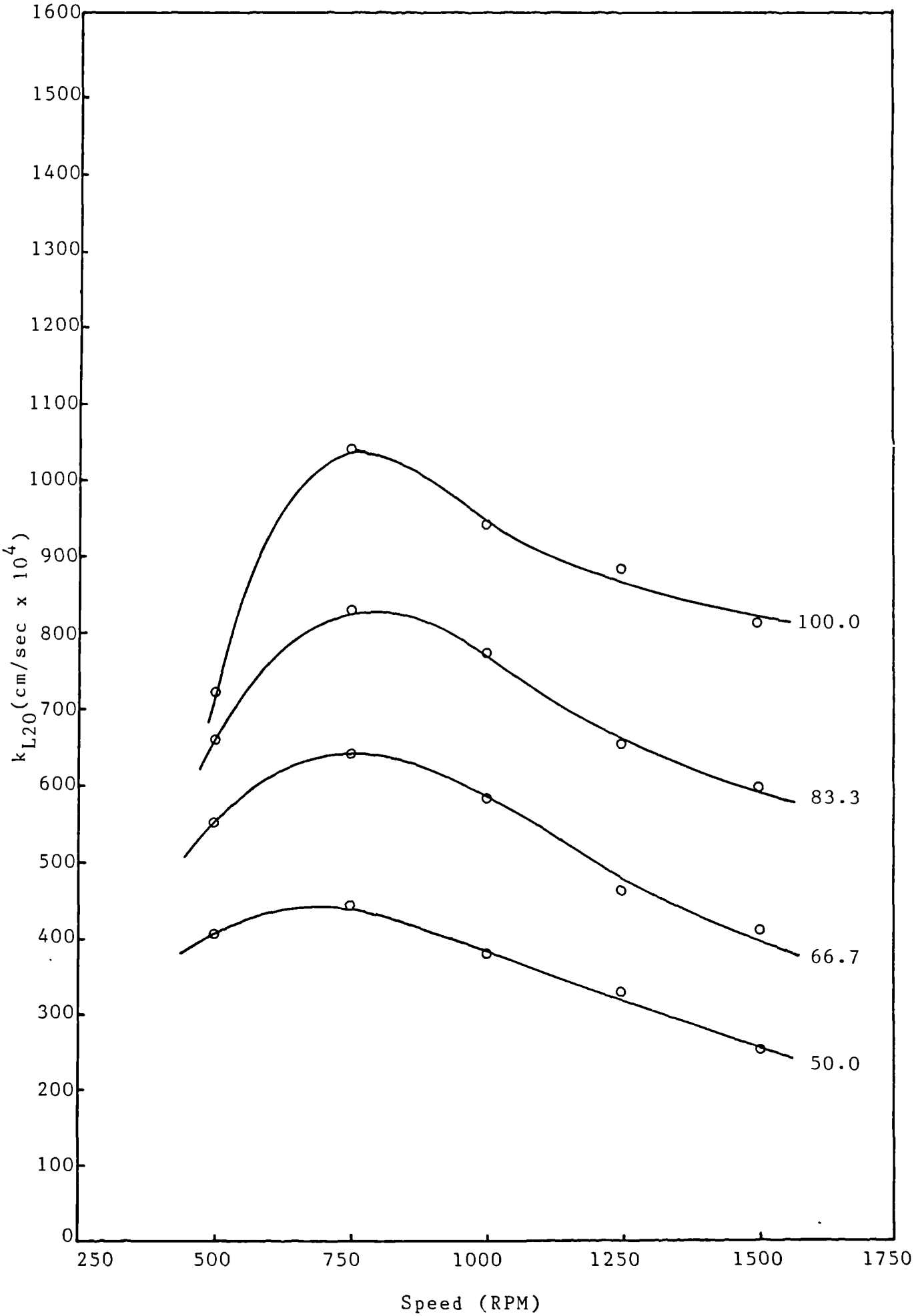

figure 8.4 Fine mesh disc in a vertical, fixed position

caused either by particles, entrained in the liquid, sticking to the plate or as an effect of the flow parameters, particularly the Weber number. These dry spots, in turn, lead to the phenomenon of film breakdown. Once the thin film formed on the surface of a rotating disc has broken up into rivulets only a certain fraction of the disc surface is wetted and thus the active mass transfer area is decreased. If this effect is not allowed for in the calculation of the associated mass transfer coefficient (see section 5.2.2) then the calculated value will be too low. Film breakdown could thus be a possible cause of the critical speed characteristic demonstrated by the smooth disc. In this case the speed associated with the maximum mass transfer coefficient would correspond to the film thickness where breakdown first occurs.

Equation 4.19 was developed from energy considerations and can be used to provide an accurate estimate of the speed at which film breakdown first occurs at a particular flowrate. Using this equation it can be shown that, over the range of rotational speeds and liquid flowrates used during this set of experiments, no film breakdown should occur. It would appear that film breakdown could not be a cause of the maxima found in figure 8.1. The water used during these investigation was taken from the departmental cold water supply and thus contained entrained rust particles. These tended to collect in the annulus of the absorption chamber. It is therefore possible that these particles, sticking to the disc surface, may have caused the otherwise stable film to break down.

Section 4.1.3.4 also discusses the breakdown of films formed on the surface of the perforated mesh discs. Although the scope of this work is limited enough data has been presented to conclude that film breakdown occurs under certain conditions. Koerfer (5) noted that at high speeds no film was formed above the perforations at the edge of a disc. If the speed was increased the wetted radius decreased. A series of photographic observations completed by Barbaris (31) showed that at 500 RPM and at flowrates less than 40 cm^3/sec the perforations around the periphery of a 32cm diameter disc were dry. The critical speed for a flowrate of 50 cm^3/sec (figure 8.2) is approximately 750 RPM and thus this value is comparible with the observations of Barberis. That is, the measured mass transfer coefficient begins to decrease at a speed above which dry perforations begin to form at the edge of the disc. Thus film breakdown is a possible cause of the critical speed characteristic shown by the perforated disc. With only a limited amount of hydrodynamic data available it is impossible to conclude that film breakdown is the definite cause of the decrease in mass transfer coefficients, especially at the higher flowrates. However it was felt, that as film breakdown on a perforated disc is observed as liquid circumnavigating rather than crossing the orifices that this may be associated with a certain film thickness. That is, that once the film thickness has been reduced beyond a certain limiting value the most favourable flowpath is around, rather than across the perforations. Considering the structure of the perforated material used (see chapter 2) it was felt that this limiting film thickness would be less than the average height of the burrs surrounding the holes. This situation has a useful analogy in the sea striking a rounded sea-wall. At high tides, although the level of the sea is below the top of the wall, a certain

fraction of the water has enough energy to flow over, rather than around it. If waves are present then a greater percentage of the incoming flow breaches the wall. As the tide falls, a certain limiting height is passed and liquid then flows around rather than over the restraining wall.

In order to study whether the decrease in mass transfer coefficients is associated with a particular film thickness, the film thickness's corresponding to the critical speeds were calculated. Although Koerfer (5) has presented a correlation for calculating the thickness of thin films formed on rotating perforated surfaces, the accuracy of this is uncertain (see 4.1.3.2). Therefore the centrifugal model (equation 4.6) was employed. Although this is unlikely to model the flow behaviour accurately it was felt that the error associated with each value would be approximately equal. The relative magnitude of the calculated values could therefore be compared. The film thickness for perforated discs in fixed and suspended positions were calculated at a radius of 141mm, from figures 8.2 and 8.6 respectively and tabulated in table 8.1. These are fairly constant, having, in the case of the fixed results a mean value of 59 μm and a standard deviation of about 3%. Considering that the results were based upon a limited amount of data and that the maxima are quite broad and ill defined it can be concluded that the reduction in mass transfer coefficients coincides with a particular film thickness. Although the true film thickness was unknown it was considered worthwhile comparing the calculated value with the average height of the burrs around the holes. The height of a representative selection of the burrs was measured and values in the range 50 to 150μm were found; 95μm was used as an approximate mean. The calculated limiting film thickness is therefore of the same order as the average burr height. It can thus be concluded that film breakdown is a plausable explanation for the reduction of the mass transfer coefficients associated with perforated discs at speeds beyond a critical value.

The hydrodynamics of the thin film formed on the surface of the coarse-mesh and fine-mesh discs was studied during the present investigation and the resulting observations are discussed in section 4.2.1.3.2. Considering the coarse-mesh, film breakdown was observed at speeds above 650 RPM (approximately) with a liquid flowrate of 60 cm^3/sec. When the flowrate was decreased to 40 cm^3/sec a stable film could only be maintained up to 500 RPM. Alternatively increasing the flowrate to 100 cm^3/sec allowed a stable film to be formed up to speeds of approximately 1000 RPM. Considering figure 8.3 it can be seen that the speed at which film breakdown begins roughly corresponds to the critical speed at which there is a maximum mass transfer coefficient. Thus it is possible to conclude that film breakdown causes the measured reduction in the mass transfer coefficient. Due to an inability in observing the film formed on the surface of the fine mesh disc it was impossible to study accurately the film breakdown on this surface (see 4.2.1.3.2). However it was observed that such breakdown was more pronounced than with the coarse-mesh disc. This observation agrees with the results presented in figures 8.3 and 8.4 which show that the reduction in mass transfer coefficients is greatest for the fine mesh.

TABLE 8.1.

A PERFORATED PLATE - SUSPENDED

FLOWRATE Q (cm^3/sec)	SPEED AT MAX (RPM)	Re	Ta	$\frac{Re}{Ta^2}$	δ (centrifugal) (mm)	δ (Koerfer) (mm)
50	683	337	1.35×10^6	1.85×10^{-10}	0.0628	0.0399
66.7	792	450	1.57×10^6	1.82×10^{-10}	0.0624	0.0396
83.3	833	562	1.65×10^6	2.06×10^{-10}	0.0651	0.0421
100.0	933	675	1.85×10^6	1.97×10^{-10}	0.0641	0.0412

B PERFORATED PLATE - FIXED

FLOWRATE Q (cm^3/sec)	SPEED AT MAX (RPM)	Re	Ta	$\frac{Re}{Ta^2}$	δ (centrifugal) (mm)	δ (Koerfer) (mm)
50	800	337	1.59×10^6	1.33×10^{-10}	0.0562	0.0338
66.7	883	450	1.75×10^6	1.46×10^{-10}	0.0580	0.0354
83.3	925	562	1.83×10^6	1.68×10^{-10}	0.0608	0.0380
100.0	1017	675	2.02×10^6	1.65×10^{-10}	0.0604	0.0377

An analysis of the results presented in figures 8.1 to 8.4 have indicated that once the film is reduced below a limiting thickness film breakdown occurs. As this reduces the active mass transfer area the mass transfer coefficient based upon the total disc area is reduced. Thus the efficiency of a rotary absorber operating in this area will be lowered. To maximise the performance of a rotary machine the operating conditions must be chosen so that film breakdown does not occur. The results of this section of the experimental investigation have indicated that operation should be confined to speeds below approximately 1000 RPM at flowrates up to 100 cm^3/sec. However such an operating speed is impractical for applications such as the stripper associated with a closed cycle diesel engine. The most convenient speed of operation for this device would be 1500 RPM which is equal to that of the engine. Thus the runs described in sections 8.3.6 and 8.3.7 were undertaken to determine whether by operating at higher flowrates film breakdown could be avoided. If the flowrate is increased while holding the rotational speed steady the film thickness at a given radius will be increased. Thus at 1500 RPM, if the flowrate is increased sufficiently, the film thickness at the disc periphery will be greater than the limiting value and thus no breakdown should occur. A rough estimate of the minimum flowrate to avoid film breakdown on a perforated surface rotating at 1500 RPM can be calculated by assuming that a limiting thickness of 59μm applies at the disc edge. Thus using the centrifugal model the corresponding Reynolds number can be calculated and from this the flowrate. This produces an estimate of 192 cm^3/sec. Thus if the flowrate is increased to 200 cm^3/sec the critical speed will be greater than 1500 RPM and thus the mass transfer coefficient/speed plot will not exhibit a maximum value.

8.3.3. Coarse mesh disc in a fixed, vertical position using carbon dioxide at 0.5 atmospheres

With the coarse mesh disc in a fixed vertical position the mass transfer coefficient was measured at speeds of 500, 750 and 1000 RPM and flowrates of 50.0, 66.7, 83.3 and 100.0 cm^3/sec. A carbon dioxide/nitrogen mixture with a CO_2 partial pressure of 0.5 atm was used during these experiments. Figure 8.5 plots the results of this run and compares them with those for the coarse mesh collected during the experiments discussed in section 8.3.2.

Figure 8.5 shows that the mass transfer coefficient over the measured range of variables is independent of the partial pressure of carbon dioxide in the gas phase. The average variance of the results is 1.4% which is well within the expected experimental error. Thus it can be concluded that the gas phase resistance is negligble confirming that as assumed, the system can be considered as liquid phase controlled.

8.3.4. Perforated and coarse mesh discs in a suspended, vertical position

The data collected with the perforated and coarse-mesh discs held in a suspended, vertical position are presented graphically in figures 8.6 and 8.7. These figures compare the measured mass transfer coefficients with those of the corresponding discs in a vertical position. Data was again collected at speeds of

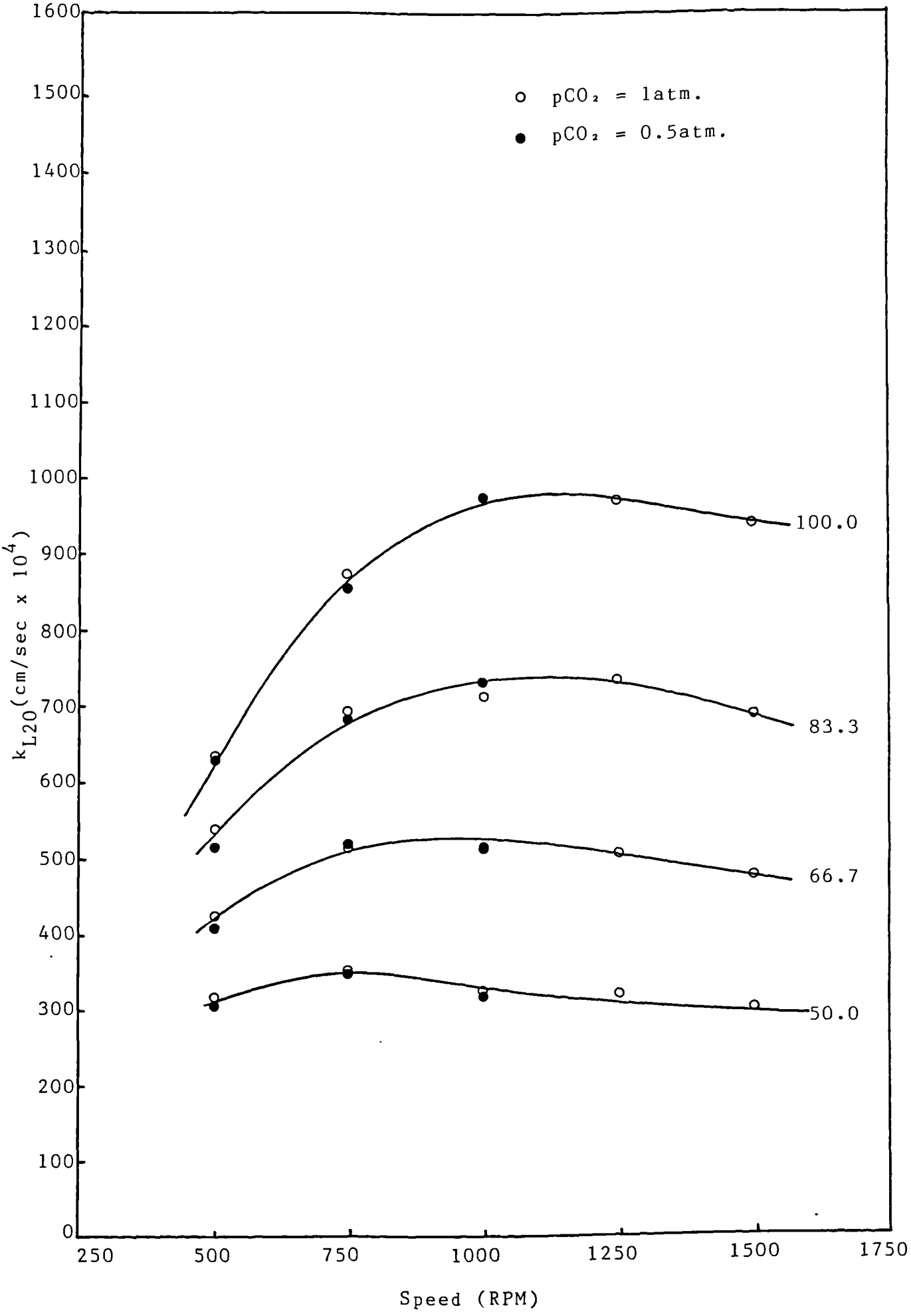

figure 8.5 Variation of mass transfer coefficient with carbon dioxide partial pressure

500, 750, 1000, 1250 and 1500 RPM and flowrates of 50.0, 66.7, 83.3 and 100.0 cm^3/sec.

Figure 8.6 shows that for each of the flowrates and speeds used the mass transfer coefficient for the perforated disc in the suspended position is greater than the corresponding value for a fixed position. The increase is greatest at the lower speeds, i.e. before the critical speed is reached and film breakdown occurs. At 500 RPM the percentage enhancement increases from 33% at 50.0 cm^3/sec to 52% at 100.0 cm^3/sec. When the rotational speed is increased at a fixed flowrate the mass transfer coefficient increases until a critical speed is exceeded. Again, as is the case with the perforated plate in a fixed position, this critical speed increases with increasing flowrate. However, for each of the flowrates used the critical speed is lower for the disc in the suspended position. Thus once the speed is increased beyond the critical point the mass transfer coefficient associated with the suspended position decreases more rapidly than when it is held in a fixed position. At a speed of 1500 RPM the percentage enhancement varies from 28% at 50 cm^3/sec down to just 8% at 100 cm^3/sec. The maximum measured mass transfer coefficient corresponds to a flowrate of 100 cm^3/sec and a speed of 920 RPM and has a value of 0.1300 cm/sec. Thus when compared with the corresponding value for a smooth plate from figure 8.1, the perforated surface provides a 2.8 fold increase in the mass transfer performance. Since no gas is present under the disc this enhancement must be due to the increased turbulence caused by the roughened surface.

From figure 8.7 it can be seen that changing the position of the coarse-mesh disc effects the mass transfer coefficient in the same ways as described above for the perforated disc. At 500 RPM the coefficient associated with the suspended position enjoys a percentage enhancement between 69% at 50.0 cm^3/sec and 51% at 100.0 cm^3/sec. However at 1500 RPM this is reduced to between 21% and 7% at 50.0 and 100.0 cm^3/sec respectively, due to an increase in the effect of film breakdown. Overall, the increase in performance due to the change in position is more pronounced for the coarse mesh disc than it is for the perforated disc. At 920 RPM the coarse mesh disc has a mass transfer coefficient of 0.1250 cm/sec and thus is 2.7 times more efficient than the smooth plate. Since the coarse mesh disc has a fractional free area considerably greater than that of the perforated disc (0.49 compared to 0.28) then when the gas phase is present on each side of the rotating discs the performance of the coarse mesh will be approximately 12% greater than that of the perforated plate.

This section of the experimental investigation has demonstrated that when the 'perforated' surfaces are lifted away from the base plate of the absorber then the mass transfer performance is enhanced. As the experiment described in section 8.3.3 has indicated that the gas phase resistance is insignificant, it was felt that this effect could not be associated with the reduction in size of the channel available for gas flow. When a 'perforated' surface is fixed against a base plate a liquid sub-layer is likely to build up in the perforations. This effect will result in an apparent reduction in the surface roughness and thus the thin liquid film will show less turbulence. When the 'perforated' plates are suspended away from the base plate the degree of turbulence will increase

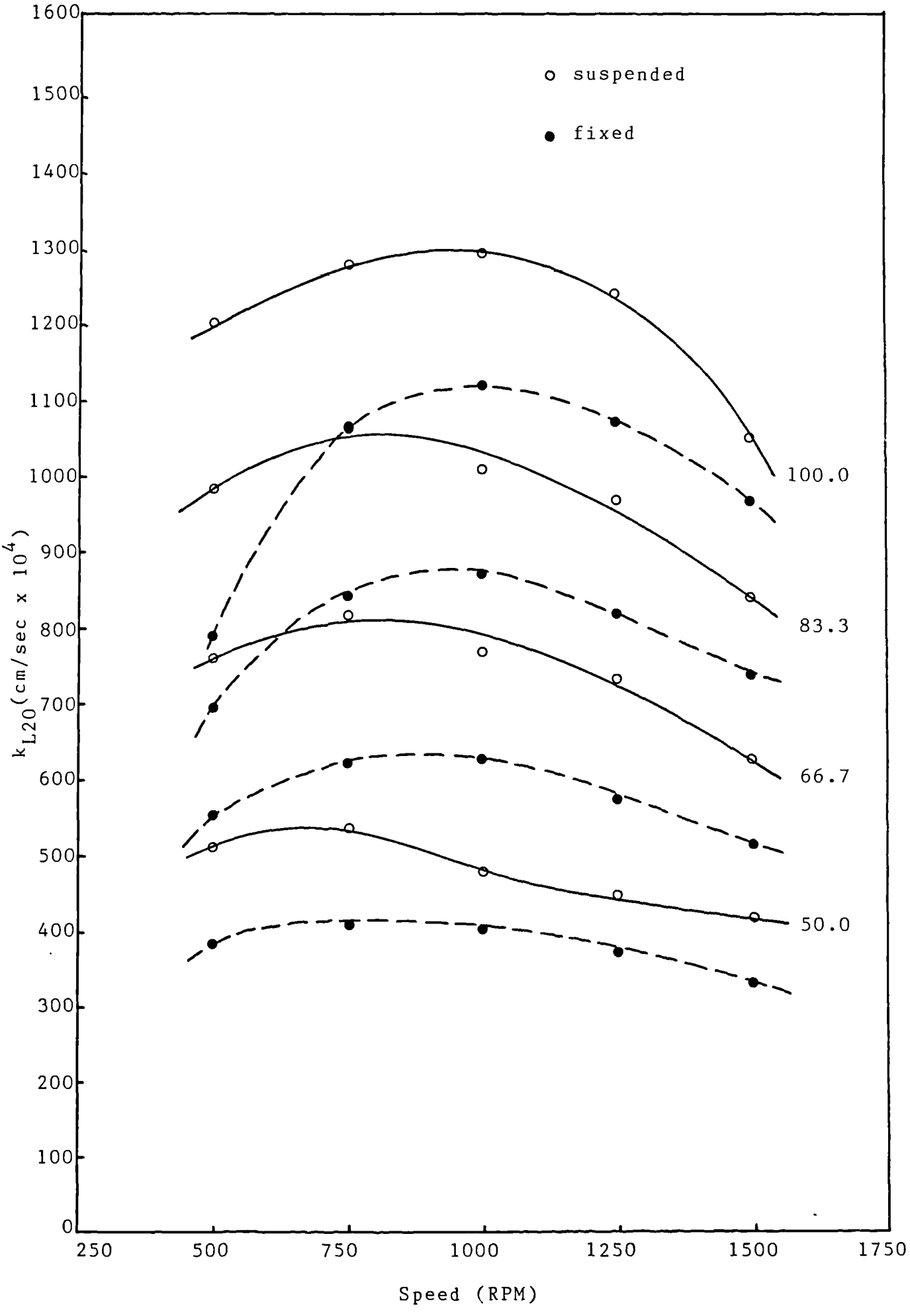

figure 8.6 Perofrated disc in a suspended, vertical position

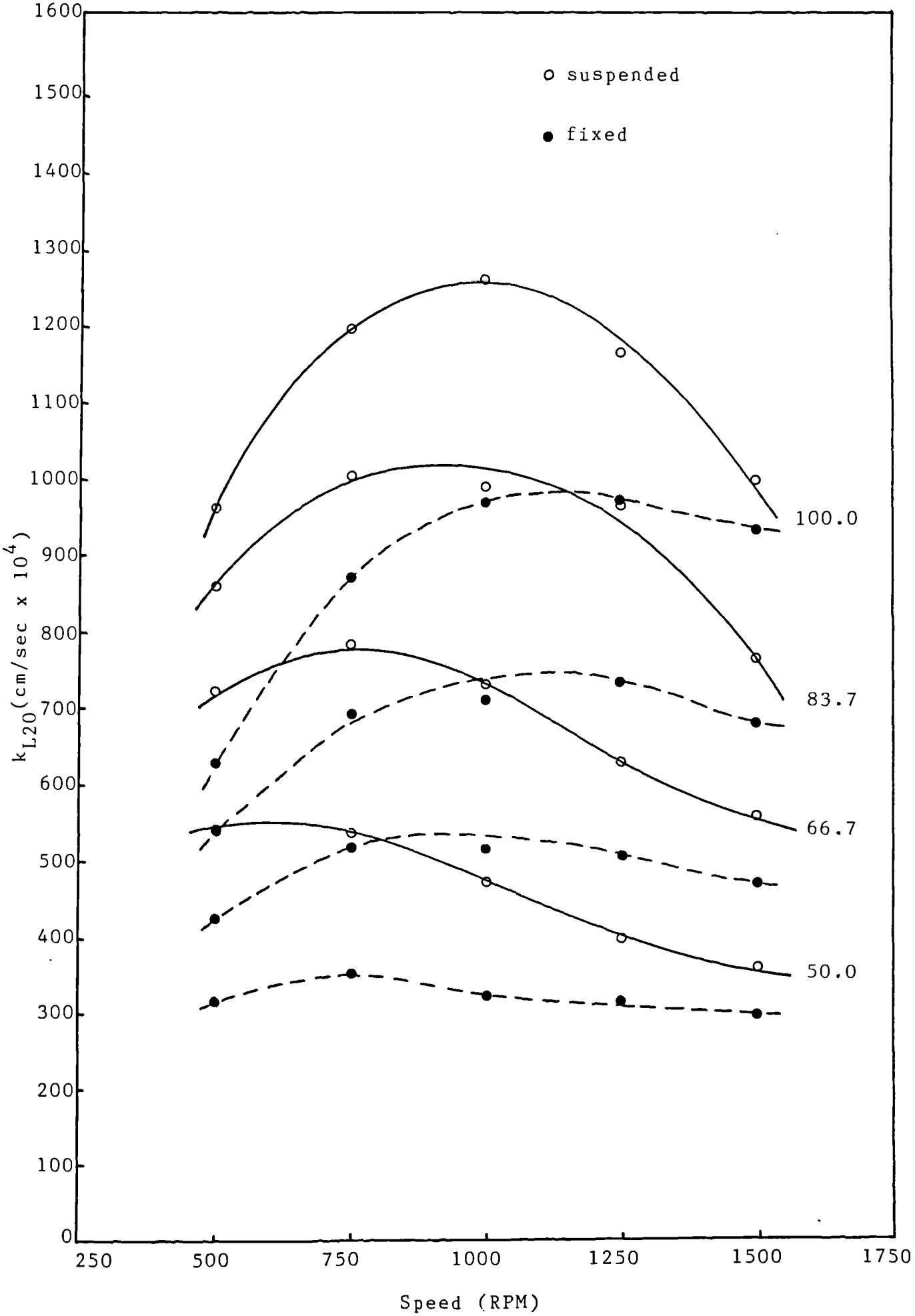

figure 8.7 Coarse mesh disc in a vertical, suspended position

and the mass transfer performance will be enhanced. The results of this section of the experimental investigation have demonstrated this phenomenon.

When considering the coarse-mesh disc it was felt that only part of the measured increase was due to the removel of a liquid sub-layer. Noting that the mesh discs have a very open, almost three dimensional structure, suspension causes the liquid film to be distributed on both surfaces. Thus the film thickness on the upper surface would be reduced and the associated mass transfer coefficient further increased. The fact that the performance of the mesh disc is enhanced to a greater extent than that of the perforated disc is evidence that this effect operates.

8.3.5. Smooth, perforated and coarse mesh discs operating in a horizontal plane

In order to determine the effect of altering the plane of rotation from vertical to horizontal, runs with the smooth, perforated and coarse-mesh discs were repeated at a flowrate of 83.3 cm^3/sec and speeds of 500, 750, 1000, 1250 and 1500 RPM. The coarse-mesh and perforated discs were used in a suspended position while the smooth plate was fixed to the base plate.

The data collected is presented graphically in figure 8.8. The corresponding results for vertical operation are plotted on the same graph to allow a comparison to be made easily. For the smooth plate the results indicate that for this surface the effect of altering the plane of rotation is negligible. The average variance between the corresponding sets of data is just 1.7%, this being well below the expected experimental error. The mass transfer coefficients associated with the perforated plate show an average variance of 2.1% and again this is below the expected experimental error. The mass transfer coefficients associated with the coarse-mesh disc display a slightly greater variance than those of the perforated or smooth discs. Although the average variance is only 4.2% the individual values range from approximately zero at the highest and lowest rotational speeds to nearly 10% in between. Although this effect may be due to experimental error it may also be a result of the change in operational inclination.

For each of the transfer surfaces employed the results for a horizontal inclination are lower than those for a vertical inclination. Although the perforated and smooth plates show only a small decrease it is highest as is that of the coarse-mesh disc, at rotational speeds close to the critical point. Thus the overall effect of changing to horizontal operation is a small reduction in the maximum mass coefficient associated with a particular flowrate. Since the hydrodynamics of the thin film formed on a rotating perforated surface is not fully understood it is difficult to suggest why this observed decrease should occur. As the discrepancy increases with an increase in the fractional free area of the surface it may be associated with either leakage or with the re-distribution of the film to the underside of the disc (as discussed in the previous section). Alternatively the effect may be caused by the spray formed by the disc surface, the volume of which increases with an increase in the 'roughness' of the surface. In the limited size

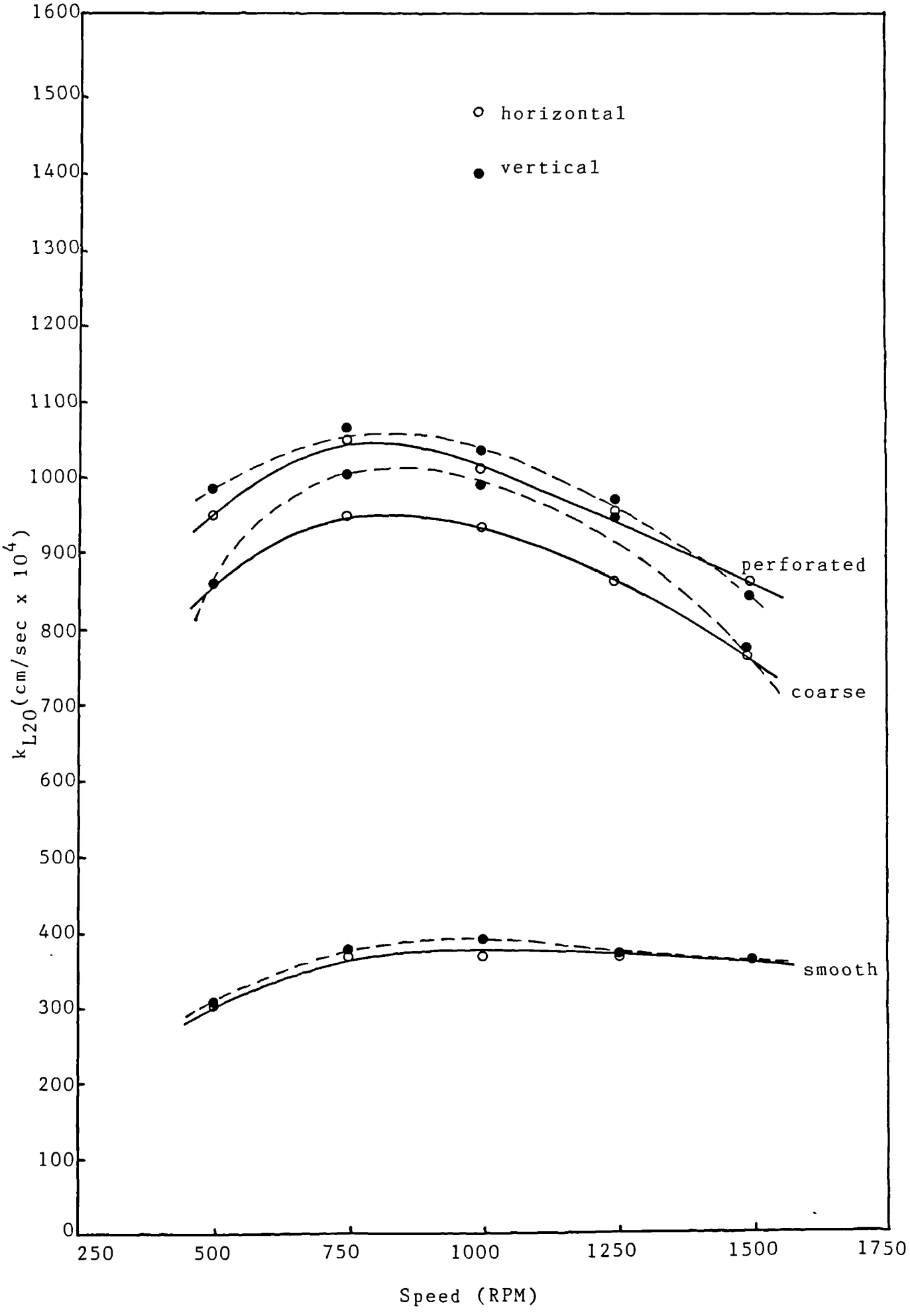

figure 8.8 Horizontal operation of coarse mesh, perforated and smooth mass transfer surfaces

absorption chamber used during the present investigation it may be possible that spray from the disc surface impinges on the upper support plate (see section 7.2.3) thus forming an additional area where mass transfer may occur. Altering the operational inclination may effect the degree to which this occurs and thus marginally reduce the mass transfer performance.

Although an explanation for the behaviour discussed in this section is uncertain, it is clear that the effect, even for the coarse-mesh disc, is only minimal. The results, presented by Watts (6,18) and discussed in section 2 can thus be re-considered. Watts used a smooth disc in a vertical position and found, that in a wavy-flow regime, the mass transfer coefficient for a carbon dioxide/water system was less than that predicted by Venkataraman's (3) 'approximate' model. As this model had been shown by Venkataraman to be capable of producing accurate predictions for laminar flow these results contradicted the work completed on inclined planes (as discussed in section 2). The investigation of the analytical technique adopted by Lim and outlined in section 6.2, showed, that provided samples were collected carefully this technique should provide accurate measurements. The results of this section of the experimental mass transfer investigation have indicated that this discrepancy could not be an effect of using the disc at a vertical inclination. It must therefore be concluded that the results due to Watts are too low and that this is caused by an undefined experimental error. Watt's results are further discussed, and compared with those of other experimental investigations (including the present investigation) in section 8.4.

8.3.6. Smooth, perforated and coarse-mesh discs at flowrates in excess of 100 cm^3/sec at a rotational speed of 1500 RPM

The set of experiments discussed in this section formed an investigation of the effect of using flowrates in excess of 100 cm^3/sec (the maximum flowrate used during the previous experiments). A speed of 1500 RPM was chosen, because in addition to this being the operational speed of the proposed nitro-diesel engine, it allowed flowrates up to 266.7 cm^3/sec to be used without encountering appreciable nozzle choking. Runs were completed for the coarse-mesh and perforated discs in vertical/fixed, and horizontal/suspended positions. This allowed the effect of each of these parameters to be determined at the higher flowrates. The smooth disc was used in a horizontal position so that its performance could be compared with those of the 'perforated' surfaces.

Figures 8.9 and 8.10 present the data collected during this section of the experimental investigation. Figure 8.9 compares the results for the perforated and coarse-mesh discs in fixed and suspended positions (the results discussed in sections 8.3.5 and 8.3.7 show that at 1500 RPM the effect of disc inclination is negligible). The results for the coarse-mesh disc in a suspended position are on average some 9% greater than those for a fixed position. This therefore agrees with the data discussed in section 8.3.4. The perforated plate shows an increase between 20% at 100 cm^3/sec and 45% at 266.7 cm^3/sec when comparing the results collected in suspended and vertical positions. If these results are compared with those discussed in section 8.3.2 it can be seen that once the

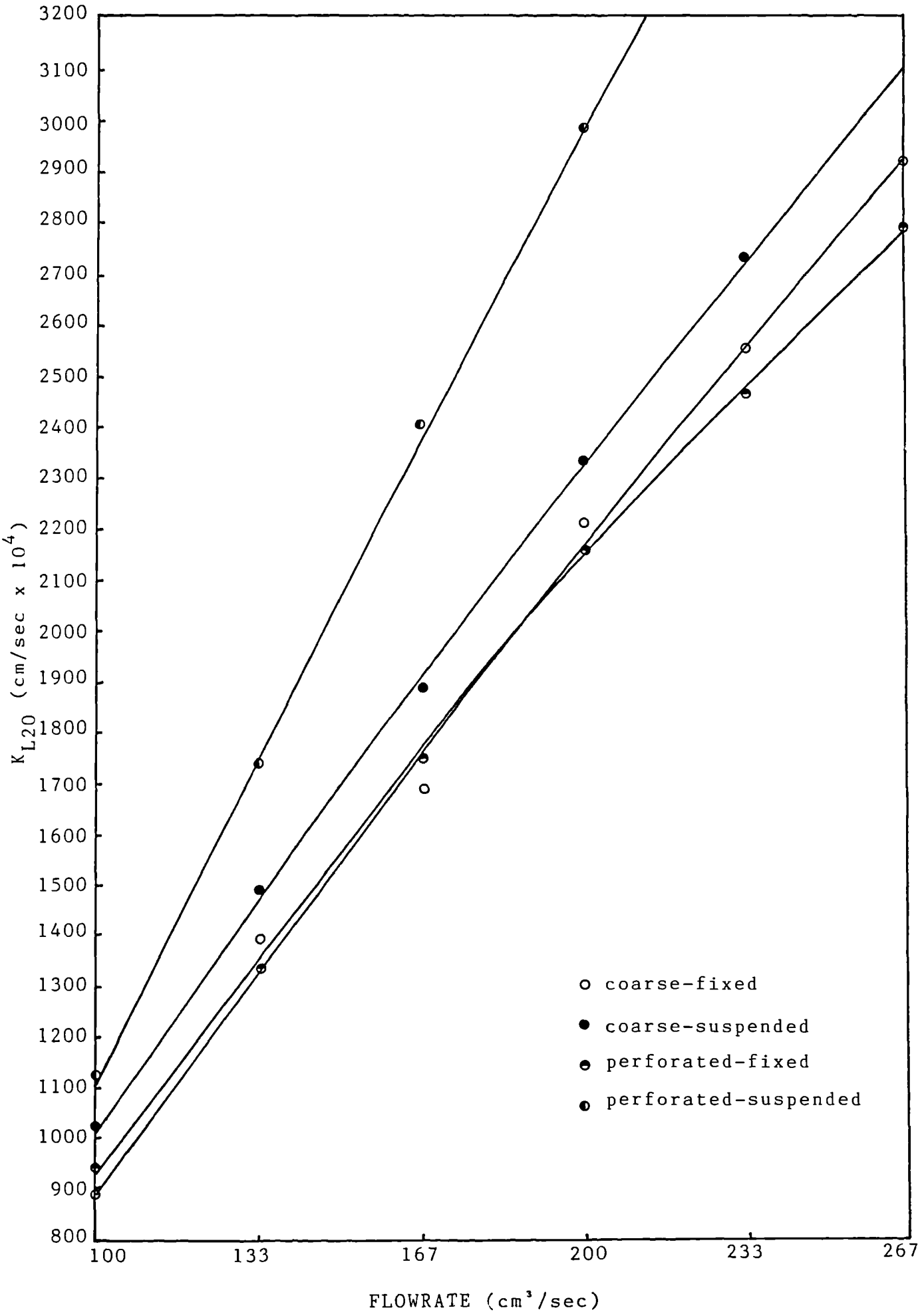

figure 8.9 Perforated and coarse mesh discs at flowrates in excess of 100 cm^3/sec at a rotational speed of 1500RPM

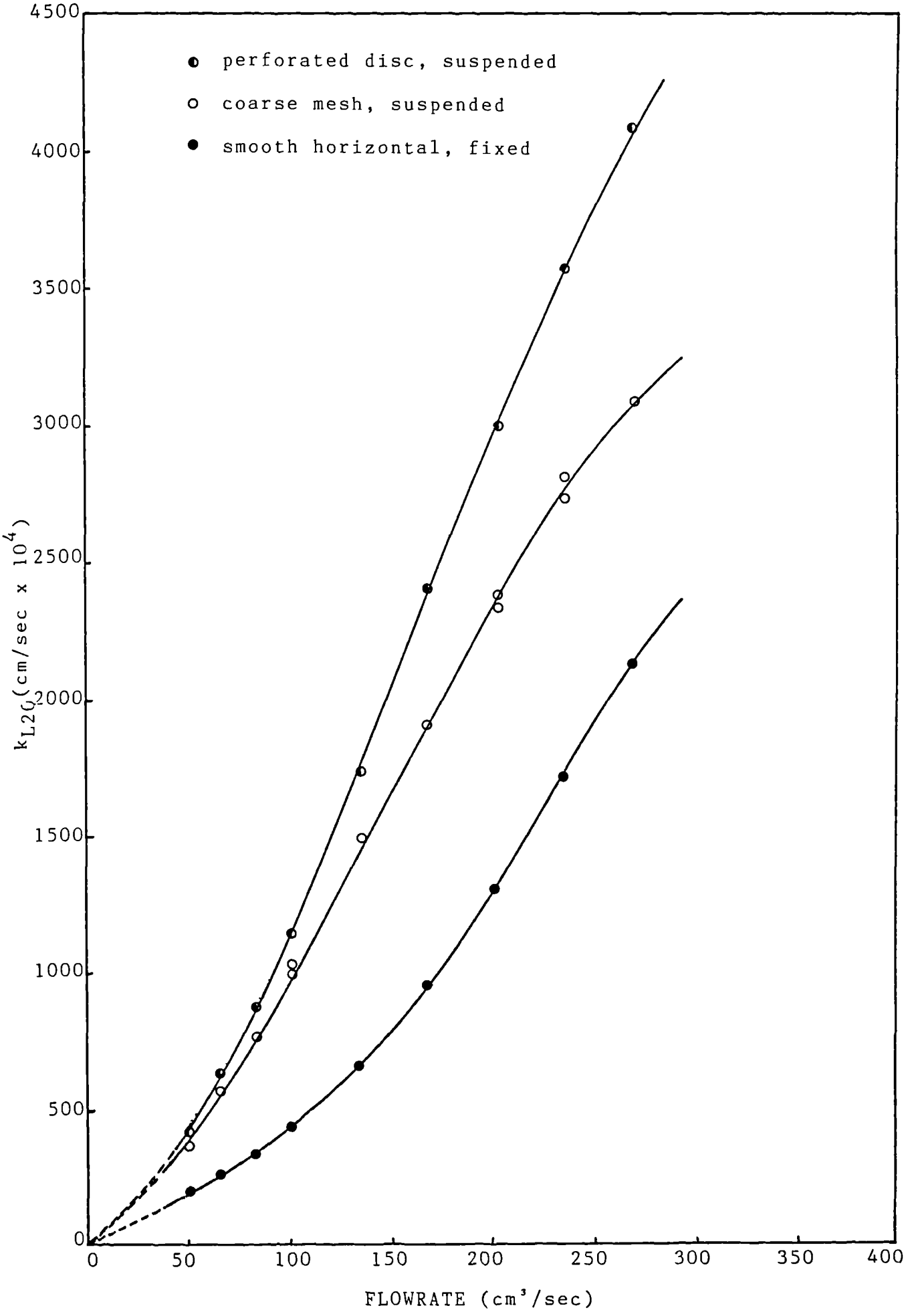

figure 8.10 Smooth, perforated and coarse mesh discs at 1500RPM

flowrate is increased beyond 100 cm^3/sec the performance of the coarse-mesh disc is greater than that of the perforated disc when the discs are in a fixed position.

Figure 8.10 compares the performance of the coarse-mesh, perforated and smooth discs, using all relevant data. At all flowrates between 50.0 and 266.7 cm^3/sec and a speed of 1500 RPM, the perforated disc in a suspended position exhibits the greatest mass transfer performance. At 50.0 cm^3/sec the mass transfer coefficient of this disc is some 1·2 times greater than that of the coarse-mesh and 2·1 times greater than that of the smooth disc. At 150 cm^3/sec these values have become 1·2 and 2·5, whilst at 250 cm^3/sec, 1·3 and 2·0 respectively. The performance of the perforated disc is therefore approximately 20% higher than that of the coarse-mesh and 100% greater than the smooth plate. If the increase due to the fractional free area of the 'perforated' discs is allowed for (see section 8.3.4) then the performance of the perforated and coarse-mesh discs is approximately equal and in the order of 160% greater than that of the smooth plate. Under these conditions the films formed on the coarse-mesh disc will be present on both surfaces, as discussed in section 2. If this is the case then the performance of the coarse-mesh will be approximately 30% greater than that of the perforated disc and 270% greater than the smooth disc.

The data collected during this section of the experimental investigation indicates that greatly enhanced rates of mass transfer can be obtained by increasing the flowrate. Between 100 and 200 cm^3/sec the gradient of the mass transfer coefficient/flowrate plot, for each of the disc surfaces employed, gradually increases. Thus doubling the flowrate more than doubles the associated mass transfer coefficient. The limiting film thickness analysis discussed in section 8.3.2 indicated that, for the perforated plate over this range of flowrates, the effect of film breakdown is reduced, until beyond 200 cm^3/sec the plate is completely wetted. This gradual increase in gradient is therefore a reflection of this improved liquid distribution. Once a continuous film is formed (i.e. once the flowrate exceeds 200 cm^3/sec approximately) the gradient of the curve begins to decrease with increasing flowrate. This section of the curve therefore reflects the true form of the function between flowrate and mass transfer coefficient.

The data collected for the coarse-mesh disc was used to study the applicability of Higbie's penetration theory to this structure. By using the centrifugal model, an expression for the residence time of liquid on the disc surface was obtained (equation 4.8). Although the centrifugal model applies only to laminar flows it was felt that in absence of a reliable turbulent model this would suffice. Therefore at each of the flowrates between 100 and 266.7 cm^3/sec and at 1500 RPM the mean residence time was calculated. Between the nozzle outlet and periphery of the disc there are 90 wires and holes. Thus the average time for fluid to cross one section of the disc was caculated from the mean residence time. Higbie's penetration theory assumes that mass transfer takes place in a series of steps with residence time θ, during which time mass transfer occurs by molecular diffusion. At the end of each step the fluid is completely mixed. The measured mass transfer coefficients were therefore compared with those predicted by equation 5.8, using the mean time for fluid to cross one wire (and hole)as the

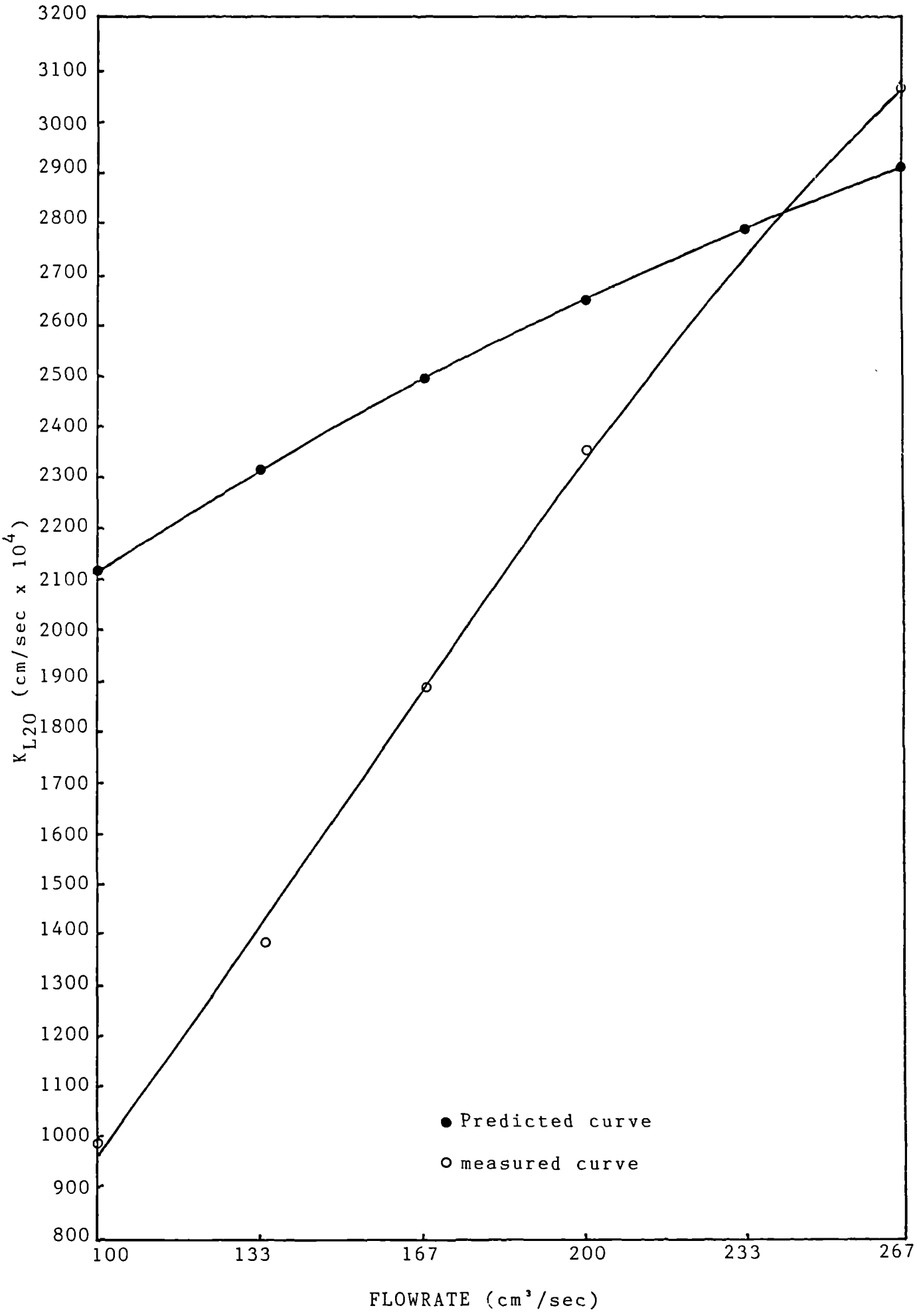

firgure 8.11 Comparison of results for coarse mesh disc with those predicted using the 'penetration' theory

penetration time, θ. Figure 8.11 presents the results of this analysis graphically. Up to a flowrate of approximately 233 cm^3/sec the actual mass transfer coefficient is less than that predicted by Higbie's theory. Above this value the measured mass transfer coefficient is greater than the predicted value. This implies that at flowrates below 233 cm^3/sec an element of mass transfer (as defined by Higbie) is greater than the time associated with one wire. For example at 100 cm^3/sec one element is equal to 4·5wires approximately. At flowrates in excess of 233 cm^3/sec θ is equal to less than one wire. The fact that the penetration time is not equal to a set number of wires at all flowrates is an indication that turbulence increases with increasing flowrate.

This analysis showed that the penetration theory could not be applied directly to the mesh structures without allowing for the effect of turbulence. The fact that the results were of the same order as the predicted values was a good indication of the accuracy of the experimental technique.

8.3.7. Coarse mesh disc at flowrates in excess of 100 cm^3/sec at speeds between 1250 and 1500 RPM

Data was collected using the coarse-mesh disc in a suspended, vertical position at speeds between 1250 and 1500 RPM with flowrates greater than 100 cm^3/sec. The maximum flowrate available at a particular speed was dependant on the ability of the pick-up tube nozzle to perform without choking. This flowrate varied from 200 cm^3/sec at 1250 RPM to 266.7 cm^3/sec at 1500 RPM. Figure 8.12 plots this data graphically.

Although only a limited amount of data was collected, especially at the highest flowrates, figure 8.12 demonstrated a number of important features. At 166.7 cm^3/sec the mass transfer coefficient/rotational speed curve goes through a maximum at approximately 1350 RPM. This is comparable with the data discussed in sections 8.3.2 and 8.3.4 illustrating that, as noted, the position of this maximum increases as the flowrate is increased. The characteritic curves at 200 cm^3/sec and above show no such maximum. This implies that at these flowrates no film breakdown occurs below a speed of 1500 RPM. This observation can be compared with the predictions of the limiting film thickness concept outlined in section 8.3.2. For a perforated disc this analysis suggested that only at flowrates below 192 cm^3/sec would film breakdown cause problems. As the maximum mass transfer coefficient associated with a particular flowrate occurs at a greater speed for the coarse-mesh disc then it does for the perforated disc, it would be expected that its limiting flowrate would be lower, as the results of this section of the experimental investigation demonstrates. The removal of the maximum from the characteristic curve at high flowrates allows the data to be compared favourably with that of other authors, particularly Koerfer (5) and Lim (4). This is discussed further in section 8.4.

The data collected during this section of the experiental investigation also provided further information regarding the effect of surface inclination on the measured performance.

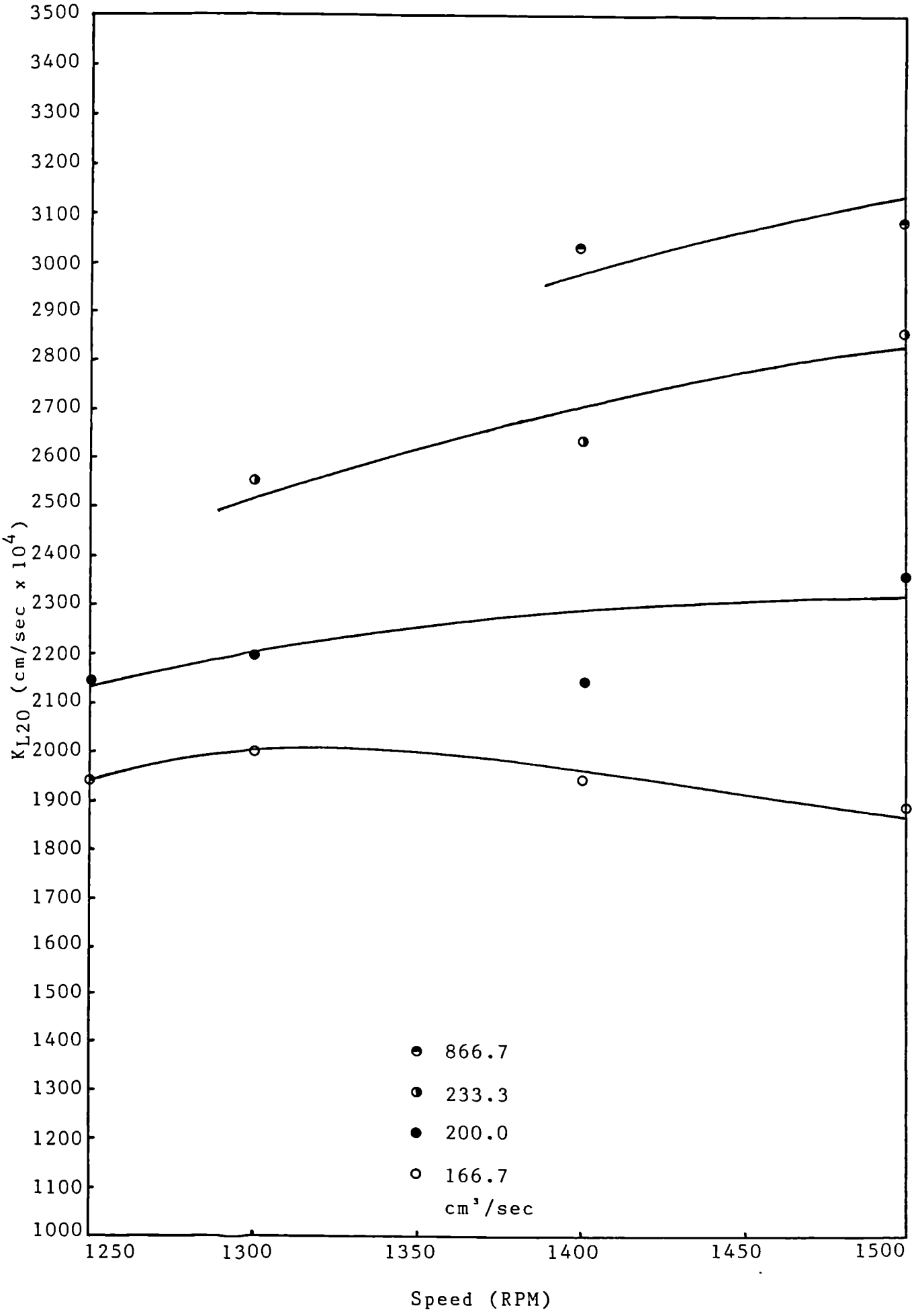

figure 8.12 Coarse mesh disc at flowrate in excess of 100cm³/sec atspeeds between 1250 and 1500RPM

The mass transfer coefficients for the various flowrates employed at a speed of 1500 RPM were compared with the corresponding data for the disc in a horizontal suspended position (see figure 8.10). The average variance of these points was only 2%. Thus, as shown previously in section 8.3.5 the disc inclination has only a negligible effect on the mass transfer performance at 1500 RPM.

8.3.8. Mass transfer associated with the liquid layer in the annulus of the absorption chamber

As a result of the way liquid is removed from the rotary absorption rig (see section 7 for a full description) a turbulent liquid layer is formed in the annulus of the absorption chamber. The inner surface of this is exposed to the gaseous phase and thus will contribute to the overall mass transfer rate. Data was therefore collected with the 'shroud' (described in section 7.2.9) in position. Rotational speeds between 500 and 1500 RPM were employed with flowrates of 50.0 and 100.0 cm^3/sec (at 500 RPM flowrates of 83.3 and 50.0 cm^3/sec were used). Because of the 'shroud' the area available for mass transfer was limited to the face of the annular layer alone. Thus the collected data was used to calculate a mass transfer coeffficient representing the performance of this additional area. Appendix K presents the analysis developed in order that the results of the preceeding sections could be modified to allow for this annular correction factor.

The results of this section of the experimental investigation were therefore used to correct the previously measured mass transfer coefficients so that they refered only to the disc and not the disc and annular layer. Table 8.2 shows the unmodified and modified mass transfer results and indicates the percentage error between them.

It can be seen from Table 8.2 that the error involved increases with increasing speed and decreases with an increase in flowrate. The increase with speed is only an apparent increase and is due to the onset of film breakdown discussed previously. As the annular layer does not break down the relative magnitude of its active area compared with that of the thin film increases. Thus the mass transfer associated with this area gradually becomes more important. The error due to this annular correction decreases with increasing flowrate because the overall mass transfer coefficient increases more rapidly than that of the peripheral liquid layer. This is a further indication of the enhancement caused by the waves formed on the surface of the thin rotating film. The effect of this correction factor is most pronounced when considering the performance of the smooth disc. At 1500 RPM the actual mass transfer coefficient is between 10 and 13% lower than the value measured previously. For the coarse mesh and perforated plates the magnitude of this error is approximately halved. One implication of this is that the enhancement achieved by replacing a smooth disc with a perforated disc is even greater than previously indicated (see section 8.3.4).

Although the error associated with the annular layer is significant it is likely that in future developments liquid will be removed in the same manner. The additional mass transfer due to this layer would thus be present and would therefore have to be allowed for in the design calculation. The mass transfer coefficients measured and discussed during the previous sections would therefore be more appropriate than the modified results.

	SMOOTH				COARSE-MESH				PERFORATED			
	$50cm^3/sec$	%	$100cm^3/sec$	%	$50cm^3/sec$	%	$100cm^3/sec$	%	$50cm^3/sec$	%	$100cm^3/sec$	%
500	0.0199	9	0.0280	9	0.0522	4	0.0831	3	0.493	4	0.0952	3
750	0.0217	9	0.0388	9	0.0515	4	0.1160	3	0.0515	4	0.01245	3
1000	0.0203	11	0.0426	9	0.0449	5	0.1218	3	0.0459	5	0.1256	3
1250	0.0189	12	0.0412	9	0.0375	6	0.1126	4	0.0423	6	0.1197	3
1500	0.0170	13	0.0419	10	0.0332	7	0.0953	4	0.0394	6	0.1006	4

Table 8.2: Mass transfer coefficients corrected for the effect of the peripheral liquid layer

8.3.9. Variation of mass transfer coefficients with radius for fine-mesh and smooth discs

Data was collected for the fine-mesh and smooth discs at radii of 116 and 84mm. The speeds and flowrates used were the same as employed in the previous experiemnts where the pick-up nozzle was positioned at a radius of 141mm. Thus the data from this section of the experimental investigation could be compared with the relevant information presented in the preceeding sections. The discs were held in a fixed position with their planes in the vertical position.

Figures 8.13 and 8.14 present the results collected for the smooth and fine-mesh discs respectively at a flowrate of 83.3 cm^3/sec. Data for these discs at a radius of 141mm is also plotted. The resulting curves for both surfaces are similar in certain respects. At low rotational speeds, the characteristic mass transfer coefficient decreases towards the centre of the disc. At high rotational speeds the inverse is true. This behaviour can be explained with respect to the film breakdown phenomenon discussed previously. At a given flowrate the film thickness is greater at the centre of the disc than it is at the periphery. As the provision of a thin film is known to enhance the associated mass transfer properties of a particular piece of equipment the rate would therefore be expected to fall as the centre is approached. At flowrates where it is known that film breakdown does not occur such behaviour is demonstrated. At conditions corresponding to film breakdown the measured mass transfer coefficient is reduced in proportion to the size of the dry area. Thus if, as suggested, film breakdown is the result of reducing the film thickness below a limiting value it will first appear at the edge of the disc. Therefore at a thickness below the critical value the disc surface will be dry up to a radius which falls as the flowrate is reduced. The increase in mass transfer coefficients shown at high rotational speeds is thus a function of this phenomenon. Although their actual magnitiude is reduced the proportion of the disc surface which is wet is increased, the measured values showing an overall increase.

The amount of data collected during this section of the experimental investigation was limited by the design of the pick-up nozzle. Although the orifice size had been designed to allow flowrates up to 100 cm^3/sec to be collected at speeds as low as 500 RPM and a radius of less than the smallest used, choking still occurred. It was felt that this was due to the shape of the nozzle itself and that improvements in its design (for example, by allowing divergent expansion of the fluid after it had entered the orifice) would have improved the performance.

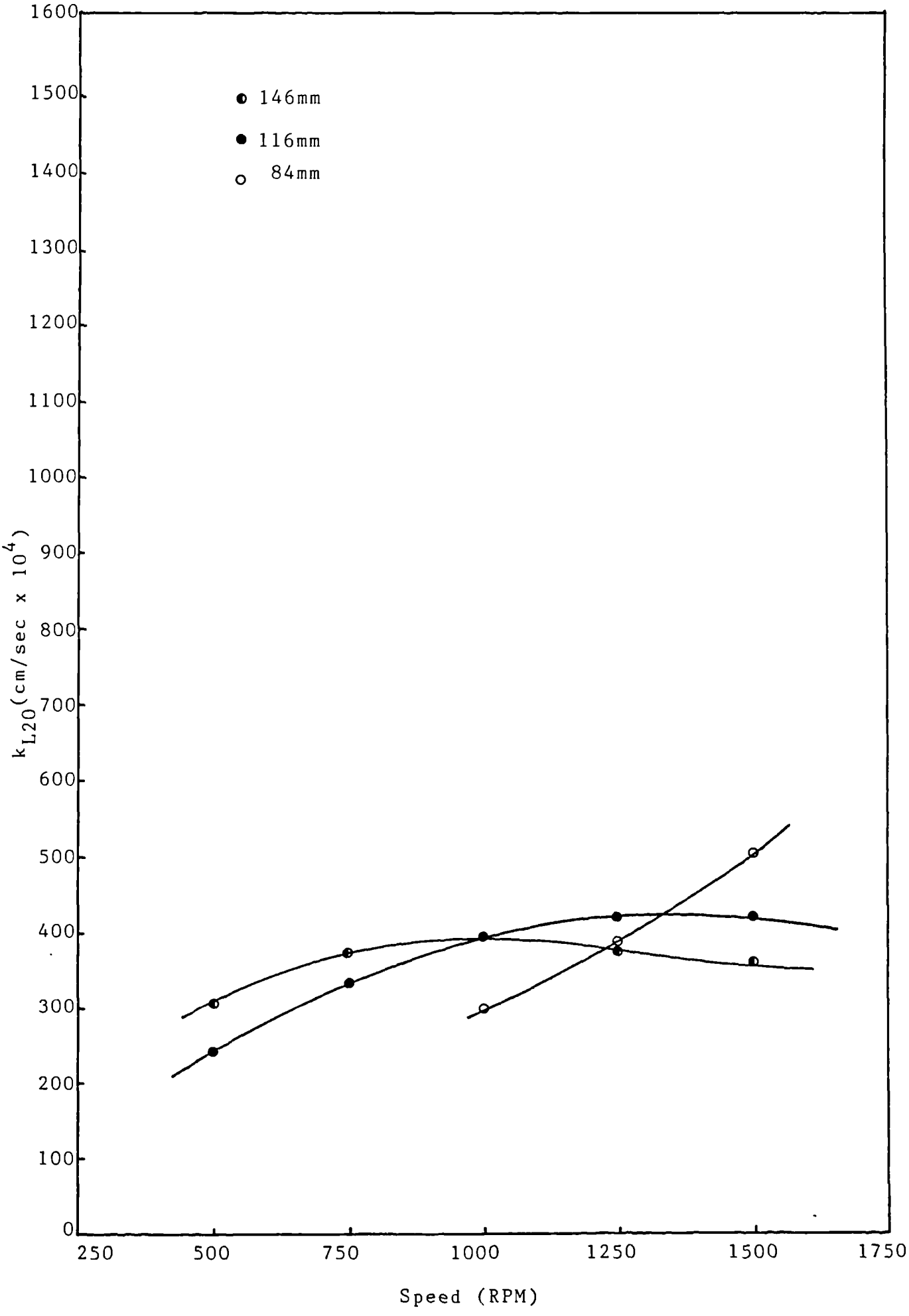

figure 8.13 Variation with radius for a smooth disc

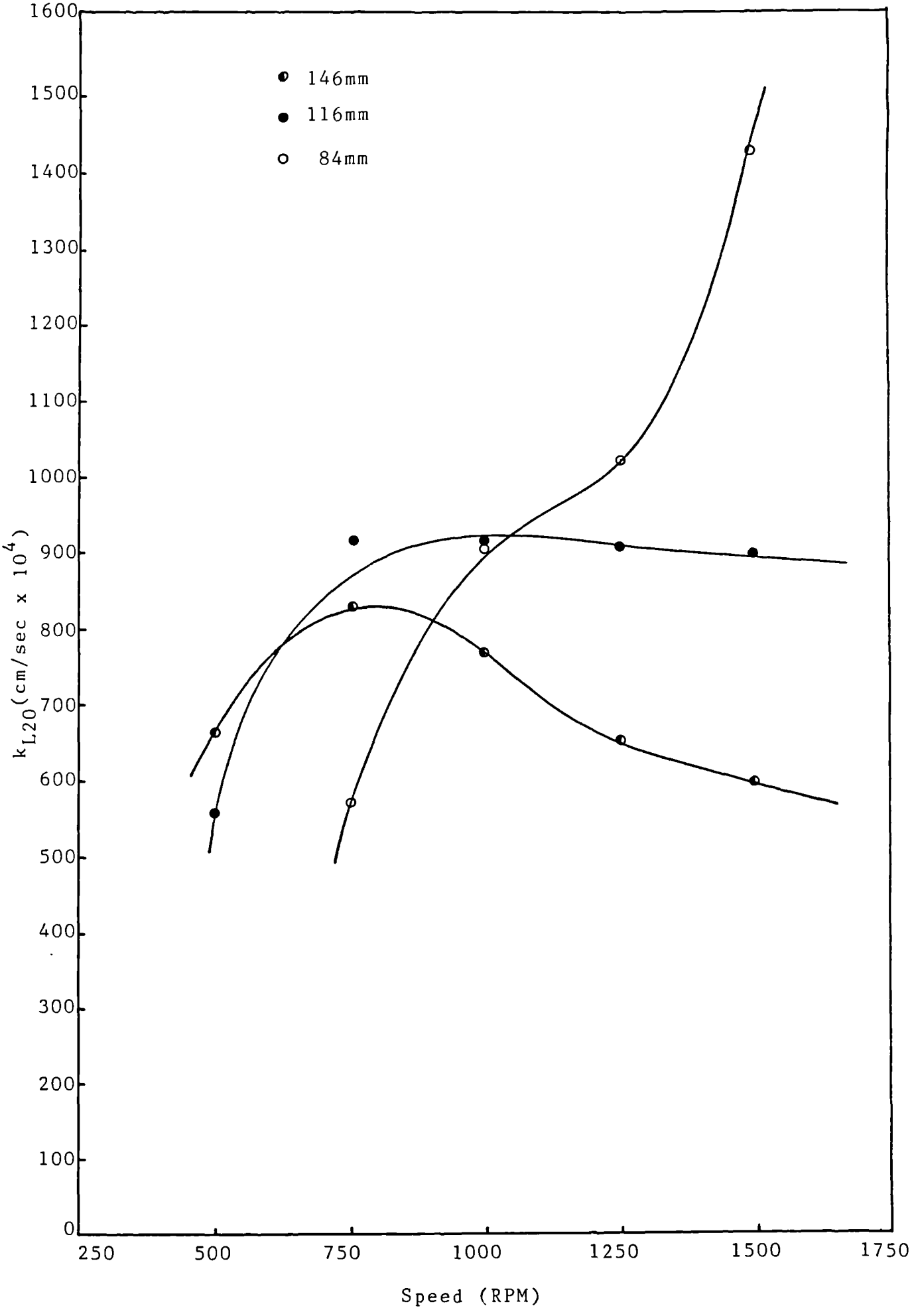

figure 8.14 Variation with radius for a fine-mesh disc

8.4. Comparison of the results of the present investigation with those of previous experiments and theoretical predictions

This section compares the results of the present work with the results from previous experimental investigations of rotary absorption systems. These results have been re-analysed using the methods described in section 5.2, so they are directly comparable with those of a carbon dioxide/water system at 20°C. In addition Venkataraman's 'approximate' theory has been used to predict mass transfer coefficients for the present system assuming a laminar film is formed.

Figure 8.15 illustrates the rotational speed and liquid flowrate ranges over which results have been published. This indicates that Lim (4) was concerned with mass transfer at low liquid flowrates (less than 60 cm^3/sec) and at intermediate rotational speeds (227 to 1110 RPM). Koerfer (5) employed high flowrates during his investigation of perforated surfaces (greater than 300 cm^3/sec) but only used speeds up to 600 RPM. Although the experimental results of Watts (6) covered a large range of flowrates and speeds the number of actual data points are limited (only three rotational speeds being employed). The results of the present investigation were designed to investigate high rotational speeds (up to 1500 RPM) at liquid flowrates between those used by Koerfer and Lim. Therefore although a considerable amount of date is available only a limited amount is directly comparable.

Figure 8.16 compares the results for the smooth disc at a flowrate of 50 cm^3/sec and between speeds of 200 and 1500 RPM with values predicted from the 'approximate' theory. For smooth plates at low rotational speeds the thin film formed will basically be laminar in nature, although a regular pattern of surface waves may be present at intermediate rotational speeds, (figurte 4.1(b) illustrates this behaviour). The 'approximate' theory (shown by Venkataraman to produce accurate predictions for laminar films) should therefore provide good estimations of mass transfer coefficients especially at low rotational speeds. Figure 8.16 illustrates that the results of the present investigation and those due to Watts are quite well modelled by the this theory. However the results of Lim's investigation are considerably different, increasing almost exponentially with increasing rotational speed. The results of Watts follow the approximate theory closely although they are slightly lower. As discussed in section 2 this is rather an incongrous result because the formation of waves should enhance, rather than decrease the associated mass transfer coefficient. The analysis technique used by Watts to measure the gas loading has been studied during this study of available analysis techniques. This indicated that the method should provide reliable results. (See section 6). However in such a technique the method used to collect and store samples is critical (and prone to error) and thus could be a possible cause of the observed behaviour. The results of the present investigation are slightly greater than those predicted by the 'approximate' theory. However at the higher rotational speeds the mass transfer coefficient passes through a maximum value before decreasing slightly. This behaviour is not demonstrated by the results of Watts or predicted by the 'approximate' theory. This phenomenon was discussed in section 8.3.2, and, it was suggested that it could be a result of the thin film breaking down due to entrained solid

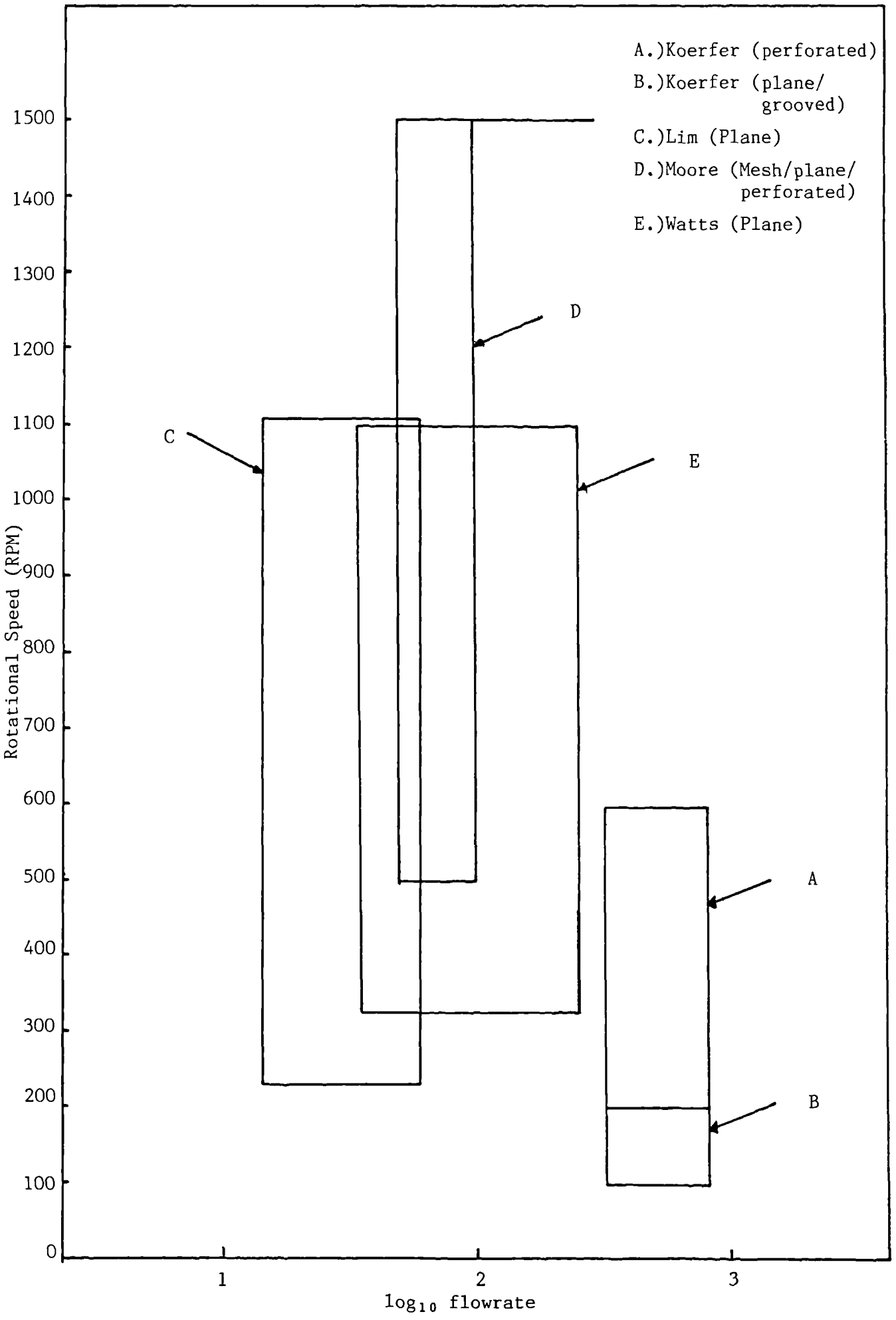

figure 8.15 Ranges of flowrate and rotational speed used by investigators of centrifugal mass transfer systems

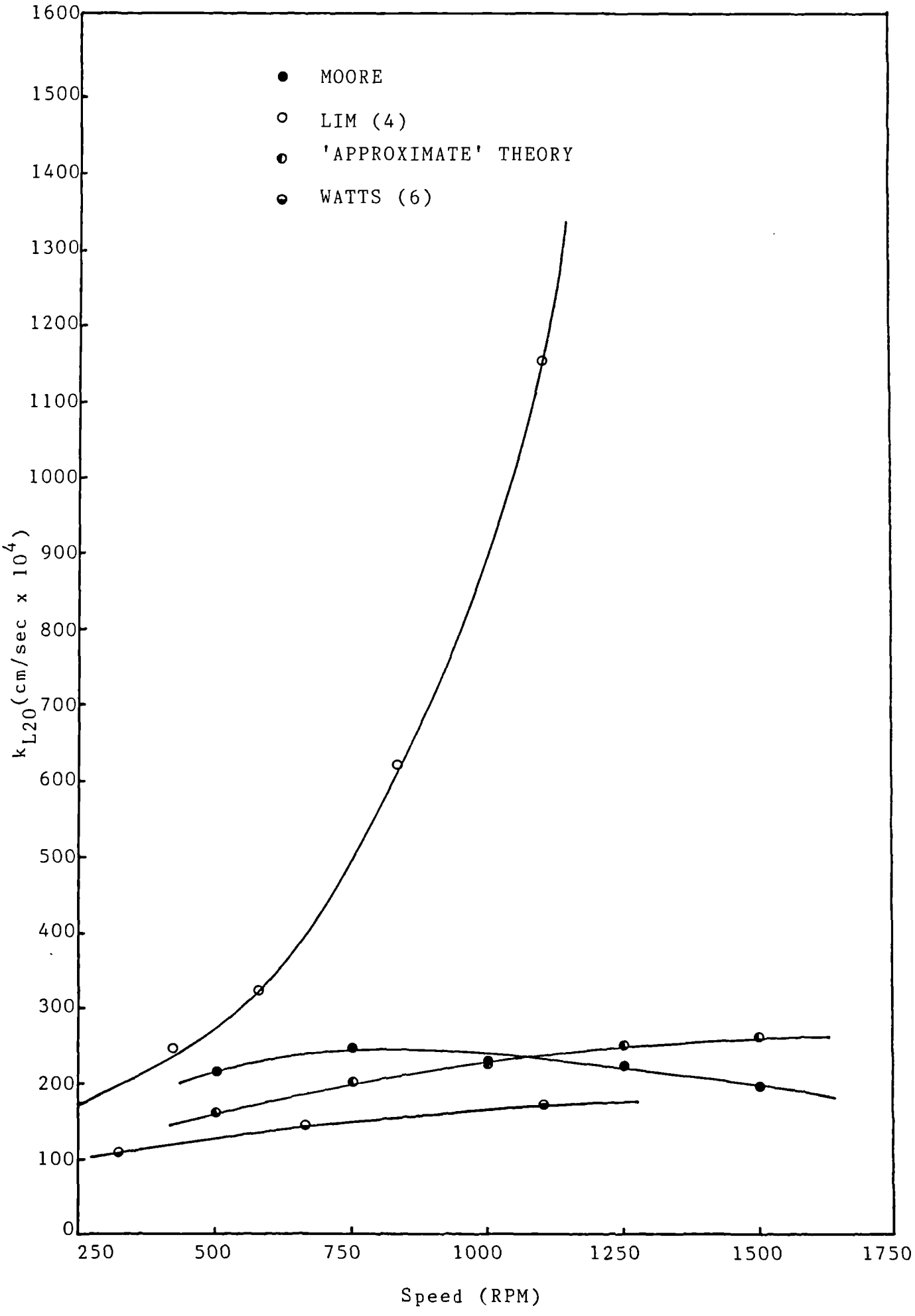

figure 8.16 Comparison of results for smooth discs

contaminents, in the liquid phase, sticking to the rotating surface. Watts used clean distilled water in his experiments and therefore the results would not demonstrate this characteristic. Similarily the 'approximate' theory does not allow for the occurence of film breakdown. The results of Lim at a flowrate of 50 cm^3/sec vary markedly from the comparable data of both the present and Watts investigation as well as the predictions of the 'approximate' theory. In addition these results do not compare favourably with those of the present investigation for the perforated and mesh discs or with the extrapolated results of Koerfers' work for perforated and smooth plates (see figure 8.17 and the following discussion). At 50 cm^3/sec and a rotational speed of 600 RPM the perforated disc used in the present investigation has an associated mass transfer coefficient of 400 x 10^{-4} cm/sec. From figure 8.17 the corresponding value for Koerfers' investigation is approximately 250 x 10^{-4} cm/sec. At these conditions the results of Lim indicate that the smooth disc has an associated mass transfer coefficient of approximately 400 x 10^{-4} cm/sec, which is of the same order as that for the perforated plate. As the film on the perforated plate shows a greater amount of turbulence than that on the smooth plate its mass transfer coefficient in theory should be larger. This behaviour is demonstrated when the data of Koerfer for perforated and smooth plates is compared. At 200 RPM and 500 cm^3/sec Lim's results show a mass transfer coefficient of approximately 150 x 10^{-4} cm/sec which can be compared with a value of approximately 50 x 10^{-4} cm/sec for the extrapolated results of Koerfer. The reason for the apparent discrepancy between Lims' results and those of the other investigations is not clear, however it is possible that it could be a result of the method used to collect samples from the disc surface. As described in section 2 a scoop device was employed so that the variation of mass transfer coefficient with radius could be analysed. In all other experiments liquid was collected from the periphery of the rotating disc. Lim indicated that problems were encountered using the scoop and that to successfully withdraw samples a syphoning effect had to be employed. The collected liquid samples were analysed by directing the flow from the scooping device to the flow cell of a dissolved oxygen analysing electrode. These electrodes have been shown to be particularly pressure sensitive and as the syphoning effect is likely to alter the liquid pressure, this may have caused the recorded readings to be greater than the actual film composition. Because the raw data collected by Lim has not been published it it impossible to check that the method used to analyse this was applied correctly. Therefore no firm conclusions can be made concerning this apparent discrepancy.

Figure 8.17 compares the mass transfer data collected by Koerfer for the perforated surface with that from the present investigation. Koerfer employed rotational speeds up to 600 RPM at flowrates from 300 to 960 cm^3/sec and thus the only data that could be directly compared was that collected in excess of 100 cm^3/sec. This represented a rotational speed of 1500 RPM. As can be seen from figure 8.17 the data compares well, the mass transfer coefficient at 1500 RPM being approximately 2·1 times greater than that at 600 RPM. This would indicate that at a particular flowrate the mass transfer coefficient increases slightly less than linearily. This agrees with the trends shown by the data discussed in the previous sub-section.

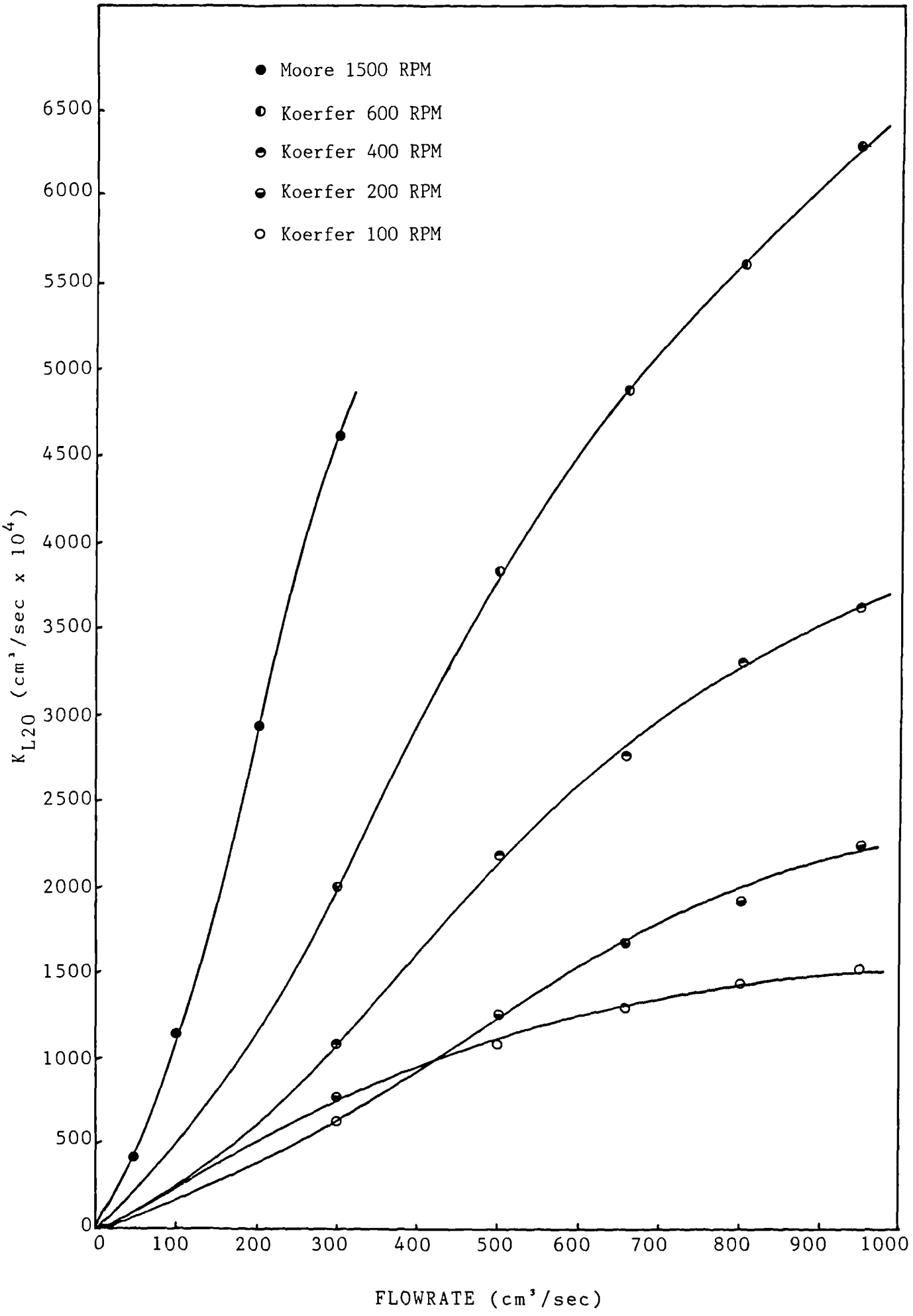

figure 8.17 Comparison of data for perforated plates

9.0. Experimental mass transfer investigation using the carbon dioxide/aqueous diethanolamine system

9.1. Introduction

The experiments in which water was replaced by aqueous diethanolamine are discussed in this section. In general the experimental procedure adopted was the same as that presented in section 8.2. The modifications that were required are outlined in section 9.2 below. The aim of these experiments was two fold. Firstly, it was hoped that the results would demonstrate the degree of enhancement attained when replacing a physical solvent by a chemical solvent in a rotary system. Secondly, the results were to be used to ascertain whether the equations, outlined in section 5.3, could accurately predict the experimentally measured enhancement factors. The contact surfaces employed were limited to the coarse mesh disc and the smooth plate. The effect of interfacial 'turbulence' could thus be determined. Section 9.3 presents the results calculated from these investigations and compares them with the corresponding results discussed in section 8.3.

9.2. Experimental procedure

The experimental procedure adopted during the series of runs where aqueous diethanolamine was employed as the liquid phase, was virtually identical to that outlined in section 8.2. The differences that did exist are discussed below.

As discussed in section 6 the outlet concentration of carbon dioxide in the liquid phase was to be measured by chromatographic analysis. The gas sensing membrane probe was therefore not required during these experiments and thus did not have to be calibrated at the beginning of each day. Flow was diverted from the electrode flow cell by keeping valve 36 on the sample line closed.

The rig was set up before the commencment of a run in exactly the same fashion as that described in section 8.2.3 except that valve 33 was closed and valve 34 opened. This diverted the outlet flow from the rotary rig towards tank 2 and away from the drain. In this way the chemical solvent could be stored under a blanket of nitrogen before being either regenerated (in the column) or being used again in the rotary rig. Once the initial rotational speeds, liquid flowrate and radial position had been attained the apparatus was left for five minutes to allow the system to reach 'equilibrium'. (i.e. a constant outlet acid gas loading). After this time a small sample was extracted from the outlet liquid line through stopcock 35 and the liquid temperature recorded. In order that a representative sample was collected the following procedure was adopted. The stopcock was fully opened and liquid allowed to run to a waste bottle for 15 seconds, thus flushing out the connecting tubing with fresh liquid. A sample bottle was then placed below the stopcock and quickly filled to overflowing. This was then sealed with an air tight lid. In this way the sample was only exposed to a source of oxygen (the atmosphere) for a negligible period. Oxidative degradation of the sample could therefore be neglected. The sample bottle was marked with the corresponding run number and stored until it could be analysed once the experimental run had been completed. Once a sample had been taken either the liquid flowrate or the rotational speed was changed to the next value of interest and the apparatus left for a further three minutes. Once all of the data required had been collected the rig was run down and drained as described in section 8. The absorption chamber was then thoroughly cleaned to remove all traces of DEA.

During runs where a partially loaded solution was employed as the liquid feed, a preliminary calibration had to be completed before experimental data could be collected. This allowed the inlet gas loading to be calculated. The rig was started up in the manner described except that pure nitrogen was used as the gas phase. After two minutes a sample was withdrawn using the procedure outlined above. The correct carbon dioxide flowrate was then established and the required experimental data collected. This sample was also used to measure the molal DEA concentration of the inlet liquid stream (see section 6.4).

The samples collected during an experimental run were analysed using the chromatographic technique outlined in section 6.3.4. This analysis was completed as soon as possible after the

samples had been collected to minimise errors associated with degradation and diffusion from solution. After the analysis had been completed the excess sample was placed in a waste bottle until disposal could be arranged.

9.3 Experimental Results

Mass transfer data was collected for the carbon dioxide/aqueous diethanolamine system using the coarse-mesh and smooth surfaces in fixed, vertical positions with a carbon dioxide partial pressure of 1 atmosphere. Liquid flowrates between 66.7 and 233.3 cm^3/sec and a rotational speed of 1500 RPM were employed. The results of these investigations are presented in appendicies H.1 and H.2 for the coarse-mesh and smooth plates respectively. These tables also present the calculation steps required to predict the relevent chemical enhancement factors by the method outlined in section 5.3. The physio-chemical data required for these was prepared using the methods discussed in section 5.4. The tables were designed so that the upper block presents the data necessary in the calculation of the measured enhancement factor (ϕ_M) while the lower block leads to the theoretical enhancement factor (ϕ_C).

The measured enhancement factor is the ratio of the measured rate of mass transfer (N_{DEA}) to the rate of mass transfer in a purely physical system with identical fluid hydrodynamics (i.e. $k_{LT} \cdot A \cdot Ci_{DEA}$).

The theoretical enhancement factor is a function of the rate of reaction between carbon dioxide and ethanolamine molecules. As discussed in section 5.4.7 the value of the reaction rate constant for this system is unclear. Two distinctly different values have been reported in the literature and thus ϕ_C has been calculated for each of these. Case (1) assumes a value of k_2 equal to $1.0 \times 10^6 cm^3/mol\ sec$. while case (2) uses $5.8 \times 10^6 cm^3/mol.sec$. Evidence suggests that the former is the most reliable figure (see 5.4.7).

For the coarse mesh disc the measured enhancement factor varies from approximately 10 at a flowrate of 66.7 cm^3/sec to approximately 3 at 233.3 cm^3/sec. The calculated enhancement factors also decrease as the flowrate is increased. At 66.7 cm^3/sec case (1) predicts an enhancement of 2·7 while case (2) predicts a 5·7 fold increase. At 233.3 cm^3/sec the enhancements are 1·1 and 1·6 respectively. The degree of chemical enhancement decreases with increasing flowrate because the physical mass transfer coefficient (and thus transfer rate) shows a corresponding increase. As discussed previously (section 2) the potential effectiveness of a chemical reaction is limited by the relative magnitude of the rate of reaction and physical mass transfer coefficient. As the coarse mesh is characterised by particularly high mass transfer coefficients at high flowrates the addition of a relatively 'slow' chemical reaction such as that for DEA provides a less significant improvement than at low flowrates.

Table H.1 indicates that for the coarse-mesh surface the measured enhancement factor is greater than the calculated value for both cases considered at all liquid flowrates. In addition the ratio $\phi_M : \phi_C$ is approximately constant especially for case (2). The penetration theory model devised by Brian et al (52) and discussed in section 5.3 was used to predict the theoretical degree of enhancement. In this model the liquid flow pattern was assumed to be such that liquid flows down over a piece of absorber packing in slug, laminar flow. In addition it was assumed that absorption took place by molecular diffusion alone whilst the liquid phase was exposed

to the gas phase for a given contact time. Between exposures the liquid was completely and instantaneously mixed, thus each slug began each contact-time interval with a flat concentration profile. The contact time between successive mixing points was so short that the absorbing species never penetrated deeply enough to approach the wall of the packing. The liquid depth could therefore be assumed to be infinite for mathematical modelling.

When this model is used together with the equations representing an irreversible second order chemical reaction system the following differential equations can be derived:

$$\frac{\delta^2 a}{\delta Z^2} - \frac{\delta a}{\delta \theta} = ab \qquad 9.1$$

and

$$rq \frac{\delta^2 b}{\delta Z^2} \quad q \frac{\delta b}{\delta \theta} = ab \qquad 9.2$$

where a,b,r,q,Z and θ are defined as,

$$a = C_{CO_2}/C^i_{CO_2}$$

$$b = C_{DEA}/C^\circ_{DEA}$$

$$r = D_{DEA}/D_{CO_2}$$

$$q = C^\circ_{DEA}/C^i_{CO_2}$$

$$Z = (k_2 C^\circ_{DEA}/D_{CO_2})^{1/2} \; y$$

where y is the distance into the liquid phase (cm),

and $$\theta = k_2 C^\circ_{DEA} t$$

i.e. the dimensionless time of contact.

The following boundary conditions were imposed upon the simultaneous solution of these differential equations,

At $\theta = 0$, and at any $Z>0$ $\quad a = 0, \; b = 1$ 9.3

At $Z = 0$, and at any $\theta>0$ $\quad a = 1, \; \frac{\delta b}{\delta Z} = 0$ 9,4

and as $Z \to \infty$, and at any θ $\quad a = 0, \; b = 1$ 9.5

These boundary conditions contain the assumption that chemical equilibrium prevails at the beginning of the contact-time interval; thus a = 0. Peaceman (49) has shown that the liquid hold-up in a gas absorption column is sufficient to ensure that this assumption is a good one for cases of practical importance. Similarily this assumption should apply to the thin film developed upon the surface of a rotating disc.

To solve the differential equations (9.1 and 9.2) Brian approximated these by time-centred implicit finite - difference equations analogous to the equation of Crank and Nicholson (107). The solution of these implicit equations was greatly simplified by linearizing according to the method of Douglas (108). An IBM - 704 digital computer was programmed to solve these equations for a variety of combinations of r and q. For these values the computer developed a and b as functions of Z and θ; at selected values of θ, ϕ was evaluated from;

$$\phi = \sqrt{\frac{\pi}{4\theta}} \int_0^\infty a\,dZ + \sqrt{\frac{\pi}{4\theta}} \int_0^\infty q(1-b)\,dZ \qquad 9.6$$

where the first integral in this equation represents the total amount of carbon dioxide in the liquid phase after a contact interval θ and the second integral represents the disappearance of the diethanolamine and thus the amount of carbon dioxide which has been removed by chemical reaction.

The physical absorption coefficient is related to the contact time for the penetration model by;

$$k_L\ (\text{phys}) = 2\sqrt{\frac{D_{CO_2}}{\pi t}} \qquad 9.7$$

and thus θ can be re-defined in terms of k_L(phys) i.e.,

$$\theta \equiv k_2 C^\circ_{DEA} t = \frac{4}{\pi}\left[\frac{k_2 C^\circ_{DEA} D_{CO_2}}{k_L(\text{phys})^2}\right] \equiv \frac{4}{\pi} \cdot Ha \qquad 9.8$$

Ha, the Hatta number, is a more general variable than θ and as previously discussed in section 5.3 can be interpreted as a measure of how rapid the chemical reaction is, relative to physical absorption in an absorber characterised by a mass transfer coefficient of k_L(phys). For a particular value of the Hatta number the chemical enhancement available from a reaction with a rate constant of k_2 can be deduced by using the method and figures described in section 5.3.

The 'crude' model developed by Venkataraman (see section 2) applied Higbie's penetration theory to the process of mass transfer in a thin rotating film. He demonstrated that even when the said film was laminar and its surface was wave free the values predicted were some 25% less than those measured. It would appear that this

was due to the interface stretching as the film expanded which caused a velocity component perpendicular to the disc surface to develop, as his 'approximate' theory which considered this effect modelled the process accurately. At higher rotational speeds and liquid throughput surface waves are formed even on a smooth disc. The 'approximate' model is unable,under these conditions, to predict the system mass transfer coefficient accurately as it is unable to represent the eddy mixing caused by the surface waves. On roughened surfaces the 'approximate' theory is of even less value as the thin films are, even at low rotational speeds, 'turbulent'. As noted above the actual chemical enhancement measured for the coarse mesh disc was significantly greater than that predicted from the equations and figures developed by Brian et. al. using a model based upon the penetration theory. It is thus probable that this inaccuracy is also a result of the turbulent nature of the thin film. Therefore to produce an accurate method of predicting the chemical enhancement factor this interfacial 'turbulence' has to be accomodated. The simplest method would be to replace the molecular diffusivity (D_{CO_2}) with a turbulent or eddy diffusivity, however values of this quantity are not generally available. Koerfer (5) attempted to model the mass transfer process on a perforated disc by assuming that mass transfer occurs in a number of concentric rings. The applicability of this technique to the process occuring on a mesh surface has been studied in section 8.3.6. This demonstrated that the width of these rings varies with both rotational speed and liquid flowrate and thus it would be difficult to use this method to modify the theory of Brian.

Considering the results for the smooth plate it can be seen that the measured enhancement factor decreases from 10.4 at 66.7cm^3/sec to 2.5 at 233.3 cm^3/sec. Again this is due to a corresponding increase in the relative magnitude of the physical mass transfer coefficient of the system. Comparing the measured enhancement factor with those calculated from theoretical considerations, it can be seen that for case (2) a good agreement is shown. For case (1) the ratio $\phi_M : \phi_C$ varies from 2.2 at 66.7cm^3/sec to 1.9 at 233.3cm^3/sec. The evidence suggests that the rate constant used in case (1) is the most accurate and thus, as for the coarse-mesh, the measured enhancement factor is significantly greater than that predicted using the penetration theory. This discprepancy is probably due to the interfacial mixing caused by the surface waves and to model this effect accurately an eddy diffusivity would have to be used in place of a molecular diffusivity.

Although the results of this section of the experimental investigation are limited they have demonstrated that for a rotary system,models based upon the penetration theory can not be used to predict the enhancement due to an associated chemical reaction. It appears that this is due to the turbulent nature of the thin film flow. To model this system accurately an eddy-type diffusivity would have to be used rather than a molecular diffusivity. These results have been used in Appendix C to calculate the size of absorber necessary to satisfy the requirements of the closed cycle nitrodiesel engine outlined in section 1.2.

10.0 CONCLUSIONS

The aim of the present investigation was to study the properties of the thin films formed under the action of centrifugal forces on the surface of various perforated materials. The experimental section of this work consisted of three main areas: a hydrodynamic study of films formed on discs constructed from woven meshes, a mass transfer study using a system comprised of carbon dioxide and water and a similar study where aqueous solutions of DEA were employed as the liquid phase. This section summarises the investigation and presents conclusions drawn from the observations and results.

The results of the hydrodynamic investigation indicate that, with each of the meshes employed, a stable film can be maintained at speeds in excess of approximately 200 RPM. In the context of perforated plates, stability indicates a film which demonstrates no leakage through the perforations rather than one which does not exhibit film breakdown. Observations of the stable films, show, that over distinct ranges of rotational speed and liquid flowrate the air liquid interface is disturbed. This disturbance can be classified as either regular surface waves spiralling out from the inlet nozzle or random turbulence. At a fixed flowrate the degree of interfacial turbulence is enhanced by an increase in the rotational speed. As a result of the improved gas/liquid mixing caused by this turbulence the coefficient representing mass transfer between these phases should also be enhanced, particularly at high speeds. To check this conclusion a smooth, plane disc was used in the mass transfer investigations as a laminar, base case. During the hydrodynamic investigation it was observed that as the rotational speed was increased dry areas began to form around the periphary of the discs. This phenomenon was particularly marked at the lower flowrates. Due to the difficulty in observing the film surface it was impossible to categorize this breakdown accurately. However as it results in a reduction in the available transfer area it was felt that its prescence would be indicated in the mass transfer results.

The mass transfer coefficient representing the co-current absorption of carbon dioxide into water was measured using a specially constructed rotary device, for three perforated materials (a fine mesh disc, a coarse mesh disc and a plane disc with a regular array ofpunched holes). A smooth plate was also employed in order to gain results for a laminar film. At all rotational speeds it was found that for each of the surfaces the measured mass transfer coefficient increased with increasing flowrate. The mass transfer coefficients associated with the perforated plates were significantly higher than those for the smooth plate. This represents the increase in interfacial turbulence that is a feature of the higher flowrates and rougher surfaces. The increase with flowrate was most pronounced for the punched disc and least for the plane. For all flowrates below 100 cm^3/sec it was found that when the rotational speed was increased at a fixed flowrate the associated mass transfer coefficient passed through a maximum. The position of this maximum increased with increasing flowrate. The degree of reduction experienced at speeds in excess of this critical point was most pronounced for the fine mesh followed by the punched plate the coarse mesh and the plane disc.

In the case of the mesh discs this phenomenon was coincident with film breakdown and it was thus concluded that the reduction in performance indicated a decrease in transfer area, rather than transfer coefficient. Previous work had indicated that film breakdown on a punched plate was caused by the liquid film circumnavigating rather than crossing the perforations. It was felt that the onset of this behaviour could be caused by the film thickness falling below a critical value and that this could be the cause of the behaviour demonstrated by the punched plate. Calculation using a 'centrifugal' model showed, that within an allowable experimental/analytical error the maximums occurred at a constant film thickness. Using this approach it was possible to predict a flowrate where film breakdown would only occur at speeds above 1500 RPM, i.e. the mass transfer coefficient would show no maximum. Tests at high flowrates indicated the accuracy of these predictions. The behaviour of the smooth disc was more difficult to explain. Hydrodynamic investigations showed no reason for a reduction in the mass transfer performance and correlations prepared for predicting the onset of film breakdown, indicated that no breakdown should occur. However as 'dirty' water was being used it was felt that the entrained rust particles could cause breakdown at higher than normal flowrates.

A number of experimental runs were repeated at carbon dioxide pressures of 0.5 atmospheres rather than one atmosphere. The associated mass transfer coefficients showed only a negligible variation. It was thus concluded that, as assumed, the transfer process was liquid phase controlled.

Experiments were completed with various discs held in vertical and horizontal planes in order to determine the effect of disc inclination on the mass transfer performance. It was concluded, that in general, this variation caused only minimal change in the associated mass transfer coefficient. Thus practical rotary machines would be capable of operation in any plane of orientation. This is important if such technology is to be successfully applied to undersea applications (i.e. the scrubber of a nitro-diesel engine) or floating structures. The variation of mass transfer coefficient with radius was examined for the smooth and fine-mesh discs. At low rotational speeds the mass transfer coefficient was found to decrease as the nozzle was approached. Such reduction was a function of the increase in film thickness and associated reduction in turbulence. At higher rotational speeds, i.e. above that where a maximum is demonstrated in the overall coefficient, the inverse is true. It was felt that this was again a result of film breakdown. Breakdown occurs at the outer edge of the disc, thus the associated overall coefficient is artificially reduced. Therefore as the nozzle is approached, and the proportion of dry disc reduced, the mass transfer coefficient appears to increase. It is possible that these results could be used to estimate the magnitude of the overall mass transfer coefficient in the absence of film breakdown.

The results of this investigation indicated that at 1500 RPM and flowrates greater than 200 cm^3/sec (i.e. conditions pertinent to practical developments) the mass transfer coefficient for the punched plate was greater than that of the coarse mesh.

However allowing for the enhancement due to the undersurface contact it was concluded that the coarse mesh disc would provide greater overall rates of transfer/unit volume. It was this surface that was thus employed in the experiments involving the chemical system. Although the results of this investigation were limited they were sufficient to conclude that a significant increase in the rate of mass transfer could be attained. As had been expected it was found that the degree of chemical enhancement decreased with increasing flowrate. This reduction is caused by the fact that the reaction between carbon dioxide and diethanolamine is relatively slow, and that the rate of physical mass transfer in this system is very high. Although the magnitude of enhancement is decreased it is significantly higher than that estimated by use of predicitive methods. These estimates were based upon a penetration type model of mass transfer where the liquid phase flows in slug laminar form. It was thus concluded that the assumptions inherent in its application could not be applied to the turbulent film formed in a rotary device.

This investigation was designed so that the data obtained could be used to study the possibility of adopting rotary technology to the design of a scrubber for a closed cycle nitro diesel engine. This analysis is outlined in Appendix C. The results of this investigation indicate that for the duty required the most practical solvent would be sea-water. Although the use of DEA reduces the number of plates necessary (by about 5 times) it involves incorporating regeneration and tankage facilities into the machine. It is estimated that these would occupy more space than is saved. The chemical system would be more attractive if a solvent were used which was more reactive than diethanolamine. Unfortunately these substances tend also to be more reactive with oxygen and thus suffer greater chemical degradation.

Dow's proprietry solvent 'Gas-Spec FS-IL' may provide the basis for an attractive system. This solvent could not be utilized during the present investigation as a sample could not be obtained.

11.0 RECOMMENDATIONS FOR FUTURE WORK

It is recommended that a number of topics either investigated in, or outlined by the present work be subject to further research. These are summarized below:-

- The breakdown of films on mesh discs should be studied further in order that operation can be avoided in regimes where this ocurrs. Information regarding the mechanism of breakdown would be useful when designing or analysing other types of disc.

- The operation of discs constructed from wires woven radially and circumferentially should be analysed. It is possible that such discs would reduce the amount of film breakdown thus significantly increasing mass transfer rates.

- The distribution of the films formed on mesh discs should be analysed in order to determine whether, as suggested these exist on both surfaces simultaneously. It is considered than an improved visualisation technique must be developed before such observations could be undertaken. Mass transfer measurements using equipment designed so that the gas phase is distributed above and below the rotating disc should be capable of providing quantitative estimates of this effect. Such a determination would have to be undertaken before multi-perforated-plate machines could be designed.

- A considerable amount of data has been produced concerning the performance of single plate machines. The disc materials used in this investigation have been shown to be capable of providing very high rates of mass transfer. It is thus suggested that future work should be more concerned with the performance of multiple plate machines than with further improvments in the characteristics of the individual discs.

- Further work with chemical solvents is recommended. The present work indicated that even when utilising a relatively slow reaction a significant enhancement could be attained. Thus in systems characterised by fast reactions, especially where a high degree of removal is required, it is possible that this could result in considerable miniaturisation. In the case of the nitro diesel engine such size reduction may outweigh the size of regeneration equipment, thus making the chemical system the more attractive option.

- If a chemical system were utilised in the scrubber designed for a closed cycle nitro diesel engine further work would be required before the regeneration system could be designed.

NOMENCLATURE

A	area available for mass transfer	(cm^2)
C	concentration of solute (carbon dioxide) in the solvent (water)	(g/cm^3)
C_o	concentration of reactant (diethanolamine) in the solution (aqueous diethanolamine)	(g/cm^3)
C*	concentration of free gas (carbon dioxide) at at the surface of the reactant solution (aqueous diethanolamine)	(g/cm^3)
ΔC	concentration driving force	(g/cm^3)
D	diffusivity of gas (carbon dioxide) in the solution	(cm^2/sec)
D_o	diffusivity of reactant (diethanolamine) in the solution	(cm^2/sec)
E	fractional free area	(-)
f	friction factor (equivalent of Fanning friction factor in full tube flow)	(-)
H	Henry's law coefficient	(mol/l.atm)
Ha	Hatta number = $(k_2.D.C_o)^{1/2}/k_L$	(-)
I	Ionic strength	(g.io/ℓ)
i_+, i_-, i_g	Ionic contributions due to cation, anion and gas respectively	(-)
k	Individual mass transfer coefficient	(cm/sec)
K	Overall mass transfer coefficient	(cm/sec)
k_2	second order rate constant	(ℓ /mol.sec)
Kc	stoichiometric equilibruim constant for the primary reation between carbon dioxide and DEA	(mol/ℓ)
M	concentration of DEA before carbonation	(mol/ℓ)
N	overall rate of mass transfer	(g/sec)
P	concentration/diffusion parameter	(-)
Q	volumetric flowrate	(cm^3/sec)

R	gas constant	
R	rate of mass transfer/unit area	($g/cm^2/sec$)
Re	Reynolds number = $Q/r\nu$	(-)
r	radius of disc	(cm)
s	fraction of surface renewed in unit time (Dankwerts' theory)	(-)
t	time; residence time of a film on the surface of a rotating disc	(sec)
T	temperature	(°C)
Ta	Taylors number = $\omega r^2/\nu$	(-)
V	film velocity	(cm/sec)
$\overline{V}$	average film velocity	(cm/sec)
y	depth of liquid measured from the disc surface	(cm)
Z	number of moles of (diethanolamine) reactant which reacts with one mole of (carbon dioxide), gas	(-)

Greek

α	degree of carbonation i.e. mols CO_2/ mol DEA	(-)
δ	film thickness	(cm)
σ	surface tension	(g/sec^2)
ρ	desnity	(g/cm^3)
θ	exposure time (penetration theory)	(sec)
ϕ	chemical acceleration factor	(-)
ν	kinematic viscosity	(cm^2/sec)
ω	angular velocity	(sec^{-1})
γ	shear stress	($g/cm\ sec^2$)

Subscripts

a	approximate value
b	bulk of solution

CO_2	referring to carbon dioxide
DEA	referring to diethanolamine
e	at edge of disc
g	gas phase
i	at the inlet/nozzle
L,1	liquid phase
O_2	oxygen
r	at a particular radius
s	at the surfaceof the film
20	at 20°C
ω	at the wall/disc surface
w	water

Superscripts

b	bulk
i	interface
o	outlet

REFERENCES

1) Bromley, L.A., 'Saline water conservation research' Water resources centre, University of California, San Diego contribution no. 100, 24-30 (1965)

2) Aroesty, J., Gross, J.F., Illickal, M.M., and Maloney, J.V., Digest seventh international conference of medical biological engineering Stockholm, p.527 (1967)

3) Venkataraman, R.S., 'Mass transfer to an expanding interface' Ph.D Thesis Leeds University (1966)

4) Lim, S.T., 'Hydrodynamics and mass transfer processes associated with the absorption of oxygen in liquid films flowing across a rotating disc' Ph.D Thesis University of Newcastle Upon Tyne (1980)

5) Koerfer, M., 'Hydrodynamics and mass transfer of thin films flowing on rotating perforated discs' Internal report University of Newcastle Upon Tyne (1982)

6) Watts, B.E., 'The flow, heat and mass transfer characteristics of a rotating disc' Ph.D Thesis University of Wales (1971)

7) Bell, C., 'The hydrodynamics and heat transfer characteristics of liquid films on a rotating disc' Ph.D Thesis University of Newcastle Upon Tyne (1975)

8) Emmert, R.E., and Pigford R.L., 'A study of gas absorption in falling liquid films' Chem. Eng. Prog. 50, 87 (1954)

9) Davies, J.T., and Bradley P.J., 'Research project Dept., Chemical Engineering, Cambridge University (1960)

10) Downing A.L., and Truesdale G.A., 'Some factors affecting the rate of solution of oxygen in water' J. Appl. Chem. 5, 570 (1955)

11) Striba, C., and Hurt, D.M., 'Turbulence in falling liquid films' A.1. Che.E. Journal, 1, 178, (1955)

12) Allen, J.M., 'Some studies on falling liquid films' Ph.D Thesis Manchester college of Science and Technology (1962)

13) Jackson, M.L., 'Liquid films in viscous flow' A.1. Che.E. Journal, 1, 231, (1955)

14) Portalski, S., 'The mechanism of flow in wetted wall columns' Ph.D Thesis, University of London (1960)

15) Duckler, A.E., and Bergelin, O.P., 'Characteristics of flow in falling liquid films' Chem. Eng. Prog., 48, 557 (1952)

16) Clegg A.J., 'Studies of film flow on wetted wall columns' Ph.D Thesis, University of Surrey (1969)

17) Perciful, J.C., MSc Thesis, Rice University, Houston Texas

18) Wood, R.M., and Watts, B.E., 'The flow, heat and mass transfer characteristics of liquid films on rotating discs' Trans Act. Instn. Chem. Engineers., 51, 315 (1973)

19) Charwat, A.F., Kelley, R.E., and Gazley, C., 'The flow and stability of thin liquid films on a rotating disc' J. Fluid. Mech, 53 (2), 227-255, (1972)

20) Davies, J.T., and Warner, K.V., 'The effect of large scale roughness in promoting gas absorption' Chem. Eng. Sci., 24, 231 (1969)

21) Lim, S.T., Unpublished work

22) Higbie, R., 'The rate of absorption of a pure gas into a still liquid during short periods of exposure' A.1. Che. E. Trans, 31, 365 (1935)

23) The Underwater engineering group; economic planning department, London. 'The market for underwater power sources' Report UR5 (1973)

24) Jones, M.E.W., 'A feasibility study into the use of manned, large, one atmospheric underwater structures for subsea production of oil and gas' University of Glasgow, Dept. of Mechanical Engineering (1980)

25) Emslie, A.G., Bonner, F.T., and Peck, L.G., 'Flow of a viscous liquid on a rotating disc' J. Appl. Physics, 29, 858 (1958)

26) Clare, H., and Jeffs, R.A., 'Some measurements of the thickness of a fluid film on a spinning disc' Natural Gas Turbine Establishment, Draft report 12.12.60

27) Jones, G.C.A., 'Some mathematics relevant to the flow of a fluid film on a spinning disc' National Gas Turbine Establishment, Eng. report Note no. 40, June 196

28) Marshal, W.R., (Jnr), Adler, C.R., 'Performance of spinning disc atomisers Parts 1 and 2' Chem. Eng. Prog. 47, (10), 515 & 601 (1951)

29) Butuzov, A.I., and Rifert, V.G., 'Experimental investigation of heat transfer to evaporating liquid film on a rotating disc' Izv. Vug. Mashin., 2, 81 (1972) or B.L.L. RTS 9462

30) Hartley, D.E., and Murgatroyd, N., 'Criteria for break up of thin liquid layers flowing isothermally over solid surfaces' Int. J. Heat and Mass Transfer, 13, 1133 (1970)

31) Barberis, K., Private Communication

32) Raimondi, P., Toor, H.L., 'Interfacial resistance in gas absorption' A.1. Che. E. Journal, 5, 86 (1959)

33) Matsuyama, T., 'The rate of absorption of CO_2 in water' Mem. Fac. Engng. Kyoto Univ. 15 (1953)

34) Dankwerts, P.V., and Kennedy, A.M., 'Kinetics of liquid film processes in gas absorption' Trans. Inst. Chem. Eng. 32s, 54 (1954)

35) Tung, L.N., and Drickamer, H.G., 'Diffusion through an interface' J. Chem. Phys. 20, 6 (1962)

36) Schrage, R.W., 'A theoretical study of interphase mass transfer' Columbia Univ. Press, N.V. 75 (1953)

37) Kwanten, F.J.G., AND Huiskamp, J., 'Gas absorption towers part A' Gas purification processes for air pollution control, edited by Nonhebel, G., (1972)

38) Whitman, W.G., 'The two film theory of gas absorption' Chemical and Metallurgical Engineering, 29, 146 (1925)

39) Dankwerts, P.V., 'Significance of liquid film coefficients in gas absorption' Ind. Eng. Chem. 43, 1460 (1951)

40) Davies, J.T., 'Turbulence Phenomena' Chapter 4, Academic Press, New York (1972)

41) Beek, W.J., and Kramers, H., 'Mass transfer during single drop formation' A.1. Che. E. Journal, 12, 127 (1966)

42) Kishinervsky, M.K., and Damilav, A.V., Z. Prikl, Khim 22, 1173 (1949)

43) Dankwerts, P.V., and Sharma, M.M., 'The absorption of carbon dioxide into solutions of alkalis and amines (with some notes on hydrogen sulphide and carbonyl sulphide) Chemical Engineer, October, 244-279 (1966)

44) Thomas, W.J., and Adams, M.J., 'Measurments of diffusion coefficients of carbon dioxide and nitrous oxide in water and aqueous solutions of glycerol' Trans. Faraday. Soc., 61, 668 (1965)

45) Dankwerts, P.V., 'Gas liquid reactions' McGraw Hill (1970)

46) Shewood, T.K., and Pigford, R.L., 'Absorption and extraction' 2nd Edition pp 317-339 Mc Graw Hill (1952)

47) Hatta, S., Technical reports. Tohuku. Imp. Univ. 8, 1 (1928-29) and 10, 119 (1932)

48) Van Krevelen, D.W., and Hoftyyer, P.J., Rec. Trav. Chim. 67, 563 (1948)

49) Peaceman, D.W., 'LIquid-side resistance in gas absorption with and without chemical reaction' Sc.D. Thesis: Mass Inst. Technol. Cambridge, Massachusetts (1951)

50) Dankwerts, P.V., 'Absorption by simultaneous absorption and chemical reaction' Trans. Faraday Soc. 46, 300 (1950)

51) Perry, R.M., and Pigford, R.L., 'Simultaneous absorption and chemical reaction' Ind. Eng. Chem. 45, 1247 (1953)

52) Brian, P.L.T., Hurley, J.F., and Ha ssel Fini, E.H., 'Penetration theory for gas absorption accompanied by a second order chemical reaction' A.1. Che. E. Journal 7, 226 (1961)

53) Brian, P.L.T., 'Gas absorption accompanied by an irreversible reaction of general order' A.1. Che. E. Journal 10, 5 (1964)

54) Asarita, G., 'Mass transfer with chemical reaction' Elsevier, Amsterdam (1967)

55) Dankwerts, P.V., Kennedy, A.M., and Roberts, D., 'Kinetics of CO_L absorption in alkaline solutions Part 11: Absorption in a packed column and tests of surface renewal models' Chem. Engng. Sci. 18, 63 (1963)

56) Hikita, H., Asai, S., Ishikawa, H., and Honda, M., 'The kinetics of reactions of carbon dioxide with monoethanolamine, diethanolamine and triethanolamine by a rapid mixing method' Chem. Eng. Journal, 13, 7 (1977)

57) Babak, V.N., Babak, T.B., Kholpanov, L.P., Malyusov, V.A., and Zhavoronkov, N.M., 'Absorption complicated by an irreversible second-order chemical reaction in the liquid phase in short-time contact of a gas and liquid' Theo. Found. Chem. Engng. 15(2), 101-108 (1981)

58) Sada, E., Kumayawa, H., and Butt, M.A., 'Gas absorption with consecutive chemical reaction absorption of carbon dioxide into aqueous amine solutions' Canad. J. Chem. Eng. 54, 421 (1976)

59) Coldrey, P.W., and Harris, I.J., 'Kinetics of the liquid phase reaction between carbon dioxide and DEA' Canad. J. Chem. Eng. 54, 566 (1976)

60) Nunge, R.J., and Gill, W.N., 'Gas liquid kinetics: the absorption of carbon dioxide in DEA' Al. Che, E. Journal 9, 469 (1963)

61) Olander, D.R., 'Silultaneous mass transfer and equilibruim chemical reaction' A.1. Che. E. Journal 6, 233 (1960)

62) Van Krevelen, D.W., and Hoftyzer, P.J., 'Sur la solubilité des gay dans les solutions aqueous (the solubility of gasses in aqueous solution)'
from, Chimie et Industrie, Numero Speciale du xxl Congres International de Chimie Industrielle, Bruxelles, Sept (1948) p. 168

63) Long, F.A., and Mc.Devit, W.F., 'Activity coefficients of non-electrolyte solutes in aqueous salt solutions' Chem. Rev., 51, 119 (1952)

64) Kothari, P.J., and Sharma, M.M., 'Kinetics of reaction between CS_2 and amines' Chem. Engng. Sci. 21, 391 (1966)

65) Thomas, W.J., and Furyer, I.A., 'Diffusion measurements in liquids by the Guoy method' Chem. Engng. Sci. 17, 115 (1962)

66) Sharma, M.M., 'Kinetics of reaction of carbonyl sulphide and carbon dioxide with amines and catalysis with Bronsted bases of hydrolysis of COS' Trans. Faraday Soc. 61, 681 (1965)

67) Jensen, M.B., Jorgensen, F., and Faurholt, C., 'Reactions between CO_2 and amino alchols - I. Monethanolamine and Diethanolamine' Acta. Chem. Scand. 8, 1137 (1954)

68) Sharma, M.M., 'Kinetics of gas absorption' Ph.D. Thesis 1964, University of Cambridge

69) McNeil, K.M., 'Kinetics of gas absorption - the effect of catalysis on rates of absorption of carbon dioxide into aqueous amine and amine-potash solutions' Ph.D. Thesis, University of Cambridge (1965)

70) Mason, J.W. and Dodge, B.F., 'Equilibruim absorption of carbon dioxide by solutions of the ethanolamines' Trans. Am. Inst. Chem. Eng. 32, 27-48 (1936)

71) Reed, R.M., and Wood, W.R., 'Recent design developments in amine gas purification plants' Trans. Am. Inst. Chem. Eng. 37, 363 (1941)

72) Lee, J.I., Otto, F.D., amd Mather, A.E., J. of Chem. Eng. Data 17(4), 465-468 (1972)

73) Jeffrey, P.G., and Kipping, P.J., 'Determination of CO_2 and N_2O in solutions of MEA' Analyst 87, 594-95 (1962)

74) Jones et al J. of Chem. Eng. Data 4 (1), 85 (1959)

75) Strohecker, R., Vom Wasser 12, 128-34 (1937)

76) Papp, S., Zeitschnift fur Analytische Chemie 125, 349-69 (1943) [Chemical Abstracts 37. 48376]

77) Papp, S., Zeitshrift fur Analytische Chemie (27, 167-73 (1944)

78) Legler, C., Wasserwirt-Wassertech 18, 187-90 (1968) [Chemical Abstracts 69: 89627e]

79) Weisgerber, P., and Kosfield, E.G., Mrt. Ver. Grosskessel-besitzer 72, 176-80 (1961) [Chemical Abstracts 56: 2288g]

80) Hammerton, D., and Garner, F.H., 'Determination of CO_2 in water' Trans. I.Chem.E. 32, S18 (1954)

81) Rogers, D.E., 'Determination of carbon dioxide and aggr-essive carbon dioxide in water' N.Z.J.Sci. 16(4), 875-93 (1973)

82) Clarke, F.E., Analytical Chemistry 19, 889-91 (1947)

83) American Society for testing and materials (1971) ASTM Standard D513-71 [also 1969: D513-697 and 1971: D1293-65]

84) British Standards BS 2690: Part 5: 1967

85) Midgley, D., 'Investigations into the use of gas-sensing membrane electrodes for the determination of carbon dioxide in power station waters' Analyst 100, 386 (1975)

86) Gaunt, H., and Shanks, C., Chem. and Ind. Apr. 18, 651 (1964)

87) Warner, K.V., 'Gas absorption into water flowing over slotted and smooth plates' Ph.D. Thesis, University of Bradford (1967)

88) Park, K., Kennedy, G.H., and Dobson, H.H., 'Comparison of a gas chromatographic method and pH/alkalinity method for determination of total carbon dioxide in water' Anal. Chem, 36, 1686 (1964)

89) Swinnerton, J.W., Linnenborm, V.J., and Check, C.H., Anal. Chem. 34, 483 (1962)

90) Harvey, Determination of the carbon dioxide content of sea water' Anal. Chem. 37, 274 (1965)

91) Farrow, M.K.A., 'A simple non-graviometric method for the determination of CO_2' J. Sedinent. Petrol. 47(2), 551-3 (1977)

92) Wall, K.H., 'The variation of pH in a solution saturated with calcium carbonate' Analyst, 91, 795 (1965)

93) Severinghaw, J.W., 'Measurements of blood gases: PO_2 and PCO_2' Ann. N.Y. Acad. Sci., 148, 115 (1968)

94) Bailey, P.L., and Riley, M., 'Performance characteristics of gas sensing membrane probes' Analyst, 100, 145 (1975)

95) Swanson, B., Private Communication

96) Journier, J., and Philbert, A., 'Equations of the absorption of CO_2 by three ethanolamines' Compt. Rend. 260 (9), 2521-2 (1965)

97) Scott, 'Standard methods of chemical analysis'
5th ed. Vol.1 p235-7, Van Nostrand, N.Y. (1939)
6th ed. vol.1 p298, Van Nostrand, N.Y. (1962)

98) Layan, F., and Lelong, B., 'Apparatus and method for determining alkanolamine combined H_2S or SO_2' Fr. Demande 2,142,412, Jun 1971

99) Carmasi et al 'Determining acid gases combined with basic solutions' Fr. Demande 2,142,573 March 1973

100) Koci and Jelink 'Determination of the amount of SO_2 and CO_2 absorbed in MEA solutions' Czech 138,106 September 1970

101) Dow Chemical Company of Canada 'Gas conditioning fact book' 2nd edition, 1962

102) Pearce, R.L., Grosso, S., and Cringle, D.C., 'Amine gas treating solution analysis : a tool in problem solving' Proc. 59th annual conven. gas processors assoc. page 150-162

103) Kohl, A., and Risenfeld, F., 'Gas purification' Gulf publishing company, 3rd edition 1979

104) Cryder, D.S., and Maloney, J.O., 'The rate of absorption of carbon dioxide in diethanolamine solutions' Trans. Am. Inst. Chem, Eng. 37, 827-852 (1941)

105) Kovalenk, S.A., et al 'Effect of various factors on the pH of aqueous solutions of ethanolamines' Uzb, Khim. Zh 13(4), 44-46 (1969) [Abstract : 72 104594]

106) Volodin, N.I., Paskov, V.P., et al 'Preparation of a polynomial description and nomogram for determining the pH value of carbonated solutions' Zh. Prikl. Khim (Leningrad) 48(2), 435-437 (1975) [abstract : 83 21592]

107) Crank, J., and Nicholson, P., Proc. Cambridge Phil. Soc. 43, 50 (1947)

108) Douglas, J., Jr. Trans. Am. Math. Soc. 89, 484 (1958)

109) Hofmeyer, B.G., Schotten, H.G., and Lloyd, W.G., 'Contamination and corrosion in monoethanolamine gas treating solutions' Paper presented at National meeting of American Chemical Society Dallas, Texas (April 8-13) 1956

110) Lloyd, W.G., and Taylor, Ind. Eng. Chem, 46 (Nov), 2407-2415 (1954)

111) Frazier, H.D., and Kohl, A.L., Ind. Eng. Chem. 42 (Nov), 2282-2292 (1950)

112) Kaplan, L.G., 'Cost-saving process recovers carbon dioxide from power-plant fluegas' Chem. Engng. November 29 215-16 (1984)

113) St. Clair, J.H., and Simister, W.F., 'Process to recover carbon dioxide from flue gas gets first large scal tryout in Texas' Oil and Gas Journal 81(7), 109-113 (1983)

114) Ballard, D., 'How to operate an amine plant' Hydrocarbon Processing 45(4), 137-144 (1966)

115) Polderman, L.D., and Steele, A.B., 'Why diethanolamine breaks down' The Oil and Gas Journal, 206, July 30 (1956)

116) Hikita, H., Asai, S., Ishikaura, H., and Uku, K., 'Absorption of carbon dioxide into aqueous diethanolamine solutions' Chem. Eng. Commun. 5, 315-22 (1980)

117) Dankwerts, P.V., 'The reaction of CO_2 with ethanolamines' Chem. Engng. Sci. 34, 443-446 (1979)

118) Kennard, M.L., and Melsen, A., 'Mechanisms and Kinetics of diethanolamine degradation' Ind. Eng. Chem. Fundam, 24, 129-140 (1985)

APPENDIX A: PRELIMINARY EXPERIMENTS

A1: Batch Regeneration Experiments

A small scale batch regeneration system was constructed to allow a series of preliminary experiments to be undertaken. The aim of these was to study the effect that regeneration had on a number of solution properties. It was hoped that the results would provide useful information for both the design of the regeneration system and the analysis of solution acid-gas content. More specifically the investigation was planned so as to obtain a series of samples which could be analyzed for:-

i) amine strength: carried out by titration as discussed in section 6.4
ii) CO_2 content (in the form of carbonate ion): using the physical method outlined in Appendix B.
iii) pH: by use of a 'Beckman' combination electrode and meter.

the results of these analysis could then be used to determine whether:

i) a correlation of pH against mol%CO_2 would be a useful method for taking on-line measurements of the solution acid gas loading.
or ii) by regenerating DEA in this fashion whether the solution was degenerated to any extent.

The equipment constructed for these experiments is illustrated in figure A1. A round bottomed flask was used as the reboiler, heat being provided by an electric heating mantle rated 300W. This was lagged to minimise heat losses. The reboiler flask was provided with three openings as shown. Both side arms were 3/4" diameter while the centre port was 1.1/2" diameter. One side arm was used as a sampling port and was stoppered while the experiments were underway. Samples were withdrawn by a syphoning effect through capillary tubing. The second side arm was used to return liquid condensed in the overhead cooler to the reboiler flask. The central opening led to a 2" diameter packed column filled with 1/8" rasching rings. The packed bed had a depth of 20". The vapour (steam/carbon dioxide) formed in the reboiler passed up through the packed bed and was condensed in a Leibig condensor. The carbon dioxide evolved was vented through a port in the reflux vessel.

A solution of known diethanolamine concentration was carbonated by bubbling pure carbon dioxide through it. The gas used was pre saturated with aqueous DEA by forcing it to pass through a vessel filled with a solution of the same concentration. The pH of this solution was recorded at a standard temperature. The acid gas loading of the sample was calculated from the change in weight of the absorption flask, and double-checked using the physical method discussed in Appendix B.

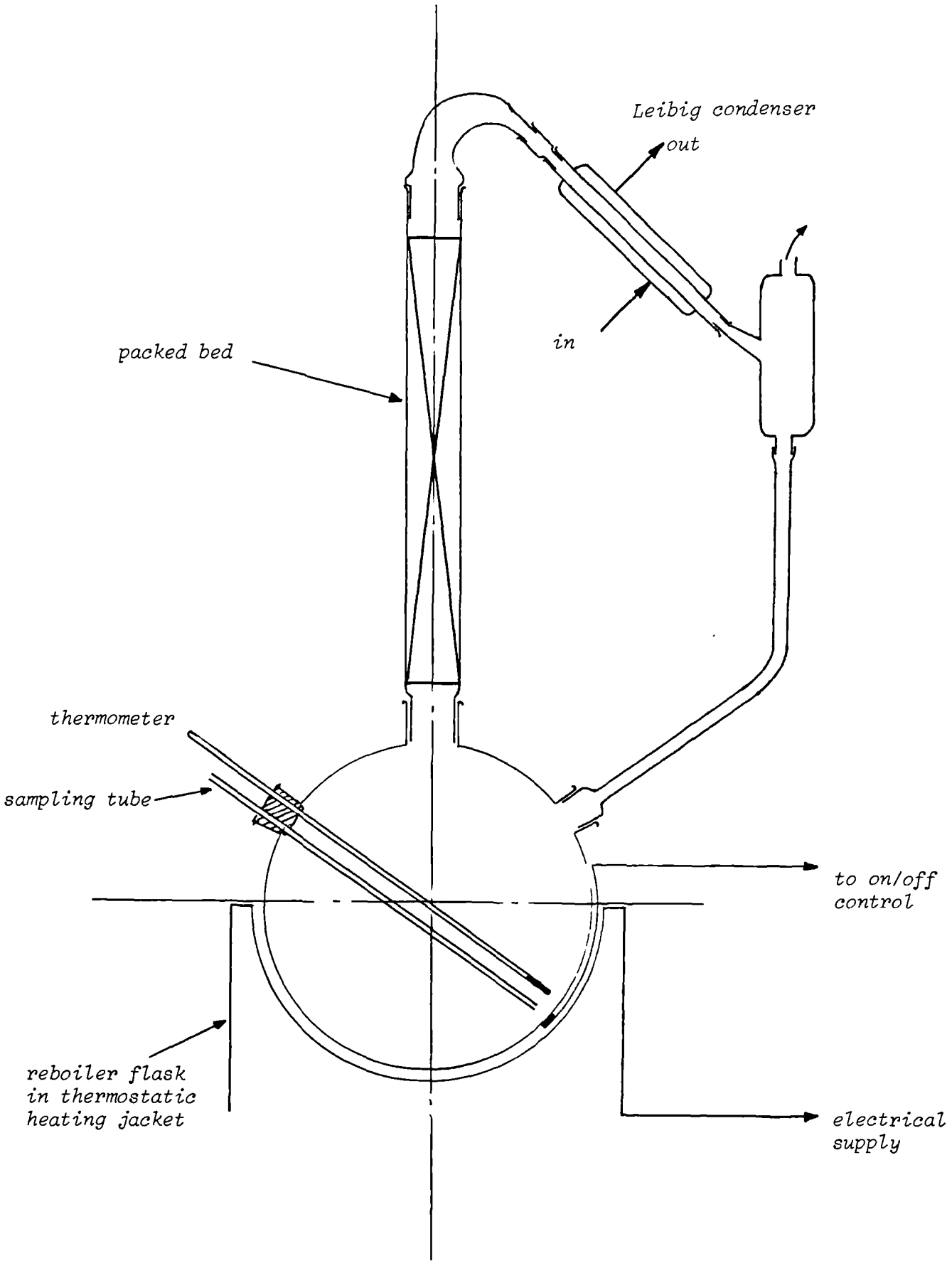

figure A1, Apparatus for preliminary investigation

The carbonated solution was placed in the heating flask of the small scale rig and brought to boil. Samples were taken periodically and storred in stoppered glas containers until they could be analysed. Boiling was maintained for 2 hours. Analysis of the samples indicated that total regeneration had been attained fairly rapidly (in approximately half an hour). By this time the solution pH had attained approximately the same value as that of an un-carbonated specimen. Analysis of the samples taken after this time showed that although the solution remained basically uncarbonated the pH decreased marginally. Determination of the diethanolamine concentration indicated that this decrease in pH was associated with a corresponding decrease in DEA concentration.

These results indicated that a degree of solution degradation had occurred. As high temperatures were known to cause thermal decomposition the wall temperature of the heating flask was monitored using a copper/constantan thermocouple. With the heating mantle at full power (300W) this was measured at 350°C. It has been demonstrated previously that surface temperatures in excess of approximately 150°C can cause some significant degradation and thus, at 350°C the degree of degradation would be severe. To study further the effect of thermal degradation the de-carbonated solution was continuously re-boiled for a further 19 hours. At the end of this time the solution was discoloured significantly more viscous and had a distinct, pungent odour. Each of these characteristics can be attributed to the formation of high molecular weight species (a result of thermal degradation).

To limit the degree of degradation in further experiments the current to the heating mantle was controlled by the vessel surface temperature so that it could not exceed 150°C. The experiment described above was thus repeated, the solution again being constantly reboiled for 19 hours. At the end of this period, although slight discolouration had occurred, the solution viscosity did not appear to have increased significantly and no odour could be detected. It was thus concluded that thermal degradation had been avoided. It is possible that the discolouration observed could have been an effect of oxidation as no precautions were taken to keep oxygen out of the system.

A series of regeneration runs was then carried out to investigate further the relationship between pH and acid gas loading. As shown previously, virtually total regeneration could be achieved and this could be demonstrated by the measurable rise in pH. However when the same solution was once more carbonated and regenerated the pH corresponding to a CO_2 free solution was marginally reduced. With each successive carbonation and regeneration a further small decrease was noted. Thus although the surface temperature was limited some degradation of the amine was occurring. Measurement of the DEA concentration confirmed this conclusion.

It can thus be concluded that the measurement of solution pH can be utilised to provide an indication of the acid gas loading of a sample of diethanolamine. However in order that an accurate value is obtained a calibration must be completed after each regeneration. Since the calibration curve linking solution pH and carbonation ratio is not linear a number of solutions must be analysed to provide the required data. As the physical method for

determination of acid gas loading is particularly slow this calibration procedure would be rather inconvenient. For this reason an analysis technique based upon the use of chromatography was prefered (see section 6).

Although the pH analysis method was not finally adopted in the mass transfer experiments, this set of preliminary observations provided useful information regarding the phenomenom of solution degradation. Such data was used when designing the solution regeneration system.

A2: Corrosion Tests

Since both copper and brass had been used in sections of the regeneration system, it was decided that the susceptibility of these materials to aqueous solutions of deithanolamine (with and without dissolved carbon dioxide) should be investigated. Because the data available in the literature, regarding such systems was limited and rather inconclusive in its results, it was decided that the corrosion rate under a number of conditions should be measured. A series of simple tests was thus set up. The conditions to be investigated were:-

i) Ambient temperature (carbon dioxide free solutions)
ii) Ambient temperature (with a fully loaded solution)
iii) At an elevated temperature (approximately 110°C) (no carbon dioxide)
iv) At an elevated temperature (approximately 110°C) (with a fully loaded solution)

Each of these tests is discussed below.

a) ambient temperature measurements

The corrosion rate at ambient temperature was measured by calculating the weight loss of a small sample of material which was suspended in the relevant solution. The solution was slowly circulated by the use of a magnetic stirrer. Six samples of each material were analysed, three in carbon dioxide free solutions (of diethanolamine concentrations 1M, 2M and 3M) and three in fully loaded solutions (of the same strengths). Each sample consisted of a 20mm square sheet of the relevant material the brass being 1.66mm thick and the copper 3.0mm. The duration of the test was 934ksecs.

Table A1 presents the results of these experiments in terms of mm lost/year of immersion. This would thus allow a corrosion allowance to be incorporated in the design of an operational piece of equipment.

The results show that the rate of corrosion for each solution concentration is greatest when no carbon dioxide is present. Furthermore the rate of corrosion increases with increasing solution concentration. This would indicate that the species which is responsible for the corrosion phenomenom is the ethanolamine ion (i.e. when CO_2 is dissolved in solution it reacts with the anion forming the carbamate and thus effectively reduces the corrosivity of the solution). The copper samples showed less resistance to corrosion than did the brass samples. This would indicate that only the copper ions in the brass alloy are subject to the corrosion reaction.

b) elevated temperature measurements

The rig previously employed in the preliminary batch regeneration experiments was used to measure the corrosion rates at temperatures similar to those experienced in the reboiler. In each of the two experiments undertaken samples of brass and copper were suspended above and below the surface of the aqueous diethanolamine solution located in the glass boiling flask. The solution was then

brought to the boil using the controlled temperature method previously discussed. In the first series of experiments carbon dioxide was continuously bubbled through the boiling solution via a glass tube passing through the sample point. This modelled a system where free carbon dioxide was present. In the second experiment a carbon dioxide free solution was employed. In each case the diethanolamine solution concentration was 2 Molar and the duration of the test was one hour. Table A.2 presents the results and the calculated corrosion rates in mm/year.

Comparing the results at the elevated temperature with those at ambient it can be seen that the calculated corrosion rates in all cases were higher. This is particularly true for the carbonated solutions where, for example with a submerged brass sampled, the corrosion rate increased by a factor of 100. For a similar sample in an uncarbonated solution the corrosion rate increased by approximately 2·5 times. It is thought that these large increases in corrosion rates for carbonated solutions is a result of the carbon dioxide being free (rather than being combined in solution) and thus capable of causing corrosion itself. These results thus indicate the importance of insuring that all carbon dioxide is removed from the DEA before the solution enters the reboiler, whilst it is perculating down through the packing. Operation of the regeneration system constructed for the present investigation was thus designed to avoid carbonated solutions being treated in the brass reboiler vessel. Additionally, because the results indicated that the rate of corrosion was significantly lower, below rather than above the surface of an uncarbonated solution the level in the reboiler was controlled so that the copper heating coils were never exposed.

TABLE A.1

Material: Brass

Sample no.	DEA Concentration	Dissolved CO_2	Initial Weight	Final Weight	mm/ Year
A	3M	yes	5.6278	5.6234	0.022
B	3M	no	5.6804	5.6448	0.178
C	2M	yes	5.6370	5.6340	0.015
D	2M	no	5.6145	5.5935	0.106
E	1M	yes	5.5761	5.5749	0.006
F	1M	no	5.5675	5.5537	0.070

Material: Copper

Sample no.	DEA Concentration	Dissolved CO_2	Initial Weight	Final Weight	mm/ Year
G	3M	yes	10.7670	10.7604	0.033
H	3M	no	10.8922	10.8466	0.226
I	2M	yes	10.6757	10.6719	0.019
J	2M	no	10.6442	10.6238	0.101
K	1M	yes	10.4825	10.4795	0.003
L	1M	no	10.7928	10.7754	0.086

TABLE A.2

Sample: 2M DEA fully loaded with CO_2

Material	Position	Initial Weight	Weight at End of Test	mm/ Year
Copper	Suspended	10.7004	10.6984	2.567
Copper	Submerged	10.7494	10.7472	2.826
Brass	Suspended	5.6636	5.6626	1.284
Brass	Submerged	5.5932	5.5919	1.670

Sample: 2M DEA non carbonated

Material	Position	Initial Weight	Weight at End of Test	mm/ Year
Copper	Suspended	10.6978	10.6969	1.156
Copper	Submerged	10.7461	10.7459	0.257
Brass	Suspended	5.6616	5.6609	0.932
Brass	Submerged	5.5914	5.5912	0.266

Appendix B: A PHYSICAL METHOD FOR DETERMINING THE CARBON DIOXIDE CONCENTRATION OF A SAMPLE OF DIETHANOLAMINE

This method was based upon a standard analytical technique for determination of carbon dioxide in limestone, dolomite, magnesite, strontianite, witherite, spathic iron ore, carbonates of sodium and potassium and bicarbonates in baking powder. The procedure utilised is based upon the evolution of carbon dioxide from a sample of known size (mass or volume) by addition of a less volatile acid. The carbon dioxide so evolved is absorbed in soda lime and the change in weight measured.

The apparatus used for this determination was a modified 'Knorr' alkalimeter. This is illustrated in figure B1 below.

The following procedure was used to analyse a given sample. A water aspirator was attached to the outlet of tube H and air pulled through the apparatus for approximately 10 minutes. The absorption vessel (G) was then weighed and this value recorded. Once the absorption vessel had been re-attached the water supply to the condensor (D) was switched on. A sample of known weight (approximately 50g) was then introduced into the dry alkalimeter (vessel C) and, with the stopcock 'B' closed 50ml of dilute sulphurine was placed in the acid funnel (B). The acid was then allowed to run slowly down on the sample at a rate which did not evolve the gas so rapidly that it could not be absorbed in 'G'. Between 1 and 2 ml of acid were retained in the funnel to act as a seal and the stopcock was then closed.

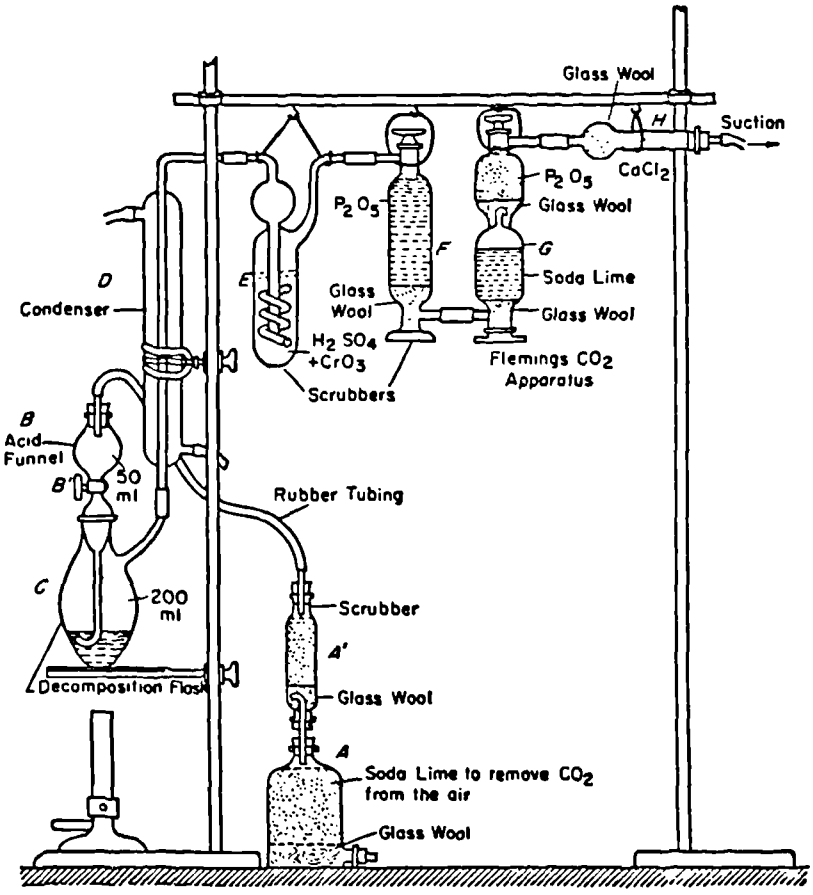

When violent action had ceased the solution was heated (by an indirect flame) to boiling and maintained there for approximately three minutes. An indirect flame was used to protect the organic sample from excess heating which could have caused charring and/or solution degradation (i.e. irreversible reaction of diethanolamine and carbon dioxide molecules (see section 3)). Gentle suction was then applied to the absorption end of the apparatus and at the same time stopcock B' opened. This allowed the rest of the acid to flow into the alkalimeter flask and produced a through current of air, purified (i.e. dried and removed of all CO_2) by the contents of flasks A and A'. This suction was gentle at first and then was gradually increased. Air was drawn through the train for 20 minutes to force all of the evolved carbon dioxide into the absorption vessel.

The vacuum pump was then stopped and the absorption tube detached and weighed. The difference between this measurement and the original weight was thus equal to the amount of carbon dioxide in the sample analysed. Knowing the concentration of DEA in the original sample (see section 6.4). The acid gas loading (mols CO_2/mol DEA) could thus be calculated.

The accuracy of this analytical equipment was checked by analysing a series of specially prepared samples of known carbon dioxide content. The measured acid gas loading using the procedure outlined above was, in all cases, within 3% of the actual value. The accuracy of this physical method was thus demonstrated.

Appendix C: CALCULATION OF THE SIZE OF A SCRUBBER REQUIRED FOR A NITRO-DIESEL ENGINE OF SPECIFIED DUTY

a) Introduction

In this section the required size of scrubber to remove carbon dioxide at a specified rate from a gas stream of particular composition is calculated. The results are then discussed.

Typical conditions of the inlet and outlet gas streams were specified by the Marine Engineering Department as:-

inlet gas pressure		2 atm
inlet gas flowrate		2 kg/min
inlet gas composition (on dry basis)	O_2	8 wt%
	N_2	68 wt%
	CO_2	24 wt%
rate of CO_2 removal		0.3 kg/min

Thus the partial pressure of carbon dioxide at the inlet and outlet can be calculated i.e.,

inlet partial pressure	0.338 atm
outlet partial pressure	0.142 atm

The size of absorber required to perform a specified duty is a function of a number of parameters of the system. These have been fixed in the following calculations as,

type of discs		coarse mesh
inner radius of disc		10 cm
outer radius of disc		40 cm
rotational speed		1500 RPM
flowrate/disc		200 cm^3/sec
liquid temperature	water	@ 15°C
		@ 1°C
	DEA	@ 20°C

Thus the physical mass transfer coefficient representing this particular system can be extracted from the results of the experimental investigation. At 20°C figure 8.9 indicates that the mass transfer process is represented by an overall mass transfer coefficient of 0.2330 cm/sec. This can be altered to allow for temperature dependance by the method previously outlined. Thus at 15°C the system mass transfer coefficient will be approximately 0.2114 cm/sec and at 1°C, approximately 0.1695 cm/sec.

For the proposed system, the mass transfer area per disc is 1178 cm^2. However as the liquid phase is exposed to the gas phase below, as well as above the surface of each disc this will be enhanced. The minimum amount of extra surface area available is equal to the size of the perforations. This assumes that the liquid film remains entirely on the surface of the disc. The mass transfer area is thus increased by 49% i.e. the active area per disc is 1755 cm^2. If, however, the liquid film is dispersed through

the mesh so that it exists equally on both sides of the plate the active area will be doubled, i.e. the area per disc = 2356cm². The number of discs required to provide the specified duty can thus be calculated for each of these figures. The actual value will therefore be somewhere in between.

b) Determination of absorber size for water at 15°C

The rate of mass transfer in the rotary absorber can be expressed as;-

$$N = V.C_b^\circ = k_{Lphys}.A.\Delta C \qquad C.1$$

Where C is the concentration driving force. To simplify the calculation an arithmetic mean driving force was used in place of a logarithmic mean. This can be shown to add an additional error to the calculation of approximately 2.0%. Thus C.1 can be rewritten as:-

$$k_{Lphys}.A.\left(\frac{C_i^i + C_i^\circ - C_b^\circ}{2}\right) = V.C_b^\circ \qquad C.2$$

and thus re-arranging

$$C_b^\circ = \frac{k_{Lphys}.A\ (C_i^i + C_i^\circ)}{2V + k_{Lphys}\ A} \qquad C.3$$

therefore the outlet liquid concentration can be calculated and from this the rate of mass transfer per plate. The number of plates required is then equal to the specified overall rate of mass transfer divided by the rate of mass transfer per plate.

At 15°C and with inlet and outlet gas streams as specified above, the interfacial concentration at the inlet of the machine (C_i^i)is 6.76 c 10^{-4}g/cm³ and at the outlet (C_i°) is 2.84 x 10^{-4} g/cm³.

Thus the rate of mass transfer per plate is between 0.092 and 0.106 g/sec and therefore between 55 and 47 of the specified plates are required. The total liquid through-put of the device would therefore be in the order of 37 m³/hr.

c) Determination of absorber size for water at 1°C

For water at 1°C the interfacial concentration of carbon dioxide at the inlet of the machine would be 1.08 x 10^{-3} g/cm³ and at the outlet, 4.53 x 10^{-4} g/cm³. Thus using equation C.3 the calculated rate of mass transfer per disc would be in the range 0.131 to 0.153 g/sec. Therefore between 39 and 33 of the specified plates would be required to give the requisite performance. A machine of this size would require a total liquid through-put of approximately 26 m³/hr.

This analysis indicates that as the inlet liquid temperature is decreased the number of plates required to perform a specified duty is also decreased. This is because the system mass transfer coefficient decreases approximately as a function of the

square root of temperature while the interfacial concentration is almost inversely proportional to the temperature.

d) Determination of absorber size for a 2M solution of DEA at 20°C

If it is assumed that the average degree of carbonation over the surface of each plate (i.e. α) is 0.2 then using the data outlined in section 5.4, the ratio H water/H DEA can be shown, at 20°C, to be 0.968. Thus the physical solubility of carbon dioxide in a 2M solution of DEA is 96.8% that for water. The interfacial concentration can be calculated at the inlet and outlet, using the CO_2 partial pressures specified above, i.e.,

$$C_i^i = 5.61 \times 10^{-4} \text{ g/cm}^3$$

$$C_i^\circ = 2.36 \times 10^{-4} \text{ g/cm}^3$$

Therefore using the chemical acceleration factor determined during the experimental investigation (i.e. $\phi_m = 3.4$ at 200 cm^3/sec and 1500 RPM) the rate of absorption per plate can be calculated from:-

$$\text{Rate per plate} = k_{L\text{phys}} \cdot \phi_m \cdot A. \left(\frac{C_i^i + C_i^\circ}{2}\right) \qquad C.4$$

Thus, using the two limits of area outlined above, the rate of mass transfer per plate lies between 0.554 and 0.744 g/sec. Therefore to remove carbon dioxide at the specified rate between 6 and 10 plates are required. At this rate of absorption and a flowrate of 200 cm^3/sec the outlet carbonation ratio rises by between 0.04 and 0.05 (mol/mol) per circulation. Thus the estimated average value of α, (i.e. 0.2) is too high (assuming the solution is completely stripped between each circulation), and so the rate of mass transfer due to a machine of this size would be higher than calculated.

No work has been undertaken to determine how easy it is to strip carbon dioxide from a solution of DEA in a rotary system. Therefore it is impossible to calculate either how many extra 'regeneration' plates would be required or to what extent the carbonation ratio could be reduced per pass. Obviously the degree of extra miniturisation available by using DEA rather than water as the solvent is largely dependent on this factor. Further work must be undertaken to quantify this unknown.

e) Conclusions/Recommendations

Even though it is impossible to quantify the exact size of machine necessary to perform the required duty when using DEA as the solvent, a number of relevant conclusions can be drawn. By employing a chemical solvent in the place of a liquid phase which absorbs physically, the number of plates required to perform a specified absorption duty is reduced. However considering the extra complexity introduced it is felt that this reduction must be of considerable magnitude to make a chemical system the most attractive (i.e. smallest) alternative.

In a system employing a chemical solvent, facility has to be made to regenerate the loaded solution. This can take place in two ways. If the solution is at an elevated pressure it can be flashed removing a certain fraction of the absorbed gas (i.e. equilibrium is moved to the left at lower pressures). This technique is employed in industry with potash solutions where inlet pressures are of the order of 20 bar. Alternatively the solution is boiled and stripped using steam generated in the reboiler of the regeneration system. Normally this technique is used in amine systems. Diethanolamine is easily stripped of carbon dioxide and almost pure solutions can be obtained. Obviously when using this technique, heat has to be supplied to the loaded solution in order to raise its temperature to the boiling point. In industry this is completed in two stages. The feed to the regeneration column is raised to approximately 75°C by passing it through a heat exchanger using liquid leaving the reboiler as the heating medium. The remainder of the necessary energy is supplied by steam heating in the reboiler vessel. To adapt this scheme for use in a rotary system would necessitate the gas stripper being constructed in three sections; an absorber containing approximately 10 plates, a centrifugal heat exchanger, and a reboiled centrifugal stripping unit equipped with an unknown number of plates. Heat could be supplied to the reboiler section of the stripping unit by the hot exhaust gasses (which need to be cooled before entering the absorption chamber). A considerable amount of work has already been published concerning thin-film centrifugal heat exchange units, and thus the design of this section should not pose too many difficulties. However before the stripping section could be engineered, research would be required to investigate the feasibility/practicality of adopting this type of process to centrifugal technology.

Although exact details of the form of a chemical stripper cannot be outlined here, the above discussion indicates that such an item would be far more complex than a machine employing a physical solvent. Therefore to be of benefit such a system would have to provide extensive miniturisation of the absorption vessel. The calculations presented above indicate that, by replacing water with a 2M aqueous solution of diethanolamine, approximately 50 less plates are required for a nitro diesel engine of the specified size. This decrease is considerably reduced if low temperature water is employed (as would be possible in an undersea environment). In a practical multiplated machine it may be possible to employ 1mm thick plates with a plate/plate seperation of just 1mm. Thus 50 plates would only occupy a depth of 100mm. It thus appears that the extra equipment required to regenerate a chemical solvent would occupy more space than is saved. In addition, when using a chemical solvent, a certain volume of tankage would be required and extra expense would be encountered as degenerated solution would have to be either regularly regenerated or replaced.

Thus overall the results of this investigation have indicated that the most practical machine would be one in which sea water (at a low temperature) was employed as the liquid phase. However, this is not to say that if a more suitable chemical solvent than DEA could be located (i.e. one that undergoes a much faster reaction with carbon dioxide and is less susceptable to degradation, especially that due to irreversible reaction with oxygen), further miniturization could not be achieved. The proprietry amine

'Gas Spec FS-IL' may thus hold the key for further development in this field. Further experimental investigations similar to those outlined in section 9 using this material are thus recommended.

APPENDIX D

DATA FOR THE EXPERIMENTAL INVESTIGATIONS EMPLOYING CARBON DIOXIDE AND WATER

TABLE D.1

DISC SURFACE: COARSE_MESH DISC POSITION: FIXED
SURFACE INCLINATION: VERTICAL

SPEED (RPM)	FLOWRATE (cm^3/sec)	TEMP (°C)	$p.CO_2$ (atm)	kL20 (cm/sec)
500	50.0	15.5	1.0	0.0320
500	66.7	15.5	1.0	0.0430
500	83.3	15.5	1.0	0.0543
500	100.0	15.8	1.0	0.0633
750	50.0	15.8	1.0	0.0345
750	66.7	16.0	1.0	0.0518
750	83.3	15.3	1.0	0.0691
750	100.0	15.5	1.0	0.0876
1000	50.0	15.3	1.0	0.0323
1000	66.7	15.8	1.0	0.0515
1000	83.3	15.5	1.0	0.0718
1000	100.0	15.5	1.0	0.0976
1250	50.0	16.0	1.0	0.0318
1250	66.7	16.0	1.0	0.0504
1250	83.3	13.6	1.0	0.0730
1250	100.0	13.1	1.0	0.0964
1500	50.0	13.3	1.0	0.0295
1500	66.7	13.8	1.0	0.0470
1500	83.3	13.8	1.0	0.0679
1500	100.0	13.8	1.0	0.0930

TABLE D.2

DISC SURFACE: FINE_MESH DISC POSITION: FIXED
SURFACE INCLINATION: VERTICAL

SPEED (RPM)	FLOWRATE (cm^3/sec)	TEMP (°C)	$p.CO_2$ (atm)	kL20 (cm/sec)
500	50.0	23.0	1.0	0.0408
500	66.7	22.7	1.0	0.0549
500	83.3	21.0	1.0	0.0664
500	100.0	21.2	1.0	0.0721
750	50.0	21.0	1.0	0.0446
750	66.7	21.2	1.0	0.0644
750	83.3	19.7	1.0	0.0832
750	100.0	20.0	1.0	0.1041
1000	50.0	20.2	1.0	0.0377
1000	66.7	20.2	1.0	0.0584
1000	83.3	20.2	1.0	0.0767
1000	100.0	17.0	1.0	0.0939
1250	50.0	17.8	1.0	0.0316
1250	66.7	17.5	1.0	0.0459
1250	83.3	16.0	1.0	0.0654
1250	100.0	16.0	1.0	0.0886
1500	50.0	16.0	1.0	0.0247
1500	66.7	16.3	1.0	0.0406
1500	83.3	16.3	1.0	0.0593
1500	100.0	16.5	1.0	0.0806

TABLE D.3

DISC SURFACE: SMOOTH DISC POSITION: FIXED
SURFACE INCLINATION: VERTICAL

SPEED (RPM)	FLOWRATE (cm^3/sec)	TEMP (°C)	$p.CO_2$ (atm)	kL20 (cm/sec)
500	50.0	16.3	1.0	0.0218
500	66.7	16.3	1.0	0.0275
500	83.3	16.0	1.0	0.0307
500	100.0	16.0	1.0	0.0326
750	50.0	16.3	1.0	0.0238
750	66.7	14.3	1.0	0.0312
750	83.3	14.1	1.0	0.0374
750	100.0	14.1	1.0	0.0426
1000	50.0	14.3	1.0	0.0227
1000	66.7	14.3	1.0	0.0312
1000	83.3	14.3	1.0	0.0392
1000	100.0	14.3	1.0	0.0466
1250	50.0	14.6	1.0	0.0214
1250	66.7	13.3	1.0	0.0293
1250	83.3	13.1	1.0	0.0370
1250	100.0	13.3	1.0	0.0455
1500	50.0	13.3	1.0	0.0195
1500	66.7	13.6	1.0	0.0277
1500	83.3	13.6	1.0	0.0362
1500	100.0	13.8	1.0	0.0463

TABLE D.4

DISC SURFACE: PERFORATED_PLATE DISC POSITION: FIXED
SURFACE INCLINATION: VERTICAL

SPEED (RPM)	FLOWRATE (cm^3/sec)	TEMP (°C)	$p.CO_2$ (atm)	kL20 (cm/sec)
500	50.0	12.4	1.0	0.0386
500	66.7	12.4	1.0	0.0550
500	83.3	12.6	1.0	0.0695
500	100.0	12.4	1.0	0.0788
750	50.0	11.2	1.0	0.0410
750	66.7	11.0	1.0	0.0620
750	83.3	11.2	1.0	0.0845
750	100.0	11.2	1.0	0.1059
1000	50.0	11.5	1.0	0.0402
1000	66.7	11.7	1.0	0.0624
1000	83.3	11.7	1.0	0.0869
1000	100.0	11.0	1.0	0.1120
1250	50.0	11.0	1.0	0.0370
1250	66.7	11.5	1.0	0.0814
1250	83.3	11.5	1.0	0.0814
1250	100.0	11.2	1.0	0.1071
1500	50.0	12.0	1.0	0.0327
1500	66.7	12.4	1.0	0.0514
1500	83.3	12.6	1.0	0.0732
1500	100.0	11.0	1.0	0.0965

TABLE D.5

DISC SURFACE: COARSE_MESH DISC POSITION: SUSPENDED
SURFACE INCLINATION: VERTICAL

SPEED (RPM)	FLOWRATE (cm^3/sec)	TEMP (°C)	p.CO_2 (atm)	kL20 (cm/sec)
500	50.0	10.4	0.5	0.0541
500	66.7	10.4	0.5	0.0718
500	83.3	10.4	0.5	0.0858
500	100.0	10.4	0.5	0.0960
750	50.0	11.1	0.5	0.0536
750	66.7	10.1	0.5	0.0785
750	83.3	10.4	0.5	0.1004
750	100.0	10.4	0.5	0.1198
1000	50.0	10.6	0.5	0.0473
1000	66.7	10.8	0.5	0.0730
1000	83.3	10.8	0.5	0.0988
1000	100.0	11.1	0.5	0.1258
1250	50.0	11.8	0.5	0.0400
1250	66.7	12.1	0.5	0.0628
1250	83.3	10.0	0.5	0.0958
1250	100.0	10.0	0.5	0.1169
1500	50.0	10.4	0.5	0.0357
1500	66.7	10.4	0.5	0.0558
1500	83.3	10.4	0.5	0.0767
1500	100.0	10.4	0.5	0.0997

TABLE D.6

DISC SURFACE: PRFORATED_PLATE DISC POSITION: SUSPENDED
SURFACE INCLINATION: VERTICAL

SPEED (RPM)	FLOWRATE (cm^3/sec)	TEMP (°C)	p.CO_2 (atm)	kL20 (cm/sec)
500	50.0	13.1	0.5	0.0512
500	66.7	13.1	0.5	0.0760
500	83.3	13.3	0.5	0.0979
500	100.0	13.3	0.5	0.1203
750	50.0	13.3	0.5	0.0536
750	66.7	13.6	0.5	0.0817
750	83.3	13.8	0.5	0.1066
750	100.0	13.1	0.5	0.1282
1000	50.0	13.3	0.5	0.0483
1000	66.7	13.8	0.5	0.0767
1000	83.3	13.8	0.5	0.1010
1000	100.0	14.1	0.5	0.1296
1250	50.0	10.2	0.5	0.0448
1250	66.7	10.2	0.5	0.0734
1250	83.3	10.4	0.5	0.0970
1250	100.0	10.4	0.5	0.1240
1500	50.0	10.8	0.5	0.0419
1500	66.7	11.1	0.5	0.0624
1500	83.3	11.4	0.5	0.0841
1500	100.0	11.6	0.5	0.1050

TABLE D.7

DISC SURFACE: COARSE_MESH DISC POSITION: FIXED
SURFACE INCLINATION: VERTICAL

SPEED (RPM)	FLOWRATE (cm^3/sec)	TEMP (°C)	p.CO_2 (atm)	kL20 (cm/sec)
500	50.0	20.0	0.5	0.0307
500	66.7	20.0	0.5	0.0409
500	83.3	20.2	0.5	0.0517
500	100.0	20.2	0.5	0.0636
750	50.0	19.0	0.5	0.0346
750	66.7	19.0	0.5	0.0512
750	83.3	19.0	0.5	0.0682
750	100.0	19.0	0.5	0.0858
1000	50.0	19.2	0.5	0.0319
1000	66.7	19.2	0.5	0.0514
1000	83.3	19.2	0.5	0.0735
1000	100.0	19.5	0.5	0.0976

TABLE D.8

DISC SURFACE: COARSE_MESH DISC POSITION: SUSPENDED
SURFACE INCLINATION: HORIZONTAL

SPEED (RPM)	FLOWRATE (cm^3/sec)	TEMP (°C)	p.CO_2 (atm)	kL20 (cm/sec)
500	83.3	12.6	0.5	0.0862
750	83.3	12.8	0.5	0.0944
1000	83.3	12.1	0.5	0.0937
1250	83.3	12.1	0.5	0.0866
1500	83.3	12.1	0.5	0.0765

TABLE D.9

DISC SURFACE: PERFORATED_PLATE DISC POSITION: SUSPENDED
SURFACE INCLINATION: HORIZONTAL

SPEED (RPM)	FLOWRATE (cm^3/sec)	TEMP (°C)	p.CO_2 (atm)	kL20 (cm/sec)
500	83.3	11.4	0.5	0.0956
750	83.3	11.8	0.5	0.1045
1000	83.3	12.3	0.5	0.1012
1250	83.3	12.3	0.5	0.0940
1500	83.3	11.4	0.5	0.0865

TABLE D.10

DISC SURFACE: SMOOTH DISC POSITION: SUSPENDED
SURFACE INCLINATION: HORIZONTAL

SPEED (RPM)	FLOWRATE (cm^3/sec)	TEMP (°C)	p.CO_2 (atm)	kL20 (cm/sec)
500	83.3	12.6	0.5	0.0305
750	83.3	12.8	0.5	0.0369
1000	83.3	13.1	0.5	0.0370
1250	83.3	13.1	0.5	0.0370
1500	83.3	13.1	0.5	0.0366

TABLE D.11

DISC SURFACE: COARSE_MESH DISC POSITION: FIXED
SURFACE INCLINATION: VERTICAL

SPEED (RPM)	FLOWRATE (cm^3/sec)	TEMP (°C)	p.CO_2 (atm)	kL20 (cm/sec)
1500	100.0	16.5	0.5	0.0888
1500	133.3	16.8	0.5	0.1392
1500	166.7	14.8	0.5	0.1698
1500	200.0	16.0	0.5	0.2217
1500	233.3	16.3	0.5	0.2559
1500	266.6	16.3	0.5	0.2925

TABLE D.12

DISC SURFACE: PERFORATED_PLATE DISC POSITION: FIXED
SURFACE INCLINATION: VERTICAL

SPEED (RPM)	FLOWRATE (cm^3/sec)	TEMP (°C)	p.CO_2 (atm)	kL20 (cm/sec)
1500	100.0	10.8	0.5	0.0940
1500	133.3	10.2	0.5	0.1336
1500	166.7	10.0	0.5	0.1754
1500	200.0	10.4	0.5	0.2165
1500	233.3	10.6	0.5	0.2472
1500	266.7	10.6	0.5	0.2794

TABLE D.13

DISC SURFACE: COARSE_MESH DISC POSITION: SUSPENDED
SURFACE INCLINATION: HORIZONTAL

SPEED (RPM)	FLOWRATE (cm^3/sec)	TEMP (°C)	p.CO_2 (atm)	kL20 (cm/sec)
1500	83.3	12.3	0.5	0.0765
1500	100.0	12.3	0.5	0.1023
1500	133.3	12.6	0.5	0.1492
1500	166.7	10.4	0.5	0.1887
1500	200.0	10.1	0.5	0.2341
1500	233.3	10.4	0.5	0.2733

TABLE D.14

DISC SURFACE: PERFORATED_PLATE DISC POSITION: SUSPENDED
SURFACE INCLINATION: HORIZONTAL

SPEED (RPM)	FLOWRATE (cm^3/sec)	TEMP (°C)	$p.CO_2$ (atm)	kL20 (cm/sec)
1500	83.3	11.4	0.5	0.0865
1500	100.0	11.4	0.5	0.1128
1500	133.3	11.4	0.5	0.1739
1500	166.7	10.1	0.5	0.2404
1500	200.0	10.1	0.5	0.2993
1500	233.3	10.3	0.5	0.3561
1500	266.7	10.1	0.5	0.4066

TABLE D.15

DISC SURFACE: SMOOTH DISC POSITION: FIXED
SURFACE INCLINATION: HORIZONTAL

SPEED (RPM)	FLOWRATE (cm^3/sec)	TEMP (°C)	$p.CO_2$ (atm)	kL20 (cm/sec)
1500	83.3	10.6	0.5	0.0367
1500	100.0	10.8	0.5	0.0456
1500	133.3	10.8	0.5	0.0665
1500	166.7	11.1	0.5	0.0945
1500	200.0	10.4	0.5	0.1309
1500	233.3	10.3	0.5	0.1711
1500	266.7	10.6	0.5	0.2132

TABLE D.16

DISC SURFACE: COARSE_MESH DISC POSITION: SUSPENDED
SURFACE INCLINATION: VERTICAL

SPEED (RPM)	FLOWRATE (cm^3/sec)	TEMP (°C)	$p.CO_2$ (atm)	kL20 (cm/sec)
1250	166.6	10.4	0.5	0.1946
1250	200.0	10.6	0.5	0.2149
1300	166.7	10.6	0.5	0.2001
1300	200.0	10.6	0.5	0.2196
1300	233.3	13.2	0.5	0.2548
1400	166.7	13.4	0.5	0.1948
1400	200.0	13.3	0.5	0.2148
1400	233.3	13.3	0.5	0.2635
1400	266.7	13.3	0.5	0.3029
1500	166.7	13.0	0.5	0.1895
1500	200.0	12.8	0.5	0.2366
1500	233.3	13.0	0.5	0.2866
1500	266.7	13.2	0.5	0.3080

APPENDIX E

DATA FOR ANNULAR CORRECTION EXPERIMENT

TABLE E.1

DISC SURFACE: SMOOTH DISC POSITION: SHROUDED
SURFACE INCLINATION: VERTICAL

SPEED (RPM)	FLOWRATE (cm^3/sec)	TEMP (°C)	$p.CO_2$ (atm)	kL20 (cm/sec)
500	50.0	10.6	1.0	0.0184
500	83.3	10.8	1.0	0.0261
750	50.0	11.1	1.0	0.0208
750	100.0	10.3	1.0	0.0365
1000	50.0	11.6	1.0	0.0231
1000	100.0	10.3	1.0	0.0391
1250	50.0	11.9	1.0	0.0242
1250	100.0	10.1	1.0	0.0423
1500	50.0	12.1	1.0	0.0244
1500	100.0	10.1	1.0	0.0430

APPENDIX F

DATA FOR EXPERIMENTS CONCERNING THE VARIATION OF THE MASS TRANSFER COEFFICIENT WITH RADIUS

TABLE F.1

DISC SURFACE: SMOOTH DISC POSITION: FIXED
SURFACE INCLINATION: VERTICAL RADIUS: 116 mm

SPEED (RPM)	FLOWRATE (cm^3/sec)	TEMP (°C)	$p.CO_2$ (atm)	kL20 (cm/sec)
500	50.0	13.6	1.0	0.0200
500	66.7	13.8	1.0	0.0244
500	83.3	13.8	1.0	0.0239
750	50.0	14.1	1.0	0.0239
750	66.7	14.3	1.0	0.0297
750	83.3	14.6	1.0	0.0336
750	100.0	12.8	1.0	0.0371
1000	50.0	13.3	1.0	0.0265
1000	66.7	13.1	1.0	0.0337
1000	83.3	13.1	1.0	0.0395
1000	100.0	13.3	1.0	0.0445
1250	50.0	13.8	1.0	0.0264
1250	66.7	13.8	1.0	0.0348
1250	83.3	13.8	1.0	0.0421
1250	100.0	11.8	1.0	0.0497
1500	50.0	12.1	1.0	0.0252
1500	66.7	12.3	1.0	0.0337
1500	83.3	12.3	1.0	0.0420
1500	100.0	12.6	1.0	0.0517

TABLE F.2

DISC SURFACE: FINE_MESH DISC POSITION: FIXED
SURFACE INCLINATION: VERTICAL RADIUS: 116 mm

SPEED (RPM)	FLOWRATE (cm^3/sec)	TEMP (°C)	$p.CO_2$ (atm)	kL20 (cm/sec)
500	50.0	14.1	1.0	0.0442
500	66.7	14.3	1.0	0.0533
500	83.3	14.6	1.0	0.0548
750	50.0	14.8	1.0	0.0549
750	66.7	14.8	1.0	0.0740
750	83.3	15.3	1.0	0.0916
750	100.0	13.3	1.0	0.1026
1000	50.0	13.8	1.0	0.0453
1000	66.7	13.8	1.0	0.0695
1000	83.3	14.1	1.0	0.0914
1000	100.0	14.3	1.0	0.1108
1250	50.0	13.6	1.0	0.0464
1250	66.7	13.8	1.0	0.0681
1250	83.3	13.3	1.0	0.0913
1250	100.0	13.6	1.0	0.1142
1500	50.0	13.8	1.0	0.0415
1500	66.7	14.1	1.0	0.0641
1500	83.3	14.3	1.0	0.0896
1500	100.0	12.6	1.0	0.1152

TABLE F.3

DISC SURFACE: SMOOTH DISC POSITION: FIXED
SURFACE INCLINATION: VERTICAL RADIUS: 84 mm

SPEED (RPM)	FLOWRATE (cm^3/sec)	TEMP (°C)	$p.CO_2$ (atm)	kL20 (cm/sec)
1000	50.0	13.3	1.0	0.0351
1000	66.7	12.1	1.0	0.0336
1000	83.3	11.8	1.0	0.0298
1250	50.0	12.3	1.0	0.0359
1250	66.7	12.6	1.0	0.0416
1250	83.3	12.6	1.0	0.0386
1500	50.0	13.1	1.0	0.0377
1500	66.7	13.6	1.0	0.0463
1500	83.3	11.8	1.0	0.0504

TABLE F.4

DISC SURFACE: FINE_MESH DISC POSITION: FIXED
SURFACE INCLINATION: VERTICAL RADIUS: 84 mm

SPEED (RPM)	FLOWRATE (cm^3/sec)	TEMP (°C)	$p.CO_2$ (atm)	kL20 (cm/sec)
750	50.0	13.3	1.0	0.0555
750	66.7	13.8	1.0	0.0625
750	83.3	14.1	1.0	0.0571
1000	50.0	14.3	1.0	0.0742
1000	66.7	12.8	1.0	0.0849
1000	83.3	12.8	1.0	0.0909
1000	100.0	13.1	1.0	0.0842
1250	50.0	17.3	1.0	0.0803
1250	66.7	17.5	1.0	0.0923
1250	83.3	16.8	1.0	0.1020
1250	100.0	17.0	1.0	0.1055
1500	50.0	17.3	1.0	0.0882
1500	66.7	17.3	1.0	0.1199
1500	83.3	15.3	1.0	0.1423
1500	100.0	15.5	1.0	0.1520

APPENDIX G

DATA FOR THE EXPERIMENTAL INVESTIGATIONS EMPLOYING CARBON DIOXIDE AND AQUEOUS DIETHANOLAMINE

Sample	Flowrate (cm^3/sec)	Temp (°C)	Henry coef (atml/mol)	Ci (g/cm^3)	DT (cm^2/sec)	kLT (cm/sec)	NH2O (g/sec)	C_b^i DEA (g/cm^3)	C_b^o DEA (g/cm^3)	NDEA (g/sc)	α out	H DEA (atml/mol)	Ci DEA (g/cm^3)	C* (mol/cm^3)	ϕ_m
A	66.7	16.3	22.9	1.92×10^{-3}	1.51×10^{-5}	0.0519	0.048	0.00	0.0090×10^{-3}	0.600	0.10	23.3	1.89×10^{-3}	4.29×10^{-7}	10.1
B	100.0	16.0	22.7	1.94×10^{-3}	1.50×10^{-5}	0.0939	0.084	0.00	0.0066×10^{-3}	0.660	0.07	23.0	1.91×10^{-3}	4.35×10^{-7}	6.1
C	133.3	16.0	22.7	1.94×10^{-3}	1.50×10^{-5}	0.1361	0.119	0.00	0.0050×10^{-3}	0.666	0.06	23.0	1.91×10^{-3}	4.35×10^{-7}	4.2
D	166.7	16.3	22.9	1.92×10^{-3}	1.51×10^{-5}	0.1782	0.153	0.00	0.0045×10^{-3}	0.750	0.05	23.1	1.90×10^{-3}	4.33×10^{-7}	3.7
E	233.3	16.5	23.0	1.91×10^{-3}	1.52×10^{-5}	0.2649	0.222	0.00	0.0040×10^{-3}	0.933	0.04	23.1	1.90×10^{-3}	4.33×10^{-7}	3.1

Sample	D CO2/DEA (cm^2/sec)	kl(1) ($cm^3/mol.s$)	kl(2) ($cm^3/mol.s$)	Co (mol/cm^3)	Function 5.27 LHS (1)	Function 5.27 LHS (2)	Function 5.27 RHS (1)	Function 5.27 RHS (2)	Function 5.29 LHS (1)	Function 5.29 LHS (2)	Function 5.29 RHS (1)	Function 5.29 RHS (2)	ϕ_c (1)	ϕ_c (2)
A	8.47×10^{-6}	1.0×10^{6}	5.8×10^{6}	1.80×10^{-3}	0.123	0.297	0.570	0.570	0.123	0.297	0.259	0.259	2.7	5.7
B	8.39×10^{-6}	1.0×10^{6}	5.8×10^{6}	1.86×10^{-3}	0.125	0.300	1.050	1.050	0.125	0.300	0.469	0.469	1.7	3.4
C	8.37×10^{-6}	1.0×10^{6}	5.8×10^{6}	1.88×10^{-3}	0.125	0.300	1.540	1.540	0.125	0.300	0.680	0.680	1.4	2.4
D	8.45×10^{-6}	1.0×10^{6}	5.8×10^{6}	1.90×10^{-3}	0.127	0.310	2.040	2.040	0.127	0.310	0.891	0.891	1.2	2.0
E	8.67×10^{-6}	1.0×10^{6}	5.8×10^{6}	1.91×10^{-3}	0.128	0.312	3.050	3.050	0.128	0.312	1.324	1.324	1.1	1.6

TABLE G.1

DISC SURFACE: COARSE_MESH DISC POSITION: FIXED
SURFACE INCLINATION: VERTICAL

GAS PRESSURE: 1.0 atm
SOLUTION COMPOSITION: 2.06 Molar

Sample	Flowrate (cm^3/sec)	Temp (°C)	Henry coef (atml/mol)	Ci (g/cm^3)	DT (cm^2/sec)	kLT (cm/sec)	NH2O (g/sec)	C_b^i DEA (g/cm^3)	C_b^o DEA (g/cm)	NDEA (g/sc)	α out	H DEA (atml/mol)	Ci DEA (g/cm)	C* (mol/cm^3)	ϕ_M
A	------	----	--------	------	------	------	-----	----	*0.0044*	----	----	--------	------	------	---
B	66.7	18.5	24.5	1.79×10^{-3}	1.62×10^{-5}	0.0270	0.0259	0.0044	0.0089	0.300	0.10	24.9	1.76×10^{-3}	4.00×10^{-5}	10.4
C	100.0	18.5	24.5	1.79×10^{-3}	1.62×10^{-5}	0.0445	0.0422	0.0044	0.0076	0.320	0.08	24.8	1.77×10^{-3}	4.02×10^{-5}	6.7
D	133.3	18.5	24.5	1.79×10^{-3}	1.62×10^{-5}	0.0649	0.0609	0.0044	0.0070	0.346	0.08	24.8	1.77×10^{-3}	4.02×10^{-5}	5.0
E	166.7	18.5	24.5	1.79×10^{-3}	1.62×10^{-5}	0.0922	0.0849	0.0044	0.0065	0.350	0.07	24.8	1.77×10^{-3}	4.02×10^{-5}	3.5
F	233.3	18.5	24.5	1.79×10^{-3}	1.62×10^{-5}	0.1670	0.1468	0.0044	0.0063	0.443	0.07	24.8	1.77×10^{-3}	4.02×10^{-5}	2.5

Sample	D CO2/DEA (cm^2/sec)	kl(1) (cm/mols)	kl(2) (cm/mols)	Co (mol/cm)	Function 5.27 LHS (1)	Function 5.27 LHS (2)	Function 5.27 RHS (1)	Function 5.27 RHS (2)	Function 5.29 LHS (1)	Function 5.29 LHS (2)	Function 5.29 RHS (1)	Function 5.29 RHS (2)	ϕ_c (1)	ϕ_c (2)
B	9.07×10^{-6}	1.0×10^{6}	5.8×10^{6}	1.80×10^{-3}	0.128	0.308	0.317	0.317	0.128	0.308	0.135	0.135	4.8	11.4
C	8.91×10^{-6}	1.0×10^{6}	5.8×10^{6}	1.84×10^{-3}	0.128	0.308	0.531	0.531	0.128	0.308	0.228	0.228	3.0	6.9
D	8.91×10^{-6}	1.0×10^{6}	5.8×10^{6}	1.84×10^{-3}	0.128	0.308	0.775	0.775	0.128	0.308	0.324	0.324	2.2	4.7
E	8.67×10^{-6}	1.0×10^{6}	5.8×10^{6}	1.86×10^{-3}	0.127	0.306	1.112	1.112	0.127	0.306	0.461	0.461	1.7	3.5
F	8.67×10^{-6}	1.0×10^{6}	5.8×10^{6}	1.86×10^{-3}	0.127	0.306	2.015	2.015	0.127	0.306	0.835	0.835	1.3	2.1

TABLE G.2

DISC SURFACE: SMOOTH DISC POSITION: FIXED
SURFACE INCLINATION: VERTICAL

GAS PRESSURE: 1.0 atm
SOLUTION COMPOSITION: 2.04 Molar

APPENDIX H

DATA FOR THE LEAKAGE EXPERIMENTS AND HYDRODYNAMICS STUDY

TABLE H.1 (LEAKAGE MEASUREMENTS)

FLOWRATE (cm^3/sec)	SPEED (RPM)	EDGE FLOWRATE (cm^3/sec) COARSE Cal1	COARSE Cal2	MEDIUM Cal1	MEDIUM Cal2	FINE Cal1	FINE Cal2
100	120	88.7	88.3	55.6	70.0	36.4	46.3
	240	95.5	98.5	96.2	*103.7	93.2	95.6
	480	99.4	*100.0	97.8	97.8	94.3	94.3
	840	95.2	99.6	95.6	99.1	95.2	96.5
	960	95.2	97.8	95.2	98.8	95.6	*100.0
	1440	93.6	94.5	96.3	95.9	96.3	98.1
	1680	95.3	95.0	98.2	99.1	99.1	*100.0
80	120	70.7	71.8	34.3	43.1	48.4	55.0
	240	79.6	80.2	80.0	81.4	69.0	68.8
	480	82.0	79.2	82.5	78.9	80.0	76.7
	840	73.9	77.6	75.0	78.9	72.0	76.8
	960	74.1	77.1	74.7	80.0	73.4	77.9
	1440	77.5	78.0	79.3	78.0	77.7	77.5
	1680	75.4	77.4	76.2	75.1	74.5	76.5
60	120	57.0	56.2	34.2	44.9	48.4	51.4
	240	61.1	58.8	61.5	62.0	60.7	59.8
	480	60.0	60.8	59.2	58.7	58.1	58.7
	840	59.3	59.8	59.8	58.9	58.7	59.1
	960	59.3	59.3	59.6	58.3	59.8	59.2
	1440	58.0	59.4	58.9	58.9	57.8	57.5
	1680	57.3	58.5	57.8	59.2	57.1	57.9
40	120	37.3	37.3	22.4	29.8	33.2	34.6
	240	40.2	40.6	39.6	39.6	39.6	40.4
	480	39.0	40.0	39.1	19.1	39.4	40.2
	840	38.9	39.3	40.4	40.0	38.9	39.3
	960	39.3	39.8	40.7	39.8	39.1	40.4
	1440	41.2	40.9	40.9	39.4	40.2	38.9
	1680	38.8	38.2	39.8	38.9	39.8	38.9
20	120	18.1	18.3	12.5	14.5	16.7	16.3
	240	20.0	20.2	20.2	20.0	20.0	19.8
	480	19.8	20.0	19.6	20.0	20.0	20.0
	840	19.1	19.3	19.2	19.6	19.2	20.2
	960	19.3	19.5	20.2	20.4	19.1	19.5
	1440	19.3	19.5	20.2	20.4	18.9	19.1
	1680	18.4	18.6	18.4	18.6	19.3	19.8

--

CALIBRATION NUMBER 1 = PLANE DISC
CALIBRATION NUMBER 2 = MESH DISC

TABLE H.2 (FLOW REGIME DATA)

FLOW CONDITION	FLOW RATE(cm^3/sec) 20	23	25	29	30	40	60	80	100	
Leakage visible to	83*	--	--	--	--	87*	93*	96*	113*	
Waves appear at	<>*	438*	--	276*	--	192*	143*	120*	113*	RPM
Waves disappear at	<>*	438*	593*	--	756*	1086*	1073*	1037*	974*	

APPENDIX I

LISTING OF BASIC PROGRAMS USED DURING THE EXPERIMENTAL INVESTIGATION

PROGRAM I.1 DATA ANALYSIS FOR CO2 ABSORPTION IN WATER

LISTING OF 'DATA-AN'

```
 10 MODE 0
 20 VDU 2
 30 PRINT "DATA ANALYSIS FOR CO2 ABSORPTION IN WATER"
 40 PRINT " "
 50 VDU 3
 60 INPUT "WHAT TYPE OF PLATE IS IN USE  ",A$
 70 PRINT " "
 80 INPUT "WHAT POSITION IS THE PLATE IN  ",B$
 90 PRINT " "
100 INPUT"WHAT RADIAL POSITION IS THE PICK-UP TUBE AT  ",R
110 PRINT
120 INPUT"WHAT SPEED IS THE MACHINE RUNNING AT ",SPEED
130 DIM DAT(14,8)
140 PRINT " "
150 INPUT"HOW MANY DATA POINTS TO BE RECORDED",H
160 HF=1
170 REPEAT
180 PRINT" "
190 PRINT"DATA SET ";HF
200 PRINT" "
210 INPUT"FLOW-RATE (SCALE)  ",DAT(1,HF)
220 PRINT"  "
230 INPUT"CONCENTRATION (mV)  ",DAT(3,HF)
240 PRINT" "
250 INPUT"TEMPERATURE (mV)  ",DAT(5,HF)
260 HF=HF+1
270 UNTIL HF=H+1
280 REM CALCULATE ACTUAL FLOWRATES
290 HF=1
300 REPEAT
310 DAT(2,HF)=DAT(1,HF)/3.6
320 HF=HF+1
330 UNTIL HF=H+1
340 REM CALCULATE ACTUAL TEMPERATURES
350 HF=1
360 REPEAT
370 DAT(6,HF)=DAT(5,HF)*24.68
380 HF=HF+1
390 UNTIL HF=H+1
400 REM CALCULATE MOLARITY OF SOLUTIONS
410 PRINT" "
420 PRINT" "
450 INPUT"LOWER (1x10 -2M) CALIBRATION POINT  ",LOW
460 PRINT
470 INPUT"IS THE GRADIENT OF THE CALIBRATION CURVE STILL 55.5 mV/decade (Y/N)"
,Y$
480 IF Y$="Y" THEN GRAD=55.5:GOTO 530
490 PRINT
500 INPUT "WHAT IS THE NEW GRADIENT  ",GRAD
520 PRINT
530 HF=1
540 REPEAT
550 DAT(4,HF)=10^(-2.0-(((-1.0*DAT(3,HF))+LOW)/GRAD))
560 HF=HF+1
570 UNTIL HF=H+1
580 REM CALCULATE HENRY'S COEFFICIENT
590 REM FROM DATA IN ASTARITA PAGE 208
600 HF=1
610 REPEAT
620 HINV=10^((1140/(DAT(6,HF)+273))-5.30)
630 DAT(7,HF)=1.0/HINV
750 HF=HF+1.0
760 UNTIL HF=H+1
770 REM CALCULATE INTERFACE CONCENTRATION
780 PRINT" "
790 INPUT"WHAT CO2 PRESSURE ARE THE READINGS AT  ",PRESS
800 HF=1
810 REPEAT
820 DAT(8,HF)=PRESS/DAT(7,HF)
830 DAT(9,HF)=DAT(8,HF)*44.0/1000.0
840 DAT(10,HF)=DAT(4,HF)*44.0/1000.0
850 DAT(11,HF)=DAT(10,HF)*1000.0
890 DAT(12,HF)=DAT(11,HF)*DAT(2,HF)/1000.0
900 HF=HF+1
910 UNTIL HF=H+1
920  REM CALCULATE MASS TRANSFER COEFFICIENTS
930 HF=1
940 IF R=1 THEN RA=141
941 IF R=2 THEN RA=116
942 IF R=3 THEN RA=84
950 AREA=(PI*(RA^2-25^2)/100)
960 REPEAT
```

```
  970 DPIV=(((DAT(9,HF)-0)-(DAT(9,HF)-DAT(10,HF)))/(LN((DAT(9,HF)-0)/(DAT(9,HF)-
DAT(10,HF)))))
  980 DAT(13,HF)=(DAT(12,HF)/(AREA*DPIV))
  982 REM   TEMPERATURE MODIFICATION OF MASS TRANSFER COEFFICIENT
  983 DX=1.21+(DAT(6,HF)-10.0)*.048
  984 DAT(14,HF)=DAT(13,HF)*(SQR(1.70)/SQR(DX))
  990 HF=HF+1
 1000 UNTIL HF=H+1
 1010 PRINT " "
 1020 MODE 0
 1030 VDU 2
 1040 PRINT " "
 1050 PRINT"                    SUMMARY OF RESULTS "
 1060 PRINT"                    ================== "
 1070 PRINT" "
 1080 PRINT"THE EXPERIMENT WAS CARRIED OUT USING A ";A$;" PLATE IN A ";B$;" POSI
TION WITH THE PICK-UP TUBE AT RADIUS ";R
 1090 PRINT" "
 1100 PRINT"ROTATIONAL SPEED FOR THIS SET OF DATA WAS ";SPEED;" (RPM)"
 1110 PRINT
 1120 PRINT
 1130 @%=132150
 1140 PRINT
 1150 PRINT"  *********************************"
 1160 PRINT"  *                               *"
 1170 PRINT"  *   FLOW RATE       I L(phys)   *"
 1180 PRINT"  *    (cm3/sec)       (cm/sec)   *"
 1190 PRINT"  *                               *"
 1200 HF=1
 1210 REPEAT
 1220 IF DAT(2,HF) >99.5 THEN GOTO 1250
 1230 PRINT"  *     ";DAT(2,HF);"          ";DAT(14,HF);"     *"
 1240 GOTO 1260
 1250 PRINT"  *    ";DAT(2,HF);"    .      ";DAT(14,HF);"     *"
 1260 HF=HF+1
 1270 UNTIL HF=H+1
 1280 PRINT"  *                               *"
 1290 PRINT"  *********************************"
 1300 PRINT
 1310 PRINT
 1320 PRINT
 1330 PRINT"THE PARTIAL PRESSURE OF CO2 FOR THIS RUN WAS ";PRESS;" (atm)"
 1340 @%=10
 1350 VDU3
 1360 END
```

PROGRAM I.2 ANALYSIS OF OASIS DATA

LISTING OF 'PLOTER'

```
 5 *LOAD "TEST2"
10REM  PROGRAM FOR THE LINKING OF DATA LOGGER AND CHROMATATOGRAPH
20  REM
25 CLS
26 INPUT "HOW MANY SCANS IN THIS RUN",A
27 PRINT:INPUT "INTER SCAN DELAY",DELAY
28 CLS
30PRINT "DATA RECALL SYSTEM VARIABLES"
40  IF ?726202=-1 THEN A$="ON" ELSE A$="OFF"
50PRINT "SUPER FAST SCAN "A$
60IF ?726198=-1 THEN B$="ON" ELSE B$="OFF"
70PRINT "FAST SCAN        "B$
80IF ?726194=0 THEN C$="ON" ELSE C$="OFF"
90PRINT "CONTINUOUS SCAN "C$
110PRINT "INTER SCAN DELAY"DELAY
120PRINT "NUMBER OF SCANS "A
121 PRINT''''''''''
122 INPUT "IS A PLOT OF THE DATA REQUIRED",D$
123 IF D$="N" THEN GOTO 500
130REM
135 CLS
140MOVE 128,100:DRAW 1151,100:DRAW 1151,1000:DRAW 128,1000:DRAW 128,100
150FOR F=1 TO 10:MOVE (128+(F*93)),100:PLOT 21,(128+(F*93)),1000:NEXT F
160FOR F=1 TO 9:MOVE 128,(100+(F*90)):PLOT 21,1151,(100+(F*90)):NEXT F
170MOVE 128,100
180FOR N=1 TO A
190X=128+(1023/((A)-1)*(N-1))
200Y=100+900*(((?(&66B0+(N*3)-1))*256)+(?(&66B0+(N*3)-2)))/65530
210 DRAW X,Y
220NEXT N
230REM
235 VDU 5
240MOVE 128,45
250PRINT "FINISH=F  INTEGRAL=I  DUMP=D"
260MOVE 700,65
270PRINT "Y SCALE  0-1 VOLT"
280MOVE 700,35
290PRINT "X SCALE  0-":DELAY*A
295 VDU 4
300INPUT F$
310IF F$="F" THEN CLS:END
320IF F$="I" THEN GOTO 500
330IF F$="D" THEN *GDUMP 1 1 3 1 1
340 GOTO 300
500REM INTEGRATION
510REM
520CLS
522    INPUT "IS AN OFFSET REQUIRED IN THE INTEGRATION",E$
523 IF E$="N" THEN OFSET=0:GOTO 530
524 INPUT "WHAT IS THE VALUE OF THE OFFSET (IN VOLTS)",OFSET
525 CLS
530AREA=0
532 CLS
535 MAX=AREA
540BASE=DELAY
541 MOVE 128,100:DRAW 1151,100:DRAW 1151,1000:DRAW 128,1000:DRAW 128,100
542 FOR F=1 TO 10:MOVE (128+(F*93)),100:PLOT 21,(128+(F*93)),1000:NEXT F
543 FOR F=1 TO 9:MOVE 128,(100+(F*90)):PLOT 21,1151,(100+(F*90)):NEXT F
544 MOVE 128,100
550FOR N=1 TO (A)-1
560PNT1=(((?(&66B0+(N*3)-1))*256)+(?(&66B0+(N*3)-2)))/65530-OFSET
570PNT2=(((?(&66B0+((N+1)*3)-1))*256)+(?(&66B0+((N+1)*3)-2)))/65530-OFSET
580AREAN=AREA+0.5*DELAY*(PNT1+PNT2)
581 IF AREAN>AREA THEN MAX=AREAN
582 AREA=AREAN
583 NEXT N
584 AREA=0
585FOR N=1 TO (A)-1
586PNT1=(((?(&66B0+(N*3)-1))*256)+(?(&66B0+(N*3)-2)))/65530-OFSET
587PNT2=(((?(&66B0+((N+1)*3)-1))*256)+(?(&66B0+((N+1)*3)-2)))/65530-OFSET
588AREA=AREA+0.5*DELAY*(PNT1+PNT2)
590X=128+(1023/((A)-1)*N)
600Y=100+900*(AREA/MAX)
610DRAW X,Y
620 NEXT N
630VDU 5
640MOVE 128,45
650PRINT "DATA PLOT=P  FINISH=F  DUMP=D"
660MOVE 700,65
670PRINT "Y SCALE 0-";MAX
680MOVE 700,35
690PRINT "X SCALE 0-";DELAY*A
700VDU 4
710 INPUT G$
720 IF G$="F" THEN CLS:END
730 IF G$="D" THEN *GDUMP 1 1 3 1 1
740 IF G$="P" THEN GOTO 130
750 GOTO 710
```

Example of output of 'PLOTER'

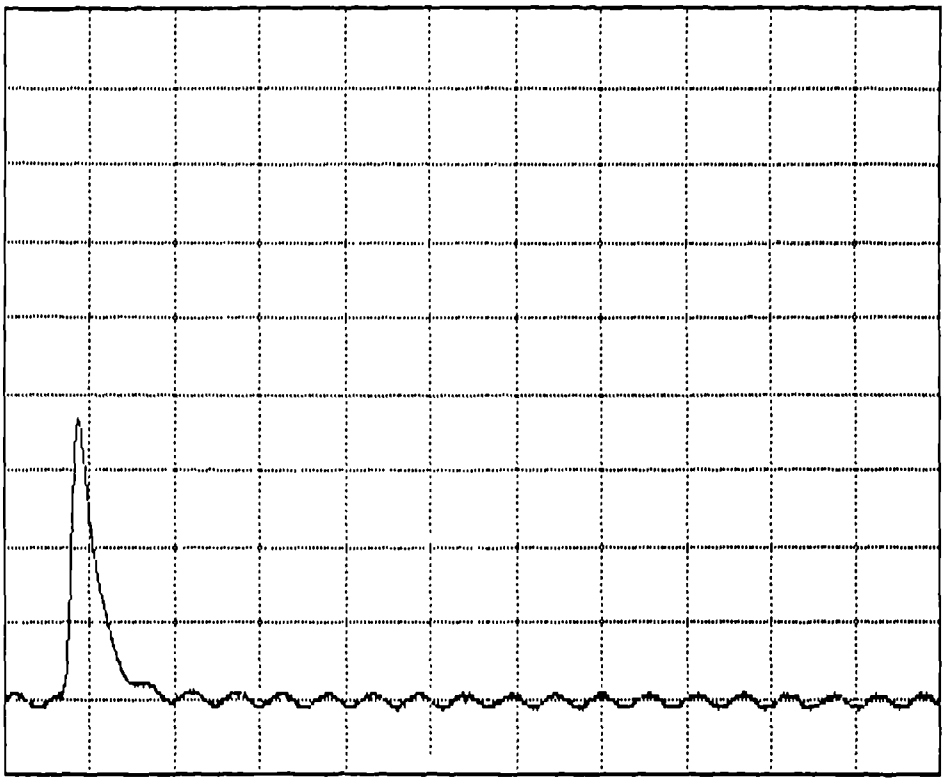

FINISH=F INTEGRAL=I DUMP=D

Y SCALE 0-1 VOLT
X SCALE 0-90000

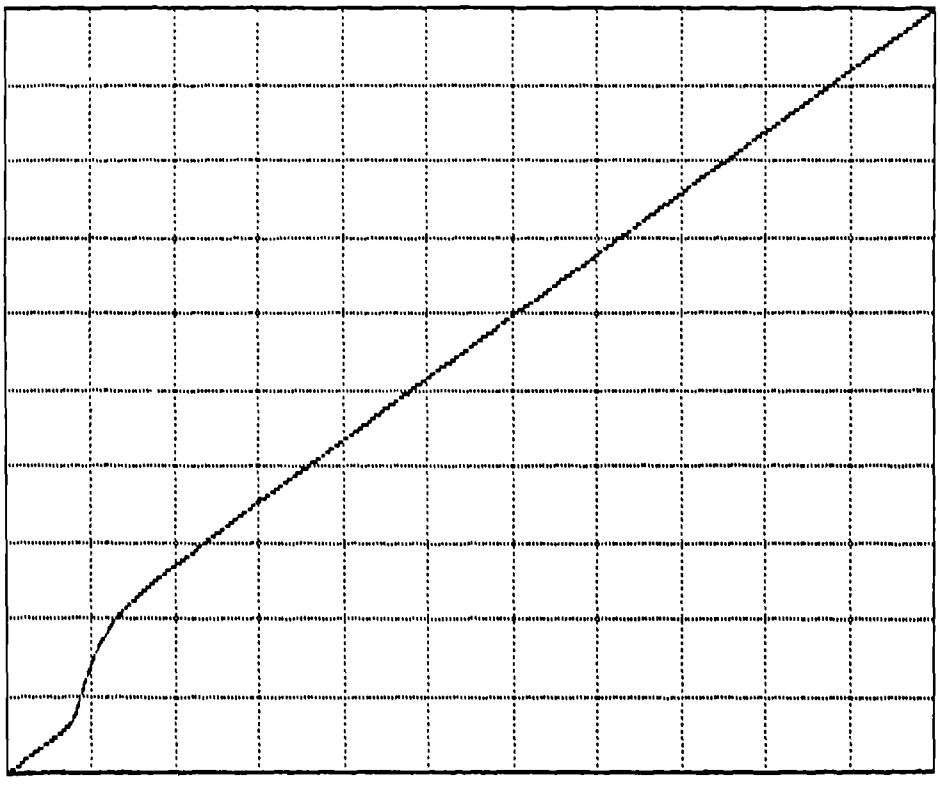

DATA PLOT=P FINISH=F DUMP=D

Y SCALE 0-9961.89839
X SCALE 0-90000

APPENDIX J

MISCELLANEOUS TABLES SHOWING PROPERTIES OF THE SYSTEM CARBON DIOXIDE/AQUEOUS DIETHANOLAMINE

DENSITY OF DIETHANOLAMINE SOLUTIONS

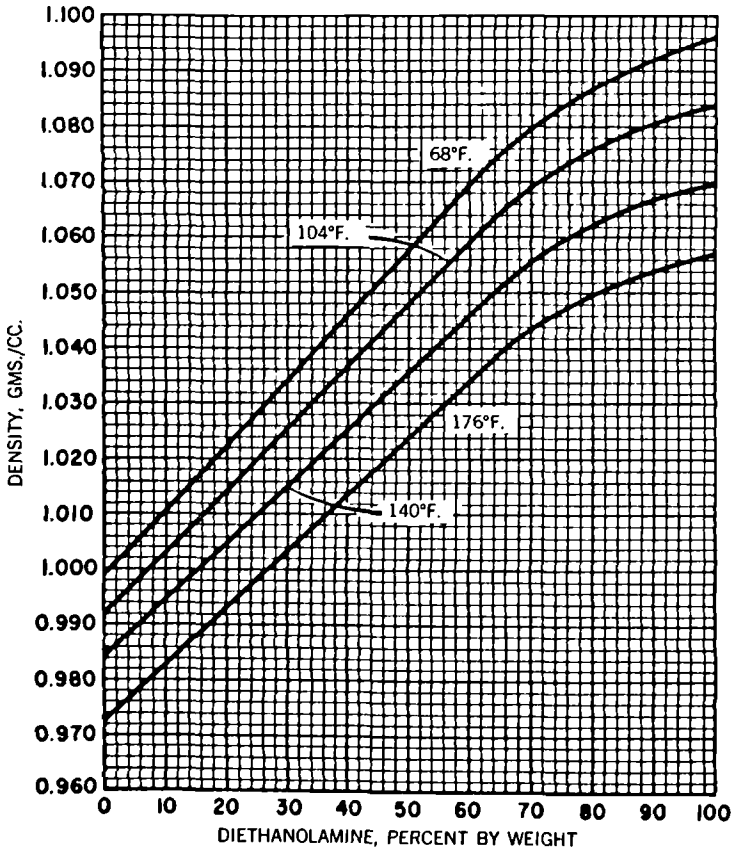

VISCOSITY OF AQUEOUS
DIETHANOLAMINE SOLUTIONS

PERCENT BY WEIGHT TECHNICAL GRADE DIETHANOLAMINE

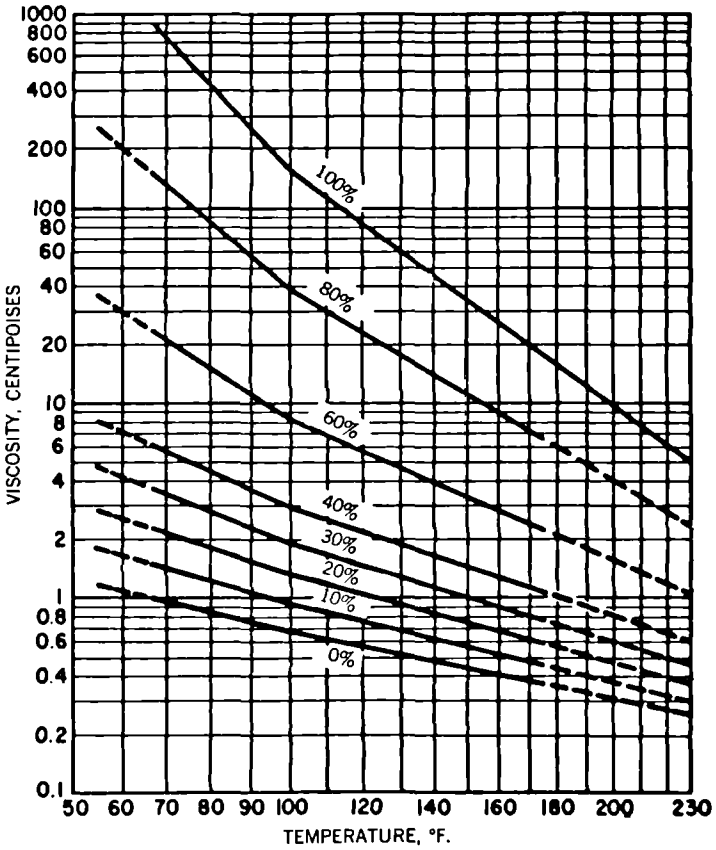

pH VALUE OF AQUEOUS DIETHANOLAMINE SOLUTIONS
PERCENT BY WEIGHT TECHNICAL GRADE DIETHANOLAMINE

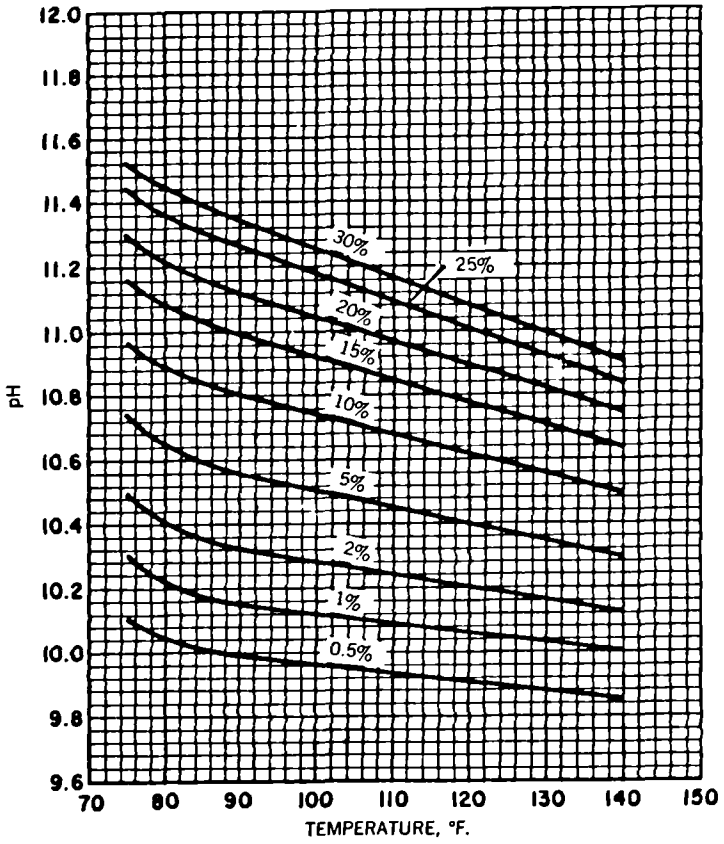

BOILING POINTS OF AQUEOUS DIETHANOLAMINE
SOLUTIONS AT VARIOUS PRESSURES

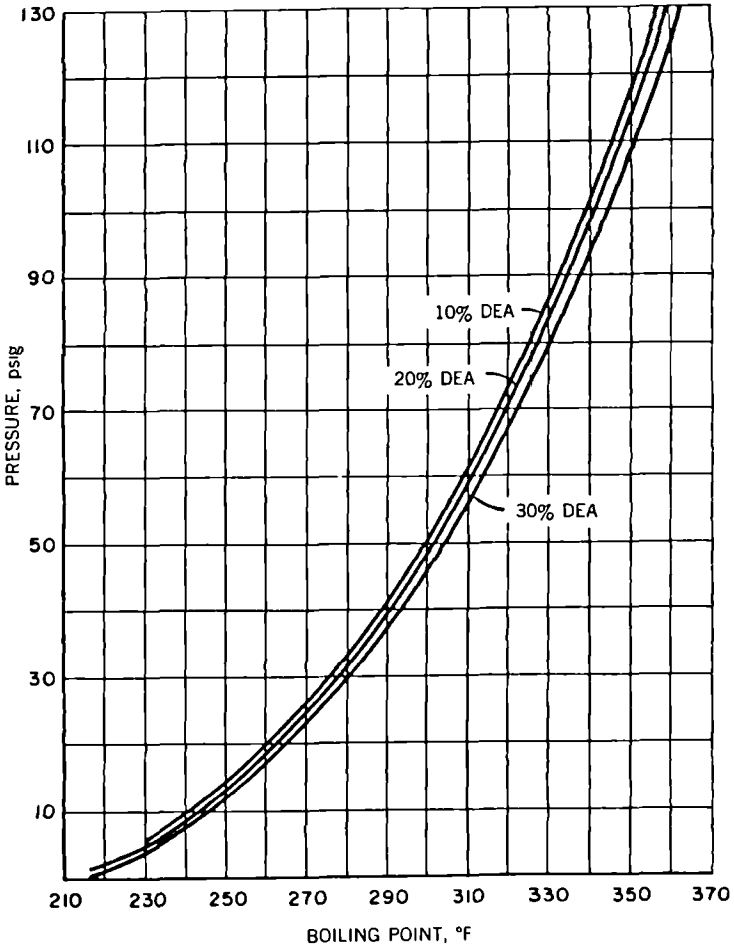

EQUILIBRIUM PLOTS OF CO_2 IN AQUEOUS DIETHANOLAMINE SOLUTIONS

5 PERCENT DEA

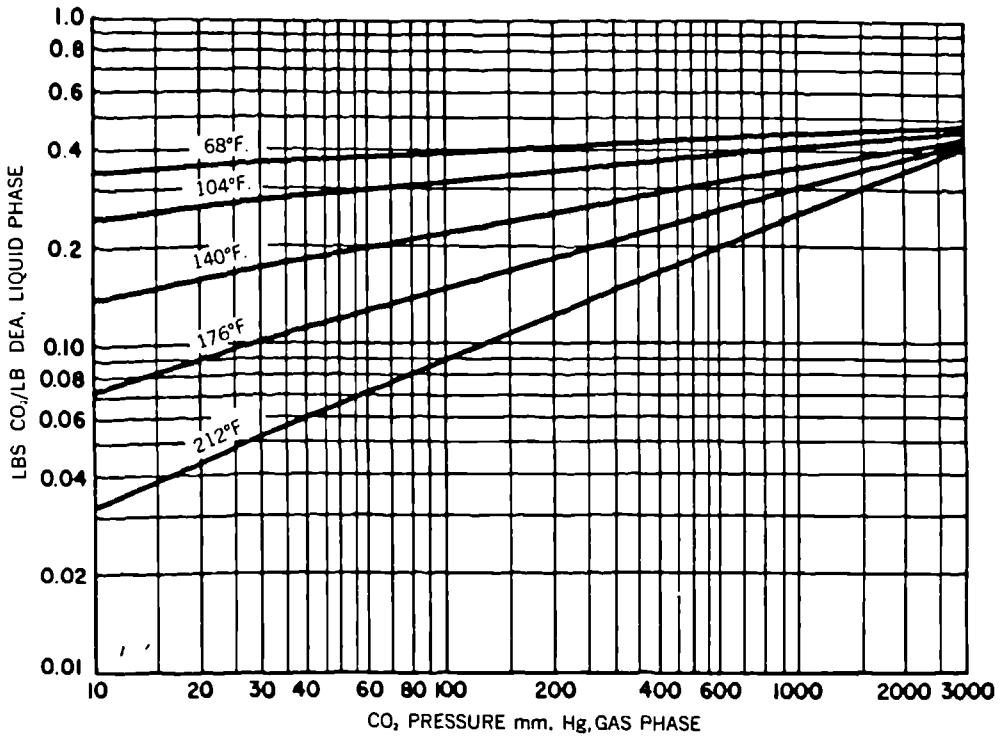

10 PERCENT DEA

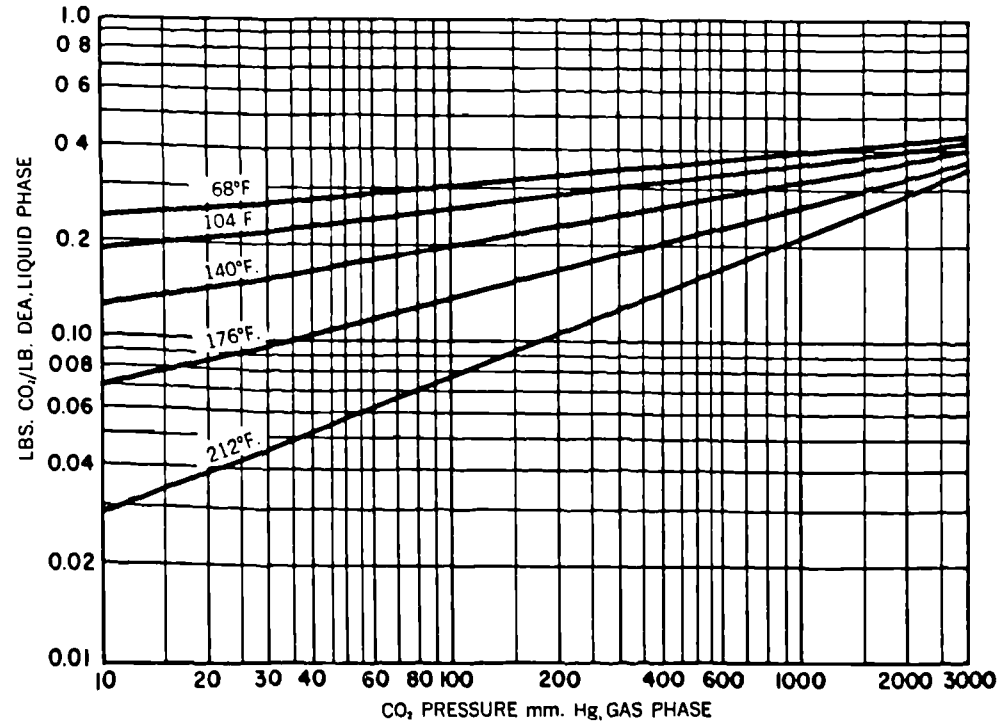

EQUILIBRIUM PLOTS OF CO_2 IN AQUEOUS DIETHANOLAMINE SOLUTIONS

15 PERCENT DEA

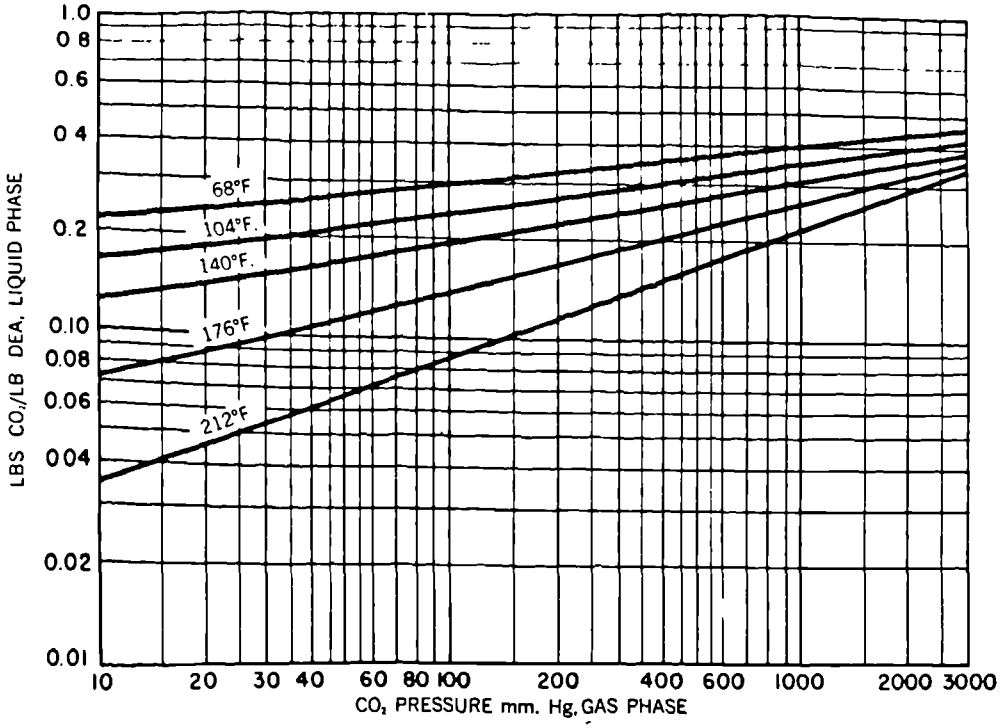

20 PERCENT DEA

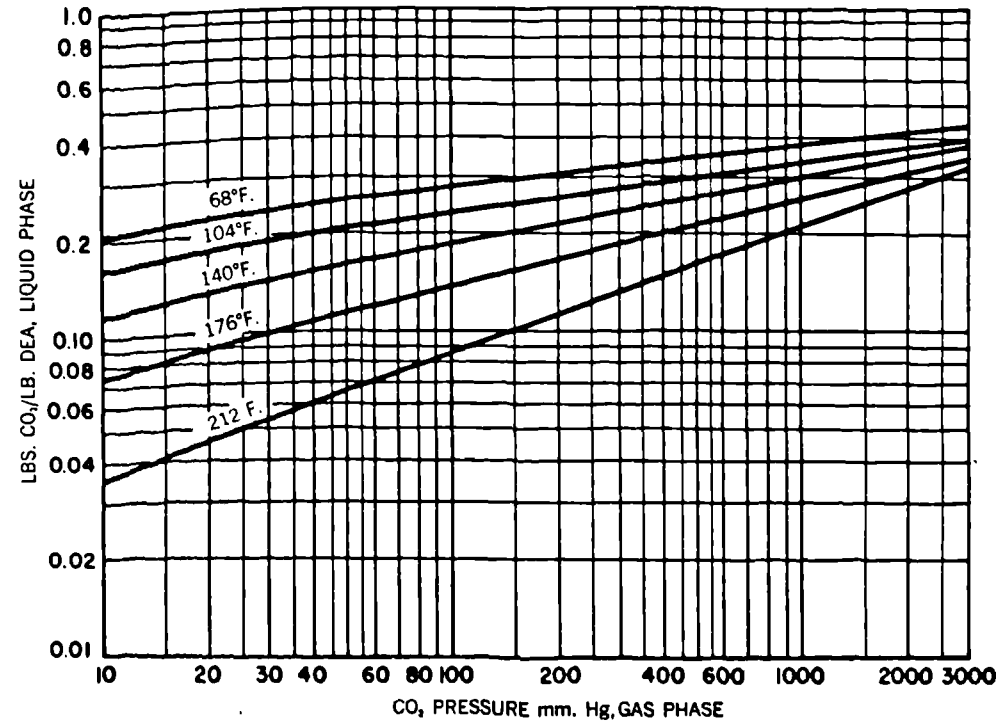

EQUILIBRIUM PLOTS OF CO, IN AQUEOUS
DIETHANOLAMINE SOLUTIONS

25 PERCENT DEA

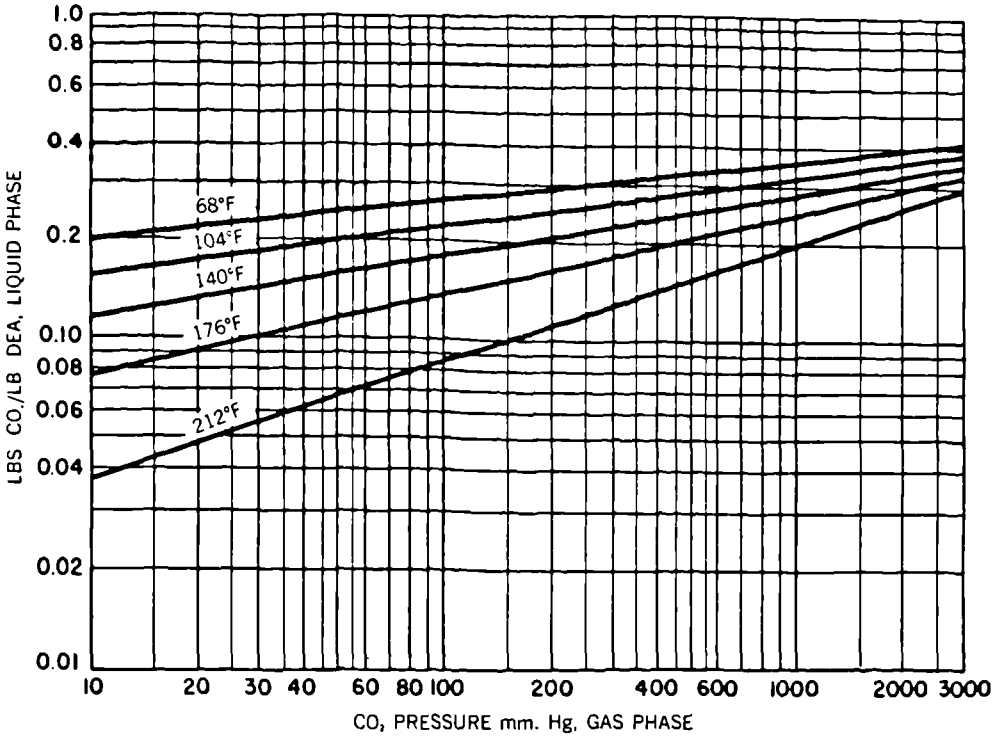

30 PERCENT DEA

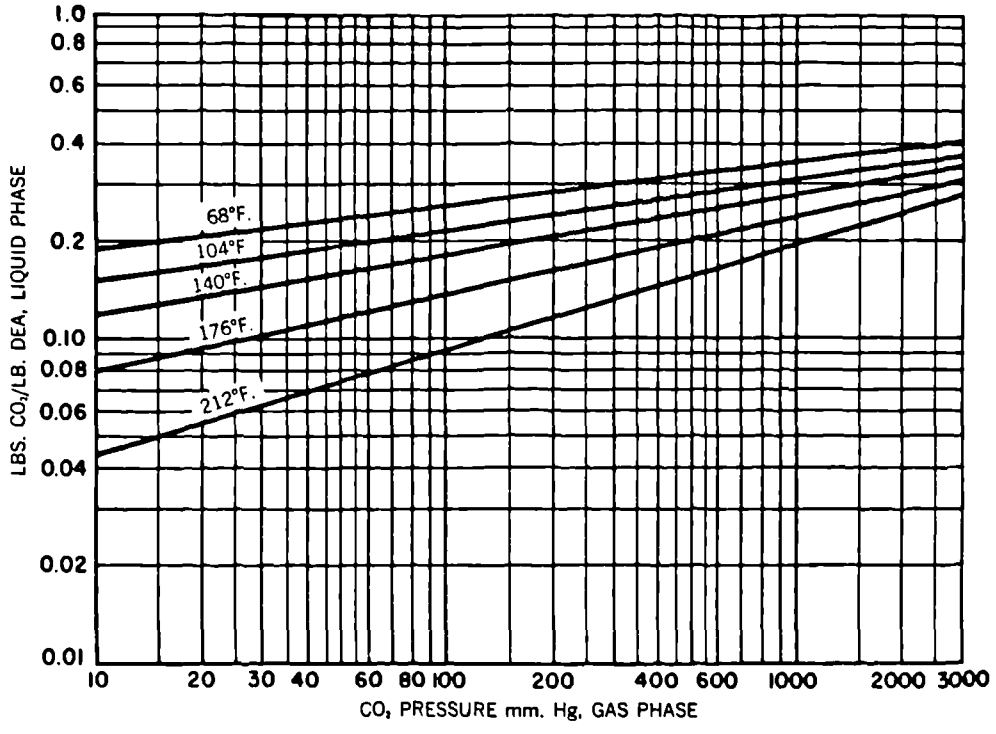

EQUILIBRIUM PLOTS OF CO_2 IN AQUEOUS DIETHANOLAMINE SOLUTIONS

35 PERCENT DEA

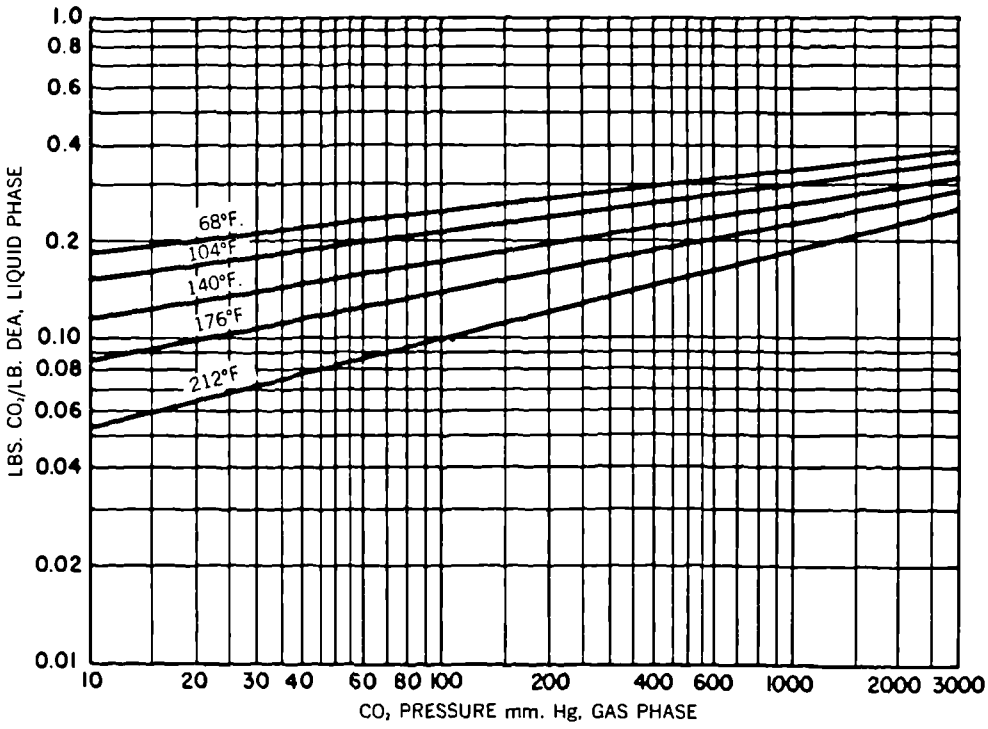

40 PERCENT DEA

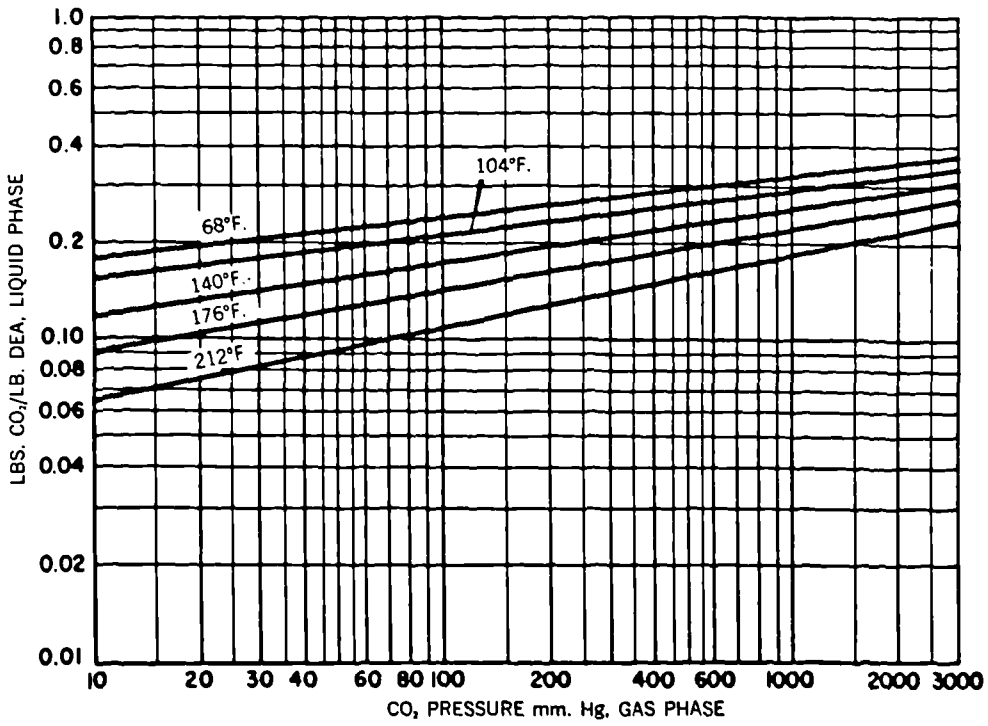

TOTAL VAPOR PRESSURES OF AQUEOUS
DIETHANOLAMINE SOLUTIONS

PERCENT BY WEIGHT

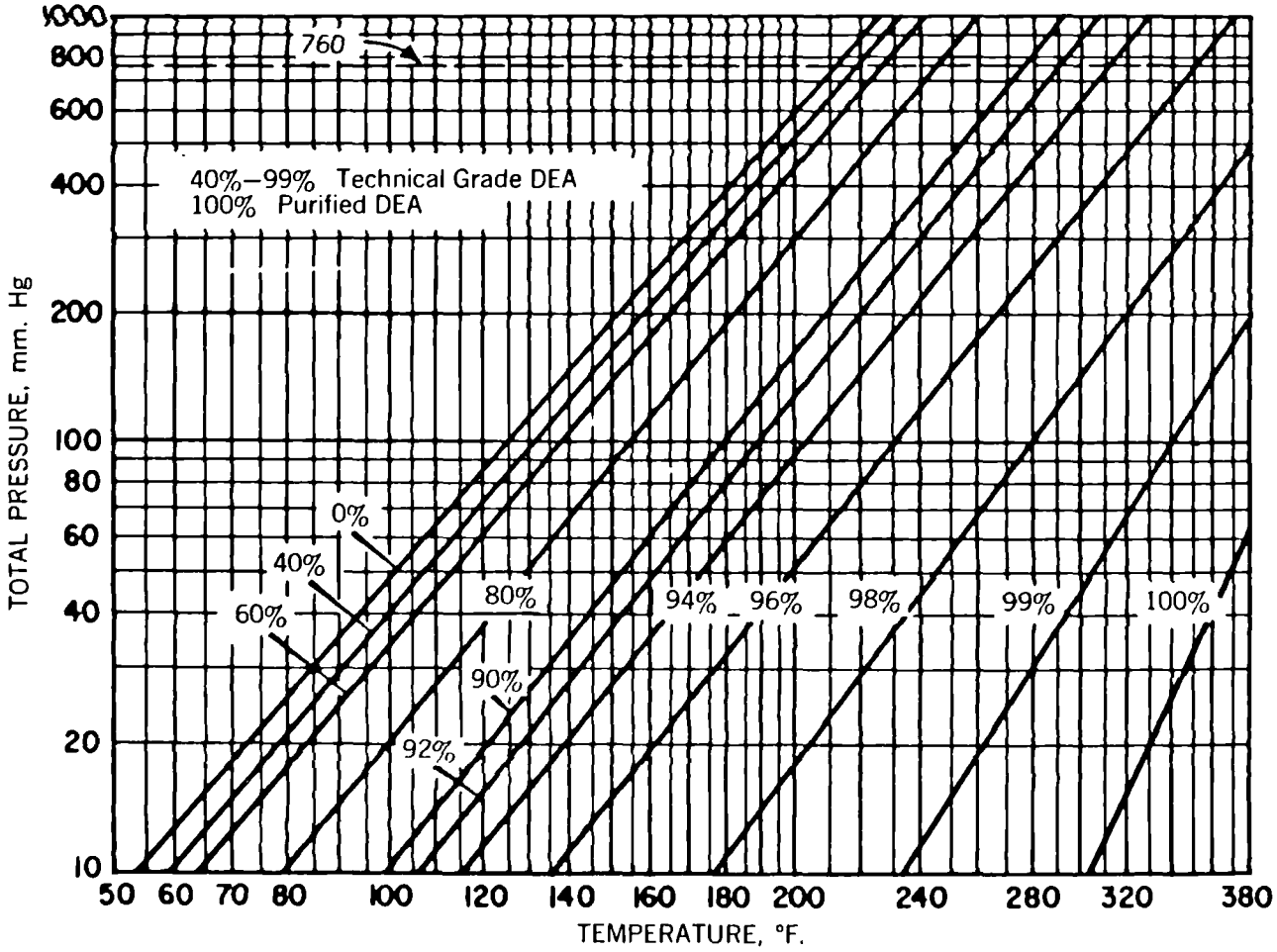

Appendix K: Miscellaneous Calculations

K1: Annular correction for mass transfer.

As described in section 8 a correction factor was measured to account for the mass transfer which occurs in the annulus of the rotary absorber. The derivation of this correction factor is outlined below.

Where mass transfer takes place in the annulus of the disc as well as across the surface of a plate, the rate of transfer is given by

$$N_o = N_p + N_A = VC_b^\circ \qquad K.1$$

where N_o = overall rate of mass transfer
N_p = mass transfer ocurring on plate
N_A = mass transfer ocurring in the annulus.

To simplify the calculation an arithmetic mean concentration driving force was assumed (this adds an error of approximately 0.5%), and thus the overall rate of mass transfer can be defined as:

$$N_o = VC_b^\circ = k_{LO}.A.\Delta C \qquad K.2$$

so
$$VC_b^\circ = k_{LO}.A\frac{(2C_i - C_b^\circ)}{2} \qquad K.3$$

or
$$C_b^\circ = \frac{k_{LO}.A.C_i}{V+1/2k_{LO}.A} \qquad K.4$$

The mass transfer occuring on the plate, N_p, can be calculated from the measured value of k_{LP} assuming the bulk CO_2 concentration at the edge of the plate is C_b^P where C_b^P is

$$C_b^P = \frac{K_{LP}.A.C_i}{V+\frac{k_{LP}.A}{2}} \qquad K.5$$

thus
$$N_P = K_{LP}.A.C_i - \frac{k_{LP}^2.A^2.C_i}{(2V+k_{LP}.A)}$$

The rate of mass transfer in the annulus is calculated similarily and thus:

$$N_A = k_{LA}.A\ \frac{(2C_i - C_b^P - C_b^o)}{2} \qquad K.6$$

where A' = annular mass transfer area.

Thus K·1, K·4. K·5, and K·6 can be combined and rearranged to provide an expression for k_{LP} (i.e. the mass transfer coefficient on the plate), i.e.,

$$k_{LP} = \frac{4V^2}{A}\left[\frac{k_{LO}\cdot A\cdot k_{LA}\cdot A'}{4V^2 - k_{LO}\cdot k_{LA}\cdot A}\right] \qquad K.7$$

at high flowrates i.e. where $4V^2 >>> k_{LO}k_{LA}.A.A'$ K.7 can be simplified to give:

$$k_{LP} = \frac{k_{LO}A - k_L A'}{A} \qquad K.8$$

This is the expression which would have been obtained if it had been assumed that the concentrating driving force was the same in the annulus as on the plate. K.8 was used to calculate the correction factors described in section 8.

K2: Calculation of required gas flowrate

The gas flowrates used during the experimental mass transfer investigation were chosen so that the interfacial concentration of carbon dioxide was approximately constant across the face of the rotary transfer surface. The following calculations show the validity of this assumption.

The flowrates of N_2 and CO_2 to the rotary test rig were controlled so that they were equal and had a value of 1.483 litres/second. Thus if the inlet gas pressure is 1 atmosphere the liquid flowrate employed is 100 cm^3/sec and the outlet bulk CO_2 concentration is 0.001 mole/litre then at 25°C the partial pressure of CO_2 drops from 0.5 atm to 0.499 atm. Therefore the interfacial concentration decreases negligibly. Assuming the bulk concentration rises to 0.003 moles/litre the CO_2 partial pressure thus falls to 0.4985 atm, again a negligible decrease. Finally if it is assumed that the outlet concentration is 0.01 moles/litre it can be shown that the CO_2 partial pressure drops to 0.496 atm.

This data can thus be used to construct a graph of outlet interfacial composition against bulk composition. This indicates that even when the outlet solution is saturated, i.e. $C_i = C_b^\circ$ the interfacial concentration only falls by 1.3%. Thus the interfacial concentration can be considered constant over the whole face of the rotating surface.

Appendix L: OPERATION OF THE REGENERATION SYSTEM

The regeneration system is described in detail in section 7.3. The following sections outline how it is operated in order to regenerate a tank full of loaded diethanolamine.

a) Priming of the reboiler with CO_2 free DEA

i) Open valve 4 to pump 1 and close valves 3 and 5.
ii) Close valve 31 and open valve 8 so that liquid is directed to the top of the column rather than the rotary absorber.
iii) Open valve 7 (recycle line) and switch on pump 1.
iv) Slowly open valve 1 until a flowrate of 200 cm^3/sec is recorded on rotameter 1.
v) Close valves 21 and 23 and ensure that valves 22 and 25 are open.
vi) Switch on pump 2 so that is controlled by the level relay.
vii) Once the high level is reached and pump 2 automatically switches on, switch off pump 1 and close valve 1.
viii) The final level in the reboiler will be at the low level.

b) Elevation of reboiler to the operational (boiling) temperature

i) Open valve 15 and clear the steam line of any condensate which may have formed.

ii) Open valve 16 followed by valve 17 until the required steam pressure is attained (steam at 3 bar has a temperature of 133.5°C)

iii) Open valves 11 and 13 fully allowing water to flow through the overhead condensor.

iv) Boiling in the reboiler is indicated by a constant temperature (approximately 110°C, as recorded by thermocouple 5) and a steady return of liquid from the condensor.

c) Feed of loaded solution to the column

i) Ensure that valves 1,2,3 and 4 are closed.

ii) Switch on the electric heater in the sump of the glass exchanger and allow the temperature to rise to the control point (95°C)

iii) Open valves 6 and 5 and switch on pump 1.

iv) Allow liquid to circulate through the glass exchanger and back to tank 2 until it attains a temperature of 70°C (as measured by thermocouple 1). This takes approximately 1/2 hour.

v) Slowly open valve 1 so that hot liquid is pumped to the top of the column. Valve 6 can be left open to maintain the liquid temperature.

vi) As regenerated solution fills up the reboiler it is automatically pumped into the brass storage tank.

vii) Liquid in the brass tank is rapidly cooled by water circulating via valve 12 through a submerged coil.

viii) Once all of the liquid from tank 2 has been delivered to the column pump 1 is switched off and valves 8,1, and 6 closed.

ix) The steam heating is switched off (by closing valves 17, 16 and 15) and once the solution has reached 30°C valve 13 is closed stopping the flow of water to the condensor.

d) Storage of regenerated solution

i) Once the liquid in the brass tank has cooled sufficiently (approximately 20 minutes) valves 24 and 21 are opened and 25 and 22 closed.

ii) Pump 2 is switched on by overiding the level control relay and the contents of brass tank 2 sent to plastic tank 3 for storage.

iii) Pump 2 is then switched off.

iv) Once the liquid in the reboiler has cooked to below 30°C (approximately 1 hour) valves 25,23 and 9 are opened and valves 21 and 24 closed.

v) Pump 2 is switched on by overiding the level control relay and the contents of the reboiler sent to plastic tank 1 for storage.

vi) Pump 2 is then switched off and valves 25, 23 and 9 closed.